ROLE OF CERULOPLASMIN SIGNALING IN ORAL CANCER METABOLISM

A Thesis submitted to the
UPES

For the Award of
Doctor of Philosophy
in
Biotechnology

By
SANIYA ARFIN

October 2023

SUPERVISOR(s)
Dr. Dhruv Kumar
Dr. Dario Di Silvestre

UPES
UNIVERSITY OF TOMORROW

School of Health Science and Technology (SOSHT)
UPES, Dehradun – 248007: Uttarakhand

ROLE OF CERULOPLASMIN SIGNALING IN ORAL CANCER METABOLISM

A Thesis submitted to the

UPES

For the Award of

Doctor of Philosophy

in

Biotechnology

By

SANIYA ARFIN

(SAP 500105605)

October 2023

Internal Supervisor:

Dr. Dhruv Kumar

Professor

School of Health Science and Technology (SOSHT)

UPES, Dehradun, Uttarakhand, India

External Supervisor:

Dr. Dario Di Silvestre

Permanent Researcher

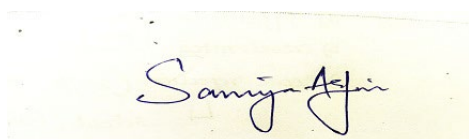Institute of Biomedical Technologies,

National Research Council, Italy

School of Health Science and Technology (SOSHT)

UPES*,* Dehradun – 248007: Uttarakhand

OCTOBER 2023

DECLARATION

I declare that the Thesis entitled "Role of Ceruloplasmin Signaling in Oral Cancer Metabolism" has been prepared by me under the guidance of Dr. Dhruv Kumar, Professor, Department of School of Health Science and Technology (SOHST), UPES. No part of this thesis has formed the basis for the award of any degree or fellowship previously.

Saniya Arfin
School of Health Science and Technology (SOHST),
UPES, Dehradun-248007, Uttarakhand

CERTIFICATE FROM INTERNAL GUIDE

CERTIFICATE FROM GUIDE

I certify that **Miss Saniya Arfin** has prepared her Long Abstract entitled **"Role of Ceruloplasmin Signaling in Oral Cancer Metabolism",** for the award of PhD degree under my guidance. She has carried out the work at School of Health Science and Technology (SoHST), University of Petroleum & Energy Studies, Dehradun.

Dr. Dhruv Kumar
Sr. Associate Professor
School of Health Science and Technology
University of Petroleum and Energy Studies
Dehradun-248007, Uttarakhand
Date: 10.02.2023

CERTIFICATE FROM THE CO-GUIDE

This is to certify that a part of the research work embodied in this Thesis entitled "Role of Ceruloplasmin Signaling in Oral Cancer Metabolism" submitted to UPES, Dehradun, for the award of the degree of Doctor of Philosophy in Biotechnology has been carried out by Saniya Arfin (SAP ID.:0500105605) under my co-supervision at Institute for Biomedical Technologies - National ResearchCouncil (ITB-CNR), Milan, Italy.

Sincerely yours,

DARIO DI
SILVESTRE
06.10.2023 10:56:06
GMT+00:00

Signature of External Co-guide

Dr. Dario Di Silvestre

Institute for Biomedical Technologies,

National Research Council

Milan, Italy

ABSTRACT

Ceruloplasmin (CP)is a protein that plays a key role in the metabolism of iron in the body by oxidation of Fe 2+ to Fe 3+ and in immune regulation in tumor cells by interacting with neutrophil derived Myeloperoxidase(MPO) to stop apoptosis. By inhibiting this interaction will allow MPO to generate HOCl resulting in caspase mediated tumor cell death. Further the free ceruloplasmin is susceptible to proteolysis leading to induction of oxidative stress mediated ferroptotic cell death suggesting CP could be a potential cancer therapeutic target.

In our study we performed in silico analysis of the Oral Squamous Cell Carcinoma data from the GDC portal and found CP expression considerably increased in high-grade oral cancer patients. Based on our findings from the analysis of protein-protein interactions and co-expression networks, it is suggested that targeting the CP-associated redox metabolism axis, iron homeostasis, and immunoregulation may hold promise as a potential therapeutic approach. This is supported by the identification of molecular hubs that characterize the high-grade OSCC phenotypes in our study. We analyzed the differential miRNA expression since the loss and gain of miRNA function promote cancer development. We have identified candidate miRNAs as well as their target genes which play important role in tumor aggressive behaviors and be further explored in oral cancer therapeutics potential gene targets. CP is a target of a downregulated miRNA in stage 4 oral cancers whose expression profile and other predicted target gene ontologies show it plays an essential role as an oral cancer metastasis promoter. A better understanding of the mechanisms of these miRNA regulation may provide useful insights for the development of effective cancer treatments.

We conducted a screening of various phytochemicals and marine compounds against CP with the aim of identifying a highly potent lead compound that could serve as a valuable foundation for the development of novel drugs with improved efficacy and reduced toxicity. The ultimate goal is to target early-stage oral cancer more effectively. We identified three phytochemicals with good docking scores, drug likeness and ADME properties. Out of these three two phytochemicals Lycoperoside F and Ardimerin digallate showed good results in MD simulations which could be further taken up for *invitro* and *invivo* studies.

ACKNOWLEDGEMENT

CONTENTS

LIST OF FIGURES

LIST OF TABLES

ABBREVIATIONS

CHAPTER 1

INTRODUCTION

1.1. OVERVIEW

Head and Neck Squamous Cell Carcinoma (HNSCC) accounts for 325,000 deaths annually and is the 8th most common cancer worldwide(Gormley et al., 2022) The HNSCC is made up of a variety of tumors affecting the upper aero digestive tract. Among the various histological types observed, squamous cell carcinoma stands as the most prevalent.
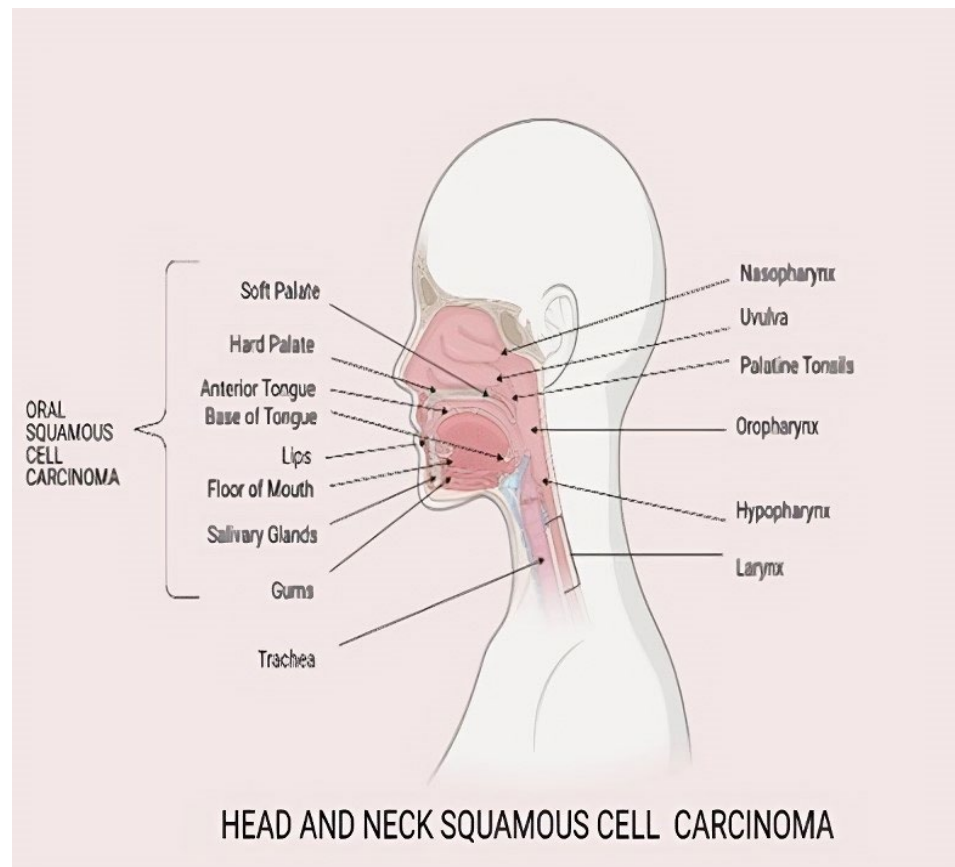
Figure 1.Oral squamous cell carcinoma sites in the Head and Neck Cancer. Oral cancer can occur in various sites within the mouth, including the lips, tongue, gums, floor of the mouth, hard and soft palate, cheeks, and even the tonsils and oropharynx.

Despite therapeutic advancements against this disease the survival probability of HNSCC patients remains considerably low. Surgical intervention, radiation therapy, and systemic treatment form indispensable elements in managing locally advanced head and neck malignancies, which continue to present significant therapeutic difficulties(*Head and Neck Cancer - The Lancet*, n.d.).

In spite of the fact there may be some overlap in treatment principles, it is important to note that the management of head and neck cancers is typically tailored to the specific site and histology of the tumor. The neoplasms affecting all oral regions are grouped as Oral cancer(Figure 1) which is the most prevalent malignancy known in the head and neck region leading to significant deaths worldwide. The prevalence of oral cancer in India is higher and accounts for one-third of the total burden of oral cancer globally(B. Gupta et al., 2017). Some of the risk factors associated to oral cancer occurrence include smoking, chewing betel leaves, excessive alcohol consumption, prolonged unhygienic oral conditions, and sustained viral human papillomavirus infections. Out of these tobacco consumption is the prime cause of cancer in developing countries(Borse et al., 2020). The diagnosis of oral cancer often occurs in advanced stages due to various factors such as lack of awareness among patients, limited availability of sensitive biomarkers, and the aggressive nature of the disease thereby, reducing the chances of cure considerably (Veluthattil et al., 2019). Another hurdle faced in curing this malignant disease is resistance to chemotherapeutic drugs (Vermorken et al., 2008). Timely treatment upon early diagnosis may improve the patient survival by 90%. This necessitates the search for specific diagnostic, therapeutic and prognostic biomarkers for oral cancer. Personalized treatment decisions are the best way to meet the needs and preferences of each patient.

Upregulation of CP, a copper-binding protein, has been observed in various types of tumors, suggesting its potential involvement in tumor development and progression (Figure 2). The increased expression of CP in tumors can have diverse implications for tumor biology. One possible consequence of CP up regulation is its association with enhanced oxidative stress management within tumor cells. CP scavenges reactive oxygen species (ROS) being an antioxidant protein, and mitigates oxidative damage. The upregulation of CP may confer a selective advantage to tumor cells by enabling them to cope with increased levels of oxidative stress often encountered in the tumor microenvironment.
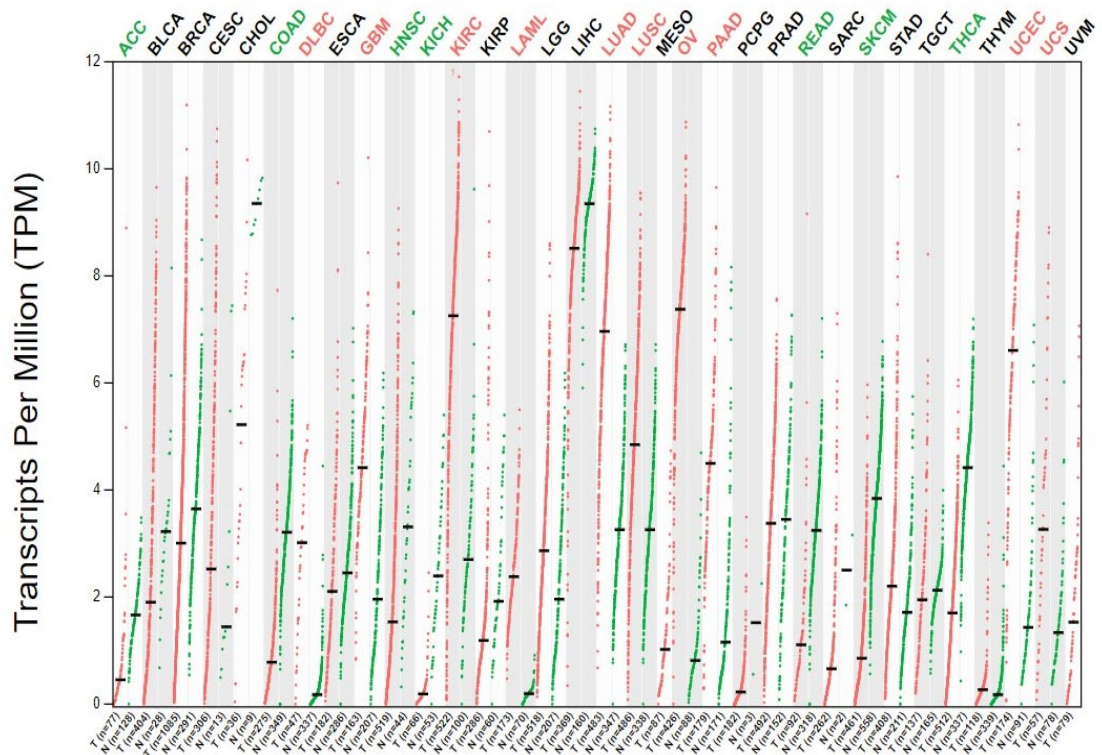
Figure 2 .Gene expression profile of CP across all tumor samples. *The Dot plot shows the CP gene expression profile across all tumor samples and paired normal tissues where each dot represent expression in samples.*

Overexpression of CP has been observed to correlate with lymph node metastasis stage and histological grade in Clear-cell renal cell carcinoma (ccRCC)(Y. Zhang et al., 2021a). Additionally, CP overexpression has been associated with activation of oncogenic pathways and poorer survival rates in ccRCC patients. In the context of breast cancer, CP has been found to correlate with immune infiltration and serves as a prognostic biomarker (C. F et al., 2021). Moreover, the expression of CP in renal cell carcinoma is associated with higher-grade tumors and reduced survival(Y. Zhang et al., 2021a)
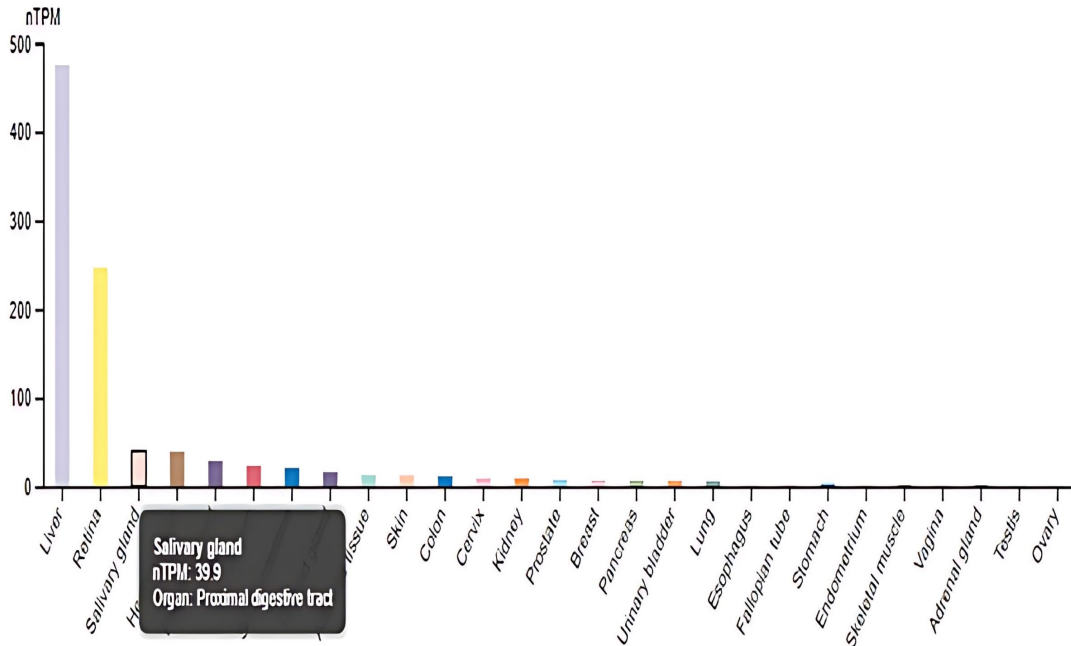
Figure 3. GTeX data showing TPM of ceruloplasmin in various tissues including normal salivary gland. After the liver, the normal salivary gland tissues exhibit an expression level of 39.9 transcripts per million (TPM) for the CP gene.

The human protein atlas shows a summary of CP expression and protein levels in the different sites within the body. Following the highest expression in liver, normal salivary gland tissues show an expression of 39.9 TPM of CP .This observation was made on analysis of the GTex dataset as shown in Figure 3.

a

b
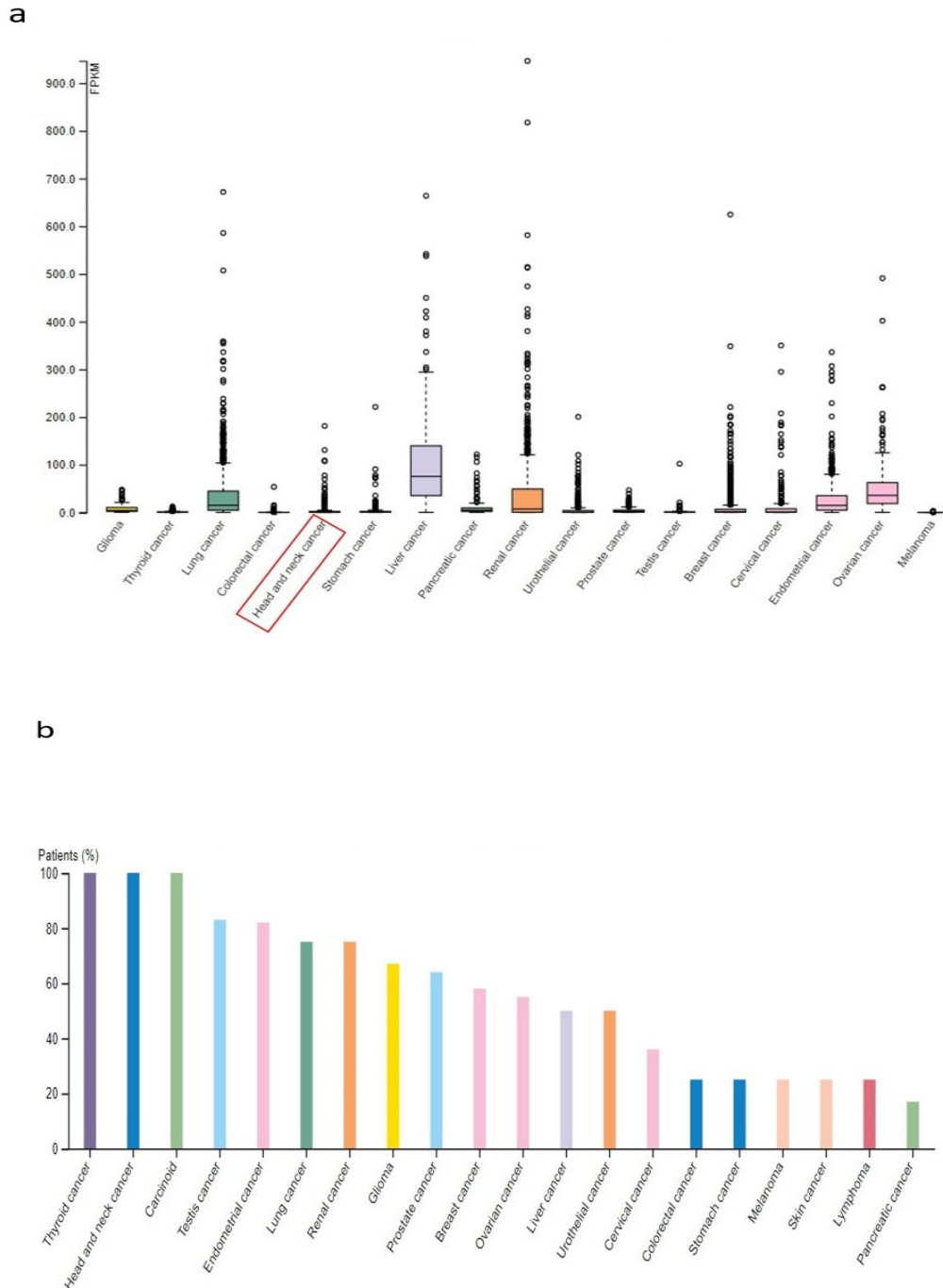
Figure 4. (a) TCGA data sets summary of mRNA expression of CP, (b) CP Protein levels summary of TCGA dataset samples. *Figure 4a shows a comparison of CP expression in head and neck cancer vs other cancer types while 4b shows the CP protein levels in all tumor types*

An overview of CP mRNA expression in the TCGA datasets as well as the protein expression summary can be seen in Figure 4. Figure 4(b) shows protein levels of CP in head and

neck cancer patients where most cancer cells showed weak to moderate cytoplasmic positivity for CP.

Anti-CP precursor antibody produced in rabbit, HPA001834 was used to stain the tissues. On comparison of head and neck cancer patients with normal samples differential staining is observed(Figure 5).
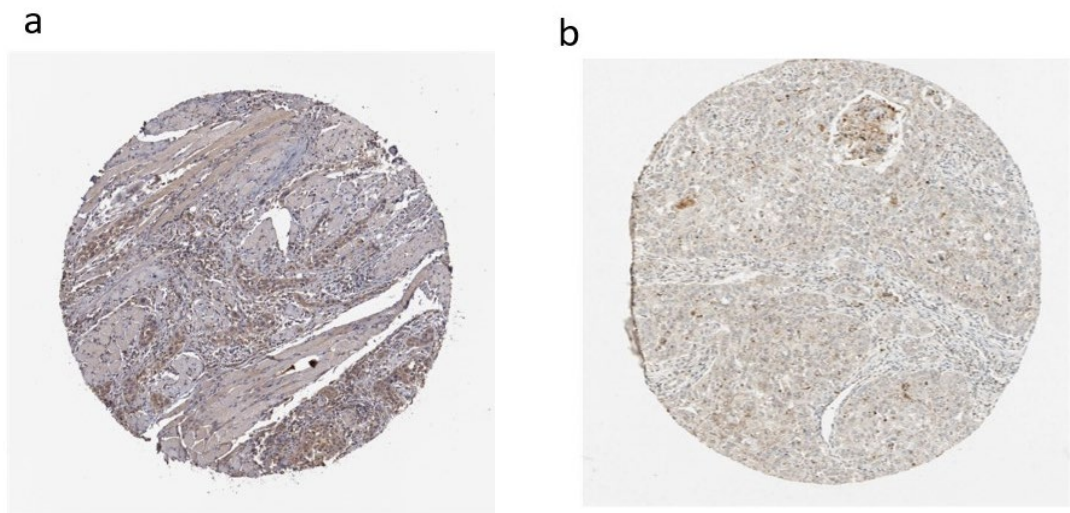
Figure 5. Staining in malignant squamous cell carcinoma obtained from head and neck cancer (patient id.2358) (a) vs the staining in normal samples(b) derived skeletal muscle of individual with (i.d. 2608)

CP exerts its influence by binding to Myeloperoxidase (MPO) and modulating its activity, specifically in the production of Hypochlorous acid (HOCl) by oxidizing chloride and other halide ions in the presence of hydrogen peroxide (H_2O_2). Previous studies have indicated that MPO, released from neutrophil granules during inflammation, does not exit into the plasma independently but necessitates CP-MPO binding(Rizo-Téllez et al., 2022)(Figure 6). Neutrophils release oxidants such as superoxides, H_2O_2, and HOCl as part of their anti-tumor cytotoxicity mechanisms.
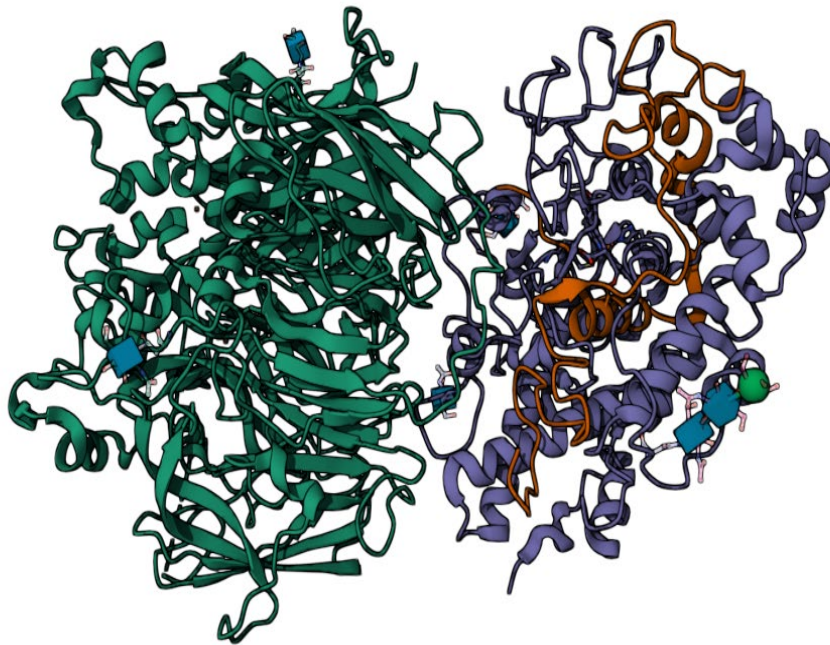
Figure 6. CP-MPO complex visualized on PYMOL. *Previous studies have reported the amino acid residues 699–710 of the extended loop of CP to be involved in interaction with the 1–27 N-terminal residues of the light chain of MPO.*

CP acts as a regulator of MPO activity by binding to it and potentially inhibiting HOCl production. This inhibitory effect may be mediated by reducing the availability of copper, a cofactor necessary for MPO enzymatic activity. Consequently, this limitation on copper availability may curtail the generation of HOCl (Hawkins & Davies, 2021). By impeding HOCl production, CP potentially helps to regulate the potentially detrimental effects of excessive oxidative damage and safeguards cancer tissues against oxidative stress. However, further research and investigation are necessary to elucidate the precise mechanism and significance of the CP-MPO interaction in processes including apoptosis and other cellular mechanisms. Based on the high affinity of CP for MPO, we hypothesize that CP-MPO binding may play pivotal roles in tumor mechanisms(Figure 7).
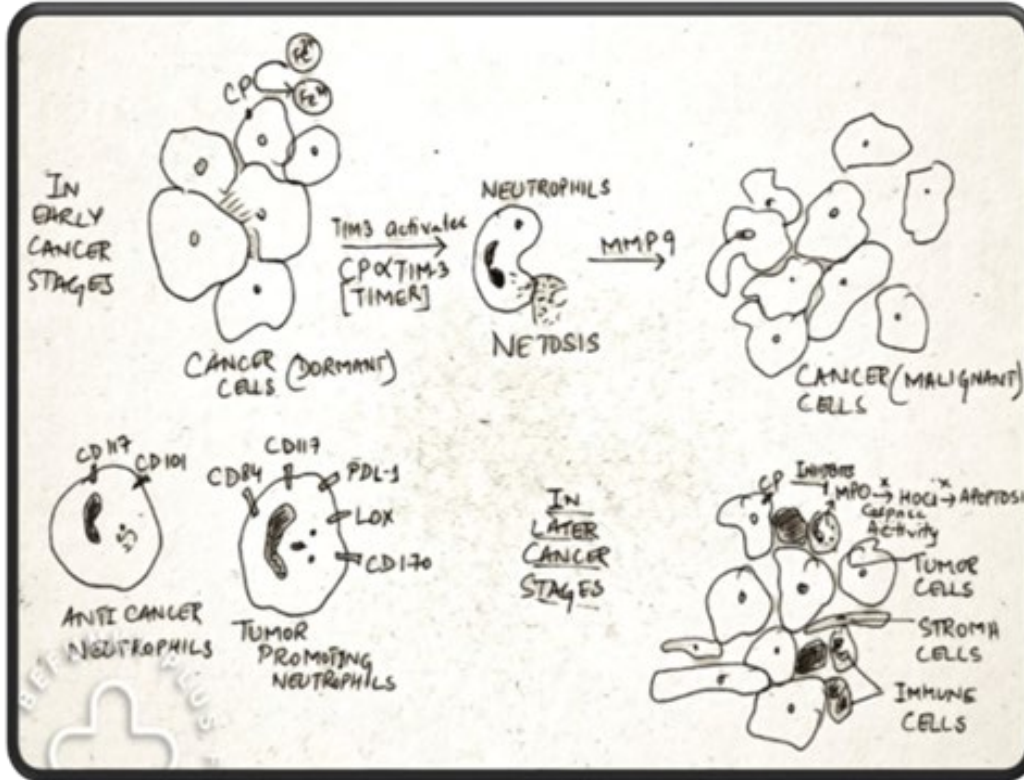
Figure 7. *An overview of CP-MPO complex inhibition and its role in ferroptotic cell death.* *In late-stage cancer, the interplay between CP, MPO, and NETosis is complex and may be influenced by various factors, including the tumor microenvironment, the immune response, and the presence of oxidative stress.*

1.2. GAPS IN THE STUDY

1.   Owing to late diagnosis of oral cancer, it is essential to identify protein biomarkers that can aid in diagnosis and targeted treatment of oral cancer patients.

2.   There have been several biomarkers identified for oral cancer through *in silico* analysis. For instance, Matrix metalloproteinase (MMPs), such as MMP-3, MMP-9, and MMP-13, have been found to show significant up regulation in oral squamous cell carcinoma (OSCC) compared to normal tissue. However, it is important to note that MMPs engage in multiple biological processes beyond cancer and their expression changes may not exclusively reflect cancer status. Similarly EGFR upregulation in oral cancer is also noted however it is also involved in normal cellular processes, and changes in its expression may not solely indicate the presence of cancer. Additionally, EGFR-targeted therapies can have adverse effects, necessitating careful patient selection for safe and effective use. Furthermore, several microRNAs (miRNAs), including miR-21, miR-31, and miR-375, have shown differential expression in OSCC compared to normal tissue. However, further research is needed to validate these miRNAs as reliable biomarkers. It is crucial to acknowledge that miRNA-based biomarkers may be prone to false positives due to variations in sample preparation and analysis methods.

3.   CP has been observed to be up regulated in a number of tumor types however there is a lack of detailed mechanistic understanding of how CP influences oral cancer metabolism which can be addressed by exploring the molecular pathways and signaling mechanisms through which CP affects cancer cell growth, invasion, metastasis, and other key processes.

4.   Investigating potential interactions with key regulators, such as oncogenes, tumor suppressors, or other proteins involved in oral cancer progression, could provide a more comprehensive understanding of CP's role.

5.   CP's immune regulatory role and MPO inhibition as well as the impact of restricting this CP-MPO interaction on cancer progression has not been previously studied.

1.3. SCOPE OF THE STUDY

In our study we first identified the expression of CP on analysis of the Head and Neck Cancer subjects submitted to The Cancer Genome Atlas database and then performed various analysis including network analysis and functional enrichments to help elucidate the mechanism of action in promoting tumorigenesis. We then determined inhibitors that can be used to target the specific role played by CP. We focused on phytochemicals and marine compounds as these bioactive molecules are preferential over other drugs as they act differentially specific to cancer cells without altering normal cells(Singh et al., 2016). Several phytochemicals have been previously studied to manifest anticancer function *in vitro* as well as *in vivo*.

1.3.1. Research Objectives

1.   Gene expression analysis of ceruloplasmin in Oral cancer patients from TCGA database and its correlation with metabolic associated genes

2.   Identification of potential inhibitor(s) for ceruloplasmin using *in silico* virtual screening approaches

3.   Evaluation of selected inhibitor(s) using Molecular Dynamics Simulation

1.3.2. Research questions/hypotheses:

1.   We hypothesized that CP up regulation in head and neck cancer promotes tumor progression by acting along the redox axis and immune regulation.

2.   We also hypothesize that CP-MPO binding maybe playing more important roles in tumor mechanism owing to the high affinity of CP for MPO.

1.4. METHODOLOGY

i) Gene expression analysis of ceruloplasmin in Oral cancer patients from TCGA database and its correlation with metabolic associated genes

1.4.1. TCGA Data Extraction

We accessed and retrieved HNSC data from The Cancer Genome Atlas (TCGA) for our study.

Data Preprocessing: The collected data underwent preprocessing, which included cleaning, alignment, and quality control.

Data Analysis: Using specialized bioinformatics tools, we performed comprehensive data analysis. This step included tasks such as identifying genetic mutations, assessing gene expression, and correlating clinical information.

Statistical Analysis: We conducted statistical analyses to uncover significant patterns, associations, or biomarkers within the dataset.

Data Visualization: The results were visualized using plots, graphs, and other visual representations to aid in data interpretation.

Interpretation: We interpreted the findings in the context of our research objectives and formulated insights and conclusions.

Reporting: The outcomes of our analysis were documented and reported, facilitating knowledge sharing and future research.

The diagram provides an overview of our TCGA data analysis workflow, highlighting the key steps and processes involved (Figure 8).
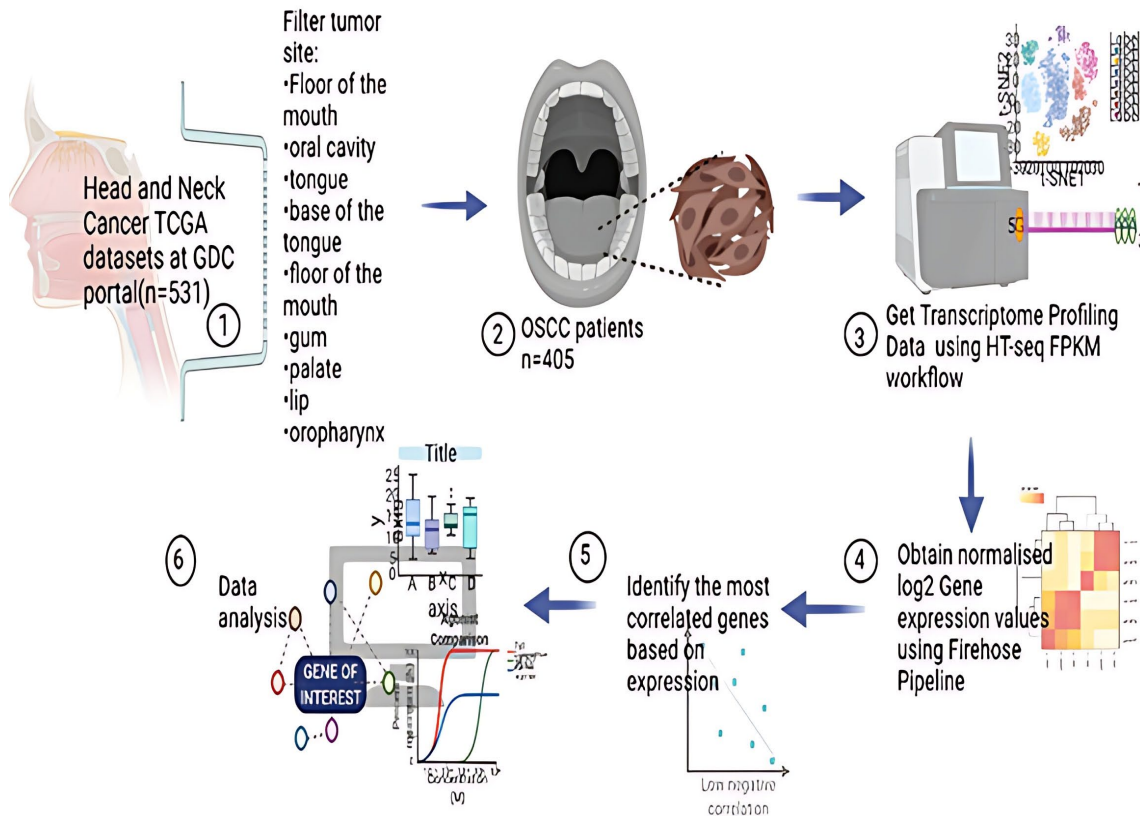
Figure 8. Workflow for TCGA data analysis of gene expression. *This involves data extraction using R followed by analysis to identify differential expression as well as epigenetic modifications.*

1.4.1.1.   GDC TCGA Database

The National Cancer Institute's Genomic Data Commons data portal provides a unified repository for cancer knowledge. It contains data from The Cancer Genome Atlas along with access to multiple other contributed datasets and enables data sharing across cancer genomic studies. (https://portal.gdc.cancer.gov/). It is a collection of 74 projects including 67 tumor sites in about 86,513 recorded cancer patients. GDC portal provides data for various cancer types and projects so we chose the specific head and neck cancer type and the TCGA project we were interested in studying.

From amongst the head and neck cancer data the transcriptomic and clinical data for OSCC were downloaded from GDC using GDC client. 405 patients with Oral cancer primary sites were selected out of the 531 Head and Neck Cancer Patients (Table1). We used the TCGA Data Portal's

search interface to define the specific criteria for data retrieval. This included selecting specific samples, data formats, molecular profiling platforms, or other relevant parameters.

Table 1.Characteristics of patients selected from the Head and Neck Cancer Dataset

Variables	N=405
Primary site(oral cancer)	Alveolar ridge - 18
	Base of tongue - 23
	Buccal mucosa - 22
	Floor of mouth - 61
	Hard palate - 7
	Hypopharynx - 2
	Lip - 3
	Oral cavity - 71
	Oral tongue - 124
	Oropharynx - 9
	Tonsil - 39
Clinical Tumor stage	Stage1–21
	Stage 2 –97
	Stage 3-106
	Stage 4-278
Tumor Grade	Grade 1-54
	Grade 2-224
	Grade 3-96
	Grade 4-7

Tumor: metastatic	Tumors- 500 Metastatic- 2
Vital status	Dead - 43 Alive -53

The transcriptome profiling data for these cases was obtained from the repository to get the mRNA expression files.

1.4.1.2.   Calculating the log2 fold change:

This is a common method used when comparing gene expression or other quantitative measurements between tumor and normal patients. The log2 fold change provides a standardized and easily interpretable metric for understanding the magnitude of differences in expression levels.

The following are the advantages of using log2 fold change in such comparisons:

Scaling and normalization: Gene expression data can have a wide dynamic range, and the distribution of expression values may vary between different samples or experimental conditions. Taking the log2 transformation helps to compress the data and improve the normality of the distribution. It also helps in reducing the impact of extreme values or outliers.

Interpretability: The log2 scale provides a more intuitive understanding of fold changes compared to linear scales. A log2 fold change of 1 means a twofold difference in expression, while a log2 fold change of 2 represents a fourfold difference. This logarithmic transformation allows for a more straightforward interpretation of the relative changes in expression levels.

Symmetry: Log2 transformation ensures symmetry around zero. In a log2 fold change calculation, an upregulation in expression is represented by a positive value, while a downregulation is represented by a negative value. This symmetry simplifies the interpretation and comparison of both upregulated and downregulated genes.

Statistical analysis: Log2 fold changes are often used as input for downstream statistical analyses, such as t-tests or linear models. These analyses assume a more normal distribution and homogeneity of variance, which are better approximated after log2 transformation.

By calculating the log2 fold change using the Firehose Pipeline in R we identified genes that show significant differential expression between tumor and normal samples. A significance level of P < 0.05 was used to determine statistical significance. The log2 fold change (FC) values obtained were subsequently utilized in various other analyses.

1.4.1.3.   The Firehose pipeline

This pipeline generates preprocessed and harmonized data for various types of genomic data, such as gene expression, copy number variation, DNA methylation, and more. Once the processed data is available, we used R to load, analyze, and visualize the data using various packages and tools.

The workflow for utilizing Firehose data in R is as follows:

- We visited the Broad Institute's Firehose website (https://gdac.broadinstitute.org/) to access the processed TCGA data generated by the Firehose pipeline(Deng et al., 2017).

- We selected the desired data type (illuminahiseq_rnaseq-gene_expression) and cancer type (oral cancer) and downloaded the processed data files. The data files were typically provided in a standardized format, such as TCGA Level 3 data. TCGA Level 3 data specifically refers to the processed data that has undergone normalization, filtering, and quality assessment steps. We relied on TCGA Level 3 data because it has undergone preprocessing steps to minimize technical variations and ensures data quality. This allows for more reliable comparisons and analyses across different tumor types and patient cohorts.

- We used R packages, such as readr and DESeq2, to load the downloaded data files into R. These packages provided functions for reading and handling various data formats, such as tab-delimited files.

- Once the data was loaded into R, various analyses were performed. Differential expression analysis packages like DESeq2 or limma were used to identify genes that were differentially expressed between tumor and normal samples. We obtained the fold change of the various genes across the subjects in comparison to normal.

- We used ggplot2, heatmaply, or survminer to create visualizations of the analyzed Firehose data. These packages offered a wide range of plotting functions for generating customized plots, such as heatmaps, survival curves, volcano plots, and more.

1.4.2. Online tools used to perform differential and correlation analysis:

The differentially expressed mRNA data was validated using online tools such as LinkedOmics, UALCAN, c-Bioportal and Oncomine.

1.4.2.1. c-Bioportal

This resource is freely available with a collection of about 20 different cancer studies and allows the multidimensional cancer genomics data sets to be explored in an interactive manner. It integrates and visualizes multidimensional data, allowing us to explore genetic alterations, gene expression patterns, and clinical outcomes across different cancer types. cBioPortal is a valuable resource for cancer genomics research and facilitates the identification of biomarkers along with potential therapeutic targets. We used c-Bioportal to obtain the correlated expression of genes in our dataset filtered on the basis of Spearman's Rho static test for expression(Cerami et al., 2012).

1.4.2.2. UALCAN

UALCAN is web portal for analyzing, and visualizing data from the Cancer Genome Atlas (TCGA) project. It enables the determination of gene expression impact on the survival of the patients. Using UALCAN we assessed the pathways perturbed in oral cancer as it also contains information for the methylation status of genes as well the differential miRNA expression of the TCGA datasets along with their genes (Chandrashekar et al., 2022).

UALCAN primarily utilizes non-parametric statistical tests for data analysis. Specifically, it employs the Mann-Whitney U test (also known as the Wilcoxon rank-sum test) to assess differential gene expression between two groups. The Mann-Whitney U test is suitable for analyzing non-normally distributed data or when the assumption of equal variances is violated. For survival analysis, it employs the Kaplan-Meier estimator to estimate survival probabilities and applies the log-rank test to evaluate the significance of variations in survival outcomes among groups. The Kaplan-Meier estimator is a non-parametric method commonly used to analyze time-to-event data, such as overall survival or disease-free survival. In addition to these statistical tests, UALCAN also provides p-values and q-values (adjusted p-values) to quantify the statistical significance of the observed differences. The q-values are calculated using the false discovery rate (FDR) correction method to control for multiple testing.

1.4.2.3.   Oncomine

This web-based data mining tool enables genome wide expression analysis. It is a collection of gene expression from micro array experiments of a variety of cancer subtypes and allows both clinical-based as well as pathology- based analysis (Rhodes et al., 2004). Data can be queried for gene-drug target pairs that can be very helpful in the discovery of biomarkers as well as therapeutic targets.

Oncomine employs the Student's t-test to assess the statistical significance of differential gene expression between two groups, such as cancer samples versus normal samples or different clinical subgroups. The t-test is commonly used when comparing means between two groups. ANOVA is utilized in Oncomine to analyze gene expression differences among multiple groups or conditions. It helps identify genes that exhibit significant variation across different cancer types, subtypes, or clinical characteristics. It also applies FDR correction to control for multiple hypothesis testing when analyzing gene expression data. FDR adjustment helps minimize the likelihood of false positive results due to conducting multiple statistical tests. Furthermore, Oncomine employs statistical methods such as the Kaplan-Meier estimator and log-rank test to assess the association between gene expression levels and patient survival outcomes. These methods enable the investigation of overall survival, disease-specific survival, or progression-free survival based on gene expression patterns. The platform employs rigorous statistical methods to ensure robust data analysis and reliable results. Hence, we used oncomine to validate our results.

1.4.2.4.   Linked Omics

This is a database presenting multi-omics data of the different cancer type's clinical data available at The Cancer Genome Atlas (TCGA) project. Linked Omics conducts integrative multi-omics analysis by merging various data types including genomics, transcriptomics, proteomics, metabolomics, and epigenomics. This approach enables a comprehensive exploration of biological systems and enhances our understanding of complex biological processes. It involves the simultaneous analysis of multiple layers of molecular data to reveal complex relationships, interactions, and regulatory mechanisms. It allowed us to obtain integrated data of mass

spectrometry (MS)-based global proteomics generated from the Clinical Proteomic Tumor Analysis Consortium (CPTAC) with the gene expression data from the TCGA samples(Vasaikar et al., 2018).

1.4.2.5. *GEPIA*

We used GEPIA to compare the TCGA gene expression results with the GTex Normal data. This web-based platform allows users to perform gene expression analysis and explore correlation patterns in large-scale cancer datasets. We also explored the tool for correlation analysis of genes along with their patient survival analysis(Tang et al., 2017). GEPIA calculates the Pearson correlation coefficient to assess the linear correlation between gene expressions of two genes across different cancer samples. The Pearson correlation coefficient assesses the strength and direction of the linear connection between two variables, offering a range of values from -1 (representing a complete negative correlation) to 1 (signifying a complete positive correlation).The p-values calculated in GEPIA to determine the statistical significance of the observed correlations indicate the likelihood of obtaining a correlation as extreme as the observed one by chance alone. We assessed the statistical significance of correlations to determine if they were statistically reliable.

1.4.2.6. *Graphpad*

This is a software that provides several statistical analysis and graphing tools: Prism and InStat. GraphPad Prism offers an intuitive interface that allows users to import their data and perform a wide range of statistical analyses, including t-tests, ANOVA, regression analysis, survival analysis, and nonparametric tests. Prism also provides tools for creating publication-quality graphs, plotting dose-response curves, performing curve fitting, and generating statistical reports.

The software utilized for generating a heat map of the differentially expressed genes in Head and Neck cancer patients was GraphPad Prism version 8.0.0 for Windows.

1.4.3. Network Analysis

1.4.3.1. STRING network analysis:

We used this biological database for generating Protein-Protein Interaction Networks on the basis of Functional Enrichment Analysis and co- expression. It represents both known and predicted

protein-protein interactions as well as uses functional associations from various sources and physical direct interactions previously established (Szklarczyk et al., 2019).

1.4.3.2. Cytoscape

We integrated our gene expression profiles with the molecular interaction networks generated by string and visualized and analyzed the network using the software Cytoscape 3.9.1. We used Cytoscape for the functional and topological analysis of the network models and the identification of network modules and molecular hubs characterizing Oral cancer phenotypes (Shannon et al., 2003).Various cytoscape applications were used for the analysis such as CyTargetLinker and bingo.

1.4.3.3. Gene Mania

GeneMANIA utilizes machine learning algorithms to predict the biological functions of genes based on their network connections and shared characteristics with known genes. GeneMANIA integrates data from various sources, including publicly available databases and experimentally derived datasets, to provide a comprehensive view of gene interactions and functions. We analyzed our gene lists using gene mania on the basis of functional classification, physical and genetic interaction as well as predicted mechanism. Each selected data set was analyzed for its predictive value on the basis of weights(Warde-Farley et al., 2010)

1.4.3.4. Gene Ontology Analysis

Gene Ontology (GO) analysis is widely used to understand the functional annotation and enrichment of genes or gene sets. It classifies genes into defined categories based on their biological processes, cellular components, and molecular functions. Gene Ontology analysis involves two main steps:

Gene Set Enrichment Analysis: This step determines whether a given set of genes shows a statistically significant enrichment in specific GO terms compared to what would be expected by chance. It helps identify the functional categories that are overrepresented within a gene set.

Functional Annotation and Visualization: After identifying enriched GO terms, the analysis assigns functional annotations to genes based on the enriched categories. This provides insights into the cellular components, biological processes, and molecular functions associated with the genes of interest. Visualization tools such as bar charts, scatterplots, and network diagrams can be used to present the results in a more interpretable manner.

GO analysis can be performed using bioinformatics tools and software packages that provide precompiled GO annotations and statistical algorithms for enrichment analysis. These tools interpret large-scale genomic or transcriptomic datasets and gain insights into the functional relevance of genes in biological processes and pathways.

We analyzed the differentially expressed genes for their Gene Ontologies using Panther classification systems , DAVID gene functional classification tool(D. W. Huang et al., 2007) as well as cytoscape

1.4.3.5.   STRING network analysis

STRING, stands for Search Tool for the Retrieval of Interacting Genes/Proteins, and is a widely-used bioinformatics database and web resource. It offers valuable information regarding protein-protein interactions, functional associations, and network analysis in a comprehensive manner(Szklarczyk et al., 2019). STRING integrates and compiles protein-protein interaction data from various sources, including experimental data, co-expression data, and curated databases. It provides a comprehensive network of interactions, enabling the exploration of known and predicted protein interactions where we can customize the visualization. It also allows to perform functional enrichment analysis to identify the enriched Gene Ontology (GO) terms, biological pathways, and protein domains associated with a set of proteins. This analysis helps uncover the biological processes and functions enriched within a protein network or a specific group of proteins. With the help of network analysis metrics string can be used to assess the properties of protein-protein interaction networks, such as node degree, clustering coefficient, and network centralities (e.g., betweenness centrality, closeness centrality). These metrics help evaluate the importance and centrality of individual proteins within the network. By integrating diverse data sources and providing a user-friendly interface, STRING facilitates network-based analyses and aids in the interpretation of complex molecular relationships.

We used this biological database for generating Protein-Protein Interaction Networks on the basis of Functional Enrichment Analysis and co- expression. It represents both known and predicted protein-protein interactions as well as uses functional associations from various sources and physical direct interactions previously established (Szklarczyk et al., 2019).

1.4.4. Gene Methylation Analysis

We used Survival Meth, MethDB and methSurv database to investigate the result of CP DNA methylation on CP expression and prognosis in OSCC patients. These databases focus on integrating DNA methylation data from multiple cancer studies and provides tools for survival analysis based on methylation profiles. MethSurv can be used to identify potential DNA methylation biomarkers associated with survival outcomes. It provides statistical analysis and ranking of DNA methylation probes or regions based on their significance and association with patient survival. We identified the different methylation sites on the CP gene body. We also analyzed survival of the patients in correlation to the differential methylation status of CP.

1.4.5. Immune correlation

Immune correlation analysis is particularly relevant in the context of cancer biomarkers, as the immune system plays an important role in cancer development, progression, and response to therapy. By examining the correlation between immune system components and cancer biomarkers, we can gain insights into the immunological aspects of cancer biology and potentially identify novel immune-related biomarkers. Here's how immune correlation analysis contributes to the study of cancer biomarkers.

1. Immune correlation analysis assesses the relationship between immune cell populations and cancer biomarkers. It explores whether specific immune cell types, such as T cells, B cells, natural killer cells, or macrophages, correlate with the presence or characteristics of cancer biomarkers. This information helps understand the immune contexture of tumors and its impact on disease progression.

2. Correlating immune-related gene expression patterns with cancer biomarkers provides insights into the molecular mechanisms underlying immune responses in cancer. It helps

identify immune-related genes that are associated with specific biomarker profiles, contributing to our understanding of immune evasion, tumor immune escape, and potential therapeutic targets.

3.   Immune correlation analysis identifies immune-related biomarkers that have predictive or prognostic value in cancer. By assessing the correlation between immune components and clinical outcomes, such as patient survival, treatment response, or disease recurrence, immune-related biomarkers can be identified that aid in patient stratification, treatment decision-making, and prognosis estimation.

With the help of TIMER database, we estimated CP's relationship with the immune cell infiltration levels (T. Li et al., 2017). Finally, the correlation of CP with the immune checkpoints was established using UALCAN.

1.4.6. Survival Analysis

c-Biopotal, Prognoscan, UALCAN and Kaplan Meier plotter databases were exploited for the correlation of CP expression with the survival probability of patients(Modi et al., 2022).

The main objective of survival analysis is to assess the likelihood of an event taking place over a given period and to identify factors that could impact the timing of the event. The Kaplan-Meier estimator is a statistical technique that is used to estimate the survival function based on observed survival times, without making assumptions about the underlying distribution of the data. It provides a stepwise estimation of survival probabilities over time and allows for the comparison of survival curves between different groups or treatment arms. Survival analysis is valuable for understanding the time-to-event outcomes in various research settings. It provides insights into prognosis, treatment efficacy, and the impact of risk factors on patient outcomes. By incorporating time-dependent information, survival analysis enables researchers and clinicians to make informed decisions in clinical practice and improve patient care.

1.4.7. miRNA Analysis

In our study, we accessed Head and Neck cancer data from the TCGA-HNSC project with the accession ID phs000178. The dataset included gene expression and miRNA expression quantification data obtained from 524 patients. We downloaded a total of 569 miRNA sequencing

files, along with 48 normal sample files, from the GDC portal using the GDC client. A workflow of miRNA analysis is shown in Figure 9.

To investigate differential miRNA expression, we employed the DESeq2 Bioconductor package in R. This package allowed us to analyze the miRNA counts data and identify differentially expressed miRNAs. We generated a volcano plot that revealed 180 upregulated and 114 downregulated miRNAs.

To further explore the miRNA expression patterns across different stages of Head and Neck cancer, we utilized the clinical data for the case patients. We selected the top 40 upregulated and top 40 downregulated miRNAs based on their significant P values (<0.000005) and fold change (>2).This analysis enabled us to identify miRNAs that exhibited significant differential expression in the different stages of HNC. The selected miRNAs serve as potential candidates for further investigation and may contribute to our understanding of the molecular mechanisms underlying oral cancer.

mirBase was used to get information published miRNA sequences and annotations(Kozomara et al., 2019). mirTarbase was used to obtain experimentally validated targets of miRNA while mirDB was used for target prediction (H. Y. Huang et al., 2022). We employed **miRWalk** to identify targets with their predicted binding sites(Sticht et al., 2018). We filtered the targets for the miRNA network from **mirDB, mirTarbase and TargetScan**.

MiEAA was used for conversion of miRNA to their miRBase ID as well conversion of precursors to their respective miRNA forms. MiEAA was also used for gene enrichment of the miRNA targets(Backes et al., 2016).

Cytoscape was used for network analysis for miRNA targets**. MirNet, miRViz** were used for confirmation of the network visualization. The differentially expressed miRNA used for the network were selected on the basis of significance (FC and p value) using ONCO.IO database.
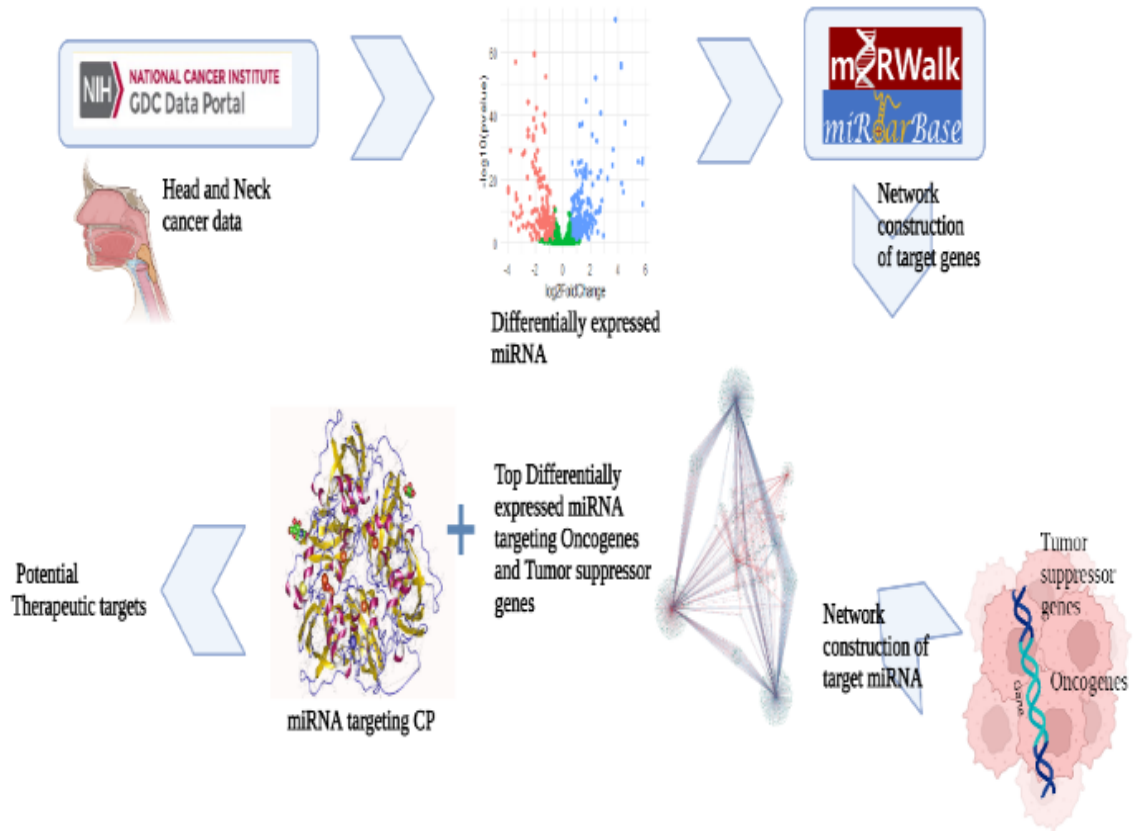
Figure 9. A workflow of Head and Neck Cancer Dataset miRNA expression analysis. The differentially expressed miRNA can we used to identify the epigenetic control of oncogenes and tumor suppressor genes in diseased state.

ii) Identification of potential inhibitor(s) for ceruloplasmin using in silico virtual screening approaches

1.4.8.   Protein Source: The Protein Data Bank (PDB)

PDB is a database that provides three-dimensional structural information of biological macromolecules, including proteins, nucleic acids, and complex assemblies. It is a valuable resource for researchers in structural biology, bioinformatics, and drug discovery. Here are some key features of the PDB:

Structural Data: The PDB contains experimentally determined atomic coordinates and other related information for a vast number of bio molecular structures. These structures are determined using techniques such as X-ray crystallography, NMR spectroscopy, and cryo-electron microscopy.

Protein Structures: The PDB offers a comprehensive collection of protein structures, ranging from enzymes and receptors to antibodies and protein complexes. Each protein structure is assigned a unique PDB ID, which allows for easy identification and retrieval. In addition to proteins, the PDB includes structures of DNA, RNA, and their complexes with other molecules. This facilitates the study of nucleic acid-protein interactions, transcription, translation, and other essential biological processes.

It also provides information about ligand binding sites within protein structures, allowing researchers to explore the interactions between small molecules (ligands) and proteins. This information is crucial for understanding drug-target interactions and designing novel therapeutics.

The PDB integrates structural data with other relevant information, such as functional annotations, sequence data, and experimental details. This integration enhances the value of the database and supports a more comprehensive analysis of the structures.

We accessed the PDB through its website (www.rcsb.org) and obtained CP protein structure .Out of the 4 available crystal structures of CP we chose 4ENZ as it was with the lowest resolution 2.6 Å (Figure 10) which is better than the other available structures. Also, in this study we hope to target CP interaction with MPO. A previous study by Samygina et al. (2013a) reported on the contact residues in the complex formed between MPO and CP. The study compared the structure of free CP (PDB ID: 4EZN, resolution of 2.6 Å) with CP bound to MPO (PDB ID: 4EJX, resolution of 4.69

Å). The complex structure identified interactions with seven unique ligands attached to CP: 2-acetamido-2-deoxy-beta-D-glucopyranose (NAG), Glycerol (GOL), Copper(II) ion, Calcium and sodium ions, Oxygen molecule, and a number of oxygen atoms(Samygina et al., 2013a). To facilitate docking studies, it is crucial to remove the ligands and preprocess the CP structure.
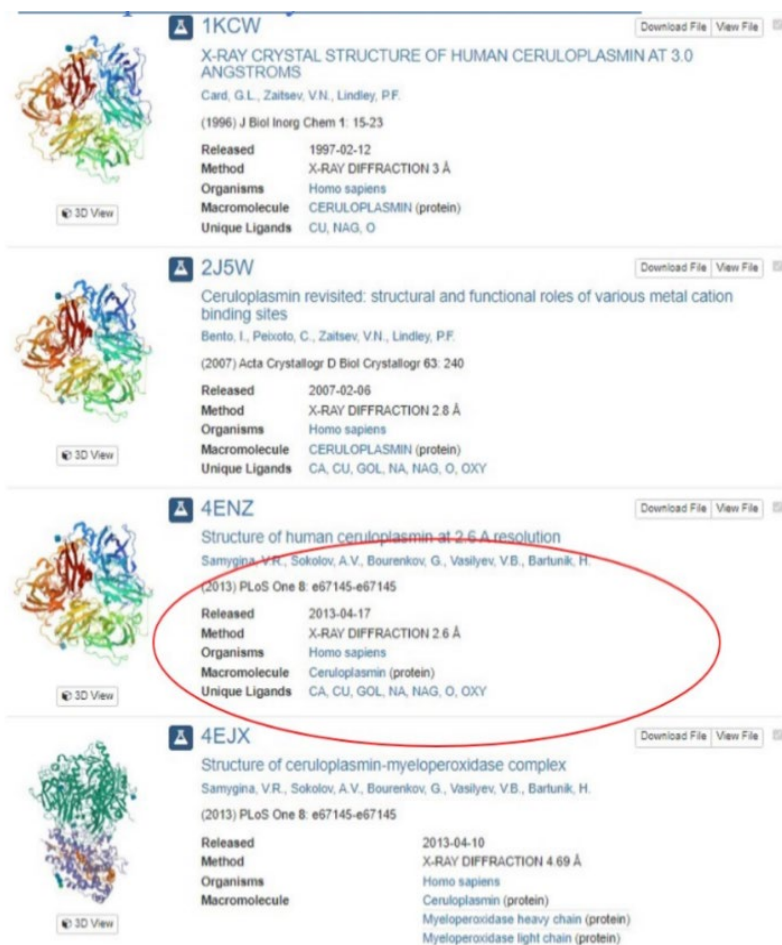
Figure 10: Structure acquisition from PDB. There are four distinct crystallographic structures of CP stored in the Protein Data Bank (PDB) out of which the one with best resolution is chosen for the study.

1.4.9. Receptor preparation

Receptor preparation is a crucial step in docking studies to ensure the accurate and reliable modeling of ligand-receptor interactions. The receptor preparation process involves:

1.   Structure Retrieval: The receptor structure is obtained from a suitable source, such as the Protein Data Bank (PDB) or other experimental or theoretical methods.

2.   Removal of Water Molecules and Heteroatoms: Water molecules, metal ions, co-factors, and other nonessential entities present in the receptor structure are removed. However, essential ions or ligands required for proper receptor function may be retained.

3.   Addition of Missing Atoms and Residues: Missing atoms or residues in the receptor structure are added to complete the protein structure. This step can involve homology modeling or comparative modeling techniques using known structures as templates.

4.   Removal of Conflicting or Erroneous Structures: Any conflicting or erroneous structures, such as alternate conformations, redundant chains, or disordered regions, are resolved or removed to simplify the receptor structure.

5.   Protonation and Ionization State Assignment: The protonation and ionization states of titratable residues (e.g., histidine) are assigned based on the desired pH conditions. Tools like PROPKA or PDB2PQR can assist in predicting these states.

6.   Energy Minimization: The receptor structure is subjected to energy minimization using molecular mechanics force fields to optimize its conformation and eliminate steric clashes.

7.   Generation of Grid Box: A grid box is defined around the active site or target region where the ligand is expected to bind. The size and dimensions of the grid box depend on the specific docking software and the target site of interest.

8.   Selection of Binding Site and Constraints: If the binding site is known or specified, the receptor can be prepared to focus on that specific region. Constraints can be applied to maintain the conformation of essential residues involved in ligand binding.

9.   Output Format: The prepared receptor structure is typically saved in a suitable file format, such as PDB or PDBQT, for compatibility with docking software.

Receptor preparation can be performed using various software tools, such as Schrodinger's Protein Preparation Wizard, AutoDockTools, or PyMOL, among others. These tools automate many of the steps mentioned above and ensure that the receptor structure is properly prepared and optimized for accurate docking simulations.

1.4.9.1.   Structure Editing:

The structure available at PDB have to be processed before use for docking. Any missing residues need to be added as well as any ligands available on them need to be removed to make all the sites available for docking(Figure 11).

1) We compared all the structures available on PDB and found that the amino acids in all structure sequences aligned so the binding site specified for any structure would be valid for the other.

2) We obtained the FASTA sequence of CP and compared it with the sequence of our structure to obtain the missing residues using EMBOSS NEEDLE of EMBL-EBI which works on pairwise alignment (Hollingsworth & Karplus, 2010).

 3) After obtaining the missing residues we built them into the 4ENZ structure using Pymol Builder. We also removed the 2 NAG (2-acetamido 2deoxy-beta-D-glucopyranose) and GOL (glycerol molecules) from the structure.
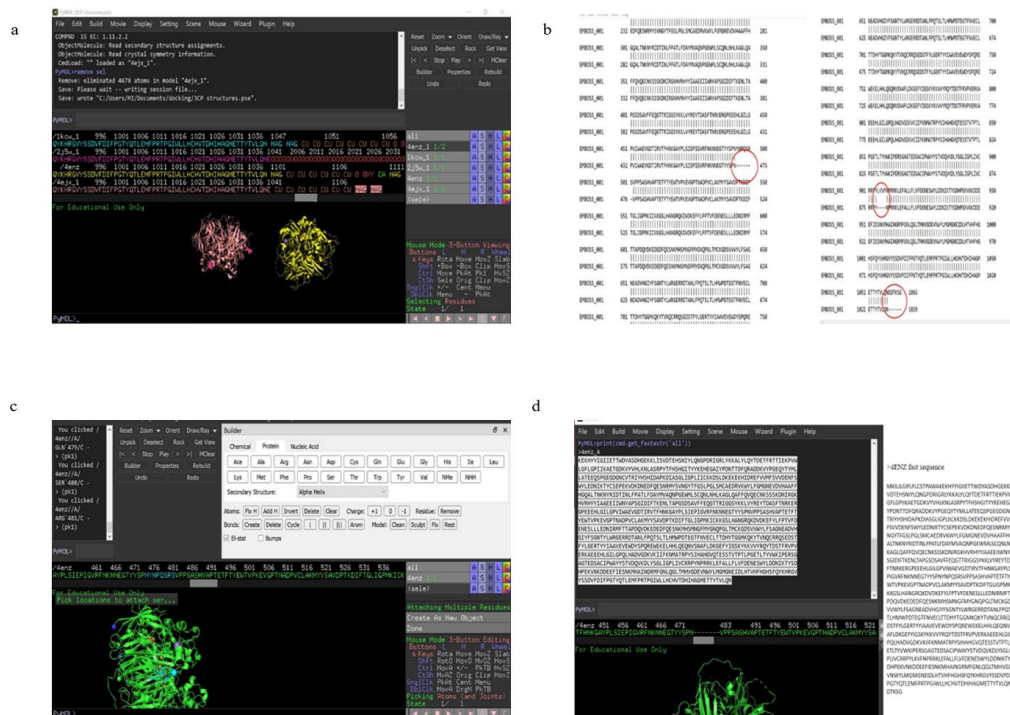
Figure 11. Steps involved in Protein preparation*. This involved identification of missing residues using EMBOSS NEEDLE followed by filling the gaps in the amino acid sequence of the available structure and building the new ceruloplasmin structure using PYMOL Builder**.*

The edited protein structure was subjected to addition of hydrogen bonds and charges in Avogadro. This was followed by energy minimization by running 5000 steps at Steepest Descent was done using Autodock Tool 4 (ADT). This was followed by conversion of the protein structure to pdbqt(Eberhardt et al., 2021).

1.4.9.2.   *Structure validation:*

The Ramachandran plot is a widely used tool in structural biology to assess the quality and validity of protein structures. It analyzes the distribution of backbone dihedral angles (Phi, ϕ, and Psi, Ψ) of amino acid residues in a protein structure.

The Phi angle refers to the rotation around the Cα-C bond, while the Psi angle represents the rotation around the C-Cα bond. These angles determine the conformation of the peptide bond and the overall shape of the protein backbone. In a Ramachandran plot, X-axis denotes the Phi angle, and the Psi angle is plotted on the Y-axis. Each point on the plot represents an individual residue in the protein structure, and the point's density in different regions of the plot reflects the prevalence of certain dihedral angle combinations.

The plot is divided into regions based on the allowed and disallowed conformations of the peptide bond. The most common regions are the "allowed" regions, where the backbone dihedral angles are energetically favorable and structurally feasible. These regions correspond to stable secondary structures, such as alpha helices and beta sheets.

We assessed the quality of the protein structure by analyzing the distribution of residues in the Ramachandran plot. A high percentage of residues falling within the allowed regions indicates a well-folded and reliable structure. On the other hand, residues in disallowed regions suggest structural irregularities or inaccuracies such as steric clashes, incorrect backbone geometry, or structural errors in the model. .

Subsequently, we validated the edited 3D structure of CP using PROCHECK and the server https://swift.cmbi.umcn.nl/servers/html/ramaplot.html. We validated our structure for the structural quality by obtaining the Ramachandran plot which analyzed the structures Phi (ϕ) versus Psi (Ψ) angle residue distribution(Hollingsworth & Karplus, 2010).

1.4.9.3.   Binding Site Identification:

The previously conducted X-ray diffraction studies of purified human CP yielded the structures 4ENZ and 4EJX. These studies revealed that CP affects the enzymatic activity of myeloperoxidase (MPO) through intermolecular contacts between the 5th and 6th domains of CP (amino acid residues 885 to 892). Additionally, residues belonging to the domain 4 (amino acid residues 511, 542-557) were found to interact with MPO. The amino acid residues 699–710 of the extended loop of CP were observed to interact with the 1–27 N-terminal residues of the light chain of MPO(Samygina et al., 2013b)(B. P. Mukhopadhyay, 2019). Furthermore, residues M668, W669, and H667 near the p-PD site of CP in domain 4 were identified as being involved in the contact. By visualizing the CP-MPO complex in PyMOL, we identified the interacting residues at the contact site as specified in the mentioned study(Figure 12).
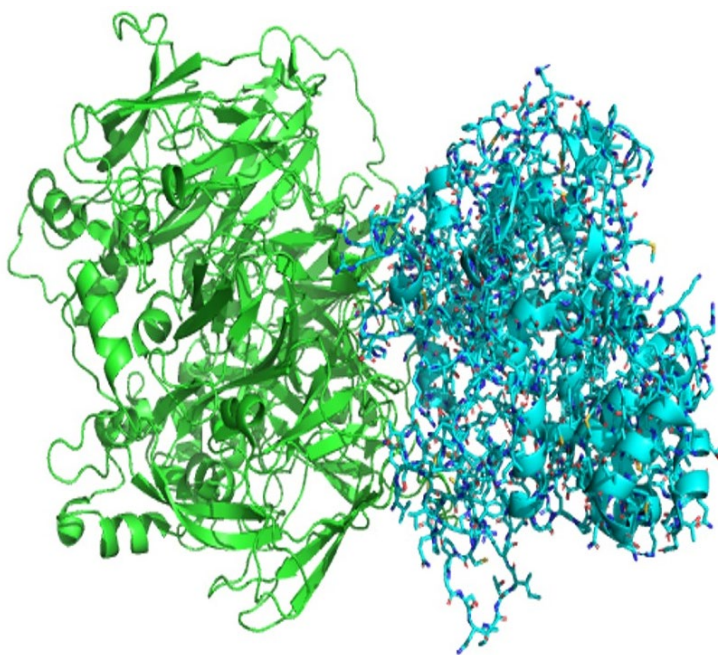
Figure 12. Ceruloplasmin involved in contact with myeloperoxidase *(Samygina et al., 2013c) (green: ceruloplasmin, Blue : myeloperoxidase)*

We visualized the CP-MPO complex on Pymol and identified the interacting residues at the contact site according to those specified in the mentioned study.

1.4.9.4. *Grid box*

Grid box generation is a crucial step in molecular docking studies as it determines the search space within the receptor where the ligand will be docked. The grid box defines the region where the docking algorithm explores different orientations and conformations of the ligand to find the optimal binding pose. To generate the grid box, the binding pocket of the receptor as identified above is used. The dimensions of the grid box are defined to encompass the active site while minimizing the search space for computational efficiency. The grid box is centered on key residues within the interacting site, and its size is adjusted to include solvent molecules/ions contributing to ligand binding. The grid spacing, or resolution, determines the density of grid points within the box. The generated grid box coordinates are saved in a suitable format for the docking software being used. Proper grid box generation is essential for accurate and reliable docking results, as it influences the exploration of ligand binding interactions within the receptor.

1.4.10. Ligand Source:

In our study we focused on phytochemicals and marine compounds as our choice of ligands for molecular docking studies. We obtained these from the following databases.

1.4.10.1. *IMPPAT 2.0*

IMPPAT 2.0 is a specific database that focuses on Indian medicinal plants, phytochemistry, and therapeutics. It is an upgraded version of the IMPPAT database, providing a more comprehensive and updated resource for researchers interested in Indian medicinal plants and their applications. IMPPAT 2.0 integrates information on the phytochemical composition of Indian medicinal plants, their pharmacological activities, and therapeutic applications. The database includes data on the chemical constituents of plants, such as alkaloids, flavonoids, terpenoids, and phenolic compounds. It also provides information on the traditional uses of these plants in various systems of traditional medicine, such as Ayurveda, Siddha, and Unani(Mohanraj et al., 2018).

1.4.10.2.　　TIPdb

TIPdb is a database that has been constructed to compile information on phytochemicals derived from indigenous plants in Taiwan with potential anticancer, antiplatelet, and antituberculosis activities. The database follows a standardized format and includes data extracted from published sources. Its purpose is to provide researchers with a consolidated resource of these bioactive compounds found in Taiwan's indigenous plant species. TIPdb aims to facilitate the exploration and utilization of these phytochemicals for various applications in cancer, platelet-related disorders, and tuberculosis research(Lin et al., 2013).

1.4.10.3.　　CMNPD

CMNPD (Comprehensive Marine Natural Products Database) is a specialized database of marine natural products that can be used for drug discovery. It compiles information on the biological activities along with the chemical structures, and sources of bioactive compounds derived from marine organisms. CMNPD serves as a centralized resource for researchers to explore the potential of marine-based drug discovery(Lyu et al., 2021).

We used phytochemicals as well as marine drugs for docking screening. Phytochemicals were downloaded from IMPPAT i.e., Indian Medicinal Plants, Phytochemistry and Therapeutics database and TIPdb for anticancer phytochemicals. The ligand preparation product, Ligprep, from Schrodinger was utilized to generate high-quality, three-dimensional (3D) structures of the ligands. Marine natural products 3D structures were downloaded from CMNPD database. A signature library was prepared with 26717 marine compounds as well as 17000 phytochemicals.

1.4.11. Preparation of Ligand:

The preparation of ligands for docking studies involves several steps to ensure their suitability and accuracy in the docking process. Ligand preparation can be performed using various software tools such as Schrodinger's Ligprep, Open Babel, RDKit, or AutoDockTools. These tools

provide automated workflows to handle most of the steps mentioned above, allowing for efficient and accurate preparation of ligands for docking studies.

After obtaining the 3D SDF structures of phytochemicals and marine compounds, the structures were first minimized using Avogadro (Hanwell et al., 2012). Subsequently, they were converted to pdbqt format, which is suitable for docking studies using Open Babel software(O'Boyle et al., 2011). To ensure high-quality, 3D structures of the ligands, the Schrodinger ligand preparation product, specifically the Ligprep module of Maestro from the Schrodinger suite (LLC, New York, NY, 2020-1), was employed. During this process, the OPLS 2004 force field was utilized for optimization and the generation of low-energy isomers of the ligands. Finally, all ligand molecules were docked using the same settings with the receptor.

Schrodinger's Ligprep is a software tool commonly used for the preparation of ligands in the context of molecular docking studies. Ligprep is a module within the Schrodinger suite, a comprehensive suite of computational chemistry software(I. J. Chen & Foloppe, 2010). Ligprep performs a series of operations to generate high-quality, 3D structures of ligands suitable for docking simulations. Some key features and functionalities of Ligprep include:

1. File Format Conversion: Ligprep supports various input file formats, such as SDF, MOL, SMILES, and PDB, allowing for flexibility in the choice of ligand representation.

2. Structure Optimization: Ligprep employs the OPLS 2004 force field to perform energy minimization and geometry optimization of the ligand structures. This helps to correct structural issues, eliminate clashes, and generate low-energy conformations.

3. Tautomeric and Stereoisomeric Handling: Ligprep considers different tautomeric and stereoisomeric forms of the ligands. It can generate all possible tautomers and stereoisomers or focus on specific states based on user-defined preferences.

4. Ionization and Protonation State Assignment: Ligprep assigns appropriate ionization and protonation states to the ligands based on the desired pH conditions. It utilizes pKa prediction algorithms to determine the likely protonation states.

5. 3D Coordinate Generation: Ligprep generates or refines the ligand's 3D coordinates by assigning bond angles and lengths, and dihedral angles to ensure a realistic and accurate representation.

6. Epitope-based Ligand Preparation: Ligprep also offers options for preparing ligands that bind to specific protein binding sites or epitopes. It allows the user to specify the binding site and adjust the ligand conformation accordingly.

7. Output Format: Ligprep provides the ligand structures in various output formats, including PDBQT, which is widely used in docking software.

By performing these operations, with the help of Schrodinger's Ligprep the ligands were prepared with improved accuracy, reliability, and compatibility for subsequent docking studies.

1.4.12. Screening of compounds:

The molecular screening of phytochemicals and marine compounds against CP involved the use of Schrodinger Glide's virtual screening workflow (VSW). In this workflow, the protein receptor was kept rigid while docking, allowing flexibility for the ligands. To facilitate the docking process, we generated a receptor grid at the site of contact between CP and MPO using Glide's Receptor grid generating panel(Friesner et al., 2004a).

After docking, the ligand poses are scored based on their predicted binding affinity and interactions with the receptor. The docking results were analyzed, and ligands with a positional root-mean-square deviation (RMSD) of less than 1.0 Å were selected. These ligands were further filtered based on favorable binding interactions. Various scoring functions are available in Glide, such as GlideScore and Prime MM-GBSA, to evaluate the ligand-receptor interactions and estimate binding energies. The binding energies of the ligands were assessed, and ligands with the most negative binding energies were considered to have the highest binding affinity or binding score, indicating a strong potential for binding to CP.

1.4.13. Analysis and visualization:

The docking results are further analyzed to identify ligands with the most favorable binding poses and interactions. This analysis d examining hydrogen bonding, hydrophobic interactions, and other key factors influencing ligand binding.

1.4.13.1.   QikProp

To ensure drug-like properties, the screened compounds were subjected to further filtering using QikProp, which generated Lipinski's rule of five parameters. This step helped eliminate compounds that violated the rule of five, which defines specific physicochemical properties important for drug-likeness.

QikProp is a software tool developed by Schrödinger that is commonly used to predict various drug-like properties of small organic molecules. It employs a range of computational algorithms and models to estimate important molecular properties and assess the likelihood of a compound having favorable pharmacokinetic and physicochemical characteristics. When using QikProp for compound filtering, several key drug-like properties are typically evaluated. These properties include:

Lipophilicity (LogP): QikProp estimates the octanol-water partition coefficient (LogP) of a compound, which is an indicator of its hydrophobicity. It provides insight into the compound's ability to cross biological membranes and influences factors such as absorption and distribution.

Solubility: QikProp predicts the aqueous solubility of a compound, which is a crucial property for its formulation and bioavailability. Poorly soluble compounds may face challenges in achieving adequate drug concentrations in the body.

Molecular weight: QikProp calculates the molecular weight of a compound. High mol. weight can be a concern due to potential difficulties in absorption, distribution, metabolism, and excretion (ADME).

Number of hydrogen bond donors and acceptors: These properties are important for assessing a compound's ability to form interactions with target molecules. The hydrogen bond donors and acceptors impact the binding affinity and potential for favorable interactions with biological targets.

Topological polar surface area (TPSA): QikProp estimates the TPSA, which provides information on the size and polarity of the compound's surface area. TPSA influences factors such as membrane permeability and can be used as an indicator of a compound's ability to cross biological barriers.

By applying QikProp to screened compounds, we assessed the likelihood of the drug-likeness of the selected ligands based on these properties. Filtering compounds based on favorable values of these properties prioritized molecules with higher potential for further development, thereby reducing the time and resources spent on compounds with undesirable characteristics. QikProp predictions are computational estimates that need further validation through experimental studies.

Pymol and Discovery Studio were employed to visually analyze the docking results by identifying the amino acids of the ligand interacting at the site on CP (Yuan et al., 2017).

1.4.13.2.   Pymol

PyMOL is primarily a molecular visualization software that specializes in rendering and analyzing three-dimensional structures of biomolecules. It provides a user-friendly interface and a wide range of visualization options to represent proteins, nucleic acids, and other macromolecules. PyMOL is highly customizable, allowing users to tailor the appearance and style of molecular representations to suit their needs. It also offers scripting capabilities, which enables users to automate tasks and perform advanced analyses(Yuan et al., 2017).

1.4.13.3.   Discovery studio

Discovery Studio is a comprehensive suite of tools designed for molecular modeling and simulation in drug discovery. It offers a broader range of functionalities compared to PyMOL, including Molecular Dynamics Simulations, Structure-based and Ligand-based Drug Design, and ADMET Prediction (Absorption, Distribution, Metabolism, Excretion, and Toxicity)(Pawar & Rohane, 2021).

In order to assess how the selected ligands will be processed by a living organism, the top 10 hits were subjected to ADME analysis using Swiss-ADME. The ADME properties of the selected compounds were evaluated according to Lipinski's rule of five, which considers factors such as pharmacokinetic properties, drug solubility, and drug likeness(Han et al., 2019).

iii) Evaluation of selected inhibitor(s) using Molecular Dynamics Simulation

1.4.14 Molecular Dynamics Simulation:

The protein CP and its three best ligand complexes wrre subjected to molecular dynamics (MD) simulations using the Desmond module within the Schrödinger suite, specifically in the Maestro environment(Ivanova et al., 2018). The ligands were chosen based on ADME analysis, XP docking, and binding interactions. The ligands, along with the protein, were prepared in the Prime module of the Schrödinger suite to rectify any inaccuracies in charge states, bond orders, missing hydrogen atoms, and side chains. A restrained energy minimization procedure was performed to alleviate strained bonds/angles and steric clashes, allowing the heavy atoms to move by a maximum of 0.3 Å (Ivanova et al., 2018).

To mimic physiological conditions, the protein-ligand complex systems were solvated in a solution containing 0.15 M NaCl and modeled using the TIP3P water model. To maintain the system's overall neutrality, counter ions (Cl- or Na+) were added to balance the net charge. Extensive MD simulations of 200 ns were carried out using the Desmond software to assess the stability of the ligand binding within the CP complex. The simulations were conducted at a temperature of 300 K, standard pressure (1.01325 bar), within an orthorhombic box of dimensions $10 \times 10 \times 10$ Å³, and using the NPT ensemble.To maintain the desired temperature, the Martyna-Tobias-Klein dynamic algorithm was employed, while the pressure was controlled by the Nose-Hoover chain method.

CHAPTER 2

LITERATURE REVIEW

CHAPTER 2.1. ORAL CANCER

2.1.1. Anatomy of the Oral cavity

The circumvallate papillae of the tongue on the inferior side, the vermilion border of the lips, and the hard-soft palate junction on the superior side all serve as boundaries for the oral cavity. The lip, the floor of the mouth, the buccal mucosa, the lower and upper gingiva or gum, the oral tongue, the retromolar trigone, and the hard palate are some of the anatomical subsite divisions of the oral cavity(Figure 13). Despite being close by, these sub sites have unique anatomical traits that must be considered when designing oncologic therapy. The overall lip cancer prevalence has been reported to be 1–2% , accounting for about 23.6–30% of all oral cancers(Alhabbab & Johar, 2022).
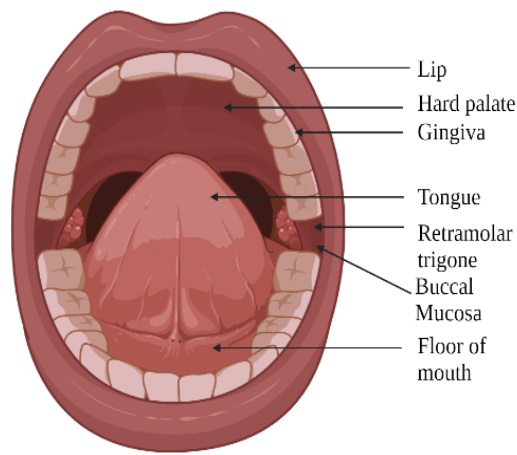
Figure 13:Anatomy of the oral cavity. The oral cavity includes lip, the floor of the mouth, the buccal mucosa, the lower and upper gingiva or gum, the oral tongue, the retromolar trigone, and the hard palate.

Hard palate cancer is a mostly squamous cell carcinoma and is not a very common representing approximately 1–3.5% of oral cavity cancers. HNC accounts for about 54,000 cases diagnosed each year worldwide (Hammouda et al., 2021). Tongue cancer when identified early, is highly curable, but it can be a serious, life-threatening form of oral cancer if not promptly diagnose and treated. However, the occurrence of tongue cancer is relatively rare(*Tongue Cancer — Cancer Stat Facts*, n.d.). 28 to 35 percent of all mouth cancers are malignancies of the mouth's floor. Men are three to four times as likely as women to get cancer of the mouth's floor. The most important

risk factors for floor of mouth malignancies are alcohol and tobacco use. Floor of the mouth cancers are also highly curable when diagnosed early(*Oral Cancer - India Against Cancer*, n.d.).

2.1.2. Oral cancer Epidemiology and Etiology

According to the Global Cancer Observatory (GLOBOCAN) the oral cavity and pharynx is one of the top most sites with highest cancer burden in both sexes accounting for 1,98,438 cases from India(Sathishkumar et al., 2023). In most ethnic groups, oral cancer affects men three times more frequently than women, according to studies. The oral cavity and pharynx cancers together rank sixth among all cancers worldwide in terms of prevalence(Warnakulasuriya, 2009). According to the most recent study from the IARC, there are more than 300.000 diagnosed cases of oral cancer worldwide, and there are roughly 145,000 fatalities each year(Rivera, 2015). The South-East Asia and Europe regions of the World Health Organization (WHO) have the highest incidence and fatality rates for oral cancer, respectively. Furthermore, a relatively high prevalence of oral cancer has also been found in India. The crude rate and age-standardized incidence rates (global) are greater in more developed regions, but mortality is higher in the less developed regions, showing socioeconomic inequality. Age of oral cancer initiation, location of the disease, etiology, and molecular biology also vary across the developing and developed worlds. Poverty, illiteracy, older ages at presentation, lack of access to health care, and inadequate treatment infrastructure are significant barriers to managing cancer. 90% of oral cancer patients in rural areas belong to lower or lower-middle socioeconomic classes, and 3.6% of them live below the poverty line, according to a review of the incidences of different cancers conducted by the Indian Council for Medical Research (ICMR) for the Cancer Atlas project.

Tobacco contains many carcinogenic molecules and is one of the top causes of oral cancer. The risk of developing squamous cell oral cancer is directly proportional to the amount of tobacco consumption over the years(Spitz et al., 1988). After tobacco cessation, this risk maybe reduced by 30% in the first 9 years and 50% for those over 9 however it does not fully abate(Macfarlane et al., 1995)(Samet, 1992). Alcohol is linked to higher oral cancer risks in nonsmokers and has a synergistic effect in the oral and oropharyngeal cancer etiology in tobacco users(Brugere et al., 1986). Other suggested causative variables include poor dental hygiene, exposure to wood dust, nutritional inadequacies, eating of red meat, and salted meat consumption(De Stefani et al., 2012).

Oral cancer has been associated with herpes simplex virus (HSV), but the virus has not been definitively implicated(Larsson et al., 1991). Head and neck cancer occurrence is increased by host variables such AIDS patients with HIV infection and transplant patients' weakened immune systems. Ataxia telangiectasia, fanconi anemia, and xeroderma pigmentosum are examples of genetic disorders that have been reported to be associated with an elevated incidence(Kutler et al., 2003)(A. T. Shah et al., 2013)(Ficarra & Eversole, 1994). Human papillomavirus (HPV) has emerged as a significant factor in the epidemiology of oral cancer. While tobacco and alcohol use have traditionally been linked to oral cancer, the prevalence of HPV-associated oral cancers is on the rise. HPV, especially high-risk strains like HPV-16, has been identified as the leading cause of a subset of oral cancers, particularly in the oropharynx. This shift underscores the changing landscape of oral cancer etiology, with HPV playing an increasingly prominent role(Lechner et al., 2022).

The incidence of oral cancer is higher among men, and it usually develops after the fifth decade. It is important to monitor patients post-therapy and alter their lifestyles in order to prevent secondary chronogenic tumors, which develop in 10% to 40% of patients after primary treatment.

2.1.3. Symptoms of Oral Cancer

Mouth cancer may be indicated by various signs and symptoms(Scully & Porter, 2001)including a sore in the mouth or on the lip that doesn't heal, red or white patch on the inside of the mouth, painful or loose teeth, lump or growth inside the mouth, pain in the mouth or ear and difficulty or pain while swallowing. Other possible signs and symptoms may include: Thickening or lump in the cheek, sore throat or feeling that something is stuck in the throat, difficulty moving the jaw or tongue, numbness in the tongue or other areas of the mouth, swelling of the jaw, changes in voice, lump in the neck, weight loss and persistent bad breath.

2.1.4. Pathophysiology of Oral cancer

Squamous cell carcinomas, which have a range of histologic grades, are the most common types of cancer of the head and neck(Johnson et al., 2020). Well-differentiated malignancies have tumor cells that closely resemble healthy squamous epithelium, whereas poorly differentiated cancers are more challenging to identify as coming from squamous epithelium(Figure 14)(Jögi et al., 2012). A small percentage of head and neck cancers are salivary gland tumors, the majority of which are adenocarcinomas. Both squamous and salivary gland carcinomas spread by the lymphatic pathway, which drains into the local lymph nodes, and by direct contiguity(Vogel et al., 2010).

.
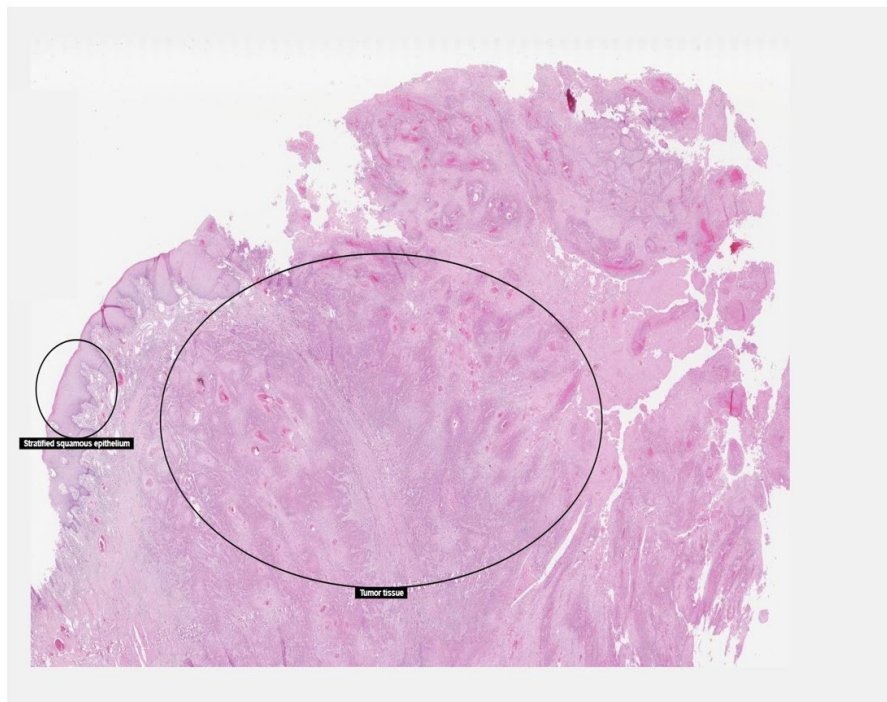
Figure 14: Section of a moderately differentiated oral squamous cell carcinoma, stained with hematoxylin and eosin for contrast. The stain can be observed to be taken up differently by the tumor tissue that has been differentiated. This figure was generated using the Human protein atlas.

The pathophysiology of oral cancer involves a complex interplay between genetic, environmental, and lifestyle factors, leading to normal cells getting transformed into cancer cells.

The pathogenesis of oral cancer is thought to start with genetic mutations in the cells of the oral cavity, which can be triggered by various factors, such as exposure to tobacco, alcohol, human papillomavirus (HPV), and chronic inflammation(X. Jiang et al., 2019). These mutations can affect the genes that regulate cell growth, division, and death, leading to uncontrolled cell proliferation and the formation of a tumor.

Oral cancer cells also exhibit altered metabolism compared to normal cells. Even when oxygen is present, they preferentially use glycolysis, which is known as the Warburg effect(Liberti & Locasale, 2016). This metabolic alteration grants cancer cells a growth edge by promoting the production of energy and biosynthetic precursors required for rapid cell proliferation(Liberti & Locasale, 2016)(Crabtree, 1929). In addition to these molecular changes, oral cancer is associated with various pathophysiological changes in the affected tissues. For example, oral cancer can cause local tissue invasion and destruction, leading to pain, difficulty swallowing, and speech impairment. It can also metastasize to other body parts, such as the lymph nodes, lungs, and liver, leading to systemic symptoms and complications (Rivera & Venegas, 2014). Furthermore, oral cancer can disrupt the normal immune response, leading to immune evasion and immune suppression(Horton et al., 2019). Cancer cells can evade immune surveillance by down regulating the expression of surface antigens and up regulating immune checkpoint molecules, such as PD-L1, which can inhibit the functioning of T cells along with rest of the immune cells[79]. Moreover, cancer cells can induce immune suppression by recruiting T regulatory cells and myeloid-derived suppressor cells to the tumor microenvironment(Y. Yang et al., 2020).

In summary, the pathophysiology of oral cancer involves complex molecular, cellular, and physiological changes that result in uncontrolled cell proliferation, metabolic reprogramming, tissue invasion, metastasis, and immune evasion. Understanding these mechanisms can help Formulate novel approaches for the prevention, diagnosis, and oral cancer treatment.

2.1.5. Oral cancer Metabolism

Oral cancer is characterized by several metabolic alterations that are critical for tumor growth and survival. These metabolic alterations can serve as potential biomarkers for oral cancer diagnosis as well as prognosis. Below, we discuss the key metabolic alterations that can be used for biomarker estimation in oral cancer.

2.1.5.1. Increased Glucose Uptake and Altered Glycolysis

Oral cancer cells exhibit increased glucose uptake and altered glycolysis, which allows them to generate energy even in the absence of oxygen. The increased glucose uptake is accompanied by upregulation of glucose transporters, such as GLUT1, and altered glycolysis, which results in increased lactate production(Zambrano et al., 2019). In cancer cells, there is a reduction in mitochondrial oxidative phosphorylation despite the presence of oxygen, resulting in decreased reliance on the TCA (tricarboxylic acid cycle) and ETC (electron transport chain) for ATP production(Luo et al., 2020). The PPP, an alternative branch of glucose metabolism, is often upregulated in cancer cells(Anastasiou et al., 2011)(Figure 15). It generates nucleotides, NADPH, and ribose-5-phosphate for DNA synthesis and antioxidant defense. This metabolic shift called Warburg effect is a hallmark of oral cancer cells and provides several advantages to cancer cells, including increased ATP production, production of metabolic intermediates for biosynthesis, and maintenance of redox balance(Heiden et al., 2009). The altered glucose metabolism in cancer cells is driven by various factors, including oncogenic signaling pathways, hypoxia-inducible factors (HIFs), and mutations in key metabolic enzymes(Marbaniang & Kma, 2018). The increased glucose uptake and altered glycolysis can be measured using metabolic imaging techniques, such as positron emission tomography (PET), which can aid in oral cancer diagnosis and staging(Walker-Samuel et al., 2013).

2.1.5.2. Alterations in Lipid Metabolism:

Oral cancer cells may alter their lipid metabolism, including the uptake, synthesis, and breakdown of lipids. These alterations can make a significant contribution to the energy needs of cancer cells and also promote tumor growth and survival. Several lipid metabolites, such as phospholipids, sphingolipids, and triglycerides, show alterations in oral cancer cells, and their levels can serve as potential biomarkers for oral cancer (Fu et al., 2021). Recent research reveals that medication resistance and altered lipid metabolism are closely connected in tumors(R. Yang et al., 2022).Some key mechanisms involved in the alterations of lipid metabolism in cancer cells are as follows:

Increased de novo lipogenesis: Cancer cells often show an upregulation of de novo lipogenesis, the process of synthesizing fatty acids from non-lipid precursors such as glucose and

amino acids. This is driven by the activation of key enzymes, including ACC (Acetyl-CoA carboxylase), FASN (fatty acid synthase), and SREBP (sterol regulatory element-binding protein) transcription factors. Enhanced de novo lipogenesis provides cancer cells with a source of fatty acids for energy production, membrane synthesis, and signaling molecule production(Koundouros & Poulogiannis, 2019).
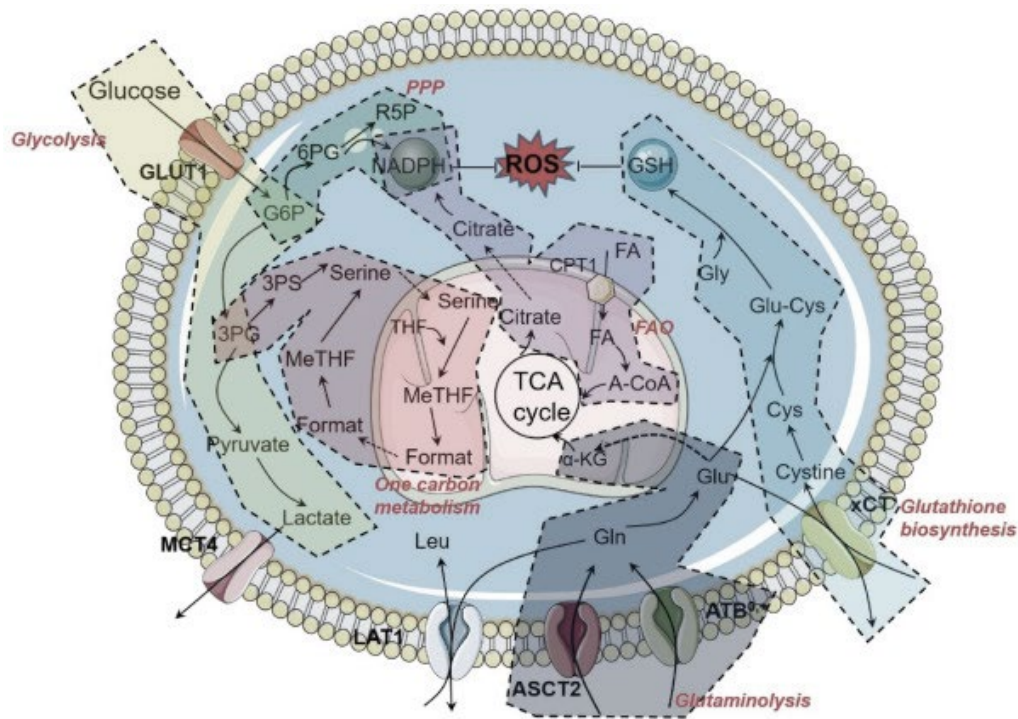
Figure 15. Alterations in the cancer cells' metabolic processes. This figure shows the precise metabolic processes that contribute to redox equilibrium, such as GSH production, fatty acid oxidation (FAO), pentose phosphate pathway (PPP), glutaminolysis, and one-carbon metabolism. (Abbreviations: α-KG, alpha ketoglutarate; 3PG, 3-phosphoglycetare; R5P, ribulose-5-phosphate; G6P, glucose-6-phosphate; 3PS, 3-phospho-serine; THF, tetrahydrofolate; MeTHF, 5,10-methylene-tetrahydrofolate; 6PG, 6-phosphoglucono-1,5-lactone; FA, fatty acid; A-CoA, acetyl coenzyme A; CPT1, carnitine palmitoyltransferase-1; (Kou et al., 2020)

Enhanced fatty acid uptake: Cancer cells increase their exogenous fatty acids uptake by upregulating fatty acid transporters such as CD36(Drury et al., 2022). This allows cancer cells to utilize exogenous fatty acids as a fuel source or for incorporation into cellular membranes.

Lipolysis of stored lipids: Some cancer cells can mobilize stored lipids, such as triglycerides, from adipose tissue or lipid droplets within the cells(Z. Li et al., 2020). This process involves the activation of lipases, including hormone-sensitive lipase (HSL) and adipose triglyceride lipase (ATGL), which hydrolyze stored triglycerides into free fatty acids that can be utilized by cancer cells(Kory et al., 2016).

Altered lipid desaturation: Cancer cells often exhibit changes in lipid desaturation, leading to increased levels of unsaturated fatty acids(Mukherjee et al., 2017). To do this, enzymes such stearoyl-CoA desaturase (SCD), which changes saturated fatty acids into monounsaturated fatty acids, are upregulated. Altered lipid desaturation influences membrane fluidity, signaling pathways, and resistance to oxidative stress in cancer cells.

Lipid droplet accumulation: Many cancer cells show an accumulation of lipid droplets, which are intracellular lipid storage organelles. Lipid droplets provide a reservoir of lipids that can be utilized during periods of increased energy demand or metabolic stress. They also play a role in protecting cancer cells from lipotoxicity, and oxidative stress.

Lipid metabolism-associated signaling pathways: Lipid metabolites and enzymes involved in lipid metabolism can activate various signaling pathways that promote cancer cell survival, proliferation, and migration. For example, lipid-derived signaling molecules like phosphatidylinositol-3,4,5-trisphosphate (PIP3) can activate the PI3K/AKT pathway, a key signaling pathway involved in cell growth and survival(P. Liu et al., 2009).

Understanding the mechanisms underlying alterations in lipid metabolism in cancer cells is important for developing therapeutic strategies that target these metabolic vulnerabilities. Targeting enzymes involved in de novo lipogenesis, fatty acid uptake, or lipid signaling pathways represents potential avenues for cancer therapy.

2.1.5.3. Alterations in Amino Acid Metabolism:

Oral cancer cells may increase the metabolism of certain amino acids, such as glutamine and serine, which are essential for tumor growth and proliferation. The levels of certain amino acids and their metabolites have shown alteration in oral cancer cells and can serve as potential biomarkers for oral cancer. For instance, GS-MS untargeted metabolomics analysis and UHPLC-MS targeted

quantitative analysis have been performed to reveal three amino acids as potential biomarkers of OSCC namely glutamate, aspartic acid, and proline(X. H. Yang et al., 2020).

2.1.5.4. Altered Redox Homeostasis:

Oral cancer cells exhibit altered redox homeostasis, which contributes to their survival and growth. The levels of oxidative stress markers, such as reactive oxygen species (ROS) and antioxidants, are altered in oral cancer cells. The alterations in redox homeostasis can be measured using various assays, such as glutathione assay and ROS detection assay, and can serve as potential biomarkers for oral cancer(Marrocco et al., 2017).

Altered redox homeostasis in cancer cells arises from various mechanisms that disrupt the balance between reactive oxygen species (ROS) generation and the cellular antioxidant defense systems. Cancer cells often experience increased production of ROS due to heightened metabolic activity, malfunctioning mitochondria, activation of oncogenes, or exposure to external factors like radiation or chemicals(Hayes et al., 2020). Dysregulation of the antioxidant systems further exacerbates the imbalance, with reduced expression or activity of key antioxidant enzymes such as superoxide dismutase (SOD), catalase, and glutathione peroxidase(Reczek et al., 2017). Dysfunctional mitochondria, characterized by mutations in mitochondrial DNA, impaired electron transport chain activity, and elevated reactive nitrogen species production, also contribute to the altered redox state(Raldine Gentric et al., n.d.). Moreover, the metabolic reprogramming observed in cancer cells, such as heightened aerobic glycolysis and dysregulated nutrient utilization, can lead to the accumulation of glycolytic intermediates and increased production of reducing equivalents, thereby promoting ROS generation(Gwangwa et al., n.d.). Dysfunctional redox signaling pathways and aberrant intracellular calcium signaling further contribute to the disruption of redox homeostasis in cancer cells(Delierneux et al., 2020). The resultant oxidative stress induces DNA damage, including strand breaks, base modifications, and adduct formation, which can further burden the cellular redox defense systems and promote genetic instability(Peluso et al., 2020). Collectively, these mechanisms contribute to the altered redox homeostasis observed in cancer cells, impacting various cellular processes, signaling pathways, and ultimately influencing cancer cell survival, proliferation, metastasis, and response to therapy.

The relationship between redox homeostasis and the major hallmarks of cancer demonstrates the impact of altered oxidative balance on cancer development and progression. Here's how redox is related to each hallmark (Figure 16):

1.   Sustained proliferative signaling: Redox signaling critically regulates cell proliferation. Altered redox homeostasis can activate signaling pathways, such as those involving growth factors and oncogenes, leading to sustained proliferative signaling(Foyer & Noctor, 2005). The Reactive oxygen species (ROS) produced by oxidative metabolism can act as secondary messengers, modulating cell cycle progression, DNA synthesis, and cell division(Checa & Aran, 2020).

2.   Evading growth suppressors: Normal cells have robust mechanisms to sense and respond to growth-inhibitory signals. Altered redox balance can disrupt these mechanisms, allowing cancer cells to evade growth suppressors(Purohit et al., 2019). Dysregulated redox signaling can impair tumor suppressor genes function, such as p53, which regulates cell cycle arrest and apoptosis as a reaction to DNA damage and oxidative stress(Budanov, 2014).

3.   Resisting cell death: Cancer cells often acquire the ability to resist cell death, enabling their survival and uncontrolled growth. Redox signaling is intricately involved in apoptotic regulation (programmed cell death)(Elmore, 2007). Altered redox homeostasis can activate survival pathways and inhibit apoptotic signaling, thereby conferring resistance to cell death(Xing et al., 2022a). For example, elevated antioxidant capacity and dysregulation of redox-sensitive proteins can interfere with apoptotic signaling pathways.

4.   Enabling replicative immortality: Normal cells have a finite replicative capacity due to the shortening of telomeres with each cell division. However, cancer cells can bypass this limitation through various mechanisms, including altered redox regulation. Elevated ROS levels can activate telomerase, an enzyme that maintains telomere length, allowing cancer cells to achieve replicative immortality(Robinson & Schiemann, 2022).

5.   Inducing angiogenesis: Redox signaling influences the process of angiogenesis, which involves new blood vessel formation to support tumor growth and metastasis(Ushio-Fukai & Nakamura, 2008). ROS can act as signaling molecules that promote angiogenesis by activating pathways such as TNF-α/NFκ-B/Snail pathway and the hypoxia-inducible factor 1 (HIFα-1) (Ziello

et al., 2007). Altered redox homeostasis can contribute to an angiogenic switch, facilitating the development of a tumor blood supply(Y. Wu & Zhou, 2010)(Aguilar-Cazares et al., 2019).

6. Activating invasion and metastasis: Redox signaling can modulate cellular processes involved in metastasis and tumor invasion. ROS has the potential to induce epithelial-mesenchymal transition (EMT), a process that enhances cancer cell migration and invasion(Pani et al., 2010). Altered redox balance can activate EMT-inducing transcription factors, remodeling the extracellular matrix, and promoting cancer cell motility and invasiveness(Park et al., 2020).

Additionally, redox homeostasis is intertwined with other hallmarks of cancer, including genomic instability and immune evasion(Kotsafti et al., 2020). Increased ROS levels can induce DNA damage and genomic instability, contributing to genetic alterations and tumor heterogeneity(Sallmyr et al., 2008). Altered redox balance can also affect immune responses by modulating immune cell functions and suppressing anti-tumor immune responses(Gostner et al., 2013).Understanding the intricate relationship between redox homeostasis and the hallmarks of cancer provides insights into the underlying molecular mechanisms driving cancer development and progression. Targeting redox-dependent pathways and restoring redox balance represent potential strategies for cancer prevention and treatment.
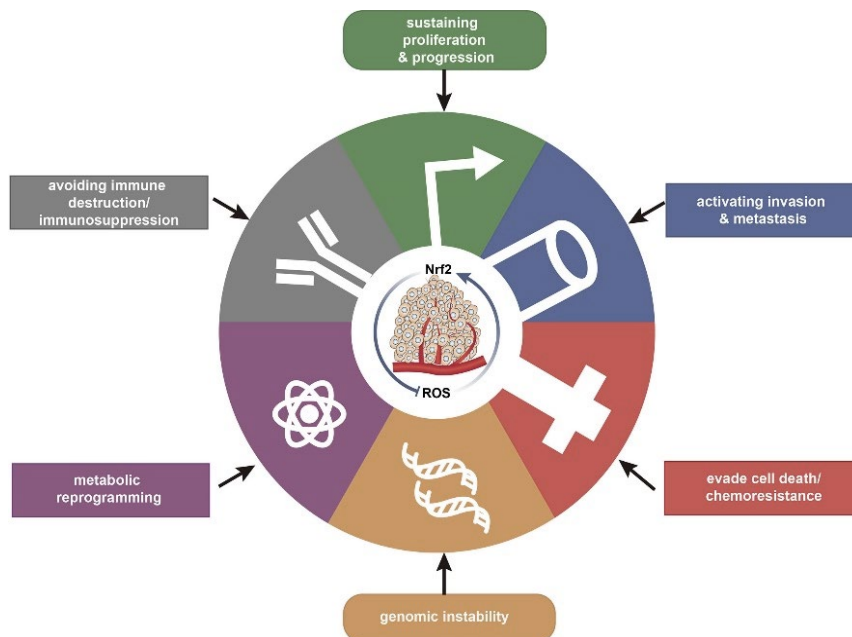
Figure 16. Relationship between redox and the main characteristics of cancer. Redox regulation influences the progression of cancer and is linked to the characteristics of cancer(Xing et al., 2022b)

2.1.5.5. Alterations in Nucleotide Metabolism:

Oral cancer cells may alter their nucleotide metabolism, including the synthesis and breakdown of nucleotides. These alterations can play a role in contributing to the energy needs of cancer cells and also facilitate tumor growth and survival. The levels of certain nucleotides and their metabolites, such as uridine and inosine, show alterations in oral cancer cells and can serve as potential biomarkers for oral cancer(Paz et al., 2007). These alterations can be measured using various assays and imaging techniques and can aid in the identification of new biomarkers and development of therapeutic strategies for oral cancer.

2.1.5.6. Iron metabolism

Iron is a vital element necessary for fundamental metabolic processes and cell division, making it indispensable for the functioning of all cells, including malignant cells. From a canonical perspective, cancer cells often exhibit accelerated proliferation rates and increased metabolic turnover, leading to a heightened demand for iron compared to non-malignant cells. Iron metabolism plays a crucial role in the development and progression of oral cancer(Guo et al., 2021). Iron is an essential nutrient required for cellular growth, proliferation, and survival(L. Zhou et al., 2018). However, Reactive oxygen species (ROS), which can result in DNA damage and mutations, are produced when there is an excessive amount of iron accumulated, ultimately leading to cancer(Ying et al., 2021).

Several studies have reported altered iron metabolism in oral cancer tissues compared to normal tissues (Brown et al., 2020). The expression of iron transport proteins, such as transferrin and transferrin receptor, is also up regulated in oral cancer cells(Torti & Torti, 2020). Furthermore, iron uptake pathways, such as divalent metal transporter 1 (DMT1) and transferrin receptor-mediated endocytosis, are up regulated in oral cancer cells. Further studies have shown that integration of Cell Cycle and JAK-STAT3 Signaling via DMT1-Mediated Iron Uptake Promotes Colorectal Tumorigenesis(Xue et al., 2016).The up regulation of iron uptake pathways in oral cancer

cells can contribute to iron accumulation and ROS generation which leads to DNA damage, mutations ultimately promoting cancer. Therefore, iron chelation therapy, which involves the removal of excess iron from the body, has emerged as a potential therapeutic strategy for oral cancer(J. C. Lee et al., 2016). Several iron chelators, such as deferoxamine, deferasirox, and deferiprone, have been tested for their anti-cancer effects in oral cancer(Bedford et al., 2013). These iron chelators have been shown to inhibit oral cancer cell growth, induce apoptosis, and decrease ROS levels (Ohyashiki et al., 2009). Furthermore, iron chelation therapy has been shown to sensitize oral cancer cells to chemotherapy and radiotherapy, potentially improving the efficacy of these treatments(Abdelaal & Veuger, 2021). However, conflicting reports challenge this viewpoint and suggest that increasing cellular and systemic iron stores may paradoxically inhibit tumor progression(Jian et al., 2013) .Therefore, it is likely that maintaining an equilibrium of iron levels, fulfilling metabolic requirements without causing cellular damage, impairing oncogenic signaling, or triggering ferroptosis, is crucial for sustaining cancer progression.

Multiple mechanisms have been identified through which iron can exert both positive as well as negative effects on tumor cell growth. Firstly, iron acts as a catalyst in non-enzymatic reactions, leading to the generation of ROS. Secondly, iron serves as a cofactor for enzymes involved in cell division, such as ribonucleotide-diphosphate reductase. Thirdly, iron regulates cell cycle control proteins, impacting cell cycle progression. Fourthly, iron participates in both pro- and anti-oncogenic signaling pathways. Lastly, iron plays a crucial role in the hypoxic response and contributes to metabolic and epigenetic reprogramming mediated by 2-oxoglutarate dioxygenases (Cabantchik et al., 2002).

A recurrent finding in numerous cancer cell types is the cell cycle arrest and activation of apoptosis in iron-depleted cancer cells(Dongiovanni et al., n.d.)(Kulp et al., n.d.). However, iron overload in cancer cells can indeed lead to tumor cell death. This occurs through various mechanisms, including the generation of reactive oxygen species (ROS) and the induction of oxidative stress. Excessive iron levels can promote the production of ROS, which can cause damage to cellular components such as DNA, proteins, and lipids. The accumulation of ROS beyond a certain threshold can trigger apoptotic pathways, leading to tumor cell death(Nogueira & Hay, 2013). Furthermore, iron overload can disrupt cellular homeostasis and interfere with essential cellular processes, including cell cycle progression and DNA repair mechanisms. These disruptions can further contribute to cell death in cancer cells.

In some cases, the combination of iron chelators, which help to reduce iron levels, and pro-apoptotic signaling can enhance the effectiveness of inducing tumor cell death(Rainey et al., 2019). The targeted reduction of iron levels in cancer cells can sensitize them to apoptotic signals, leading to increased cell death. While iron overload can have detrimental effects on cancer cells, it is important to carefully balance iron levels to avoid potential damage to healthy cells and tissues.

Ferroportin is a transmembrane protein involved in the export of iron from cells. It is primarily responsible for releasing iron into the bloodstream from cells that store or absorb iron, such as macrophages and enterocytes in the intestine(Ward & Kaplan, 2012). Hepcidin, a hormone that binds to ferroportin and causes its internalization and destruction, controls ferroportin, thus reducing iron export(Nemeth & Ganz, 2009). FPN and CP are indeed connected in terms of iron metabolism(Musci, 2014). FPN1, which mediates the outflow of ferrous iron, works with any one of the three multi-copper oxidases—hephaestin, CP, and zyklopen—that can change ferrous iron into its ferric form(Vashchenko & MacGillivray, 2013).

2.1.5.7. Avoid tumor cell death

Oral cancer cells have developed several mechanisms to avoid tumor cell death. These mechanisms help cancer cells to survive and proliferate, making them resistant to various anti-cancer treatments.

One of the mechanisms that oral cancer cells use to avoid tumor cell death is the activation of anti-apoptotic pathways. Apoptosis, or programmed cell death, is a natural process that eliminates damaged or abnormal cells. However, cancer cells can evade apoptosis by activating anti-apoptotic pathways, such as the PI3K/AKT pathway, the NF-κB pathway, and the MAPK pathway (Fulda & Debatin, 2006). These pathways can inhibit apoptosis and promote cancer cell survival.

Another mechanism that oral cancer cells use to avoid tumor cell death is the activation of DNA repair pathways. Chemotherapy and radiation therapy induce DNA damage in cancer cells, which can lead to cell death. However, cancer cells can repair DNA damage by activating DNA repair pathways, such as the homologous recombination and non-homologous end joining pathways(Helleday, 2010). These pathways can repair DNA damage and promote cancer cell survival.

Moreover, oral cancer cells can evade tumor cell death by activating autophagy, a process that recycles damaged or unnecessary cellular components. Autophagy can promote cancer cell survival by providing energy and nutrients to cancer cells under stress conditions, such as chemotherapy and radiation therapy(Yun & Lee, 2018).

Additionally, cancer cells can evade tumor cell death by activating pro-survival signaling pathways, such as the Wnt/β-catenin pathway and the Notch pathway(Katoh, 2011). These pathways can promote cancer cell proliferation and survival by regulating cell cycle progression and apoptosis.

Furthermore, Cancer Cells Evade Death via Redox Regulation. One of the key strategies employed by cancer cells is the upregulation of antioxidant defense systems. This includes an increase in the production of antioxidant enzymes that scavenge and neutralize ROS, such as superoxide dismutase (SOD), catalase, and glutathione peroxidase. By enhancing their antioxidant capacity, cancer cells can effectively mitigate the harmful effects of ROS and prevent apoptosis. The ability of cancer cells to evade death via redox regulation poses a significant challenge in cancer treatment. Therapeutic strategies that target redox imbalance and disrupt the adaptive mechanisms of cancer cells are being explored to overcome this evasion. By understanding the intricate interplay between redox regulation and cell survival in cancer, researchers aim to develop novel approaches to selectively induce apoptosis in cancer cells only.

2.1.5.8. Iron metabolism, Redox regulation and Ferroptosis in Tumors:

Ferroptosis is a form of controlled cell death characterized by an iron-dependent buildup of lipid peroxides and oxidative damage(Pu et al., 2022) It represents a unique intersection between redox regulation and cell death pathways. Unlike apoptosis or necrosis, ferroptosis specifically involves the dysregulation of cellular iron and lipid metabolism, leading to ROS accumulation and lipid peroxidation(X. Chen et al., 2020a).

Ferroptosis is tightly linked to redox signaling and cellular antioxidant defenses. One of the key players in ferroptosis is the glutathione peroxidase 4 (GPX4) enzyme, which utilizes glutathione (GSH) to detoxify lipid peroxides and maintain redox balance within cells. Inhibition or depletion of GPX4 leads to the accumulation of lipid peroxides and triggers ferroptosis(J. Li et al., 2020). The redox status of cells also influences their susceptibility to ferroptosis. Cells with lower levels of

intracellular antioxidants or reduced capacity to regenerate GSH are more susceptible to ferroptosis. On the other hand, activation of the Nrf2 pathway, which regulates the expression of antioxidant genes, can confer protection against ferroptosis by enhancing cellular antioxidant defenses.

Furthermore, iron metabolism plays a critical role in ferroptosis(X. Chen et al., 2020b). Iron is required for the generation of lipid peroxides through Fenton chemistry, where it catalyzes the production of highly reactive hydroxyl radicals. The accumulated ROS can initiate lipid peroxidation and cause oxidative damage to cellular components, ultimately triggering ferroptotic cell death.

The connection between redox regulation and ferroptosis is of great interest in cancer research and therapeutics. Interestingly, exploiting iron accumulation as a therapeutic strategy has been investigated in certain types of cancer(Morales & Xue, 2021). For instance, targeting iron metabolism through iron chelators or inhibitors of iron uptake or storage proteins can effectively induce ferroptosis in cancer cells with iron overload. This approach uses the vulnerability of cancer cells to iron-induced oxidative stress and offers a potential therapeutic avenue.

2.1.6. Treatment and Diagnosis

Microscopic inspection can be used to diagnose the majority of head and neck malignancies. Immunohistochemistry is useful in identifying poorly differentiated tumors and those with unusual morphological features(Pai & Westra, 2009). Antibodies like cytokeratin (CK), p63, and S-100 are frequently employed in diagnosing squamous cell carcinoma or salivary gland carcinomas(H. Li et al., 2020). In oropharyngeal cancers, p16 expression is routinely evaluated to assess HPV presence, providing valuable prognostic information(Golusiński et al., 2017). Molecular studies are used to evaluate (Epstein-Barr virus) EBV presence in undifferentiated tumors or to confirm the subtypes of salivary gland tumors and assess genetic alterations(Young & Dawson, 2014).

The prognosis for head and neck cancer patients varies with the histological type and location of the tumor(Pai & Westra, 2009). The 5-year survival rate is about 60% for salivary gland cancer, mouth tumors, cancers of oropharynx, and larynx, while hypopharyngeal cancer has a lower rate of around 30%. Treatment choices are contingent upon factors such as the location of the tumors, histological type, and cancer stage(Kase et al., 2021). Surgery, radiotherapy, and chemotherapy are the main treatment options for advanced cases(Figure 17). Patients with

squamous cell carcinoma may also consider immunotherapy with checkpoint inhibitors(Zolkind & Uppaluri, 2017).
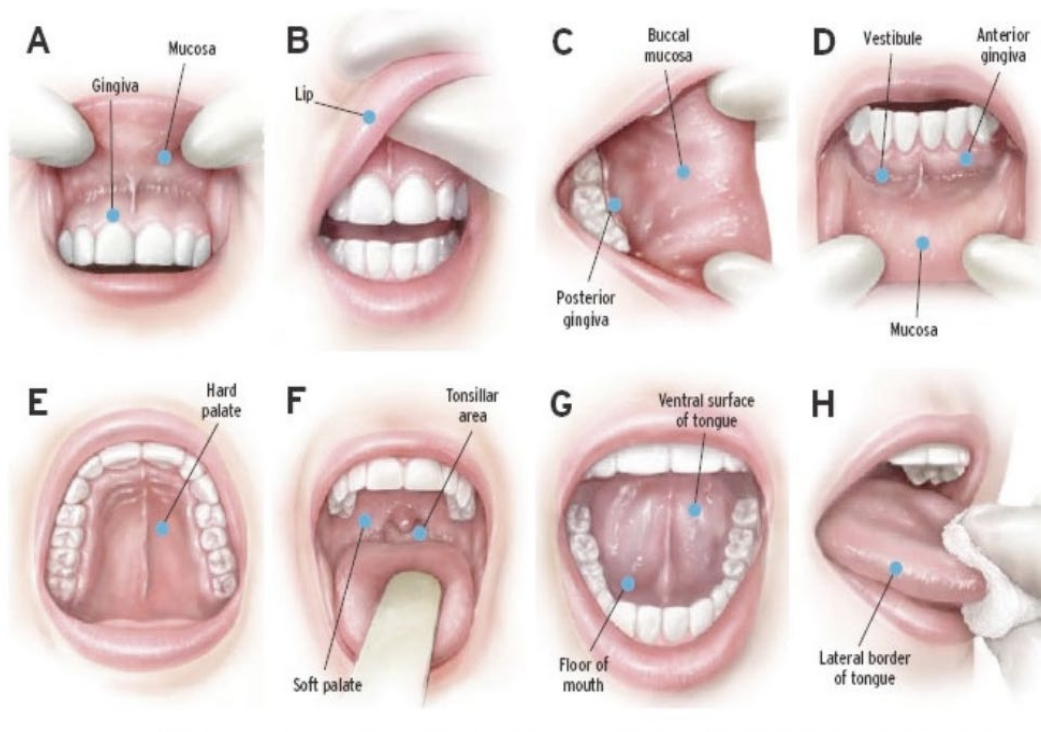
Figure 17. An eight step oral cavity inspection is part of a quick oral cancer screening. Based on work of Lindsey McCall, 2019

Several factors need to be considered when choosing a treatment for a patient. The patient's physiological age, comorbid conditions (such as heart problems), lifestyle choices (such as smoking or excessive alcohol consumption), and surgical resectability are all evaluated to determine the potential risks of complications associated with the treatment (J. P. Shah & Gil, 2009) The preferred course of treatment for OC is surgical resection, which enables precise pathologic staging and provides details regarding tumor dissemination, margin status, and histopathologic characteristics that can be utilized to guide further management based on an evaluation of risk against benefit (Moratin et al., 2021). In regionally advanced tumors adjuvant radiotherapy along with chemotherapy is used for specific indications (Warnakulasuriya, 2009). Despite advancements in the field the proportion of patients presenting with advanced disease had not changed owing to delay

in diagnosis(Varela-Centelles, 2022). This delay has been reported by several studies to be on the patient's part in seeking professional advice after the presentation of oral cancer symptoms. Further, since most oral cancers present at a late stage of the disease it is essential to identify molecular diagnostic and therapeutic markers.

Hence the following are the several reasons why identifying molecular diagnostic and therapeutic markers of oral cancer is important:

1.   Early detection: Molecular indicators can aid in the early oral tumors detection, when it is most amenable to treatment. As a result, there may be a greater likelihood for successful therapy and better patient outcomes.

2.   Precision medicine: Molecular markers can help tailor treatment to an individual patient's cancer, based on the specific genetic mutations or alterations present. This can lead to more effective and targeted treatments, with fewer side effects.

3.   Prognosis: Certain molecular markers can predict the cancer progression or recurrence likelihood, as well as the overall prognosis for the patient. This can help guide treatment decisions and monitoring strategies.

4.   Drug development: Identifying molecular markers of oral cancer can aid in new drugs and therapy development, specifically targeting the molecular pathways involved in the cancer. This can lead to more effective treatments and improved outcomes for patients.

Overall, identifying molecular diagnostic and therapeutic markers of oral cancer can help improve patient outcomes, guide treatment decisions, and improve our understanding of the disease.

CHAPTER 2.2. INSILICO BIOMARKER ESTIMATION

Various *in silico* methods have been used for identifying potential cancer biomarkers and can help guide the development of new diagnostic and therapeutic strategies. *In silico* methods refer to computational approaches that use algorithms, software, and databases to analyze large amounts of biological data. Figure 18 shows several *in silico* methods have been used to identify cancer biomarkers, including:

Genomic analysis: This involves the analysis of DNA and RNA sequencing data to identify genetic mutations, alterations, and expression patterns that are characteristic of cancer. Bioinformatics tools can be used to analyze the data and identify potential biomarkers.

Proteomic analysis: This involves the analysis of proteins in biological samples, such as blood or tissue, to identify proteins that are overexpressed or under expressed in cancer. Mass spectrometry and other proteomic techniques can be used to identify potential biomarkers.

Machine learning: This involves the use of algorithms and statistical models to analyze large datasets and identify patterns that are indicative of cancer. Machine learning can be used to identify potential biomarkers based on gene expression, protein expression, or other molecular characteristics.

Network analysis: This involves the analysis of molecular interactions and pathways to identify key players and potential biomarkers in cancer development and progression. Network analysis can be used to identify potential biomarkers based on their interactions with other molecules in the cell.
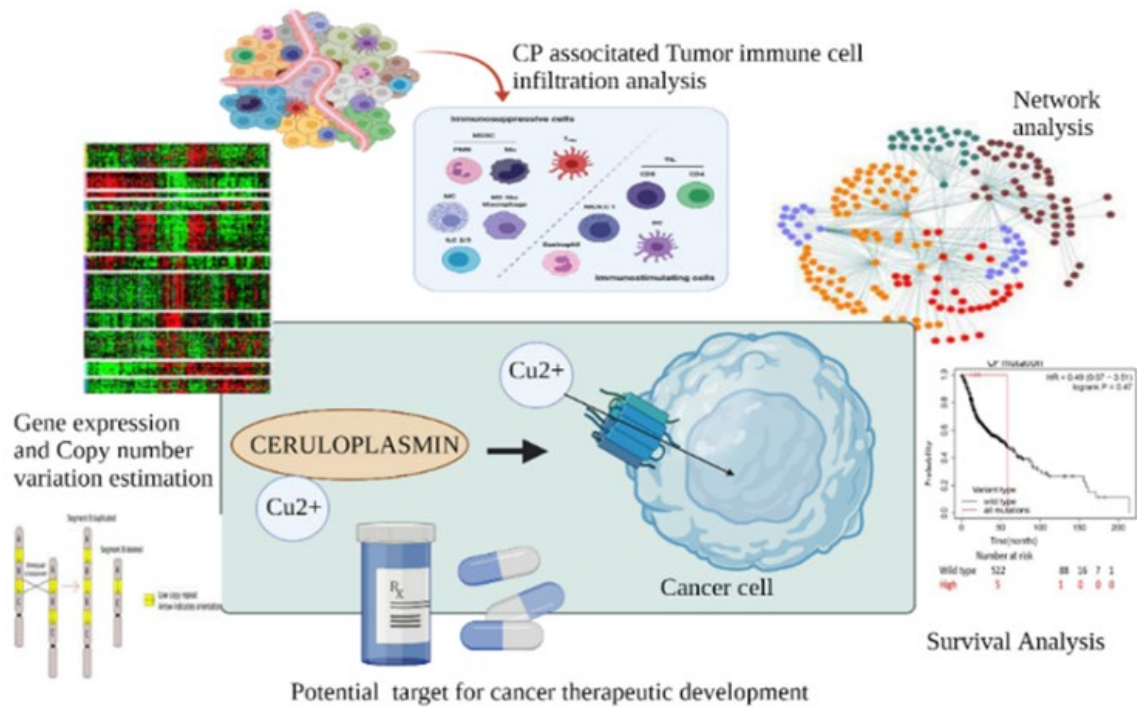
Figure 18. Workflow of biomarker estimation. The gene expression data helps us perform a number of analysis including gene interaction network analysis and correlated expression analysis to identify the pathways altered during cancer progression as well as identify the best targets in cancer therapy.

2.2.1. Differential gene expression analysis

Differential gene expression analysis is a powerful approach used to identify potential cancer biomarkers by comparing gene expression levels between cancerous and non-cancerous tissues or between different cancer subtypes. Here are key points regarding the use of differential gene expression analysis for cancer biomarker identification:

Data Generation: Gene expression data is generated using high-throughput technologies such as microarrays or RNA sequencing (RNA-seq) from cancer and normal tissue samples. These technologies provide comprehensive information on the expression levels of thousands of genes simultaneously.

Differential Expression Analysis: Statistical methods, such as t-tests, ANOVA, or advanced algorithms like DESeq2 or edgeR, are employed to identify genes that show significant differences

in expression between cancer and normal samples. The analysis helps identify genes that are upregulated or downregulated in cancer.

Fold Change and p-value: The fold change, which measures how much gene expression has changed, and the p-value, which denotes the statistical significance of the differential expression, are commonly reported by differential expression analysis. Genes with high fold change and low p-values are considered as potential biomarkers.

Calculating the log2 fold change is a common method for comparing gene expression between tumor and normal patients. It provides a standardized and easily interpretable measure of the magnitude of expression differences. By using log2 fold change, researchers can identify genes with significant differential expression, aiding in the understanding of molecular changes associated with the disease and the identification of potential biomarkers or therapeutic targets.

Biological Relevance: Identified differentially expressed genes are further analyzed for their biological functions and pathways using enrichment analysis tools such as Gene Ontology (GO) analysis or pathway analysis. This helps understand the functional implications of the identified genes and their involvement in cancer-related processes.

Validation: Differential gene expression findings need to be validated in independent sample sets or through alternative techniques like qRT-PCR or immunohistochemistry. Validation ensures the reliability and reproducibility of the identified biomarkers.

Biomarker Selection: From the list of differentially expressed genes, potential biomarkers are selected based on their biological relevance, specificity to cancer, association with clinical outcomes (e.g., survival, response to therapy), and feasibility of detection in clinical settings.

Clinical Translation: Validated biomarkers can be further developed into diagnostic, prognostic, or predictive tools for cancer. They may undergo clinical trials to assess their effectiveness and utility in patient management.

2.2.2. Differential gene methylation

Differential gene methylation status has been widely investigated as a potential biomarker for cancer. The identification of specific genes that exhibit differential methylation patterns between cancerous and normal tissues holds promise for diagnostic, prognostic, and therapeutic purposes.

Here are some key points regarding the use of differential gene methylation status as a cancer biomarker:

Cancer-Specific Methylation: Certain genes may show tumor-specific methylation patterns, with hypermethylation or hypomethylation occurring predominantly in cancer cells compared to normal cells. These differentially methylated genes can serve as potential biomarkers for cancer detection and classification.

Diagnostic Biomarkers: Differential methylation of specific genes can be utilized as biomarkers for cancer diagnosis. Methylation-specific PCR (MSP), bisulfite sequencing, or other methylation detection methods can be employed to assess the methylation status of selected gene regions and distinguish between cancerous and non-cancerous tissues or body fluids.

Prognostic Biomarkers: Gene methylation status can also provide valuable prognostic information. Methylation alterations in certain genes have been associated with cancer progression, metastasis, and patient survival. By analyzing the methylation status of specific genes, clinicians can gain insights into the potential aggressiveness of the cancer and guide treatment decisions.

Predictive Biomarkers: In addition to diagnosis and prognosis, differential gene methylation can serve as a predictive biomarker for response to specific treatments. Certain gene methylation profiles may indicate sensitivity or resistance to particular therapies, allowing for personalized treatment strategies.

Panels of Biomarkers: Rather than relying on single gene methylation analysis, panels of differentially methylated genes are often utilized to enhance the sensitivity and specificity of cancer detection and classification. Methylation profiling of multiple genes in a panel can provide a more comprehensive picture of the disease status.

2.2.3. Differential miRNA expression

Differential miRNA expression analysis is a valuable approach for identifying cancer biomarkers. By comparing the expression levels of microRNAs (miRNAs) between cancerous and normal tissues, this analysis reveals changes that are associated with tumor development, progression, and treatment response. Differential expression analysis identifies specific miRNAs that are significantly upregulated or downregulated in cancer. These differentially expressed

miRNAs can serve as potential biomarkers, distinguishing between cancerous and non-cancerous conditions.

Differentially expressed miRNAs can be used for cancer diagnosis while certain differentially expressed miRNAs correlate with clinical outcomes in cancer patients. Combining multiple miRNAs into signature panels improves the accuracy of cancer detection, enabling early intervention and better patient outcomes. They serve as prognostic indicators, providing information on disease progression, metastasis, and patient survival. Moreover, differentially expressed miRNAs often regulate key cancer-related genes and pathways, making them potential therapeutic targets. Modulating their expression or activity could restore normal cellular functions and hinder cancer progression. Specific miRNAs may be associated with drug sensitivity or resistance, allowing for personalized treatment strategies. Hence, differential miRNA expression patterns can predict treatment response.

Hence differential miRNA expression analysis, combined with functional and clinical validation, has the potential to revolutionize cancer diagnosis, prognosis, treatment selection, and therapeutic development.

2.2.4. Network analysis

Network analysis is a powerful approach used to study the relationships and interactions between entities, such as genes, proteins, or individuals, represented as nodes, and their connections, represented as edges. It provides a comprehensive view of complex systems and allows for the exploration of various biological, social, or technological phenomena.

1.   Networks consist of nodes (also called vertices) and edges (also called links). Nodes can represent individual entities, such as genes or proteins in a biological network or individuals in a social network. Edges represent the connections or interactions between nodes, which can be physical, functional, or informational relationships.

2.   Various approaches, such as correlation analysis, co-expression analysis, or protein-protein interaction data, can be used to establish connections between nodes.

3.   Network topology refers to the structural characteristics and patterns within a network. It includes measures such as node degree (number of connections), centrality (importance of nodes), clustering coefficient (degree of connectivity within a neighborhood), and modules or

communities (groups of densely connected nodes).Graph theory provides various metrics and measures to quantify and characterize network properties.

4. Graph theory offers a wide range of algorithms for network analysis. These algorithms enable researchers to perform tasks such as identifying important nodes (e.g., centrality analysis), detecting network motifs or patterns, finding shortest paths, measuring network resilience, and predicting missing or future connections.

5. It helps uncover underlying patterns, identify key nodes or influencers, assess network robustness, analyze diffusion processes, and understand the overall structure and dynamics of networks.

6. Network analysis techniques, such as graph theory and pathway analysis, can be used to identify hub genes, bottleneck genes, and estimate shortest paths in biological networks.

Hub Genes:

Hub genes are nodes in a biological network that exhibit high connectivity, meaning they are connected to a numerous other genes or proteins within the network. Hub genes play an important role in maintaining network integrity and communication, as they act as central points for information flow. They are often involved in critical biological processes, such as signaling pathways, regulatory networks, or key functional modules. Identifying hub genes can provide insights into key players or regulators within a biological system and their potential roles in disease or normal physiological processes.

Bottleneck Genes:

Bottleneck genes, also known as bottleneck proteins, are nodes in a network that act as critical points of control or regulation. They are characterized by their essential role in maintaining the flow of information or resources within the network. Bottleneck genes often have high betweenness centrality, meaning they lie on many of the shortest paths connecting different parts of the network. Disruption or alteration of bottleneck genes can have a significant impact on the overall network structure and functionality. Identifying bottleneck genes helps uncover key regulatory points and potential targets for therapeutic intervention or biomarker discovery.

Shortest Paths Estimation:

Shortest path estimation is a computational technique used to calculate the shortest route or distance between two nodes in a network. In the context of biological networks, such as gene

regulatory networks or protein-protein interaction networks, estimating shortest paths can provide insights into functional relationships, information flow, or communication patterns between different genes or proteins. Shortest path estimation algorithms, such as Dijkstra's algorithm or Floyd-Warshall algorithm, can be applied to determine the most efficient paths between nodes based on the network topology and edge weights. The shortest path analysis helps uncover key relationships, functional associations, or potential signaling cascades within the network, aiding in understanding biological processes and identifying important nodes or pathways related to disease or normal physiology.

2.2.5. Survival analysis

A statistical technique called survival analysis is frequently employed in the context of medical research to assess time-to-event data. It is widely applied in various fields, including cancer research, epidemiology, and clinical trials. Assessment of the likelihood of an event happening over time and the identification of variables that can affect the time until the event are the two main objectives of survival analysis.

There have been several biomarkers identified for oral cancer through *in silico* analysis. For instance, Matrix metalloproteinase (MMPs) have been identified as potential biomarkers for oral cancer on analysis of the gene expression data from patients with oral squamous cell carcinoma (OSCC). The study found that MMP-3, MMP-9, and MMP-13 were significantly upregulated in OSCC compared to normal tissue(Shin et al., 2021). While MMPs have been identified as potential biomarkers for oral cancer, they are involved in a wide range of biological processes, including tissue remodeling and angiogenesis. As such, changes in their expression may not specifically reflect changes in cancer status. Similarly another study reported EGFR to be significantly upregulated in oral cancer tissue(Kalinowski et al., 2012). While EGFR has been shown to be upregulated in oral cancer, it is also involved in normal cellular processes, and changes in its expression may not specifically indicate cancer. In addition, EGFR-targeted therapies have been associated with a range of adverse effects, and careful patient selection is needed to ensure that these therapies are used safely and effectively. Several miRNAs have been identified to be differentially expressed in OSCC compared to normal tissue, including miR-21, miR-31, and miR-375(Rajan et al., 2021). However more research needs to be carried out to validate these targets. Furthermore

miRNA-based biomarkers may be subject to false positives due to variations in sample preparation and analysis.

Using these *in silico* analysis procedures other biomarkers may be identified in future studies as our understanding of oral cancer biology continues to evolve.

2.2.5. TCGA data analysis

The National Human Genome Research Institute (NHGRI) and the National Cancer Institute (NCI) jointly established the Cancer Genome Atlas (TCGA), a sizable research initiative, in 2006(Tomczak et al., 2015). This project catalogs the genetic and epigenetic changes that occur in various cancer types, with the aim of enhancing our understanding of cancer biology and ultimately leading to improved diagnostic and therapeutic approaches. TCGA involved the analysis of thousands of tumor samples across more than 30 different cancer types, using a wide range of genomic and molecular profiling techniques, including DNA sequencing, RNA sequencing, methylation profiling, and proteomic analysis. The resulting data sets, which included both raw sequencing data and processed results, are now available to researchers around the world through a public data portal. The TCGA project has led to numerous discoveries in the field of cancer biology and has helped to spur the development of new technologies and analytical tools for genomic and molecular analysis.

Analyzing TCGA data involves several steps, including data retrieval, processing, analysis, and interpretation. Here is an overview of each step:

Data retrieval: TCGA data is publicly available and can be accessed through the Genomic Data Commons (GDC) data portal. Data sets for various types of cancer can be downloaded which may include raw sequencing data, processed genomic data, clinical data, and other metadata.

Data processing: TCGA data sets can be quite large and complex, and may require pre-processing before analysis. This can include steps such as filtering out low-quality data, normalizing data across samples, and correcting for batch effects.

Data analysis: Once the data has been pre-processed, a variety of analytical methods can be applied to identify patterns as well as relationships in the data. This may involve techniques such as differential expression analysis, pathway analysis, network analysis, and machine learning.

Interpretation: The results of the analysis can then be interpreted to gain insights into cancer biology as well as to develop new diagnostic and therapeutic approaches. This may involve validating findings through additional experiments or clinical trials.

TCGA data analysis can be challenging due to the large volume and complexity of the data, as well as the need for specialized computational and statistical expertise. However, the availability of TCGA data has enabled researchers around the world to collaborate and share insights, leading to numerous important discoveries in the field of cancer biology.

Working with TCGA data requires an understanding of bioinformatics and data analysis techniques. There are several bioinformatics pipelines and packages available in the R programming language that can be beneficial for analyzing and utilizing TCGA data. Some commonly used pipelines and packages:

TCGAbiolinks: TCGAbiolinks is an R package specifically designed for retrieving and analyzing TCGA data. It provides functions for data download, data preprocessing, differential expression analysis, survival analysis, and data visualization. It offers a comprehensive set of tools for TCGA data analysis.

DESeq2: A popular R program for analyzing differential expression in RNA-seq data is DESeq2. It allows the identification of differentially expressed between different groups, such as tumor and normal samples from TCGA. DESeq2 provides statistical methods and normalization techniques to account for sample variability and perform robust differential expression analysis.

limma: limma is another widely used R package for analyzing microarray and RNA-seq data. It includes functions for differential expression analysis, data normalization, and batch effect correction. limma is often applied to TCGA data for identifying differentially expressed genes and exploring molecular changes between tumor and normal samples.

Survival: The survival package in R provides functions for survival analysis, including Kaplan-Meier estimation, Cox regression, and log-rank tests. This package is useful for analyzing TCGA clinical data, such as patient survival information, and investigating the relationship between gene expression and patient outcomes.

ggplot2: ggplot2 is a powerful R package for data visualization. It offers a flexible and intuitive grammar of graphics for creating high-quality plots and visualizations. ggplot2 can be used

to generate publication-ready plots to visualize TCGA data, such as expression patterns, differential expression results, and survival curves.

CHAPTER 2.3. CERULOPLASMIN

Tumor cells synthesize markers in large quantities releasing them into the circulation during the process. Abnormal levels of these biomarkers in the patient's serum or saliva of an individual can serve as indicators of potential malignant transformations in the future. Greater than normal serum CP levels have been noticed in a number of cancers(Patil et al., 2021). CP has been explored as a potential cancer biomarker due to its involvement in various biological processes and its altered expression in cancer. Furthermore, CP's ability to regulate iron metabolism and oxidative stress makes it relevant to cancer biology. Dysregulation of iron metabolism and increased oxidative stress are common features of cancer cells. CP's role in iron oxidation and transport suggests its potential involvement in cancer-related iron dysregulation and ROS generation. As an acute-phase reactant, CP levels can increase in response to inflammation, which is often associated with cancer development and progression (*Ceruloplasmin and Acute Phase Protein Levels Are Associated with Cardiovascular Disease in Chronic Dialysis Patients - PubMed*, n.d.).Studies have indicated that CP levels may be elevated in certain types of cancer, including liver, breast, and colorectal cancer. Increased CP levels have been associated with tumor growth, metastasis, and poorer prognosis in some cases(Y. Zhang et al., 2021c). CP is typically used in combination with other cancer biomarkers or clinical assessments to improve diagnostic accuracy and prognostic value. Further research has to be done to fully elucidate the utility of CP as a cancer biomarker, including the identification of specific cancer types or stages where its measurement may be most informative.

CP, is a copper-containing protein involved in iron transport and metabolism. It plays a role in incorporating iron into transferrin, a major iron transport protein in the blood. CP also possesses ferroxidase activity, facilitating the oxidation of ferrous iron ($Fe2+$) to ferric iron ($Fe3+$), through the transfer of four electrons to oxygen, which is necessary for its binding to transferrin(Roeser et al., 1970). CP maintains iron homeostasis by transferring ferric irons to transferrin for transport outside the cell and also prevents the occurrence of the deleterious Fenton reaction (B. Jiang et al., 2016). This enzyme has also been reported to oxidize various biogenic amines such as norepinephrine, serotonin and synthetic amines like phenylenediamine and dianisidine(Vashchenko et al., 2011) has been previously described to have interactions with number of proteins such as

ferroportin, transferrin, and myeloperoxidase. Since copper plays an important role in hypoxia and CP plays a major role in copper transport, CP is a hypoxia related protein. CP expression maybe high in tumors to account for the increased iron during the rapid cancer cell proliferation. Recent research shows iron homeostasis related genes can be potential therapeutic targets. The expression of CP has been previously reported to be high in a number of tumors such as melanomas and renal cancers. However, the expression of CP in head and neck cancer hasn't been explored before.

Ceruloplasmin (4ENZ) is a multi-domain glycoprotein found in the blood that plays a crucial role in copper transport and oxidation. Its structure, as determined by X-ray crystallography, reveals several distinct domains that are responsible for its various functions. Here's an overview of the domains found in ceruloplasmin:

N-Terminal Domain: This domain is responsible for copper binding and contains six copper-binding sites. Ceruloplasmin can carry up to six copper ions simultaneously, making it an essential copper transporter in the bloodstream.

Ferritin-like Domain: This domain is involved in iron binding and regulation. Ceruloplasmin also has ferroxidase activity, which helps convert toxic ferrous iron ($Fe2+$) into ferric iron ($Fe3+$), facilitating iron transport and storage.

Glycosylation Sites: Ceruloplasmin is a glycoprotein, meaning it has carbohydrate (sugar) chains attached to certain amino acids. These glycosylation sites are crucial for its stability and function.

Signal Peptide: This is a short sequence at the N-terminus that guides the newly synthesized ceruloplasmin to the endoplasmic reticulum, where it undergoes further processing and glycosylation.

The combination of these domains allows ceruloplasmin to fulfill its roles in copper transport, copper oxidation, and iron regulation within the body. Its multi-domain structure is essential for its biological functions(Figure 19).
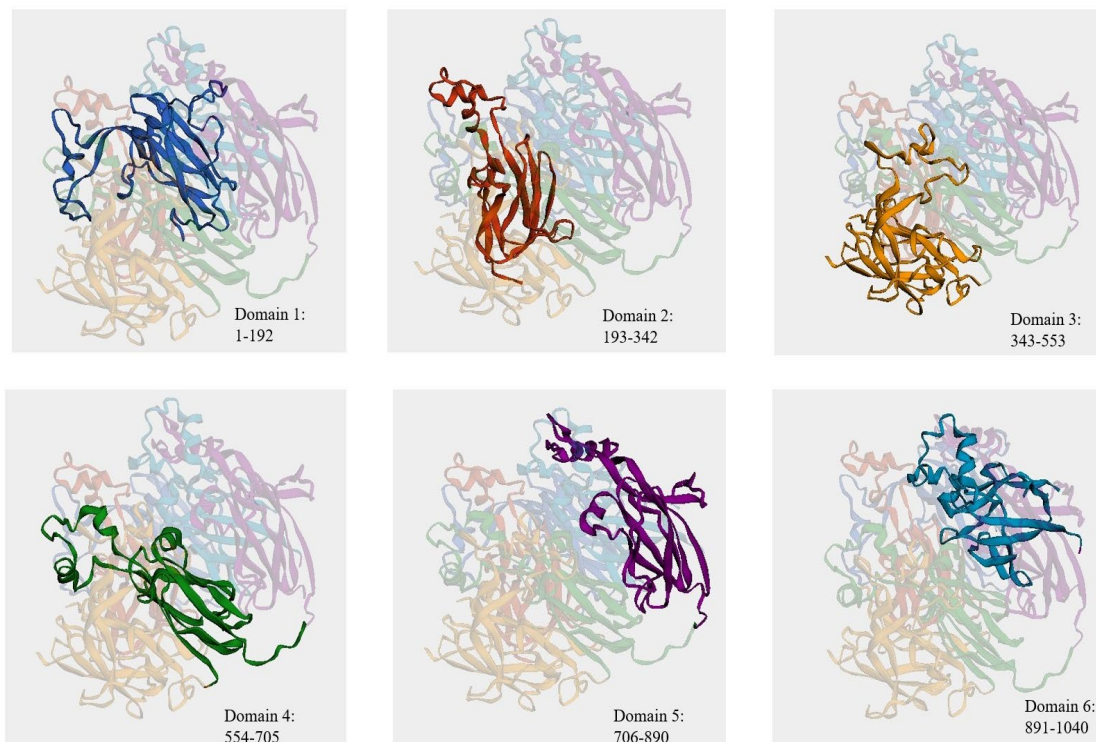
Figure 19. Protein ceruloplasmin structure from PDB (4ENZ) showing different domains (blue: domain 1, green: domain 4, sea green: domain 6, red: domain 2, orange: domain 3, purple: domain 5)

2.3.1. Ceruloplasmin in iron homeostasis

CP has been previously reported to exist in an interplay with FPN in maintaining iron homeostasis**.** Hepcidin, a hormone that binds to ferroportin and causes its internalization and degradation, inhibits iron export by causing ferroportin to be internalized and degraded. Ferroportin is a transmembrane protein involved in the export of iron from cells. CP has been shown to stabilize ferroportin on the cell surface, thereby enhancing iron export(Musci, 2014). Additionally, CP-derived copper is required for proper ferroportin function(Jończy et al., 2021). Furthermore, hepcidin, the hormone that regulates ferroportin, is influenced by CP(Kono et al., 2010). CP is involved in the oxidation of ferrous iron, which leads to increased levels of ferric iron. High levels of ferric iron can stimulate hepcidin production, resulting in the degradation of ferroportin and decreased iron export (Figure 20).
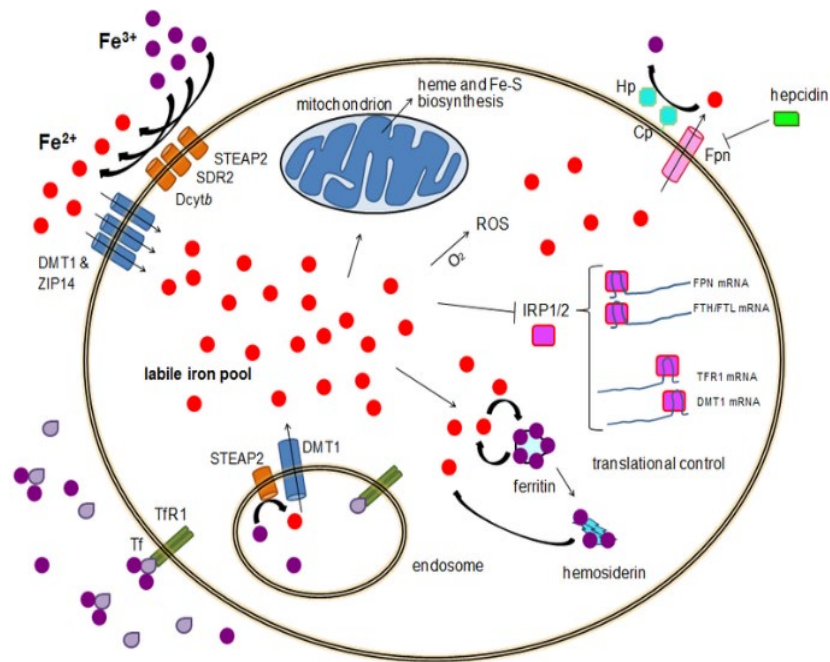
Figure 20. Schematic representation of cellular iron homeostasis. *The transporters are used to import iron. The cytoplasmic labile iron pool (LIP) is made up of intracellular iron and can be either supplied to various cell compartments or stored in ferritin for later use. Hephaestin, ceruloplasmin, and ferroportin work together to facilitate the excess iron's export, and hepcidin inhibits it(Jung et al., 2019)*

CP by converting Fe^{2+} to Fe^{3+} and promoting iron binding to transferrin, thereby limiting the labile iron pool within cells. This limitation reduces the availability of free iron for catalyzing the Fenton reaction and subsequent ROS production, thereby suppressing ferroptotic cell death. Ferroportin exports Fe^{2+} from the cytoplasm into the extracellular space, while transferrin receptor internalizes Fe^{3+} via transferrin-bound complexes into the cell where Fe^{3+} is reduced to Fe^{2+} by the action of STEAP3, allowing it to enter the labile iron pool present in the cytoplasm. Additionally, Fe^{2+} released into the extracellular space can be oxidized to Fe^{3+} by CP, enabling its uptake by transferrin for transport.

In the context of ferroptosis, Fe^{2+} plays a critical role by participating in key reactions that contribute to the development of this form of regulated cell death. In the Fenton reaction, Fe^{2+} interacts with hydrogen peroxide to produce hydroxyl radicals ($\bullet OH$), which are extremely reactive. These hydroxyl radicals can oxidize lipids in the cell membrane, initiating a chain reaction of lipid

peroxidation, which is a hallmark event in ferroptosis(Figure 21). Moreover, Fe^{2+} can also catalyze lipid peroxidation through the activity of lipoxygenases (LOXs), further contributing to the propagation of lipid peroxidation in ferroptosis. Understanding these processes provides insights into the mechanisms underlying ferroptosis and potential targets for therapeutic interventions in diseases associated with dysregulated iron metabolism(Mao et al., 2020).

According to a study done on HCC cells, CP depletion makes it more likely that cells would undergo the ferroptotic cell death that is brought on by erastin and RSL3. This results in an accumulation of intracellular ferrous iron (Fe^{2+}) and lipid ROS. On the other hand, CP overexpression successfully blocks erastin- and RSL3-induced ferroptosis in HCC cells. CP therefore inhibits ferroptosis in hepatocellular carcinoma cells via controlling iron homeostasis(Shang et al., 2020a)(Figure 22).
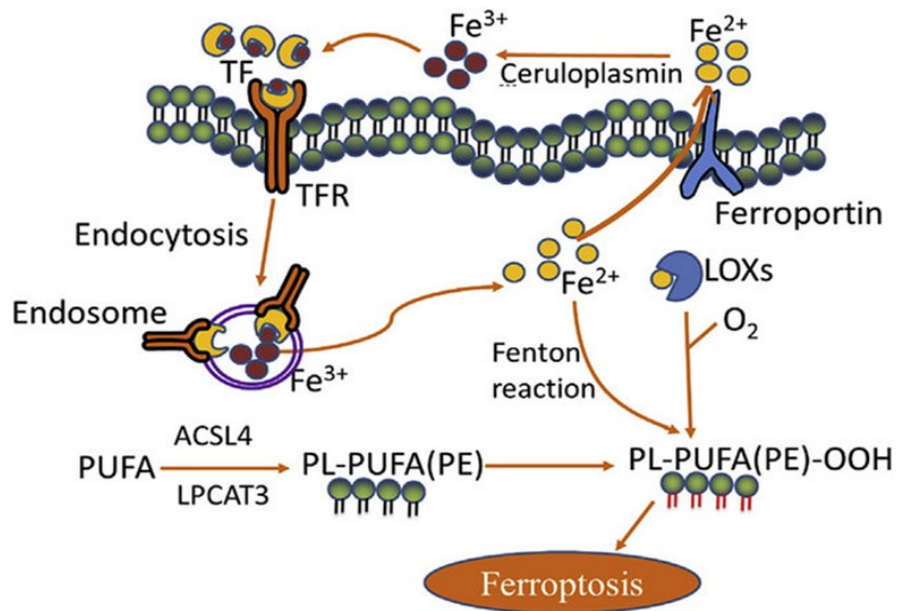
Figure 21. Iron metabolism in ferroptosis. *Ferroportin and transferrin receptor (TFR) maintain iron balance. TFR transports Fe3+ into cells, reduced to Fe2+ by STEAP3 in endosomes, then released into a labile iron pool. Fe2+ can oxidize to Fe3+ by ceruloplasmin, taken up by transferrin. Fe2+ triggers ferroptosis by lipid oxidation via Fenton reaction and lipoxygenases. LPCAT3 and ACSL4 also impact ferroptosis by regulating polyunsaturated fatty acids*(Mao et al., 2020).
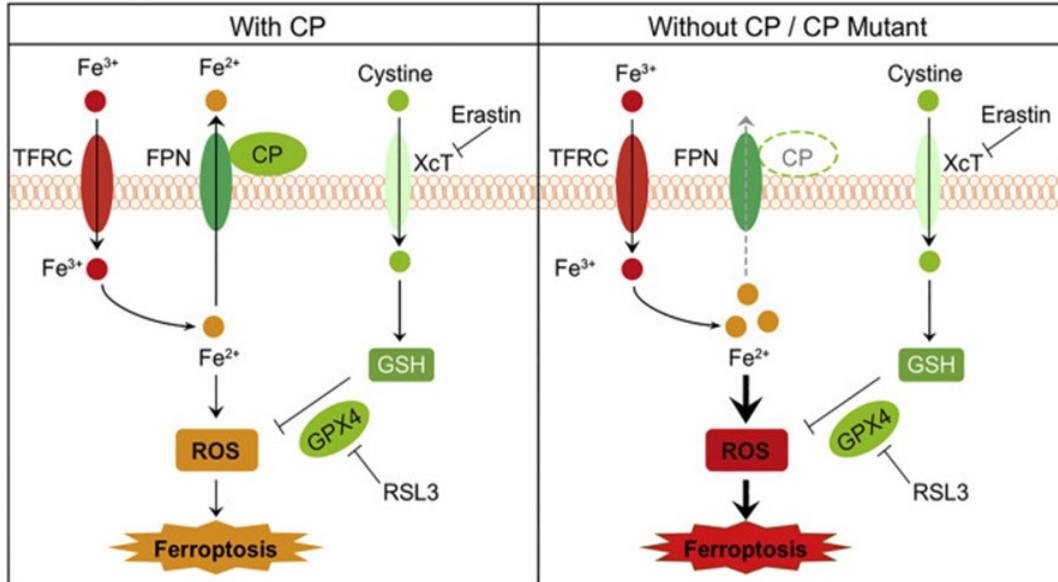
Figure 22. Ferroptosis suppression by Ceruloplasmin by regulation of iron homeostasis in hepatocellular carcinoma cells. Ceruloplasmin (CP) controls ferroptosis triggered by erastin and RSL3 through iron export. CP collaborates with ferroportin (FPN) to facilitate the release of Fe2+ from cells, thereby playing a crucial role in regulating ferroptosis induced by erastin and RSL3. In the absence of CP, intracellular Fe2+ accumulates, promoting ferroptosis. (Shang et al., 2020a).

2.3.2. Ceruloplasmin and copper

There is proof that CP connects copper and iron metabolism directly at the molecular level. Copper deficiency results in low plasma CP and iron levels as 6 atoms of copper form an integral part of CP protein structure(O'Brien & Bruce, 2010). The oxidase activity of CP is also copper-dependent. Cancer cells due to increased proliferation have an increased demand for iron. The labile iron pool within the cancer cell result in increased ROS. Tumor cells counter the oxidative stress due to the ROS built-up within the cell by transporting out excess Fe2+ ions out of the cell (De Domenico et al., 2007). A set of enzymes that change Fe2+ to Fe3+ are required for iron to be properly loaded onto transferrin (Tf), as this protein can only bind the oxidized form of the metal. Iron is extruded by Fpn as Fe2+. These enzymes, which also include CP and hephaestin, a

membrane-bound paralog of CP, are multicopper oxidases with ferroxidase activity(Bonaccorsi di Patti et al., 2018). The majority of CP processes, such as the amine oxidase activity that regulates the amount of biogenic amines in intestinal fluids and plasma, the elimination of free radicals from plasma, and the export of iron and copper to extra hepatic tissues, are dependent on the presence of the Cu centers centers(*BIOLOGICAL INORGANIC CHEMISTRY : Structure and Reactivity.*, 2018).

CP is reported to regulate and VEGF24 and HIF1A. A study on colon cancer reported proteasomal degradation of CP could result in angiogenesis inhibition by regulating HIF-1α expression and VEGFA(Y. Zhang et al., 2021a).CP is responsible for carrying iron outside a cell by ferrous ion conversion and helps reduce the built up of free radicals within the cell. Hence we suggest that CP upregulation may be tumor cells mechanism of countering the buildup of oxidative stress within the cell and avoid cell death.

2.3.3. Ceruloplasmin and MPO

It has been discovered that CP inhibits the production of myeloperoxidase (MPO), holds a pivotal role as a vital component within the innate immune system produced by neutrophils. Myeloperoxidase (MPO) is an enzyme found in certain immune cells, particularly neutrophils, which play a role in the body's defense against pathogens. It generates reactive oxygen species (ROS) as part of the immune response. The activation of caspases, a family of protease enzymes, is a crucial step in the process of apoptotic cell death. The involvement of MPO-mediated caspase activity in apoptotic cell death can be explained as follows:

1.   Reactive Oxygen Species (ROS) generation: MPO produces ROS, including hydrogen peroxide (H_2O_2) and hypochlorous acid (HOCl), as byproducts of its activity(Mütze et al., 2003). These ROS can induce oxidative stress and damage cellular components.

2.   Activation of Caspases: The increased levels of ROS generated by MPO can trigger various signaling pathways, leading to the activation of caspases(Parrish et al., 2013). Caspases are initially present as inactive procaspase forms. However, under conditions of oxidative stress, specific caspases, such as caspase-9 and caspase-3, can undergo activation through proteolytic cleavage.

3.   Mitochondrial Dysfunction: ROS generated by MPO can cause mitochondrial dysfunction. This can lead to the release of cytochrome c, a protein normally located in the

mitochondria, into the cytosol. Cytochrome c forms an apoptosome complex by binding to the apoptotic protease activating factor 1 (Apaf-1) and ATP (Garrido et al., 2006).

4.   Formation of Apoptosome Complex: The apoptosome complex, consisting of cytochrome c, Apaf-1, and ATP, promotes the activation of caspase-9. The execution phase of apoptosis begins when activated caspase-9 cleaves and activates downstream caspases, such as caspase-3(Brentnall et al., 2013).

5.   Execution of Apoptosis: Upon activation caspase-3 cleaves various cellular substrates, including structural proteins, enzymes, and DNA repair proteins(McIlwain et al., 2013). This results in the characteristic morphological and biochemical changes associated with apoptosis, such as cell shrinkage, chromatin condensation, DNA fragmentation, and membrane blebbing.

CP binding to MPO in the presence of hydrogen peroxide, prevents the oxidation of chloride and other halide ions to produce hypochlorous acid. Previous Studies have shown that MPO released from the neutrophil granules at an inflamed site do not exit to the plasma on their own and require CP-MPO binding. Neutrophils release neutrophil-derived oxidants such as super-oxides, hydrogen peroxide (H_2O_2) and hypochlorous acid (HOCl) as a mechanism of anti-tumor cytotoxicity (Singel & Segal, 2016). CP binds to MPO and regulate its activity modulating the production of HOCl by MPO. CP may act as an inhibitor by reducing the availability of copper, a cofactor required for MPO enzymatic activity, thus limiting the generation of HOCl(Chapman et al., 2013). By inhibiting HOCl production, CP may help regulate the potentially harmful effects of excessive oxidative damage and protect the cancer tissues from oxidative stress. However, the exact mechanism and significance of CP-MPO interaction in the context of apoptosis or other cellular processes require further research and investigation.

A number of crystallographic studies have been carried out to elucidate CP structure owing to the nature of function of the protein. CP is a 1065 amino acids protein with 6 domains and a multi copper active site. The copper at the tri nuclear center plays an important role in the oxidoreductase activity of CP. According to studies, MPO binds to two main 21 amino acid sequences, and the application of the Anti-P18 antibody prevents the CP-MPO association while preserving the enzyme's activity. P18 and P76, two significant binding sites, were reported (Bakhautdin et al., 2014)(Figure 23).
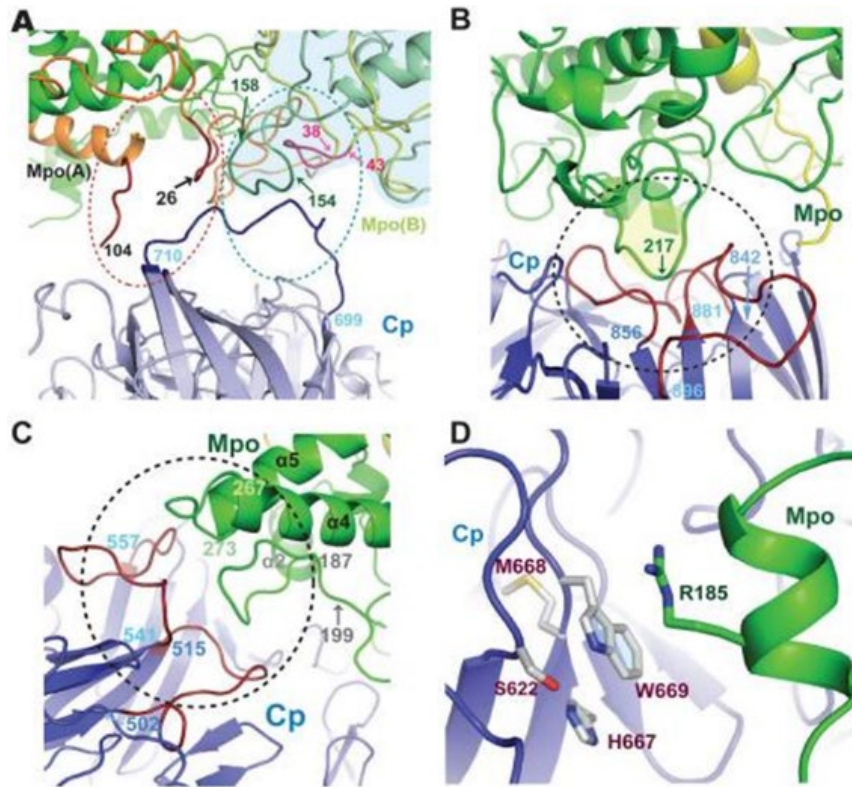
Figure 23. Interacting amino acids in ceruloplasmin-myeloperoxidase complex (Samygina et al.) (A) Interaction zone between the N-terminal of the MPO light chain and the loop spanning residues 699 to 720 of Cp.(B) Interaction of the loop comprising residues 699 to 720 of Cp with a symmetric monomer of MPO. The symmetrical Cp molecule is omitted for clarity.(C) Contact region involving loops spanning residues 542 to 557 and 618 to 624 of Cp.(D) Proximity to the phosphorylated-PD (p-PD) site of Cp within domain 4. Residues M668, W669, and H667 are depicted in stick representation.

2.3.4. Ceruloplasmin in tumors

Clear-cell renal cell carcinoma (ccRCC) histological grade and lymph node metastatic stage were found to be related to CP overexpression(Y. Zhang et al., 2021b). It was noted to be associated with poorer survival rates along and was observed to play a role in oncogenic pathways in clear-cell renal cell carcinoma (Y. Zhang et al., 2021c). Patients diagnosed with nasopharyngeal carcinoma exhibit elevated levels of CP expression in both their serum and tumor tissues compared to healthy individuals(Doustjalali et al., 2006). In a study, it was discovered that CP acts as a novel adipokine that shows increased expression in adipose tissue of obese individuals and in cancer cells associated

with obesity(Arner et al., 2014). One study indicated that the activity of the CP promoter is markedly increased in ovarian cancer, suggesting its potential as a promising cancer-specific promoter for the development of new gene therapy approaches targeting ovarian cancer. Through deletion studies, it was determined that an activator protein-1 (AP-1) site within the CP promoter plays a crucial role in regulating its activity. Activation of the CP promoter was observed upon treatment with 1-O-tetradecanoyl phorbol-13-acetate, an activator of c-Jun, while inhibition of c-jun by SP600125 resulted in suppression of the CP promoter. Additionally, the AP-1 site in the CP promoter was found to specifically interact with c-Jun both in laboratory experiments and *in vivo*. Immunohistochemical analysis of human ovarian cancer samples revealed a significant correlation (r = 0.7, P = 0.007) between the expression levels of c-Jun and CP. In a xenograft mouse model carrying SKOV3.ip1 tumors, the CP promoter demonstrated notably higher activity in the tumors compared to normal organs(C. M. Lee et al., 2004). These findings highlight the potential of the CP promoter as a target for ovarian cancer-specific gene therapies and highlight the involvement of c-Jun in its regulation. CP mRNA expression has been reported to be significantly higher in early invasive Lung adenocarcinoma(Matsuoka et al., 2018).

CP is a predictive biomarker for breast cancer that corresponds with immune infiltration(F. Chen et al., 2021). CP expression in renal cell carcinoma correlates with higher-grade and shortened survival(Zimpfer et al., 2021).

Aceruloplasminemia, which results in iron accumulation and tissue damage and is linked to diabetes and neurologic disorders, is brought on by mutations in this gene. This gene has two transcript variants, one of which codes for proteins and the other not.[Provided by RefSeq, Feb 2012](gEPIA) (M. Y et al., 2021).

One study reported that the long non-coding RNA (lncRNA) ceruloplasmin (NRCP) exhibits significant upregulation in ovarian tumors. The observed that knockdown of NRCP in cancer cells led to notable increases in apoptosis, decreased cell proliferation, and reduced glycolysis compared to control cancer cells(Rupaimoole et al., 2015).

CHAPTER 3

RESULTS AND DISCUSSION

i) Gene expression analysis of ceruloplasmin in Oral cancer patients from TCGA database and its correlation with metabolic associated genes

Part 3.1: CP expression and interaction

On analysis of the HNSCC patient's mRNA Expression on cbioportal we found 440 samples out of total 538 patients did not show alteration in CP while 90 patients showed alterations in CP. The volcano plot of the CP altered vs unaltered showed that the patients with CP alteration had alterations in a number of cancer progression related genes(Brlek et al., 2021). (CP Mean log2 expression in the altered group=7.02, standard deviation= 3.34 while that in unaltered group = 6.17, std. deviation=3.03)(Figure 24).

We highlighted a few genes that are altered in higher percentages in the CP high patients such as PIK3CA with 85% alteration in CP altered patients in comparison to just 23% alteration in the unaltered patients. PIK3CA is an unrefuted oncogene that has been previously studied to be linked to tumor metastasis(Karakas et al., 2006).
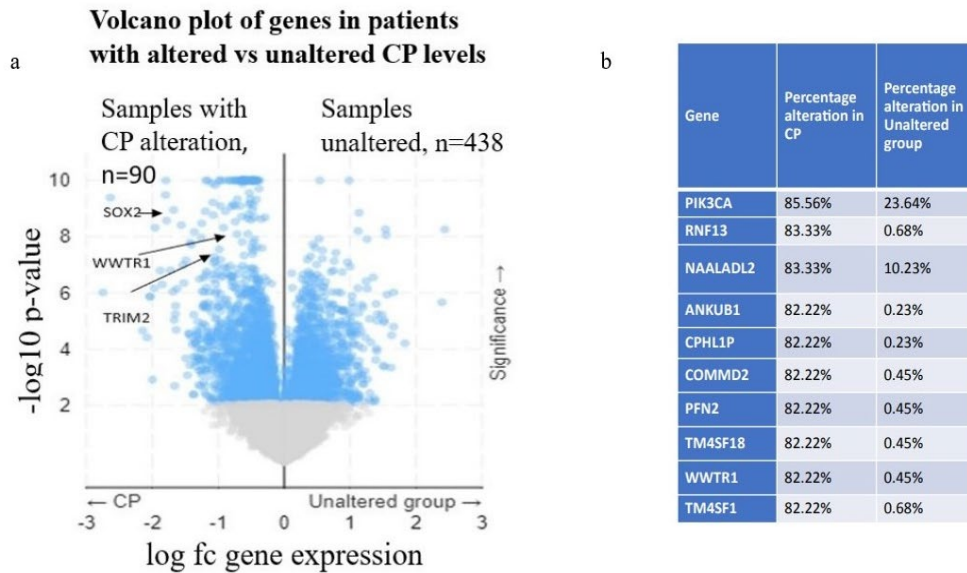
Figure 24. (a) Volcano plot showing CP alteration in TCGA HNSCC dataset. (b) A comparison of genes altered in CP altered vs unaltered patients. *From amongst a number of genes*

altered in CP altered patients SOX2,WWTR1, PI3KCA and TRIM2 are highlighted as are important cancer related genes.

The Protein expression (RPPA) analysis revealed the most significant altered protein in CP altered patients was CHEK2. CHEK2 has been associated with cancer risks. An increased CHEK 2 expression has been associated to an increased chance to develop female breast cancer, colorectal cancer, and possibly other cancers(Koen et al., 2022)(Figure 25).
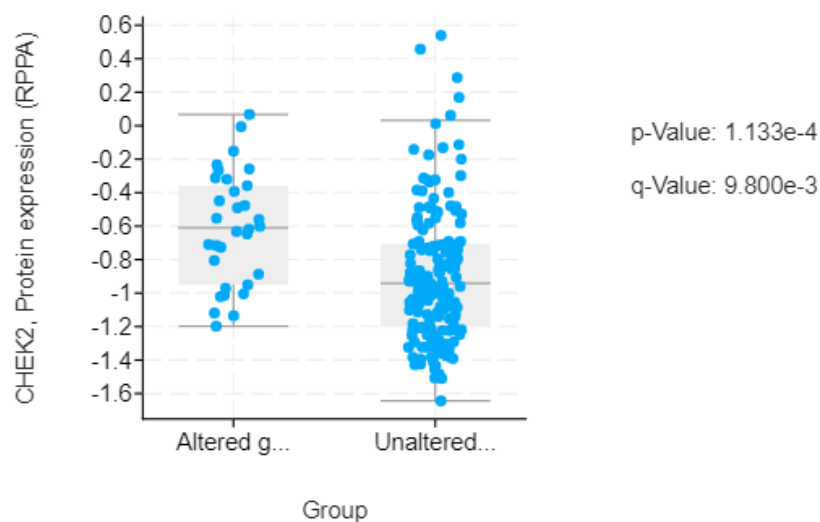
Figure 25. RPPA analysis of patients with ceruloplasmin alteration. The protein expression of CHEK2 is higher in individuals with ceruloplasmin alteration.

3.1.1. CP expression and Copy Number Variation:

On plotting the log2 expression values of CP in tumor vs normal patients we found the CP expression increased in the later stages as well later grades of Oral Cancer (Figure 26a, b). The copy number alteration also confirmed with the gene expression levels of CP (Figure 26c, d). Differential site wise analysis showed the highest expression of CP in the tissues from the base of the tongue followed by the lip tissues then tonsil while the lowest was observed in the tissues from the alveolar ridge. (Figure 26e)
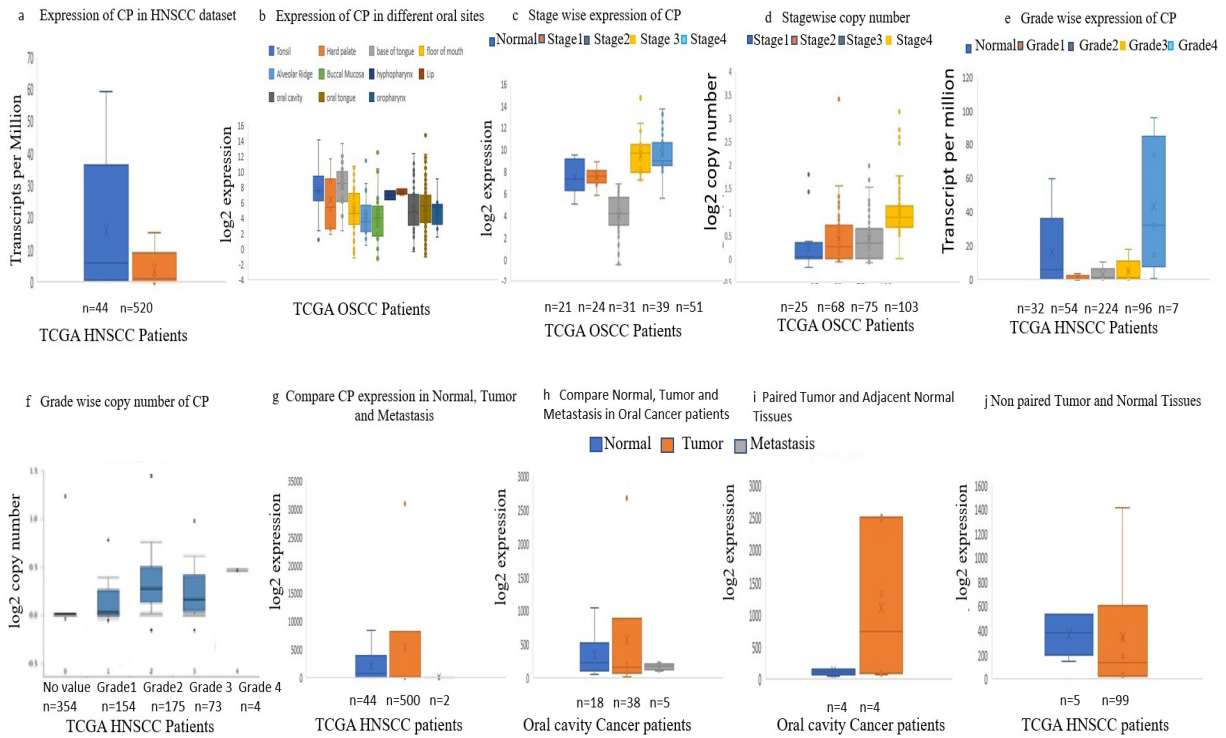
Figure 26. Expression and copy number variation of Ceruloplasmin in Oral Cancer Patients: a) CP gene expression in normal vs tumor b)Site-wise analysis of CP expression in OSCC patients, c)Stage-wise expression of CP, d) Stage-wise copy number variation, e) Grade-wise expression f)Grade-wise copy number variation)CP expression in metastatic tissues in HNSCC ,h)CPO expression in metastatic tissues in OC patients ,i) in paired tissues, j) non paired normal and tumor tissues). CP expression and copy number is higher in the later stages and grades of OC. The tissues samples from the lip showed the highest expression for ceruloplasmin.

3.1.2. Differentially expressed genes:

The log2 FC calculated for a list of 120 genes using R, were used to plot a heatmap. This heat map showed correlated expression of a number of cancer progression related genes (Figure 27). For instance, Notch1 showed correlated expression to CP. MAPK13 that was up regulated in tumors showed expression similar to CP suggesting a possible interaction. Similarly, metabolism related gene HK 1 also is up regulated in oral cancer tumors. It has been discovered that CP expression is connected with the expression of genes involved in tumor migration, including NOTCH 1, MAPK

13, CLDN 1, MMP 11, MMP 2/9, VEGFA, FAT 1, and TIAM 1, as well as other genes that promote tumor growth and invasion. In OSCC, FOXP 2 expression has been discovered to be downregulated, and its decreased expression is known to encourage tumor migration(M. T. Chen et al., 2018). An upregulated gene called TNF, which is linked to cell survival and proliferation, has been discovered in OSCC(H. L. Yang et al., 2014). FGG, whose expression is down regulated in OSCC patients, is another gene whose down regulation encourages tumor spread(M. Wang et al., 2020). One of several CC cytokine genes that secretes proteins implicated in inflammatory and immunoregulatory processes, the CCL19 gene has linked expression to CP(X. Zhang et al., 2017).
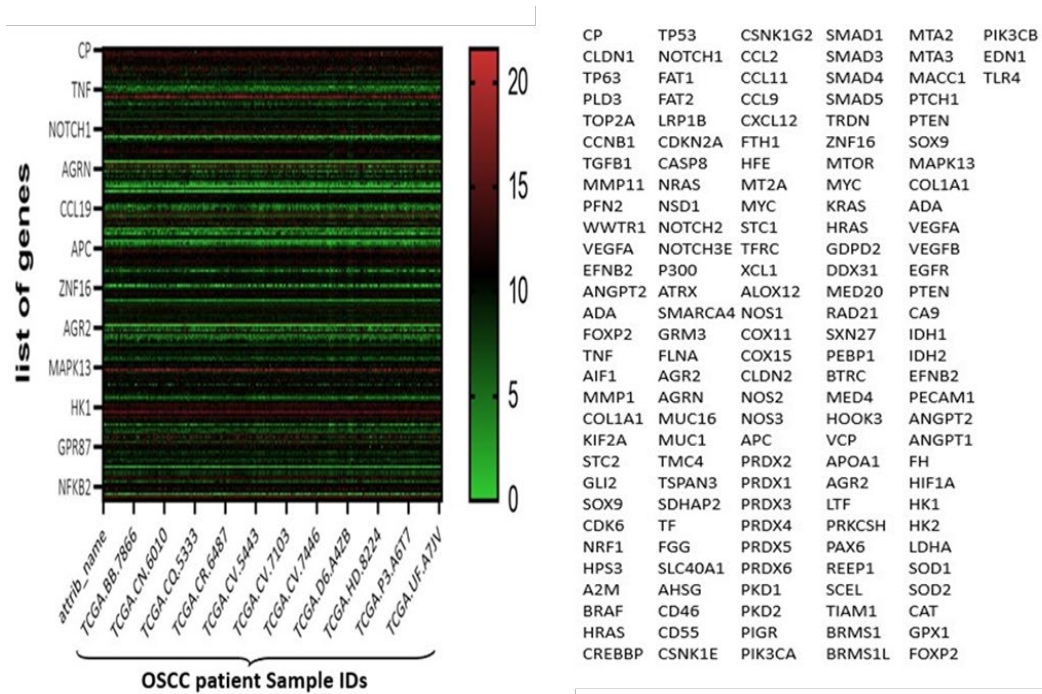
Figure 27. Gene expression heat map of various Oncogenes with ceruloplasmin in oral cancer patients. A number of other cancer progression and metastasis related genes such as VEGFA, NOTCH1, AGRN, MAPK13 are showing upregulated expression in correlation to CP expression.

3.1.3. Network analysis

We analyzed 50 genes for interaction with CP using GENEMANIA. 15 neighboring genes were found to be co-expressed with CP. CP was found to interact with LTF which plays a role in NFκB signaling. Another interacting protein can be seen is MMP9. FGG and CP are seen to share

the same function of negative regulation of apoptosis(Hoesel & Schmid, 2013) (Figure 28a). HIF-α1-alpha transcription factor network pathway documented by PID Pathways shows CP as one of the nodes in the HIF1A signaling and is observed to interact with VEGFA. This suggests CP plays an important role in this oncogenesis-associated pathways such as the HIF- α1 signaling pathway. Previous studies have reported CP is capable of regulating the HIF-2α activity via an iron/PHD cascade-dependent pathway(YM et al., 2020). This is in confirmation with observation reported by researchers that on inhibition of CP proteasomal degradation, angiogenesis could set in by HIF-1α and VEGF24 regulation.
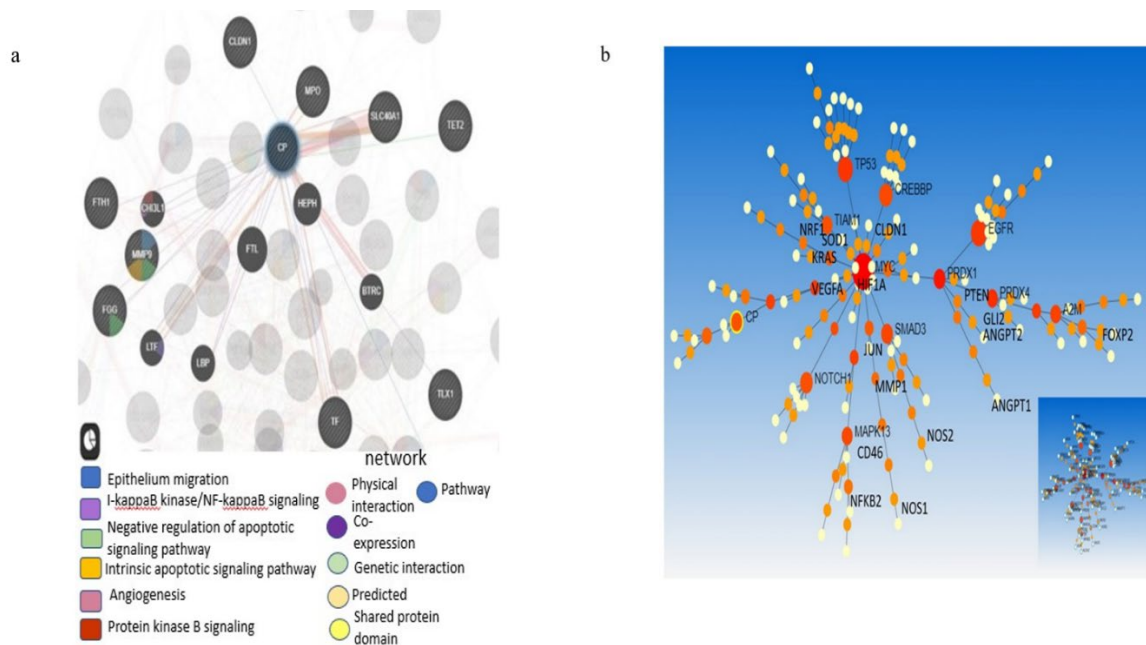
Figure 28. (a) Gene interaction network generated using Gene mania on the basis of functional annotation, (b) Cytoscape network showing CP interaction in HIF1a signaling. FGG plays a role in suppressing apoptosis and is found to show gene-gene interaction with CP. Genes related to epithelial migration such as MMP9 are also interacting while TF gene coding for transferin is showing co expression.

SLC40A1, TF, HEPH, and HMOX1 are four genes involved in iron metabolism that CP was found to interact with(Sukiennicki et al., 2019), also MMP9 that plays a role in epithelial migration (Deryugina & Quigley, 2006) and LTF in NFκB signaling. MMP9, FGG have also been associated to negative regulation of apoptotic signaling pathway and have been seen to interact with CP

(Arnould et al., 2009). CH3L1 an important angiogenesis and protein kinase B signaling pathway protein also shows protein-protein interaction with CP. This Protein-protein interaction of CP was observed on plotting string interaction networks on cytoscape. CP also interacts with genes involved in ferroptosis, tumor metastasis and cancer progression related genes, and oncogenes as well as redox metabolism associated genes (Figure 29).
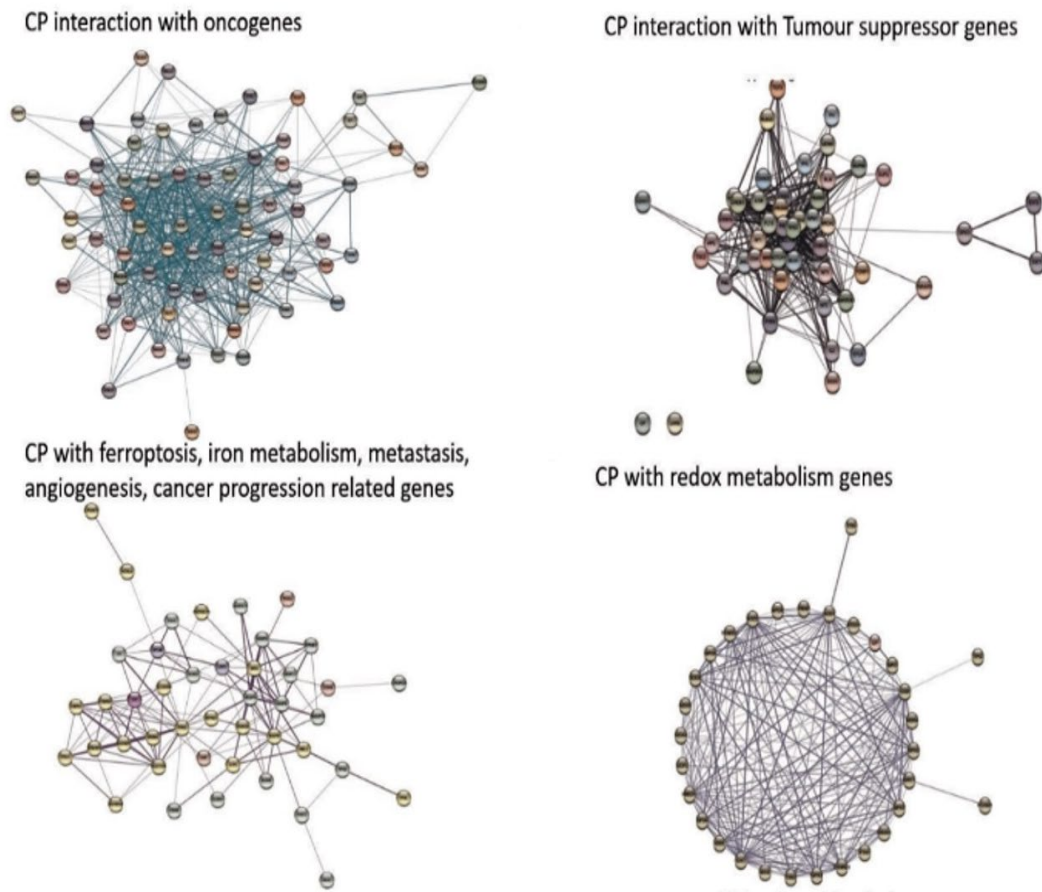
Figure 29. String and Cytoscape network analysis of CP interaction with a) oncogenes, b) tumor suppressor genes, c) interaction with angiogenesis, tumor metastasis related genes, and genes involved in iron metabolism, ferroptosis and complement system, d) oxidative stress related genes interacting with CP.MYC,HRAS,JUN,NOTCH1,Tiam1 are amongst the oncogenes showing PPI with CP while the tumor suppressors are not showing any interaction with CP.MF,CD46 and FLNA of the complement system interact with CP .FGG,MAPK13,VEGFA and the matrix

metalloproteases are amongst the migration promoting genes interacting with CP.irom metabolism related genes are also involved in PPI with CP.

Previous studies have reported high CP to result in increased IL-8 secretion (Kennedy et al., 2012). Also, there is evidence for CP-PDPK1 interaction which is responsible for AKT phosphorylation that plays a role in various pathways of cancer cells(Gagliardi et al., 2018). This provides evidence for role of CP in cancer progression by interacting with various cancer signaling related genes.

3.1.4. CP methylation:

Given the role of DNA methylation in cancer progression, the aberrant methylation of CpG sites holds promise as potential markers for disease initiation(Łuczak & Jagodziński, 2006). We analyzed CP methylation status. We identified the CpG site **cg094575255** to be significantly hyper methylated. We observed differential methylation of this site in the high-risk Oral cancer patients and it correlated to poorer survival(Figure 30).
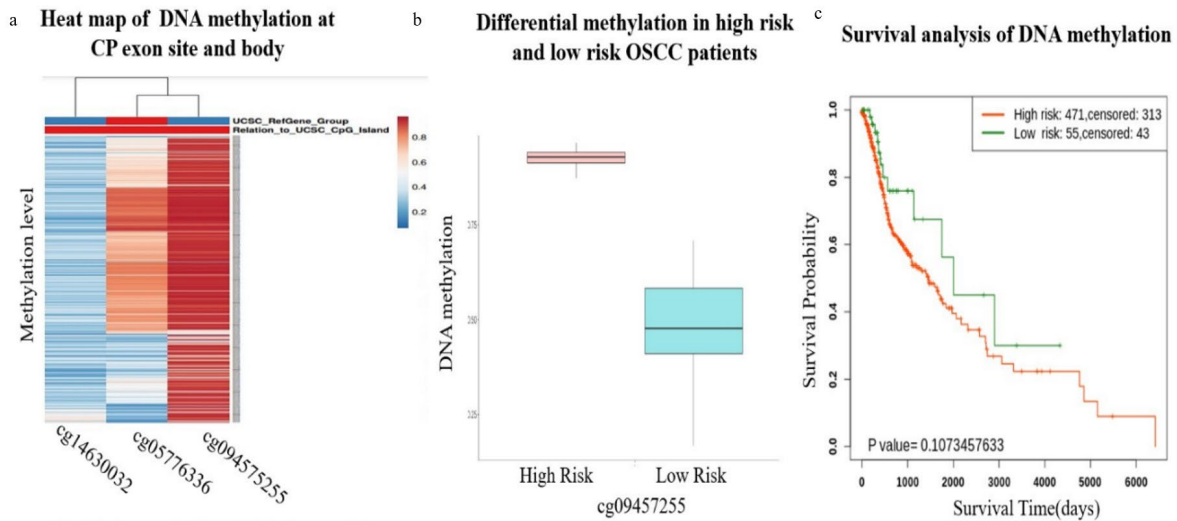
Figure 30. Heat map of CP methylation, b) differential CGP methylation in tumor vs normal, c) Impact of methylation on survival of patients. *The CpG site cg094575255 is identified to be hypermethylated differentially in tumor vs normal samples and correlated to lower survival probability. In figure 30a Red shows hypermethylation.*

3.1.5. Immune Cell Infiltration:

CP expression was observed to be linked to the expression levels of various immune cell types. High CP expression corresponded to low tumor immune infiltrating levels such as low CD8 T cells and CD4 T cells which accounts for the aggressive Oral cancer phenotypes (J. Ma et al., 2019) (Figure 31a). CP expression was observed to be positively correlated to PD-L1, CTLA-4, LAG-3, and TIM- 3 which are established negative regulators of immune response(Han et al., 2020)(Andrews et al., 2017)(Das et al., 2017) (Figure 31b). Due to this the overexpression of CP is associated to immunosuppressive role and with shorter survival. CP shows correlated expression to various immune checkpoints which could be targeted to enhance the immune response of patients limiting the tumor growth(Y. Zhang & Zhang, 2020). Therefore, CP may serve as a biomarker for the immune-related gene prognostic index in patients with oral cancer.
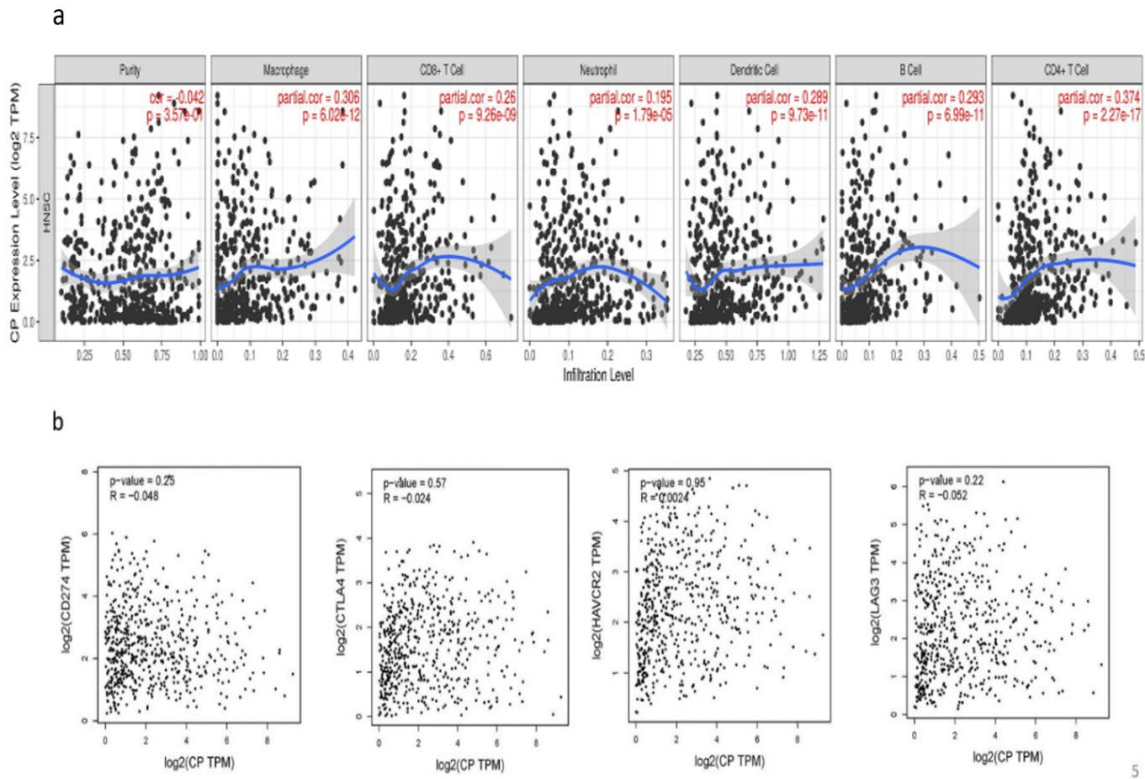
***Figure 31. a) CP expression levels in relation to tumor immunological infiltration of key immune cells, b) Expression of Negative regulators of immune response in relation to CP expression.** A lower expression of CD8+T cells and CD4+T cells in observed to be downregulated when CP expression increases.*

3.1.6. Survival Analysis:

On plotting the Kaplan-Meier survival plot for CP expression we found that the high expression of CP correlated to a worse survival (HR=1.99; p=0.14) as well as high CP mutation also was associated to reduced survival (HR=0, p=0.47) in Oral cancer patients(Figure 32).
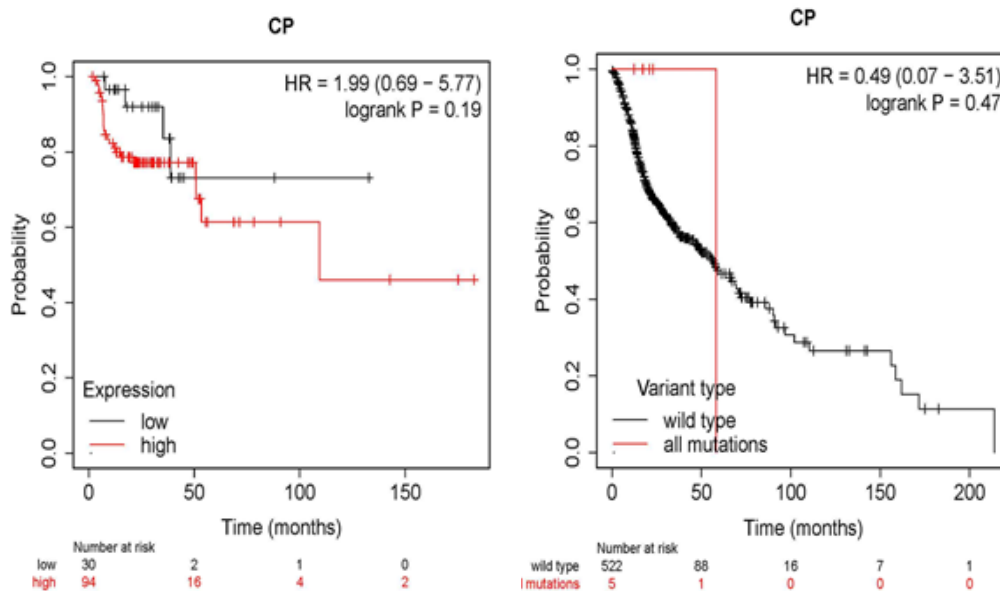
Figure 32. Survival plots for High CP expression and CP mutation. *A higher CP expression as well as mutation resulted in a lower survival of patients with time.*

Discussion of Part 3.1.

Using bioinformatics analysis, we examined the expression patterns, copy number variation, gene interactions, survival analysis, DNA methylation, and associations with immune infiltration in OSCC patients in this study. We discovered genomic changes in the CP gene in 90 patients by cBioportal analysis of the Head and Neck Squamous Cell Carcinoma TCGA, Firehose Legacy Dataset, and we also discovered changes in numerous additional oncogenes in CP altered individuals. In early cancer clinical stages and pathological grades, we found that the expression of CP mRNA and protein was downregulated; in later tumor grades and stages, it was shown to be upregulated (Figure 26). Furthermore, in patients with oral cancer, CP expression seems to be linked to metastasis and demonstrated a higher CP in paired tumor and neighboring normal.

CP expression has been observed to be connected with the expression of NOTCH 1, MAPK 13, and other genes that promote tumor invasion and development, including CLDN 1, MMP 11, VEGFA, FAT 1, MMP 2/9, and TIAM 1(Figure 27 and 29). In OSCC, FOXP 2 expression has been discovered to be down regulated, the result of which is known to encourage tumor migration. TNF, a gene linked to cell survival and growth, has been discovered to be elevated in OSCC. FGG, whose expression is downregulated in OSCC patients, is another gene whose downregulation encourages tumor spread. Oncogenes like HRAS and MYC are inversely connected with CP, whilst genes involved in glucose metabolism like HK1 have been found to be positively correlated to CP overexpression. One of the CC cytokine genes that secretes proteins involved in inflammatory and immunoregulatory processes is CCL19. In cervical cancer, increased CCL19 expression has been linked to tumor development(X. Zhang et al., 2017). Through the WNT signaling pathway, AGRN progression encourages the proliferation in rectal cancers as well as promotes tumor invasion, and migration(ZQ et al., 2021). An association between the expression of CP and inflammation has been suggested by the observation that NFκB2 is elevated while the tumor suppressor gene APC is down regulated.

Aberrantly methylated CpG sites can function as potential markers in OSCC because DNA methylation has been shown to affect gene expression(Bertucci et al., 2017) . Upregulated DNA methylation in CpG sites in tumor patients suggests an increased methylation level at specific genomic regions. This can potentially lead to gene silencing or altered gene expression patterns, which may contribute to the development or progression of the tumor. The CpG site cg09457255 that we found to have significantly altered methylation within tumor cells when compared to normal samples has been associated with a poor prognosis in individuals with HNSCC (Figure 30).

The interaction of CP with several oncogenes and genes related to oxidative stress is supported by numerous text mining and database analyses (Figure 28). Additionally, CP has been shown to participate in oncogenesis-related pathways, such as the HIF-α1 signaling pathway and to control HIF-α2 activity via an iron/PHD cascade-dependent mechanism(Tsai et al., 2020). It has been observed that under hypoxic conditions, the expression of CP, vascular endothelial growth factor (VEGF), and glucose transporter 1 (Glut-1) is upregulated as well as transcription of the CP gene promoter(M. F et al., 2005). According to a study on colon cancer, inhibiting CP's proteasomal degradation promotes angiogenesis via controlling the production of HIF-1 and VEGF(Dai et al., 2016).

By controlling iron homeostasis in hepatocellular carcinoma (HCC) cells, the previously identified glycoprotein CP plays a crucial role in iron homeostasis and suppressing ferroptosis, a type of cell death characterized by the iron-dependent accumulation of lipid hydroperoxides. Researchers found that overexpression of CP in HCC cells suppressed erastin- and RSL3-induced ferroptosis while CP depletion promoted erastin- and RSL3-induced ferroptosis cell death and led to the accumulation of intracellular ferrous iron ($Fe2+$) and lipid reactive oxygen species (ROS).L-type Ca2+ channels (LTCC) have been discovered as prospective therapeutic targets to lessen the harmful consequences of too much iron(Oudit et al., 2006). Dysregulated iron metabolism has been identified as a prognostic factor in cancer.

CP expression and CACNA1C, which codes for the calcium voltage-gated channel subunit, are positively correlated in Gepia, with the exception of the PPI interaction shown in figure 28. Additionally, CACNA1C is elevated in OSCC patients. Additionally, it has been discovered that CP is adversely linked with the invasion of CD8+ T cells. CP reduces ferroptosis because CD8+ T lymphocytes promote ferroptosis. In the presence of high CP, Interferon-gamma (IFN-ɣ), a different pleiotropic molecule linked to antiproliferative, pro-apoptotic, and antitumor mechanisms(Castro et al., 2018a), is suppressed, leading to more HIFα2 inducing arginase1 expression and NO production(Keith et al., 2012). In prior investigations, it was discovered that ARG1 has an oncogenic role in the development of HCC by accelerating the EMT process(You et al., 2018). The CP transcript is selectively silenced during IFN- activation via a cis regulatory element known as the GAIT element, which is a gatekeeper of the expression of inflammatory genes(R. Mukhopadhyay et al., 2009). HIF-2 (hypoxia-inducible factor-2) has also been discovered to be crucial for the development and spread of tumors(Roig et al., 2018). Neutrophil granules release LF and MPO when there is inflammation(AV et al., 2014). According to earlier research, CP is a gene involved in the inflammatory response. Increased CP expression was strongly correlated with low tumor immune infiltration levels, according to TIMER analysis (Figure31). It has been discovered that a number of immune cells in the TME are linked to metastasis, recurrence, and prognosis supporting cancer start and progression. In numerous malignancies, it has been demonstrated that targeting immunological check points is effective(Z. Y & Z, 2020). We discovered that the HAVCR2, IDO1, LAG3, PDCD1LG2/PDL2, TIM3, and negative regulators of T-cell immune response were overexpressed in the CP-high samples. As a result of this immunosuppressive function, excessive expression of CP is linked to a shorter survival time. Low CD8 T cells, low CD4

T cells, high B cells infiltration, M0 macrophages, M2 macrophages, as well as suppressive immunity and more aggressive phenotypes have all been linked to high CP expression.

Under hypoxic conditions the CP gene promoter transcription is induced leading to increased CP expression (M. F et al., 2005). The role of CP in conversion of Fe2+ to Fe3+ suppresses ferroptosis and inactivates the PHD1/2 leading to increased VEGFA and HIF2a which favors tumor progression. When CP expression is low MPO is high which results in increased oxidative stress promoting cancer progression. However, in the later stages of cancer CP is highly expressed leading to MPO inhibition which maybe a cancer cells mechanism of countering increasingly toxic oxidative stress. At low CP levels Erastin and RSL3 have been reported to induce ferroptotic cell death resulting from Fe2+ accumulation of and lipid reactive oxygen species (ROS) (Sukiennicki et al., 2019). However, at high CP levels erastin- and RSL3-induced ferroptosis is suppressed in HCC cells. We propose a similar mechanism of working of CP in Oral cancer patients. CP has been observed to show correlated expression with CACNA1C which codes for the L-type Ca2+ channels(Sukiennicki et al., 2019) (LTCC) which play a role in dysregulated iron metabolism in cancer cells and are potential therapeutic targets(Shang et al., 2020b). The negative correlation of CP with CD8+ T cells confirms the role of CP in ferroptosis suppression as CD8+ T cells have been reported to enhance ferroptosis. Interferon-gamma (IFN-γ) that works in antiproliferative, pro-apoptotic manner has been studied to be suppressed by CP which results in high HIF2α(Castro et al., 2018b).This increased HIF 2α levels result in arginase accumulation which promotes EMT making tumors more aggressive and undifferentiated (You et al., 2018). In case of inflammation neutrophil granules secrete LF and MPO .CP has been previously identified as an inflammatory response gene and works to inhibit MPO in the later tumor stages when inflammation sets in(AV et al., 2014). In our study we identified the miRNAs targeting CP, of which mir21 has important cancer related gene associations. mir21 expression also confirmed with CP expression levels in our queried dataset. This could be further explored for development of better Head and Neck cancer targeted therapy.

Interaction with CP inhibited peroxidase activity of Myeloperoxidase (MPO) under physiological conditions preventing HOCl production by MPO in the Tumor-Associated Neutrophils in tumor microenvironment(Masucci et al., 2019). This suppresses HOCL-mediated

caspase activity that leads to apoptosis which may be a mechanism of tumor survival in the later tumor stages. We also reported using Tumor Immune Infiltration analysis that the High CP expression shows correlated expression to PDL1 and TIM3 that activate NETosis (Kaltenmeier et al., 2021). These neutrophil extracellular traps have been previously studied to promote tumor metastasis. Furthermore MPO-CP binding prevents CP from proteolytic degradation. Therefore, we aim to target CP's immune regulation in head and neck cancer patients.

Part 3.2: miRNA expression analysis in head and neck cancer patients:

3.2.1. Differential miRNA expression

Starting from profiles retrieved by GDC portal we selected several miRNAs differentially expressed between control and HNC patients. The volcano plot in Figure33 shows the significant up regulated as well as downregulated miRNA in head and neck cancer patients. Specifically, we selected 39 upregulated miRNA and 40 downregulated, with log2FC>2 and p values <0.000005.
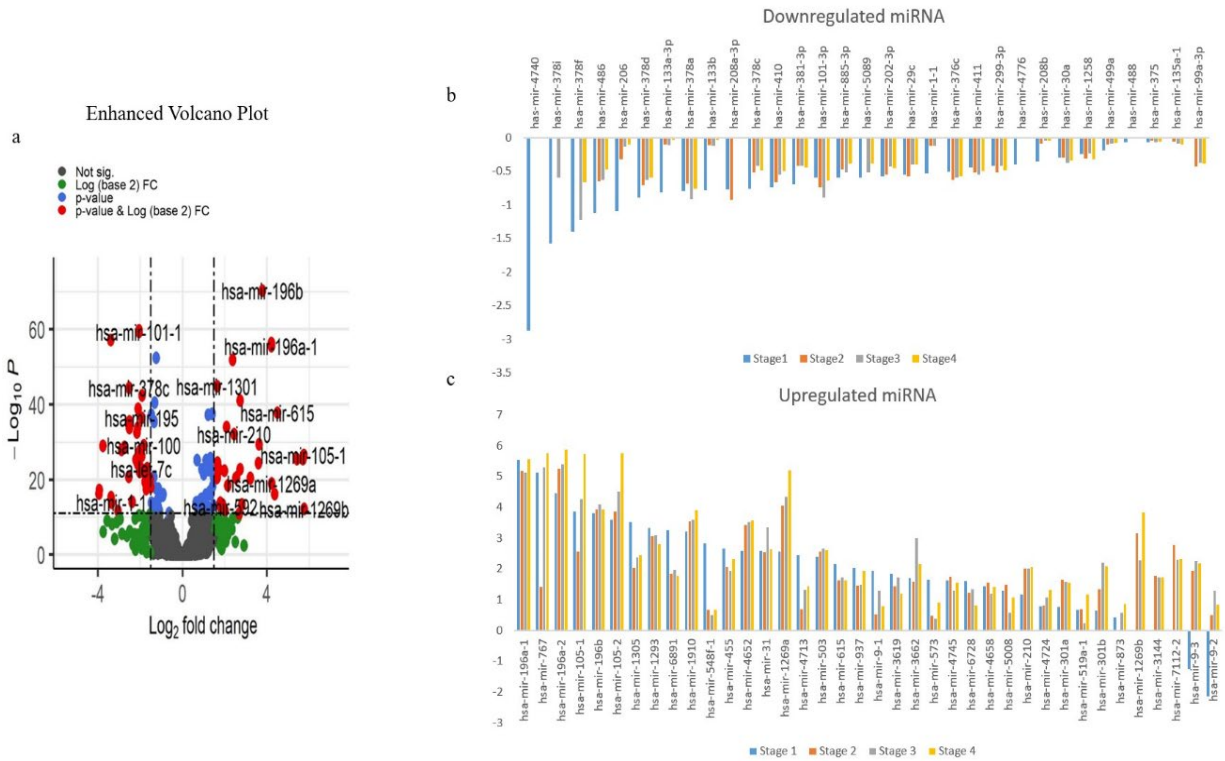
Figure 33: a) A volcano plot of FC vs P value of HNC miRNA expression, b) Stage wise down regulated miRNA in HNSC patients. c) Stage wise up regulated miRNA in HNSC patients.

We obtained the miRNA expression in the different stages of Head and Neck cancer patients and found that the miRNA expression varied across the different tumor stages. A higher number of miRNAs were down regulated in the patients in the Stage 1VB (Figure 33b, c). We found Hsa- mir-

378i to be downregulated with a fold change of 3.93 on comparison of normal samples to tumor samples of stage 1 as well as stage 3.Similarly, we observed hsa-mir-105-1, mir-196a, mir-767 one of the most upregulated miRNA to show the highest FC in stage 4 cancer patients.

3.2.2. Predicted miRNA targets:

The miRNA targets predicted from various online databases were used to build a network of interaction between the differentially expressed miRNAs and their target genes. The analysis of the upregulated miRNAs target network shows the target genes are mostly tumor suppressor genes such as CDKN1A, SMAD7, GFBR2, PDCD4, TIMP2, TP53, PTEN, CCDN1, BCL10 and IL10 (Figure 34). Similarly, a few highlighted targets of the downregulated miRNA include MAPK3, NRAS, HRAS, EGFR, CDK14, MET, MMP28, MYC which are previously reported oncogenes (Woodman & Mills, 2010) (Figure 35). Figure 34b highlights the tumor suppressor genes targeted by the upregulated miRNA. A few miRNAs can be seen to target multiple genes and similarly a number of genes are targeted my multiple miRNAs. These genes could be those involved in important processes and can be further explored as potential head and neck cancer targets.

Figure 34. Network of upregulated miRNA targets. Programed cell death related gene PDCD4 and tumor suppressor PTEN are amongst the targets of the miRNA.
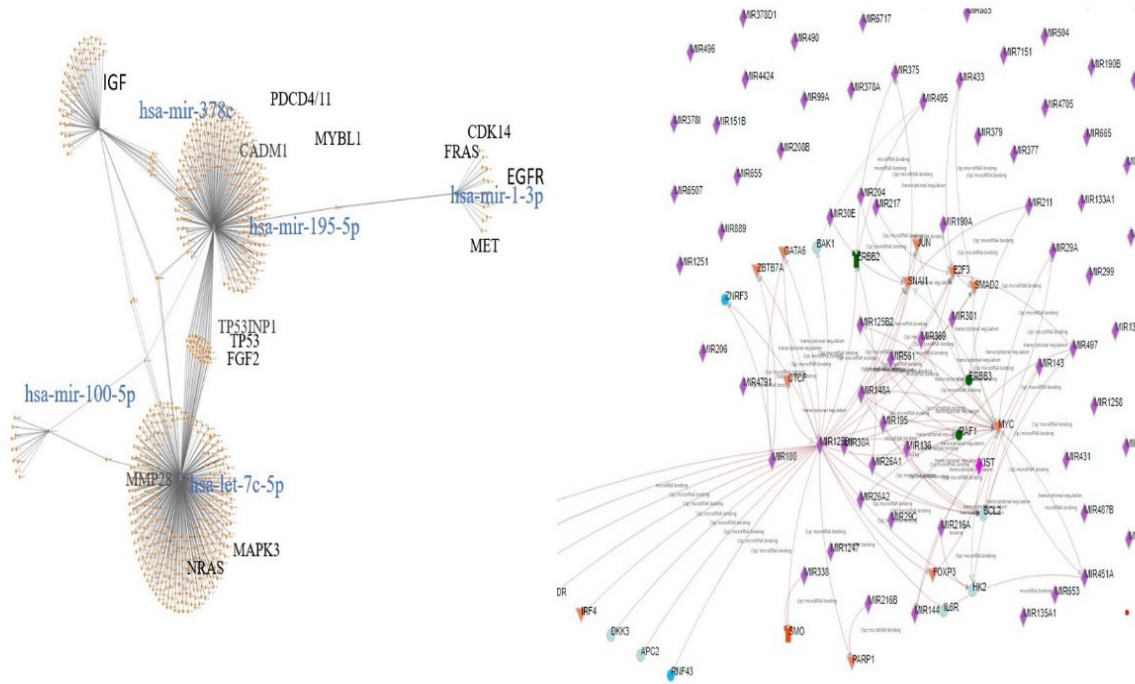
Figure 35.Network of downregulated miRNA targets. Oncogenes like MYC,SMAD2,SNAIL 1 and zinc factors are amongst the targets of the downregulated miRNA in oral cancer.

3.2.3. Experimentally validated miRNA targets:

Using Cytopscape, we created a network of the miRNA targets that have undergone experimental validation. We calculated the top downregulated and upregulated miRNAs with the highest degrees for each network's nodes (Figure 36a,b).Most genes are targeted by the upregulated and downregulated hsa-mir-301-3p. We also discovered the genes associated with the greatest number of upregulated miRNAs, with a confidence level of at least 8, or two times the average degree of elevated miRNA targets (4). Similarly, taking into account the average node degree of 5, we found the downregulated miRNA targets with degrees more than 10.Figure 36 c displays the genes that the most downregulated miRNAs target, with Vascular Endothelial Growth Factor A(VEGFA) and Ras GTPase-activating protein-binding protein 2 (G3BP2) are amongst among the genes that were most frequently targeted by the down regulated miRNA and thus allegedly up

regulated in HNC patients. According to Sa-nguanraksa and O-charoenrat (2012), VEGFA is an oncogene important for angiogenesis, vasculogenesis, and endothelial cell growth. Its upregulation is linked to endothelial cell proliferation and cell migration. According to Gupta et al. (2017), G3BP2 regulates SART3, the expression of the pluripotency transcription factors Octamer-binding protein 4 (Oct-4) and Nanog Homeobox (Nanog), as well as subpopulations of breast cancer cells(N. Gupta et al., 2017). Polypyrimidine tract-binding protein (PTBP1) has been identified as a pro-oncogenic component that has been linked to enhanced malignancy in some research on breast and bladder cancer(He et al., 2014). Tyrosine-protein phosphatase non-receptor type 4 (PTPN4), one of the genes targeted by the elevated miRNA, is important for immunity; hence, a number of uncontrolled miRNA targeting this gene ensures decreased immunity. Furthermore, STAT3 activation due to PTPN4 depletion has been shown to enhance tumor growth in colorectal cancer(B. D. Zhang et al., 2019). Another heavily targeted gene is ZNF711, whose reduction of JHDM2A and SLC31A1 in ovarian cancers has been linked to cisplatin resistance(G. Wu et al., 2021). Neuropilin-1 (NRP1), an immunoregulatory receptor, is a gene that is targeted by more downregulated than upregulated MIRNA, and regulatory T cells enriched with these receptors are seen in a variety of malignancies. This gene is an important TME checkpoint as well as a potential immunotherapeutic target(Chuckran et al., 2020). Other frequent target genes include the proto-oncogene MET and MCL1, whose overexpression is linked to both a poor prognosis and medication resistance(H. Wang et al., 2021)(Gherardi et al., 2012). In line with previously reported findings that NPTX1 upregulation inhibits tumor proliferation and migration, we discovered that NPTX1 was being targeted by higher upregulated miRNA in HNC patients. Chemotherapy is ineffective against the tumor because NPTX is downregulated (J. Wu et al., 2022).
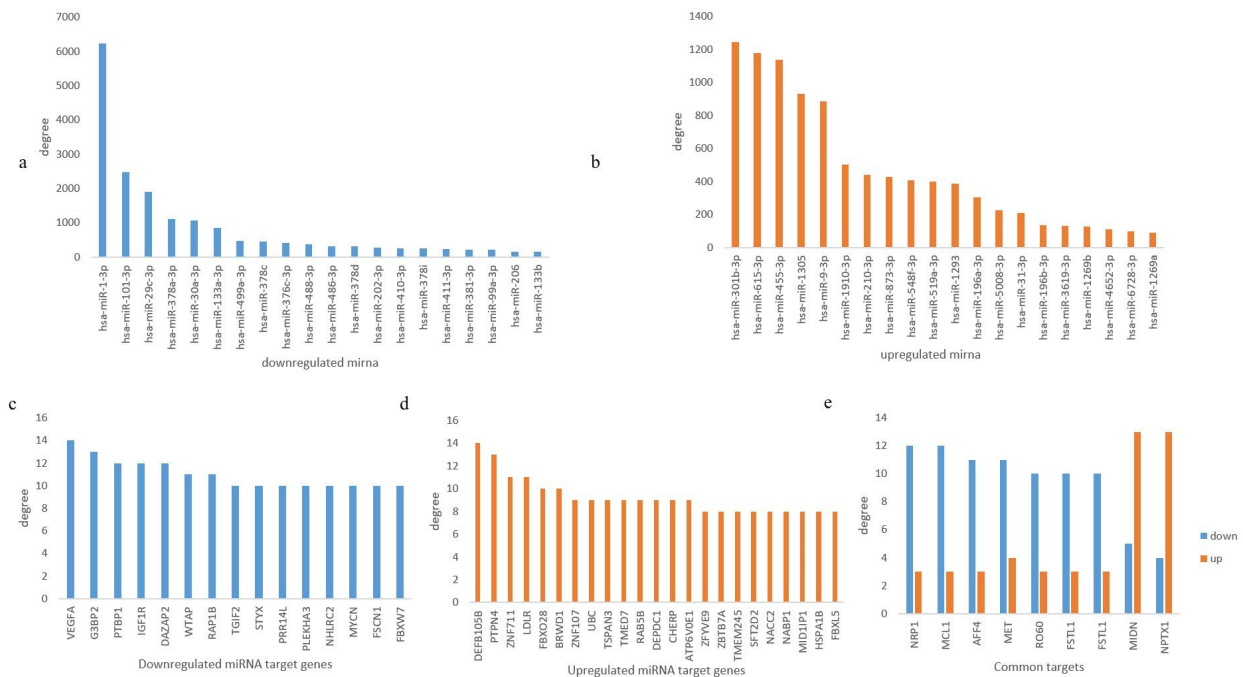
Figure 36: Top 20 down regulated miRNA with highest degree (a), Top 20 up regulated miRNA with highest degree (b) Gene targets of down regulated miRNA(c) up regulated miRNA (d) with highest degree (e) Genes targeted by both down and upregulated miRNA with significant difference in degree. *Blue bars indicate genes targeted by down-regulated miRNAs . Orange bars indicate differentially expressed genes most targeted up-regulated miRNAs.*

3.2.4. Gene Ontology enrichment analysis of predicted miRNA targets:

We obtained the gene set enrichment analysis of the targets of the miRNA using Cytoscape. We analyzed the biological processes (BP) and the pathways enriched in specifically downregulated miRNA targets and in up regulated targets separately. We found 57 biological processes and 9 pathways enriched in downregulated miRNA targets falling in <0.01 FDR category while 16 biological process and 3 pathways enriched in upregulated miRNA targets only. Figure 37 a shows all the processes and pathways enriched in upregulated miRNA targets whereas Figure 37b shows all the pathways enriched but only a few biological processes for better visualization. Since the tumor suppressor TP53 controls the transcription of 24 of the elevated miRNA's target genes, their downregulation would be linked to the development of tumors. To maintain the survival of tumor

cells, autophagy mechanisms are downregulated in tumor cells. This pathway is also enriched in targets for upregulated miRNAs.
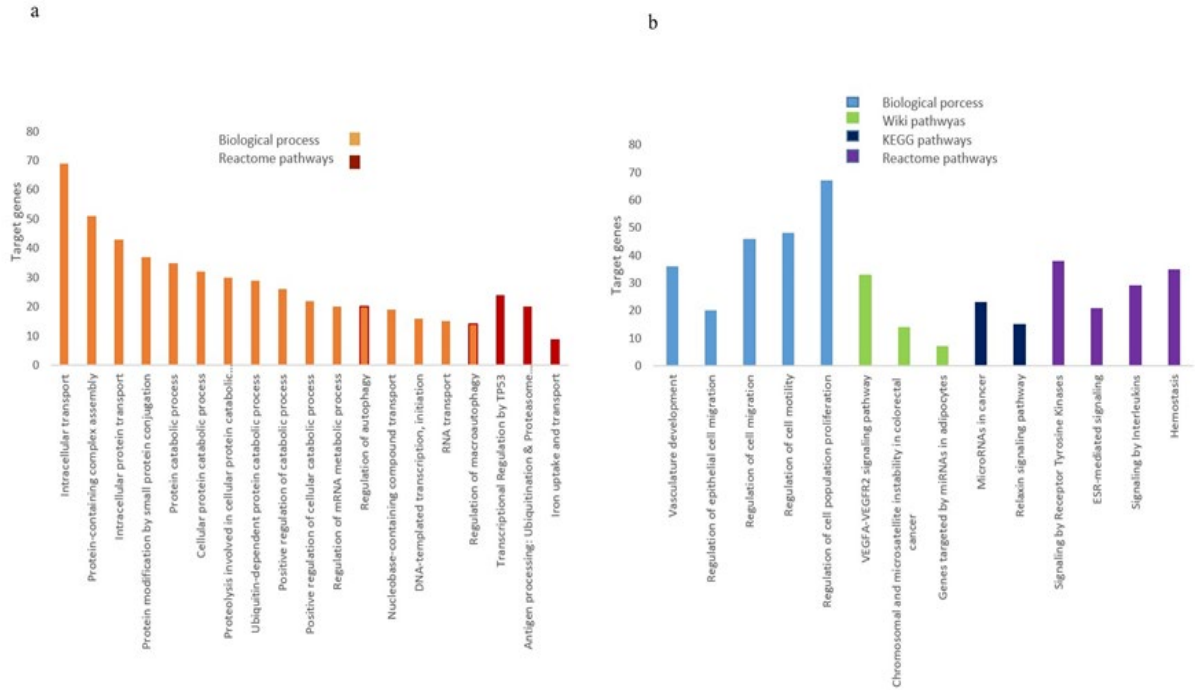
Figure 37. Gene Enrichment analysis of the upregulated miRNA (a) and downregulated miRNA(b)The upregulated miRNA targets regulate autophagy and are related to transcriptional regulation by TP53 while the downregulated miRNA targets promote vascular development, migration and motility.

Similarly, the gene ontologies of downregulated miRNA show they play roles in VEGF signaling and regulation of cell migration and motility.

3.2.5. Hub genes Targets:

The 417 genes in the network of up-regulated miRNA targets were filtered to produce a network of 36 nodes using the criteria of mean centroid value=-260.86, betweenness=515.41, and bridging=12.88. A network of 38 genes was created by filtering the down-regulated miRNA targets using the criteria of mean centroid value=-234, betweenness= 457.38, and bridging=7.53. Figure 38a highlights the genes involved in phagocytosis, immune system processes, and integrin-mediated

signaling pathways. String enrichment of these networks revealed regulated miRNA targets enriched in only biological functions. We found that the down-regulated miRNA hub genes were more frequently involved in cancer-promoting pathways, such as the activation of RAF and RhoGTPase effectors and WNT and ROBO receptor signaling. According to numerous studies, Wnt signaling upregulation promotes tumor metastasis, proliferation, differentiation, and cancer stem cell renewal (Zhan et al., 2016), playing a significant role in carcinogenesis and therapy response (Y. Zhang & Wang, 2020). Prior research by Zhou et al. (2011) demonstrated the significance of ROBO3 in the malignant transformation of cancer cells and tumor invasion in conjunction with upregulated Wnt pathway components(W. J. Zhou et al., 2011). Previous research has shown that Raf activation through the Rho GTPases affects cell adhesion, morphology, and progression by modulating the cell cycle (Beeram et al., 2005)(Cardama et al., 2017).
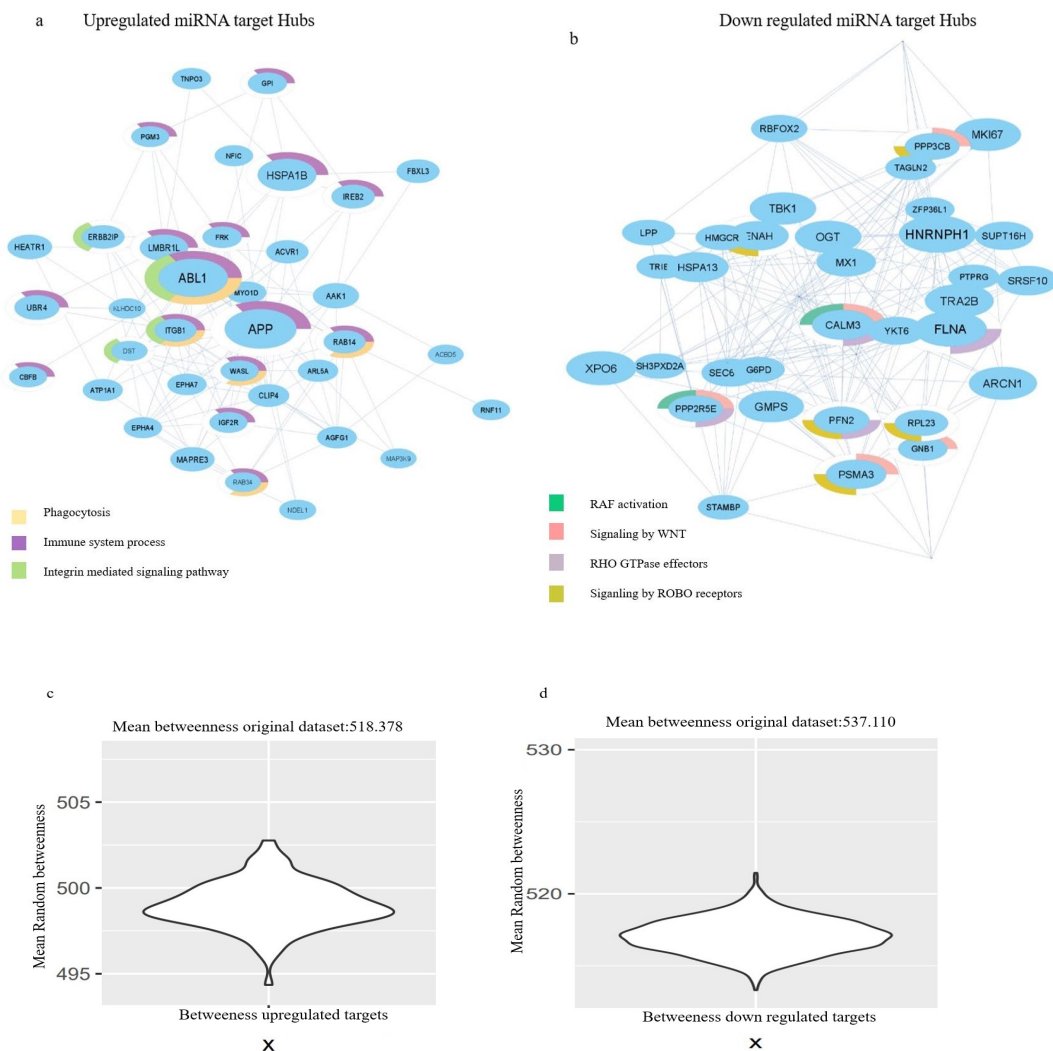
Figure 38: Upregulated miRNA target hub genes selected by (mean=515.4), bridging (mean=12.8) and centroid (mean=260.8). t (a), down regulated miRNA target hub genes selected by betweenness (mean=457.3), bridging (mean=7.5) and centroid (mean=-234.5).(b) violin plot showing average betweenness of each random network against the betweenness of the original network of upregulated targets (c) and downregulated targets (d)

3. 2.6. List of miRNAs targeting known oncogenes and tumor suppressor genes:

We obtained a list of miRNA targeting oncogenes and tumor suppressor genes. We obtained a network to identify miRNA targeting both PTEN as well as TP53. Similarly, we tried to find miRNAs that targeted the largest number of these oncogenes EGFR, MET, HRAS and TP53, NOCTH1. The threshold for the adjusted p-value (FDR) was set to 1 and the threshold for number of miRNA-target interactions was set to 2 interactions (Table3). hsa- mir-410-3p, hsa-mir-1-3p, hsa-mir-499a, hsa-mir-133, hsa-mir-139-5p are the miRNA significantly downregulated miRNA targeting the oncogenes while hsa-mir-21, hsa-mir-205, hsa- mir-106a, hsa-mir-19a-3p, hsa-mir-18a-5p are those upregulated miRNAs targeting the tumor suppressor genes.
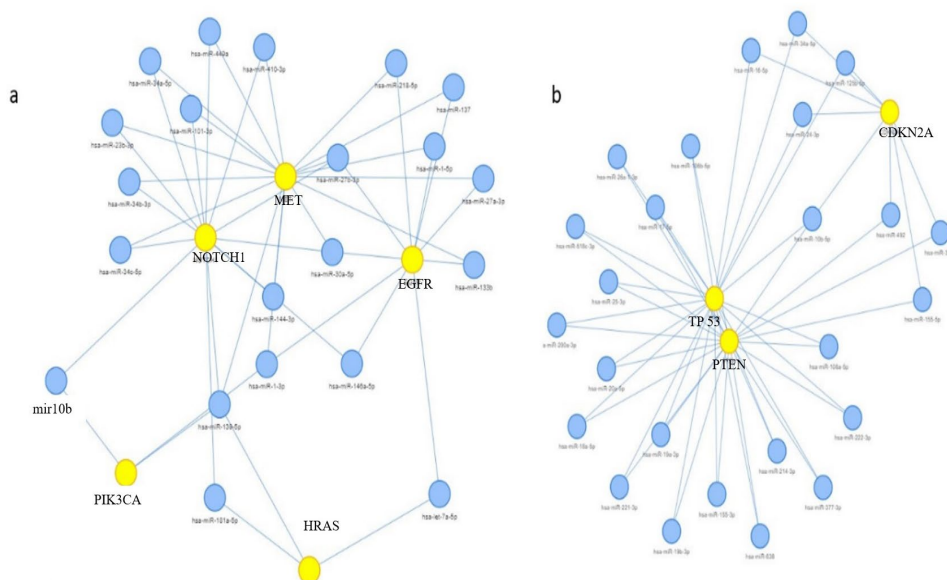
Figure 39. Experimentally validated miRNA targeting the oncogenes (a) and the tumor suppressor genes (b).

Using mirTarbase, we were able to obtain the validated mirna targeting a list of oncogenes and tumor suppressor genes. We contrasted the miRNAs that specifically target TP53 and PTEN. A list of common miRNAs that target PIK3CA, EGFR, MET, HRAS, and NOCTH1 was also created by our team (Table 1).We discovered that miR-301a-3p and miR-301b-3p, which had the highest number of gene targets compared to the most elevated miRNA in HNC patients, also targeted the tumor suppressor PTEN. While miRr-210-3p is known to target both PTEN and TP53 with 440 target genes, miR-1305, miR-196b-3p, and miR-31-3p all appear to target exclusively TP53. As a result, we suggest that additional research on upregulated miR-210- 3p would be worthwhile.

Table 2: List of tumor suppressors along with their targeting miRNA compared to the list of up regulated miRNA in head and neck cancer patients with highest number of target genes

PTEN	TP53	CDKN1A	Upregulated miRNA	degree
hsa-miR-518c-3p	hsa-miR-200a-3p	**hsa-mir-301a-3p**	**hsa-miR-301a-3p**	1543
hsa-miR-155-3p↑	hsa-miR-10b-5p↑	hsa-miR-1229-3p	**hsa-miR-301b-3p**	1246
hsa-miR-26a-1-3p↓	hsa-miR-25-3p	hsa-miR-1307-3p	hsa-miR-615-3p	1177
hsa-miR-638	hsa-miR-518c-3p	hsa-miR-130b-3p	**hsa-miR-455-3p**	1139
hsa-miR-214-3p	hsa-miR-155-3p↑	hsa-miR-18a-3p↑	**hsa-miR-1305**	930
hsa-miR-18a-5p↑	hsa-miR-26a-1-3p↓	**hsa-miR-1910-3p**	hsa-miR-9-3p	887
hsa-miR-377-3p↓	hsa-miR-638	hsa-miR-1911-3p	**hsa-miR-1910-3p**	502

hsa-miR-221-3p ↑	hsa-miR-214-3p	hsa-miR-193b-3p ↑	**hsa-miR-210-3p**	440
hsa-miR-222-3p ↑	hsa-miR-18a-5p ↑	hsa-miR-19a-3p ↑	hsa-miR-873-3p	428
hsa-miR-19a-3p ↑	hsa-miR-377-3p ↓	hsa-miR-205-3p ↑	hsa-miR-548f-3p	407
hsa-miR-106a-5p ↑	hsa-miR-221-3p ↑	hsa-miR-21-3p ↑	**hsa-miR-519a-3p**	398
hsa-miR-19b-3p	hsa-miR-222-3p ↑	hsa-miR-450-3p	hsa-miR-1293	385
hsa-miR-106b-5p	hsa-miR-19a-3p ↑	**hsa-miR-455-3p** ↑	hsa-miR-196a-3p	303
hsa-miR-17-5p	hsa-miR-106a-5p ↑	**hsa-miR-301b-3p**	hsa-miR-5008-3p	225
hsa-miR-20a-5p ↑	hsa-miR-19b-3p		**hsa-miR-31-3p**	207
hsa-miR-200a-3p ↑	hsa-miR-106b-5p		**hsa-miR-196b-3p**	136
hsa-miR-10b-5p ↑	hsa-miR-17-5p		hsa-miR-3619-3p	129
hsa-miR-25-3p	hsa-miR-20a-5p		hsa-miR-1269b	127
hsa-miR-301a-3p	**hsa-miR-1305** ↑		hsa-miR-4652-3p	111
hsa-miR-301b-3p	hsa-miR-196a-3p ↑		hsa-miR-6728-3p	97
hsa-miR-21-3p ↑	**hsa-miR-196b-3p** ↑		hsa-miR-1269a	87
hsa-miR-210-3p ↑	**hsa-miR-210-3p** ↑		hsa-miR-767-3p	69
hsa-miR-519a-3p	**hsa-miR-31-3p** ↑		hsa-miR-937-3p	69
			hsa-miR-503-3p	50

					hsa-miR-4713-3p	46
					hsa-miR-4724-3p	43
					hsa-miR-3144-3p	40
					hsa-miR-4745-3p	30

Similar to this, we discovered miR-1-3p with the highest gene targets similarly targeted MET, EGFR, and PIK3CA on examination of the miRNA targeting oncogenes with the considerably downregulated miRNA. While miR-133b targeted EGFR and MET, miR-101-3p, miR-410-3p, and miR-410-3p targeted NOTCH1 and MET. Since miR-1-3p targeted the most genes, including three oncogenes, further examination of miR-1-3p role in head and neck cancer patients' survival is recommended.

Table 3: List of oncogenes with their targeting miRNA compared to the list of down regulated miRNA with highest degree.

MET	NOTCH1	EGFR	HRAS	PIK3CA	Downregulated miRNA	Degree
hsa-miR-137	hsa-miR-139-5p	hsa-miR-1-5p	hsa-miR-181a-5p	hsa-miR-139-5p	**hsa-miR-1-3p**	6235
hsa-miR-34c-5p	hsa-miR-27b-3p	**hsa-miR-133b**	hsa-let-7a-5p	hsa-miR-10b-5p	**hsa-miR-101-3p**	2471
hsa-miR-449a	hsa-miR-30a-5p	hsa-miR-146a-5p	hsa-miR-139-5p	**hsa-miR-1-3p**	hsa-miR-29c-3p	1895
hsa-miR-34b-3p	hsa-miR-144-3p	hsa-miR-27a-3p			hsa-miR-378a-3p	1113

hsa-miR-1-3p ↓	hsa-miR-10b-5p	**hsa-miR-218-5p** ↓			hsa-miR-30a-3p	1072
hsa-miR-410-3p ↓	hsa-miR-23b-3p	hsa-miR-27b-3p			hsa-miR-133a-3p	852
hsa-miR-101-3p ↓	hsa-miR-34c-5p	hsa-miR-137 ↑			hsa-miR-499a-3p	465
hsa-miR-34a-5p	hsa-miR-449a	**hsa-miR-1-3p**			hsa-miR-378c	462
hsa-miR-1-5p	hsa-miR-146a-5p ↓	hsa-let-7a-5p ↓			hsa-miR-376c-3p	405
hsa-miR-133b ↓	hsa-miR-34b-3p	hsa-miR-30a-5p ↓			hsa-miR-488-3p	366
hsa-miR-30a-5p ↓	**hsa-miR-410-3p** ↓				hsa-miR-486-3p	319
hsa-miR-144-3p	**hsa-miR-101-3p** ↓				hsa-miR-378d	308
hsa-miR-23b-3p	hsa-miR-181a-5p ↓				hsa-miR-202-3p	269
hsa-miR-27a-3p ↓	hsa-miR-34a-5p ↓				**hsa-miR-410-3p**	264
hsa-miR-218-5p					hsa-miR-378i	251
hsa-miR-27b-3p					hsa-miR-411-3p	230
hsa-miR-139-5p					hsa-miR-381-3p	223

					hsa-miR-99a-3p	220
					hsa-miR-206	151
					hsa-miR-885-3p	147
					hsa-miR-133b	147
					hsa-miR-299-3p	136
					hsa-miR-378f	128
					hsa-miR-4740-3p	125
					hsa-miR-211-3p	119
					hsa-miR-4776-3p	109
					hsa-miR-135a-3p	67
					hsa-miR-208b-3p	52
					hsa-miR-5089-3p	44
					hsa-miR-1258	37

According to an examination of the miRNAs that target oncogenes, patients with head and neck cancer have considerably lower levels of the miRNAs hsa-miR-410-3p, hsa-miR-1-3p, has-miR-499a, has-miR-133, and hsa-miR-139-5p. Two of these miRNAs that frequently target NOTCH1 and MET are hsa-mir-410-3p and hsa-mir-499a. It has been discovered that hsa-miR-1-3p and hsa-miR-139-5p share four common targets between them: NOTCH1, HRAS, MET, and PIK3CA. Similarly, hsa-miR-21, hsa-miR-205, hsa-miR-106a, hsa-miR-19a-3p, hsa-miR-18a-5p, and hsa-miR-522 target tumor suppressor genes and are upregulated in HNSC. In addition, hsa-miR-205, hsa-miR-19a, hsa-miR-106a, and hsa-miR-21 target PTEN and TP53. Among these miRNA, has-miR-522 targets TP53 and CDNK2A.

3.2.7 miRNA targeting Ceruloplasmin

mirTarbase reports four experimentally validated miRNA targeting CP including three found in house mouse: mmu-miR-129-5p, mmu-miR-203-3p, mmu-miR-203 and one in humans:

hsa-miR-145-5p. Figure 40 shows the mir-145 is down regulated in tumors in comparison to normal patients suggesting its role in suppressing the controlling the transcription of oncogenes. Mir-145 is seen to target CP from amongst various other target genes. Lower expression of mir-145 has been observed to be associated to reduced survival of cancer patients.
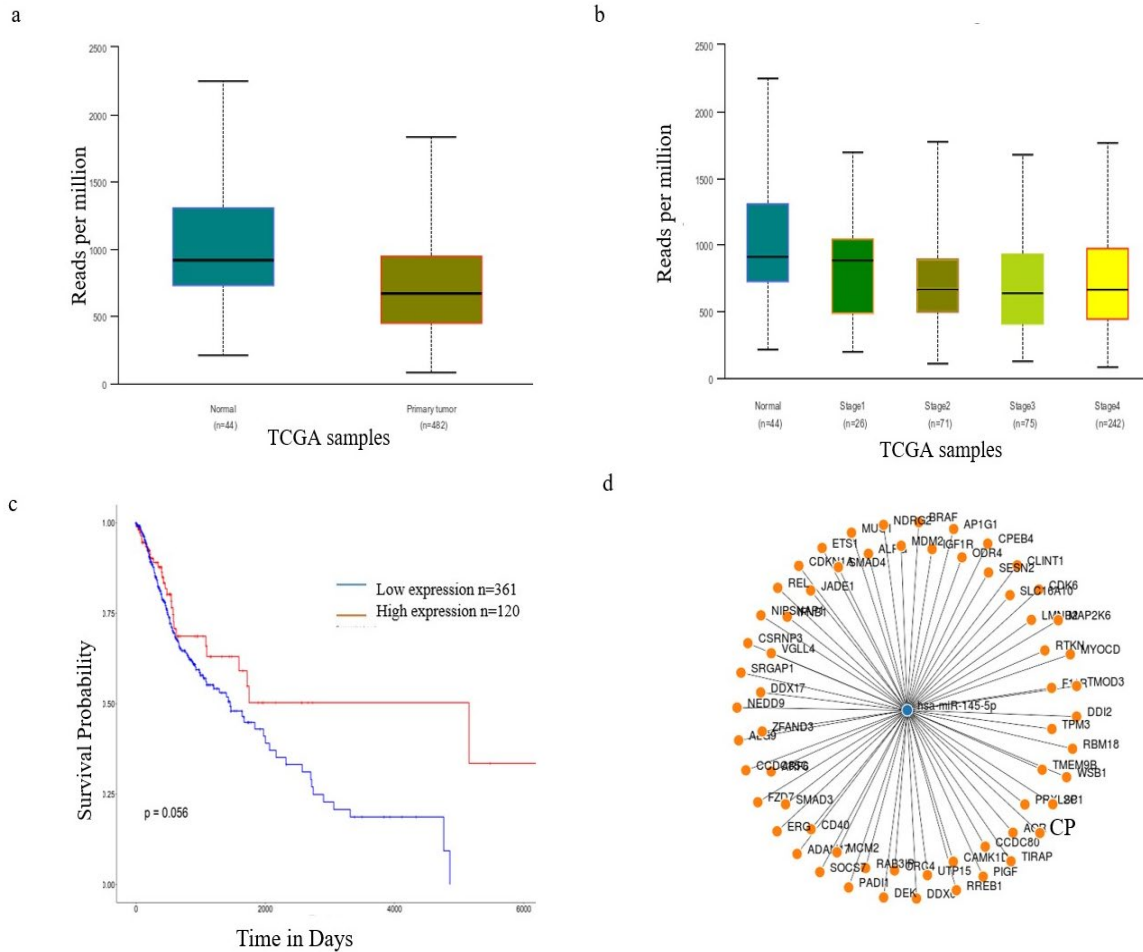
Figure 40: a) Differential expression of miR-145, b) stage wise expression of miR-145, c) survival analysis of miR-145, d) the targets of miR-145.miR145 is observed to be downregulated in tumor samples. Its lower expression confirms CP upregulation and corresponds to lower survival.

170 miRNA were predicted to be targeting CP according to miRwalk database. Out of these we identified the miRNA differentially expressed in the head and neck cancer patients in comparison to normal patients.

Table 4: List of miRNA targeting CP, significantly differentially expressed in Head and neck cancer patients

Upregulated miRNA targeting CP	Down regulated miRNA targeting CP
hsa-mir-1237	hsa-mir-125b-1
hsa-mir-1343	hsa-mir-139
hsa-mir-137	hsa-mir-1468
hsa-mir-196b	hsa-mir-204
hsa-mir-2355	hsa-mir-431
hsa-mir-3619	hsa-mir-432
hsa-mir-3940	hsa-mir-504
hsa-mir-450a-1	hsa-mir-5698
hsa-mir-4714	hsa-mir-676
hsa-mir-4726	hsa-mir-885
hsa-mir-4745	
hsa-mir-4763	
hsa-mir-5008	
hsa-mir-503	
hsa-mir-6764	
hsa-mir-6803	
hsa-mir-6887	
hsa-mir-6891	
hsa-mir-7110	

hsa-mir-7112	
hsa-mir-7850	
hsa-mir-8072	
hsa-mir-873	
hsa-mir-21	

We generated a list of miRNA targeting CP and hsa-miR-21 out of the above mentioned downregulated and upregulated miRNA has been predicted to target CP. The differential expression analysis stagewise and survival analysis of mir-21 was performed. In grade 4 patients miR21 is downregulated and CP is upregulated especially in the later stages. Furthermore, the lower expression of hsa-miR-21 expression in head and neck cancer patients was found to be correlated to lower survival rates of patients (Figure41).
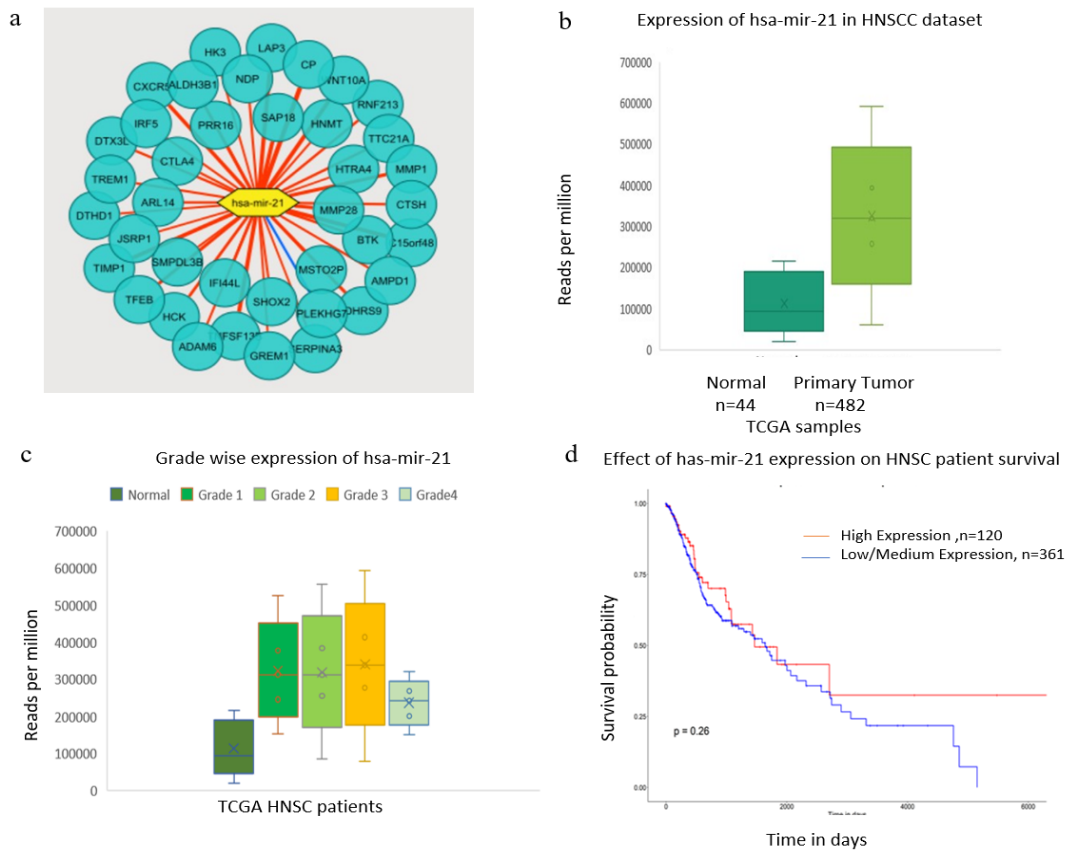
Figure 41. a)Predicted targets of miR-21 showing it targets CP, b) miR21 expression in HNSCC tumor vs normal, c)stage wise expression of miR-21, and d) its survival analysis. Higher expression of miR21 in early stages and downregulation in lager stages confirms with CP expression trend i.e. upregulated in later stage. Its decreased expression corresponds to lower survival probability in patients.

3.2.8. Mir21 Target analysis:

We used ONCO.IO for miRNA target network analysis for mir21.When mir21 is upregulated in the early tumor stages of Head and neck cancer it promotes tumor progression by targeting various tumor suppressor genes such as (C. Y. Chen et al., 2018) SMAD7(D. Ma et al., 2021), Programmed cell death gene PDCD4 (Matsuhashi et al., 2019)and TP63. However, in the later tumor stages it is downregulated which resulted in MAPK10, STAT3, NFKB, MMP3, NANOG and MYC along with CP up regulation. Hence our candidate miRNA21 could be further explored as a potential therapeutic target in Head and Neck cancer therapeutics.
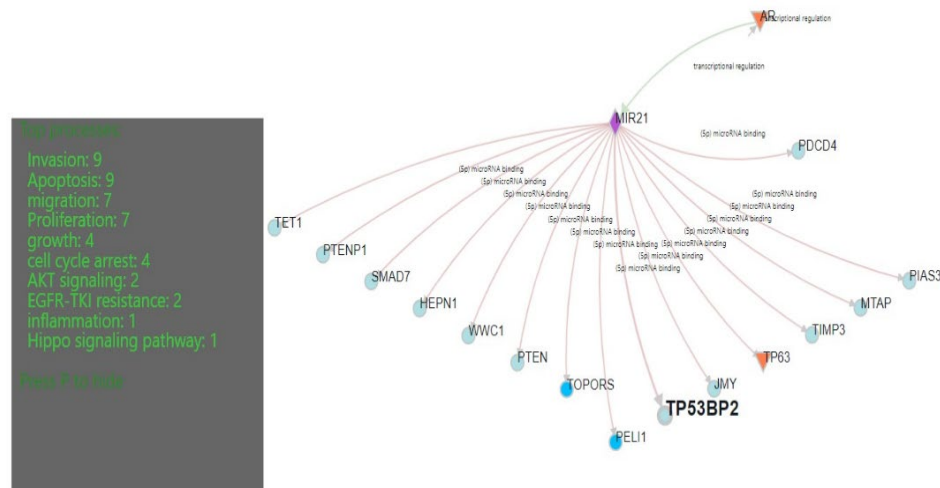
Figure 42. Targets of miR21 in the early tumor stages when it is upregulated along with summary of the processes effected.TP53 a tumor suppressor maybe inhibited in the initial cancer stages by miR21 upregulation and maybe involved in increasing tumor proliferation and inflammation.
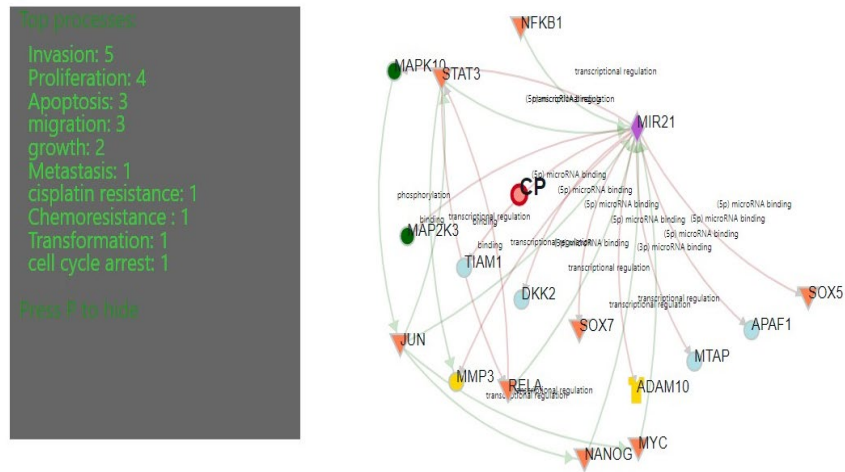
Figure 43. Targets of miR21 in the later tumor stages when it is downregulated along with a summary of the processes affected. Here in the later cancer stage miR21 downregulation leads to upregulation of MAPK3,CP, NFKB and TIAM1 promoting invasion and inducing drug resistance.

Discussion of part 3.2:

The stage IVB patients had the most downregulated miRNAs, according to the differential miRNA expression in the head and neck cancer patients in the various stages. This suggests that miRNAs associated with disease aggression may be the targets of these downregulated miRNAs. We chose the top 20 enriched phrases for the upregulated miRNAs based on the P value, which included terms like protein ubiquitination, positive regulation of angiogenesis, negative regulation of gene expression, and positive regulation of cell proliferation. Positive regulation of cell motility, the Ras signaling pathway, the upkeep of somatic stem cells, cell cycle transitions, and protein stability were among the enriched processes in the downregulated miRNA. Many of the cancer-related genes that the downregulated miRNAs target have been identified as prospective targets for cancer therapy, including transcription factors like MYC and protein kinases like MAPK(Braicu et al., 2019). In addition to being upregulated in some tumors, the long non-coding RNA (lncRNA) X-inactive specific transcript (XIST), an oncogene previously identified to promote tumorigenesis by upregulating EGFR, MAPK1, HIF1alpha, TGFB1, and WNT signaling, is also a targeted of several miRNAs that are downregulated in head and neck cancer (J. Yang et al., 2021). Another target is

ERBB2; this protein's function in human cancers and chemoresistance is significant (Tan & Yu, 2013).PTEN, TP53, and TIMP2, which is an inhibitor of metalloproteinases 2 and prevents tumor metastasis, are miRNA targets that are increased(W. Wang et al., 2019)(H. Wang et al., 2021). Tumors with downregulated SMAD7 experience epithelial to mesenchymal transition because SMAD 7 has been shown to impede TGF signaling(Matsuhashi et al., 2019). Another tumor suppressor that is inhibited in head and neck malignancies is PDCD4 (Programmed cell death protein 4)[236]. It is targeted by the increased miRNA.

The most common genetic change is identified in the TP53 tumor suppressor gene, which is mutated in roughly 70–80% of individuals with head and neck cancer (Blandino & Di Agostino, 2018). PTEN has been identified as the primary antagonistic regulator of PI3K-Akt signaling pathway activation in earlier HNC research(Vahabi et al., 2019). The miRNAs that target these tumor suppressors and are associated with decreased survival upon increased expression were the focus of our investigation. We identified 2 elevated miRNAs, hsa-mir-18a and hsa-mir-19a, which were associated with cancer-specific survival. Patients with upregulated expression of hsa-mir 18a and 19a showed lower survival rates. Numerous transcription factors, including ZEB1, ZEB2, Snail, Slug, and Twist, have been linked to tumor metastasis and the EMT process, according to studies. It has been discovered that in many cancers, the expression of these genes is elevated while the targeted miRNA is downregulated. The biggest difficulties in treating head and neck cancer are resistance to radiotherapy and resistance to chemotherapy. EGFR has been connected to therapy resistance and a bad prognosis. About 90% of HNSC patients have been shown to have overexpression of the EGFR gene. We discovered three miRNAs that were highly expressed in the EGFR, MET, and PI3K-Akt-mTOR signaling pathways(Vahabi et al., 2021). Hsa-mir-1-1, Hsa-mir-410, and Hsa-mir-139 survival research revealed that downregulation of these genes was associated with a decreased likelihood of surviving and a worse prognosis.

We discovered that downregulating hsa-mir-410 and 139 combined led to the targeting of cancers related to MDM2, MMP16, and MET. According to research by Wei et al. (2019), TRIM44 is another target that has been shown to encourage cell proliferation by controlling FRK and activating the AKt/mTor signaling pathway in malignancies(Wei et al., 2019). These miRNAs also target ITPKB, an enzyme that has been shown to control the redox balance of NOX4-dependent pathways and give cisplatin resistance in malignancies (Pan et al., 2019). The ATG16L1 gene is crucial for autophagy and is also targeted by mir-410 and 139(Jamali et al., 2022) Dickkopf-1

(DKK1), which is overexpressed in many cancers and is thought to have immunosuppressive functions in addition to being a secreted regulator of Wnt signaling. Because mir-310 and mir-139 are suppressed in HNC malignancies, its overexpression is linked to worse clinical outcomes(Haas et al., 2021). These miRNAs that were downregulated also targeted the inflammatory gene HMGB1(Kang et al., 2013). It has been noted that lncRNA CCAT1 functions as an oncogene in individuals with renal cancer, and its relationship to hsa-mir140 and 139 may be further investigated. As a result, we demonstrate that these downregulated miRNAs have targets that modulate a number of cancer-related domains, such as inflammation, drug resistance, WNT signaling, immunological suppression, and cell migration. These miRNAs may be investigated in the treatment of head and neck cancer. The tumor suppressors PTEN, Smad3, and ROR, which have been shown to regulate pathways relevant to cancer growth, have been demonstrated to be inhibited by the increased miRNA18a and 19a. When downregulated, the Sonic Hedgehog (SHH) signaling downstream target gene neogenin-1 (NEO1) is associated with basal cell carcinoma aggressiveness(Casas et al., 2017) .A lnc RNA called TP53TG1 has been investigated to improve cisplatin sensitivity in lung cancer cells and has also been investigated as a method to improve the efficacy of chemotherapy for NSCLC (Xiao et al., 2018). The NF-B signaling pathway is negatively controlled by the well-studied tumor suppressor TNFAIP3, which is reported to be downregulated in cancerous tumors(Du et al., 2019). Therefore, by up-regulating these tumor suppressive and drug-sensitizing genes targeted by these miRNAs, it should be able to enhance the clinical result of patients.

Mir-145 has been reported experimentally to be targeting CP. This miRNA was found to be downregulated in tumors and its downregulation correlated to lower survival probability in patients. We also noted that hsa-mir-21 also significantly differentially expressed in oral tumors, elevated in patients with Grade 1 and 2 OSCC, is predicted to have CP as one of its target genes. As CP is elevated at later stages, the finding that hsa-miR-21 is downregulated in grade 4 patients suggests that has-mir-21 epigenetically controls CP antagonistically .Through CP control, further research on its oncogenic significance may be done. Additionally, we used the miRwalk 2.0 website to predict the miRNA-CP interactions and discovered that hsa-miR-92a-2-5p targets CP with a target score of 79 and binds CP at the 3' UTR.

Part 3.3: ii) Identification of potential inhibitor(s) for ceruloplasmin using in silico virtual screening approaches

3.3.1. Protein structure preparation/structure validation:

The 4ENZ CP structure was downloaded from the Protein Data Bank (PDB) and subjected to several modifications. Ligands were removed, missing residues were added, and hydrogen atoms were added. . To assess the quality of the energy minimized structure, a ProSA analysis was performed. The ProSA Z-score value for CP was determined to be -10. This Z-score falls within the range of Z-scores obtained for protein structures generated by both NMR spectroscopy (represented by dark blue spots) and X-ray crystallography (represented by light blue spots) (Prajapat et al., 2014). Furthermore, in Figure 44B, the negative ProSA energies observed for the majority of amino acid residues further indicate the good quality of our structure.
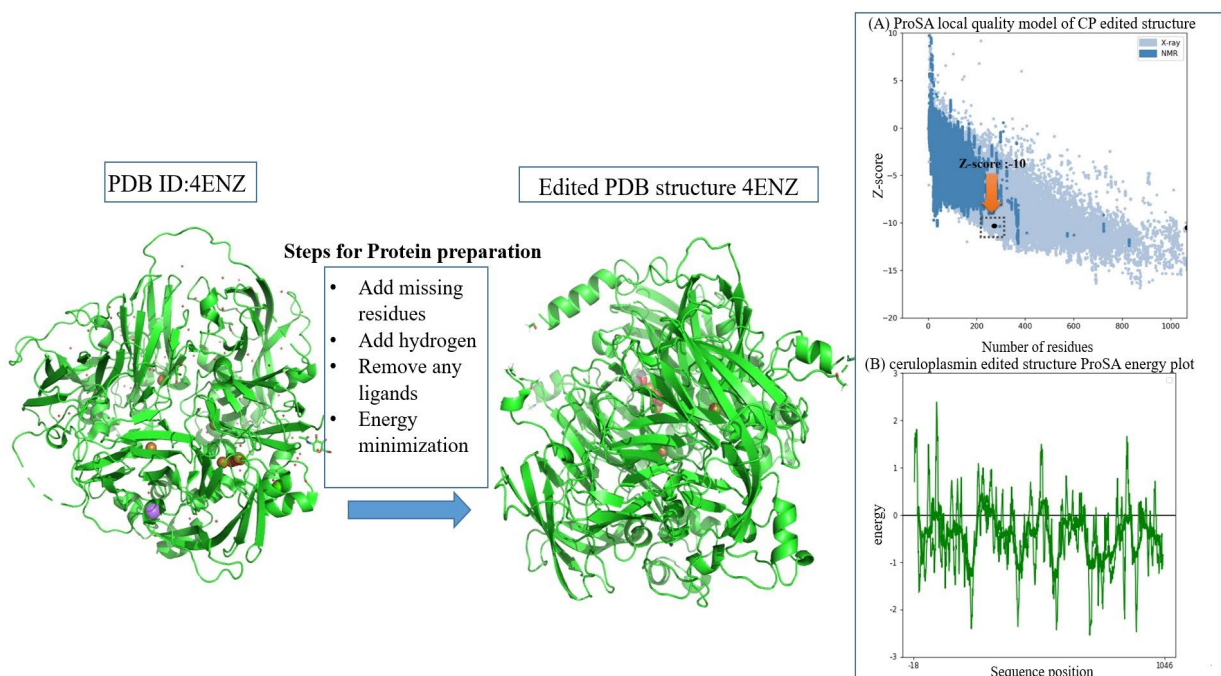
Figure 44. Protein preparation of PDB structure 4ENZ, (A) ProSA local quality model of CP edited structure (B) ceruloplasmin edited structure ProSA energy plot. *The Ramachandran plot generated against a background of phi psi probabilities validated our structure as it showed 92. 2 % Ramachandran favored regions.*

The structure was edited by H addition and neutralization of residues that do not participate in salt bridges and that are more than a specified distance from the nearest ligand atom. Addition of missing residues followed by energy minimization was saved as the 4ENZ.edited structure which was then used to obtain a Ramachandran plot, against a background of phi-psi probabilities(Figure 45).
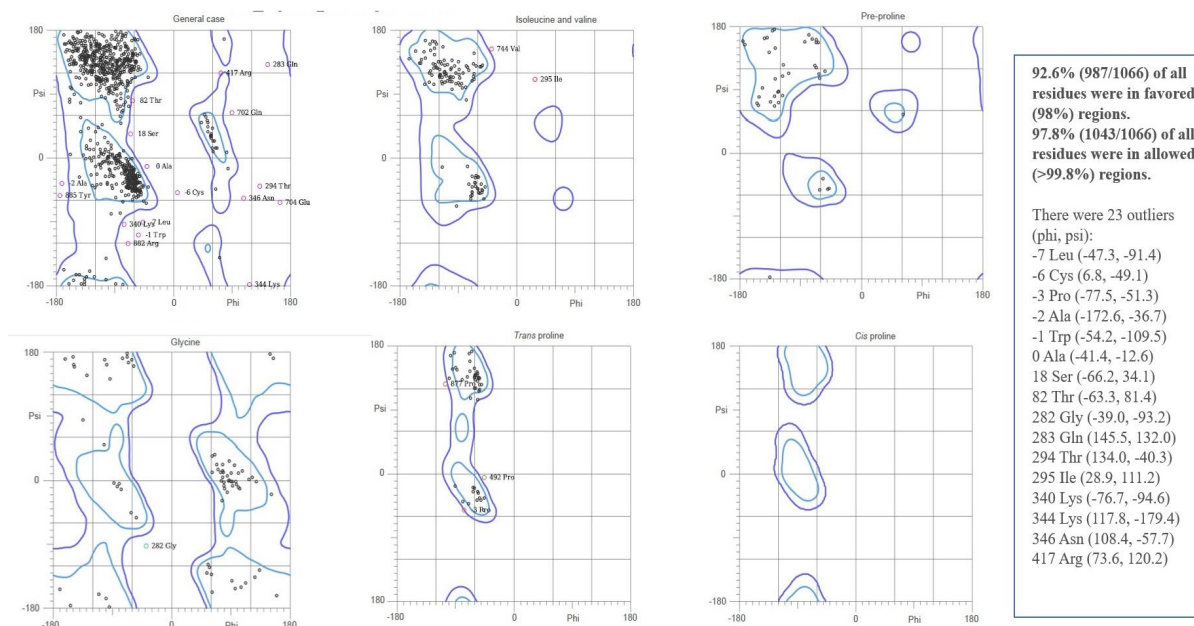
Figure 45. Ramachandran Plot for edited Ceruloplasmin structure 92.92% Rama distribution Z-score, -1.75 ± 0.25(Blue represent the helix, red means strand and green means turn and loop according to DSSP. The lines in the plot indicate the preferred areas. Outer lines encircle the area that should have 90% of all dots of the same color; the inner lines indicate the 50% area.)

In the DSSP representation, the color blue corresponds to the helix structure, red represents the strand structure, and green indicates the turn and loop regions. The lines on the plot mark the preferred regions. The outer lines enclose the area where 90% of all crosses of the same color are expected, while the inner lines indicate the 50% area.

3.3.2. Binding site:

The binding site was identified containing the following amino acid residues: **885 to 892, 511,542-557,699–710, M668, W669 and H667** which interact with myeloperoxidases binding site inhibiting the chlorinating action of myeloperoxidase(Figure 46).
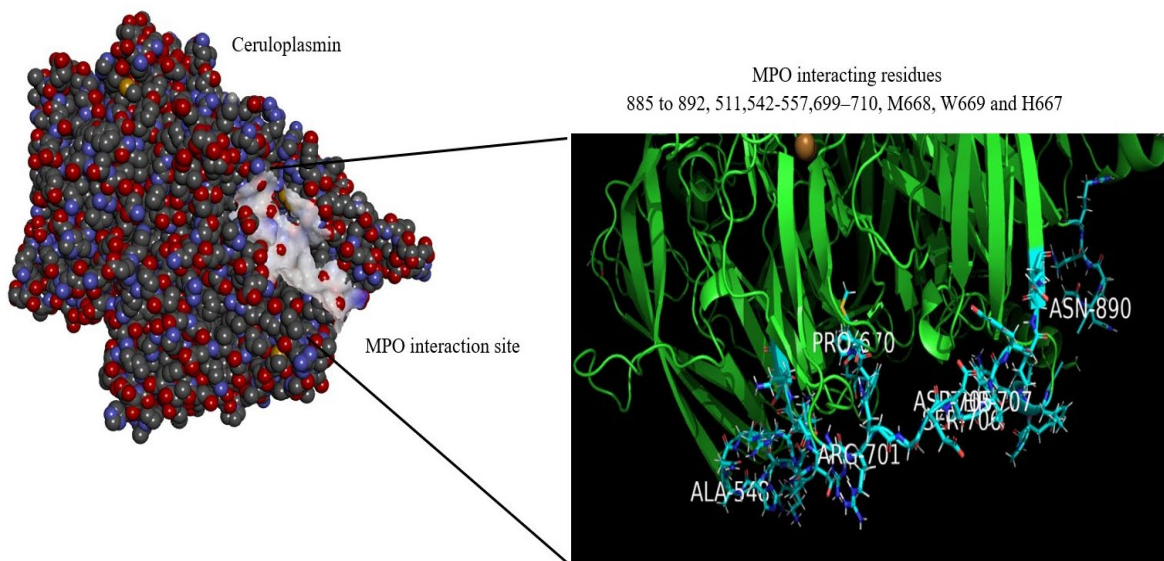
Figure 46. The amino acids on CP interacting with MPO. *The binding site contains the following amino acid residues: 885 to 892, 511,542-557,699–710, M668, W669 and H667 which interact with myeloperoxidases binding site inhibiting the chlorinating action of myeloperoxidase.3b Binding site sphere was defined for docking analysis where the control and ligands bind to CP*

3.3.3. Molecular Docking Analysis

As an initial step in Schrodinger's docking protocol, Glide is employed to conduct a comprehensive conformational search. During this search, high-energy conformers and long-range hydrogen bonds containing conformations are eliminated as they are unfavorable for receptor binding (Friesner et al., 2004b). The OPLS-AA molecular mechanics potential function is utilized to impose a cutoff for the total conformational energy, ensuring it remains within an acceptable range compared to the lowest-energy state. To achieve optimal results, the starting conformations should be within approximately 1.5 Å rmsd (root-mean-square deviation) of the correct crystallized conformation. Each ligand consists of a "core" region to which several "rotamer groups" are attached via a rotatable bond. Glide performs an exhaustive exploration of potential positions and orientations for each core conformation, specifically focusing on the region of interest on the protein.

The **Receptor Grid Box** for docking studies was set as in Figure 47.

114
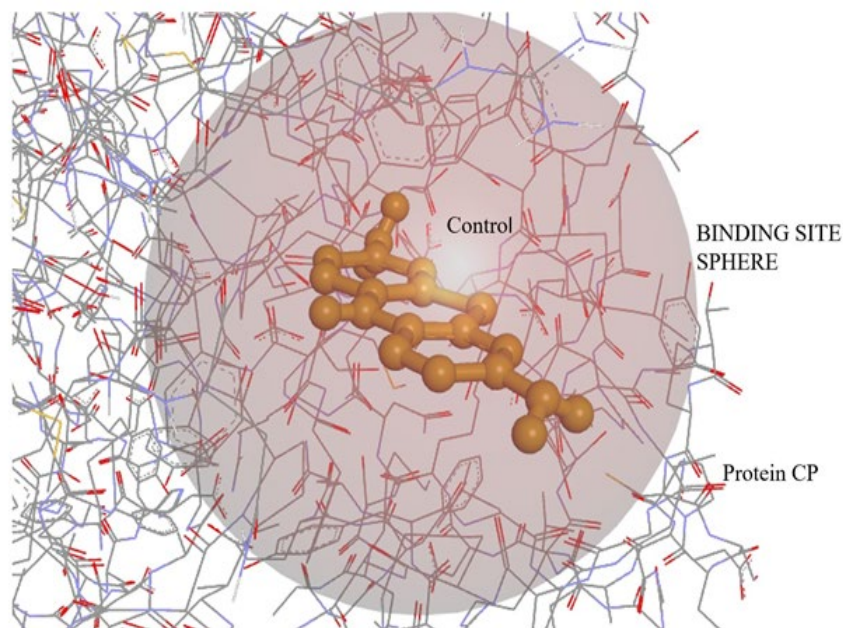
Figure 47. Defining the Binding site. *GRID_CENTER: 6.337066710810808, 109.0767157891891, 23.543311587837835,INNERBOX: 21, 24, 16, OUTERBOX: 41, 44, 36 (FORCEFIELD OPLS_2005)*

After evaluating favorable hydrophobic interactions, hydrogen bonding, metal-ligation interactions, and steric clashes, a selection is made from the best refined poses. Only a limited number, specifically 400 poses, undergo minimization on precomputed OPLS-AA van der Waals and electrostatic grids for the receptor (Elekofehinti et al., 2021). The best-docked structure is determined based on the model energy score, which encompasses multiple factors. This score includes the energy-grid score, reflecting the interaction energy within the grid; the internal strain energy, which accounts for the potential used during the conformational search; and the binding affinity predicted by the Glide Score. By considering these factors, the optimal docking pose is identified.

3.3.3.1. Control Selection:
Control: Amitriptyline:
Amitriptyline belongs to a class of medications known as tricyclic antidepressants. It exhibits various roles, including acting as an adrenergic uptake inhibitor, an antidepressant, an

environmental contaminant, a xenobiotic, and an agonist of the tropomyosin-related kinase B receptor. Structurally, it is classified as a tertiary amine and a carbotricyclic compound(Figure 48).

In a previous study, it was reported that Amitriptyline can bind to CP at specific amino acid residues, including ASN119, TRP732, ILE1016, GLN729, GLN951 (OE1), THR1033 (OG1), and THR1036 (OG1). The binding was determined to have a score of -7.78 kcal/mol. However, the study did not provide specific information about the mechanism of action of Amitriptyline in relation to CP (Merugu & Singh, 2018).
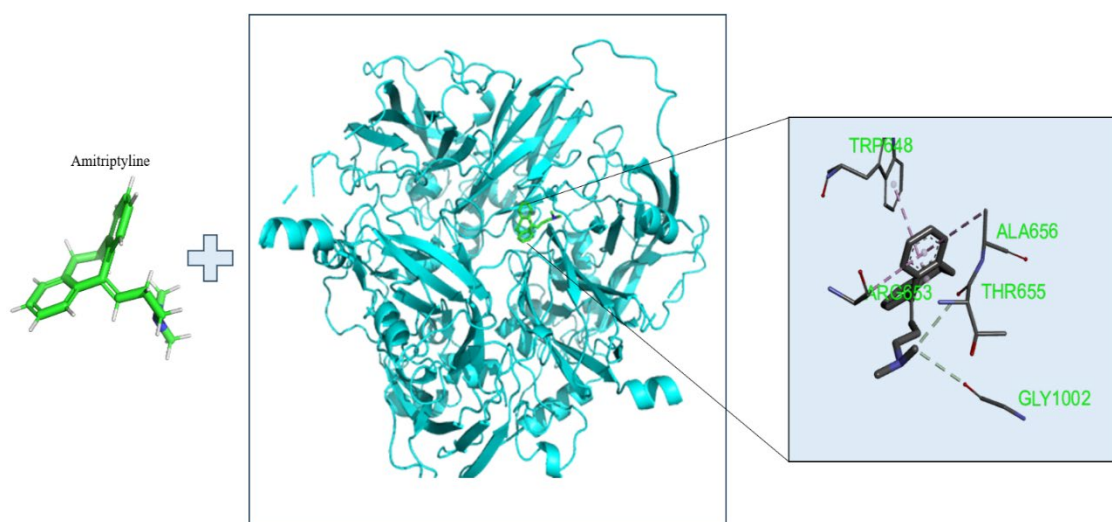
Figure 48. Control selected amitriptyline structure, its binding on ceruloplasmin and the interacting amino acids. Amitriptyline binds with a docking score: -3.5978kcal/mol and the interacting amino acids are Arg 653, Ala 656, Trp 648, Thr 655, Gly1002.

3.3.3.2. Screening of Phytochemicals and Marine compounds:

We screened a list of 17000 phytochemicals out of which 45 were best hits which were subjected to ADME Analysis using QikProp tool of Schrodinger suite.

Phytochemical Screening:

A total of 17,000 phytochemicals were screened, and 45 of them showed the most promising results. These 45 compounds were further filtered on the basis of ADME analysis using the QikProp

tool in the Schrodinger suite. Based on the results obtained from qikprop and ADME analysis, 5 phytochemicals were selected for further investigation (Table 5 and 6). Molecular docking analysis was performed to assess their binding affinities against CP (4ENZ) and the amino acids involved in the interactions.

Table 5: Molecular docking analysis of the top phytochemicals with the best binding affinities against CP (4ENZ) and their interacting amino acids.

Chemical name	Binding scores	Amino acid residues
Control-amitryptiline	-3.59	Arg 653, Ala 656, Trp 648, Thr 655, Gly1002
Xyloglucan oligosaccharide	-18.93	Asp 556, Arg 652, Glu 844, Lys841, Phe 708,Asp 705,Gln 821,Trp 669, Asp 671,Gln 702
Ardimerin digallate	-13.659	Arg 701,Gln 702, Ser 703, Glu 704, Asp 705, Ser 706, Thr 707, Lys 619, Gly 620
Mukurozioside IIb	-13.626	Lys 619,Glu 704, Ser 706,Phe 708, Asp 554, Gln 552
Lycoperoside F	-15.553	Asp 671, Asp 705, Ser 706, Thr 707,Phe 708, Asp 554,Gln 552
Uttroside B	-13.606	Gln 552, Asp 554, Trp 669, Lys 841, Phe 708, Ser 706, Asp 705, Glu 704, Ser 703

Marine Compound Screening:

In a similar manner, screening was carried out for 26,717 marine compounds. Among them, 66 compounds were identified as the best hits and were subjected to ADME analysis. Table 2 presents the interacting amino acids and docking scores of the top 5 marine compounds based on

the QikProp results (Table6). However, due to lower binding affinities compared to the phytochemicals and some compounds not binding at our site of interest in CP, these ligands were not selected for further molecular dynamics (MD) analysis.

Table 6. Molecular docking analysis of the top marine compounds with the best binding affinities against CP (4ENZ) and their interacting amino acids.

Chemical name	Binding scores	Amino acid residues
daldiniside B	-9.089	Pro3, Leu7, Cys6,Trp1, Gln 55, Ile77
arthone C	-8.124	Phe659, Trp648, Tyr646, ARg653, Ala656
engyodontiumone H	-8.091	Glu189, Phe10, His 4, Gln55, Ile65, Trp1
3-[2-[2-hydroxy-3-methylphenyl-5-(hydroxymethyl)]-2-oxoethyl] glutarimide	-9.824	Glu 189, Leu13, Phe10, Trp1, Ile77, Leu9
isonaamidine D	-8.456	Arg653, Thr655, Tyr646, Phe997, Tyr986, Phe303, Thr294

3.3.4. Calculation of drug-likeness of compounds
Drug-Likeness and ADME Analysis:
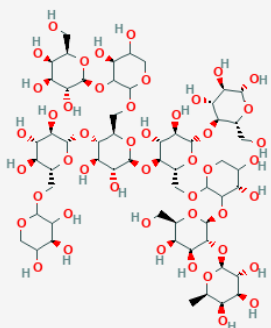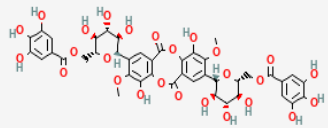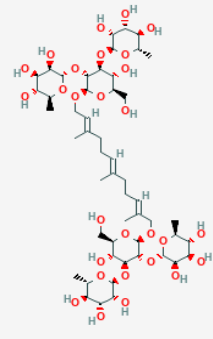
To ensure the rational design of drugs, we evaluated the molecular properties of the selected compounds to comply with Lipinski's rule of five (B. Fernandes et al., 2016)(Giménez et al., 2010).

While all the compounds showed two violations of the five rules, they did not meet the criteria of having no more than 5 hydrogen bond donors, no more than 10 hydrogen bond acceptors, a molecular weight of less than 500, less than 10 rotatable bonds, and a topological polar surface area (TPSA) not greater than 140. However, the partition coefficient (log P) for all compounds was less than 5 (Table 7).Using the QikProp tool, we predicted significant ADME properties of our selected ligands. The number of metabolites binding to human serum albumin provided insights into the percent of human oral absorption (Aman et al., 2021). We also assessed the predicted aqueous solubility of the drugs (QPLogKhsa) as well as the cell's permeability (QPLogS). The results of the physicochemical properties and ADME parameters of these ligands suggest their potential as drug candidates for further studies.

Table 7 presents the ADME properties of the top 5 phytochemical hits, while Table 8 displays the ADME properties of the top 5 marine hits.

Table 7.ADME of the top 5 phytochemical hits

Compound	Molecular formula	ADME Properties (Lipinki's Rule of Five)	Properties Value	Structure	Drug likeliness
XLLG xyloglucan oligosaccharide	C57H96O47	Molecular weight (<500Da) LogP (<5) H-Bond donor(5) H-bond acceptor (<10)	1387.215 g/mol -2.62 28 47		no

			3		no
		Violations			
Ardimerin digallate	C42H40O26	Molecular weight (<500Da)	960.75 g/mol		no
		LogP (<5)	1.45		
		H-Bond donor (5)	14		
		H-bond acceptor (<10)	26		
		Violations	3		
Mukurozioside IIb	C51H86O28	Molecular weight (<500Da)	1147.21 g/mol		no
		LogP (<5)	4.38		
		H-Bond donor (5)	16		
		H-bond acceptor (<10)	28		
		Violations	3		
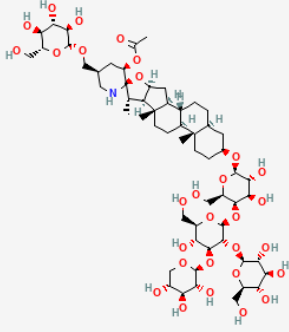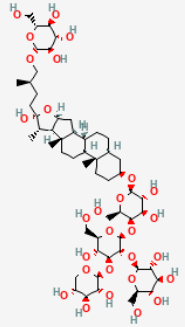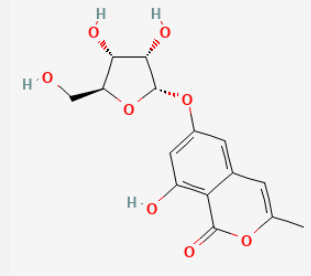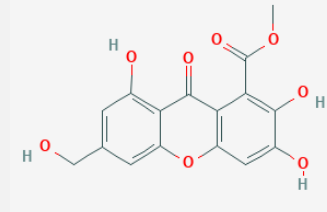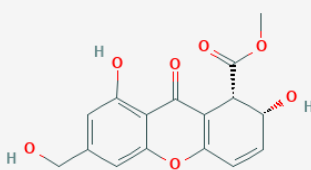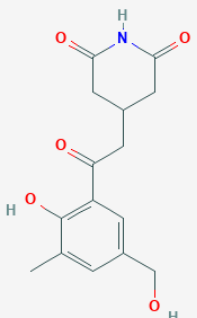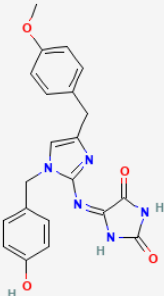
Lycoperosi de F	C58H95NO29	Molecular weight (<500Da)	1270.378		no
		LogP (<5)	4.95		
		H-Bond donor (5)	17		
		H-bond acceptor (<10)	30		
		Violations	3		
Uttroside B	C56H94O28	Molecular weight (<500Da)	1215.342		
		LogP (<5)			
		H-Bond donor (5)			
		H-bond acceptor (<10)			
		Violations			

Table 8.ADME of the top 5 marine hits

Compound	Molecular formula	ADME Properties (Lipinki's Rule of Five)	Properties Value	Structure	Drug likeliness
Daldiniside B-CMNPD24886	C15H16O8	Molecular weight (<500Da) LogP (<5) H-Bond donor (5) H-bond acceptor (<10) Violations	324.287 2.12 3 9.8 0		yes
arthone C-CMNPD30269	C16H12O8	Molecular weight (<500Da) LogP (<5) H-Bond donor (5) H-bond acceptor (<10)	332.266 1.98 2		yes

		Violations	6.45 0		
engyodontiumone H-CMNPD24551	C16H14O7	Molecular weight (<500Da)	318.282		yes
		LogP (<5)	2.29		
		H-Bond donor (5)	1		
		H-bond acceptor (<10)	6.65		
		Violations	0		
3-[2-[2-hydroxy-3-methylphenyl-5-(hydroxymethyl)]-2-oxoethyl] glutarimide-CMNPD24436	C15H17NO5	Molecular weight (<500Da)	291.303		yes
		LogP (<5)	1.29		
		H-Bond donor (5)	2		
		H-bond acceptor (<10)	6.45 0		
		Violations			

isonaamidine D -CMNPD9669	C21H19N5O4	Molecular weight (<500Da)	405.412		yes
		LogP (<5)	2.45		
		H-Bond donor (5)			
		H-bond acceptor (<10)	3		
		Violations	7.5		
			0		

3.3.5. Visualization of the Docked complexes:

The ligand docking calculations were performed using the extra precision (XP) mode of Glide. Based on the ADME analysis and docking scores, we selected three ligands as the best hits.

- Ligand 1, XXL xyloglucan oligosaccharide, exhibited a high binding score of -18.93. The docking results revealed 14 short hydrogen bonds formed with the amino acids on CP.

- Ligand 2, Lycoperoside F (TIP011972), achieved a docking score of -15.5. It formed 11 hydrogen bond interactions and 5 hydrophobic interactions with CP.

- Ligand 3, Ardimerin digallate (TIP009181), demonstrated a binding score of -13.6. It engaged in 7 hydrogen bonds with CP, along with a salt bridge with Lys619 (Figure 49).

Furthermore, Uttroside B (TIP012195) exhibited a binding score of -13.6, forming 8 hydrogen bonds and 4 hydrophobic interactions with CP. Mukurozioside IIb (TIP011396.1) formed 10 hydrogen bonds and 8 hydrophobic interactions with CP, also with a binding score of -13.6.

(a)

a

- 8 polar
- 5 hydrophobic
- 17 H bonds-7short

Interacting amino acid residues

Ligand1

b

c

(b)

a

- 9 polar
- 6 hydrophobic
- 11 H bonds

Interacting amino acid residues

Ligand 2

b
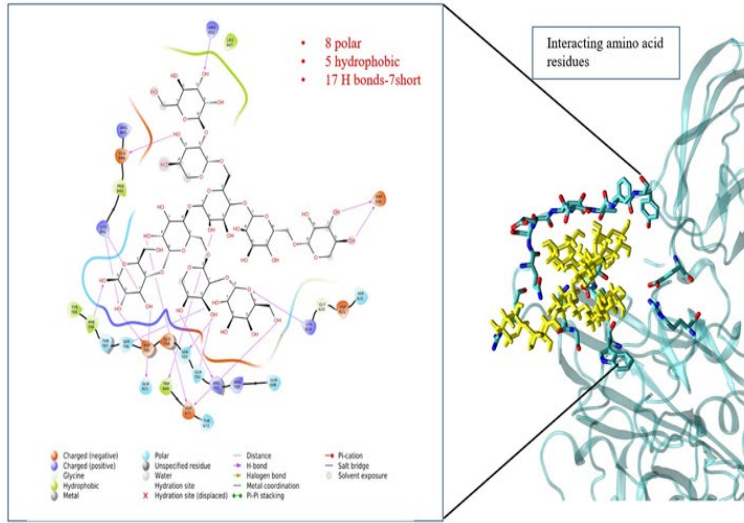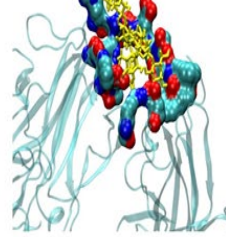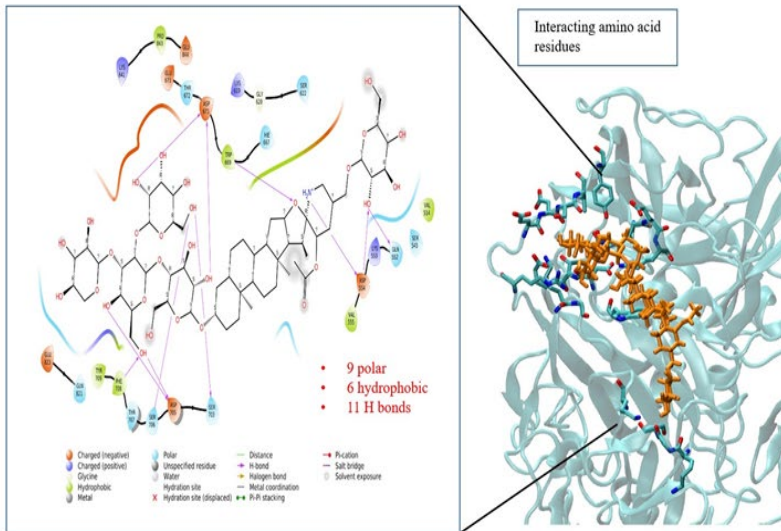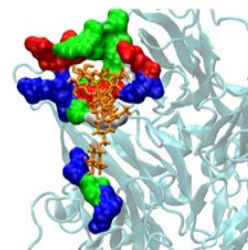
c
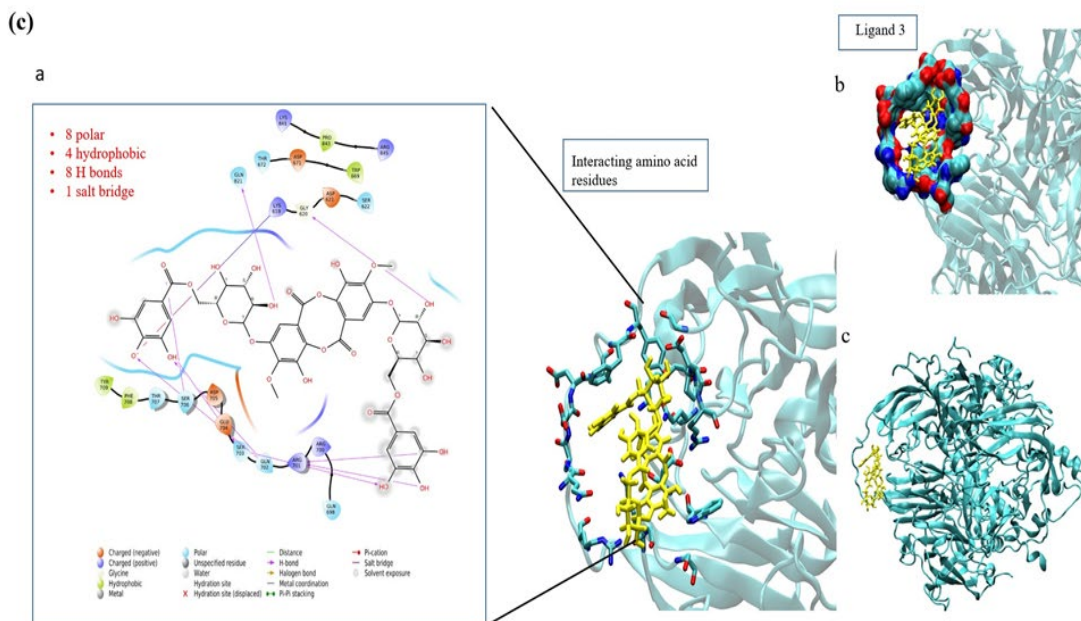
Figure 49. Interaction of ceruloplasmin with phytochemicals showing highest binding affinities in the order: a)Ligand 1: XXL xyloglucan oligosaccharide-Hit 1, b)Ligand 2: Lycoperoside F (TIP011972)-Hit 2, c)Ligand3: Ardimerin digallate (TIP009181)-Hit 3 respectively.

All three top ligands exhibited a minimum of 7 hydrogen bonds and 5 hydrophobic interactions, indicating their potential as promising hits for further analysis through MD simulations.

iii) Evaluation of selected inhibitor(s) using Molecular Dynamics Simulation

MD was performed on all 5 best hits obtained after docking and ADME analysis, using Desmond Simulation Package from Schrodinger which was run to check ligand – protein binding stability over 100ns.

3.3.6. Protein RMSD:

The protein RMSD analysis provides insights into the structural conformation changes of the protein and ligand during the simulation. It involves aligning all frames of the protein to a

reference backbone and calculating the RMSD based on atom selection. Changes greater than 1-3 Å indicate significant conformational changes in the protein during the simulation.

Figure 50 depicts the root mean square deviation (RMSD) of the three ligands with the highest binding scores. The atomic positions for the regions corresponding to CP and Hit1 (XXL xyloglucan oligosaccharide) exhibit notably small variations, indicating a stable binding of the ligand to the protein. Smaller RMSD values indicate a more stable ligand-protein complex(Kufareva & Abagyan, 2012).

In the case of the Hit2 (Lycoperoside F) complex, the protein shows insignificant deviation and attains stability (< 4.5 Å) throughout the simulation. However, the ligand exhibits larger deviations towards the end (> 10 Å).

In the Ardimerin digallate CP complex, the protein remains stable throughout the simulation, while the ligand displays comparably stable behavior (< 4 Å) with minor fluctuations (> 5 Å) around 100 ns. These fluctuations decrease to 3.5 Å by the end of the simulation. This indicates that the selected natural compounds binding to the CP-MPO interaction site result in a stable protein conformation with minimal or no conformational changes during the 200 ns simulation.

The control amitriptyline, shows substantial deviation with an RMSD value of 105 Å at 35-40 ns, which decreases to 45 Å at 100 ns and then reaches a stable equilibrium state until the end of the 200 ns simulation.

The simulations for Hit 2 and Hit 3 binding to CP show more variation in RMSD values for these ligands before stabilizing around a fixed value. The ligand RMSD values indicate the stability of the ligand in relation to the protein's binding site. Similar RMSD values between the ligand and the protein in Hit1 and Hit2 suggest that the ligands remain bound to the protein's binding site throughout the simulation. In the case of Hit 3, the lower RMSD values towards the end suggest that the ligand moves away from the binding pocket.
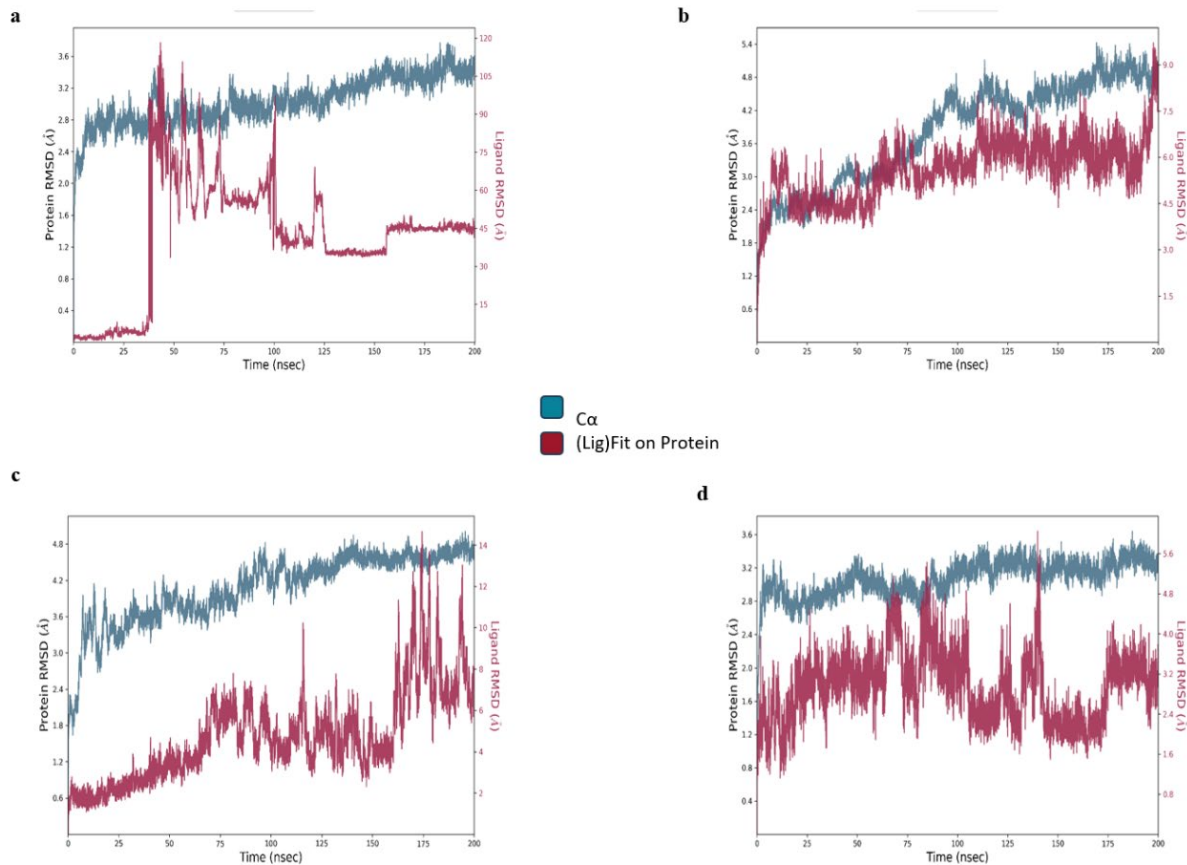
Figure 50. a) Protein-Ligand RMSD of CP-control, b) RSMSD of CP-Hit1, c) RMSD of CP-Hit2, d)RMSD of CP-Hit3. The simulation for Hit 2 and Hit3 binding at ceruloplasmin shows more variation in RMSD values for these ligands before getting stabilized around a fixed value. The atomic position's behavior is notably small for the regions corresponding to the CP and Hit1 i.e., XLLG xyloglucan oligosaccharide.

3.3.7. Protein-ligand contact mapping:

During the MD simulation, we analyzed the interactions between the protein amino acids and our ligands. The docked complexes were examined for four types of protein-ligand interactions: hydrogen bonds, hydrophobic interactions, ionic interactions, and water bridges. The stacked bar charts in Figure 51 illustrate the normalized protein-ligand interactions over the course of the trajectory(Dubey et al., 2014).

For the first hit, hydrogen bonds and water bridges were predominantly observed throughout the simulation, with minimal hydrophobic interactions (Figure 51). Hydrogen bonds play a crucial role in drug specificity, absorption, and metabolism. On the other hand, all three hits displayed hydrophobic interactions, and hit 3 also exhibited ionic interactions. These findings make Hit 2 and Hit 3 more promising drug candidates for docking with CP (Wade & Goodford, 1989).

In the XLLG xyloglucan oligosaccharide complex, Glu704, Ser706, and Phe708 residues formed hydrogen bonds for 100% of the simulation time. Gln821 and Glu844 residues showed hydrogen bond formation for more than 75% of the total simulation duration. Additionally, Val888 formed water bridges for 30% of the simulation time and exhibited hydrophobic interactions for 10% of the duration. Trp669 displayed hydrophobic interactions for 40% of the time and also formed water bridges for 30% of the simulation.

In the Lycoperoside F complex, hydrogen bonds were observed with residues Lys619, Asp671, Thr672, Glu673, and Asp705 for 100% of the simulation. Trp669 showed hydrophobic interactions for 50% of the time and formed water bridges. Asp554 formed water bridges for 50% of the time, along with ionic interactions for 10% of the duration, and hydrogen bonds for the remaining 45%.

In the Ardimerin digallate complex, Trp669 and Tyr709 residues exhibited hydrophobic interactions for 40% and 25% of the 200 ns simulation, respectively. They also formed water bridges for about 20% of the time. GLN673 formed water bridges for over 70% of the simulation period. Gly844 formed hydrogen bonds for 100% of the simulation time, while Glu704 and Gln702 formed hydrogen bonds for approximately 70-75%.

The residues in the control amitriptyline complex mostly showed hydrophobic interactions, with only Glu633 forming hydrogen bonds for 40% of the duration.

Based on the overall analysis of the MD simulation, Lycoperoside F displayed potential dynamic stability compared to the other selected natural compounds and the control molecule.
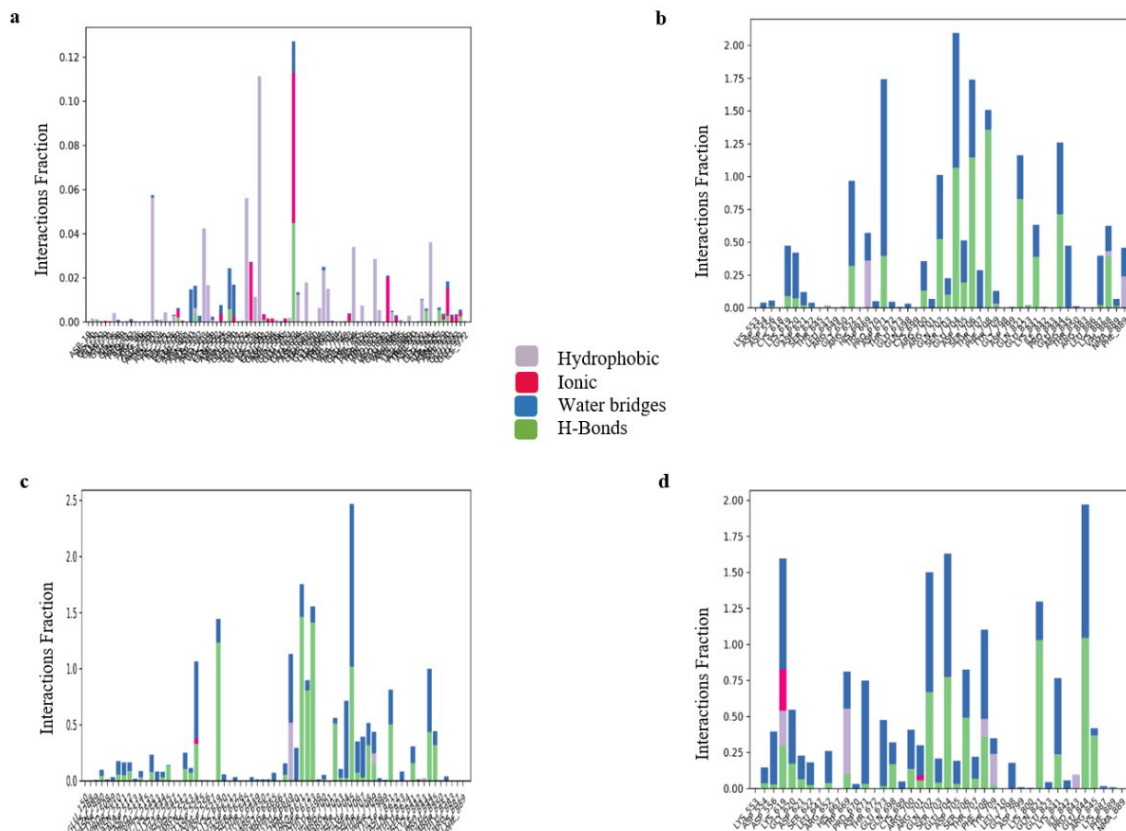
Figure 51: Protein-Ligand interaction over more than 30.0% of the simulation time in the selected trajectory (0.00 through 200.01 nsec) of control (a) Hit 1(b), Hit2 (c), Hit3(d). The docked complexes are analyzed for the following protein-ligand interactions: Hydrogen Bonds, Hydrophobic interaction, Ionic interaction and Water Bridges

3.3.8. RMSF analysis:

The RMSF (Root Mean Square Fluctuation) value provides insight into the specific variations of atoms/residues in each complex's protein and ligand molecules. The Protein RMSF analysis of the three selected phytochemical complexes revealed low fluctuations throughout the simulation time. The protein residues in all docked complexes exhibited stability (< 3 Å) with minor residual fluctuations (Figure 52(a)). However, the ligand RMSF analysis showed some atomic fluctuations. In the case of XLLG xyloglucan oligosaccharide, the ligand residues exhibited fluctuations with RMSF values below 3 Å. On the other hand, the ligand molecule of Lycoperoside

F displayed substantial fluctuations, reaching a maximum RMSF value of 8 Å. Hit 3 Ardimerin digallate showed atomic stability (< 3 Å) with acceptable fluctuations. Interestingly, the control compound amitriptyline showed a very high RMSF (Figure 52a, b).

i)
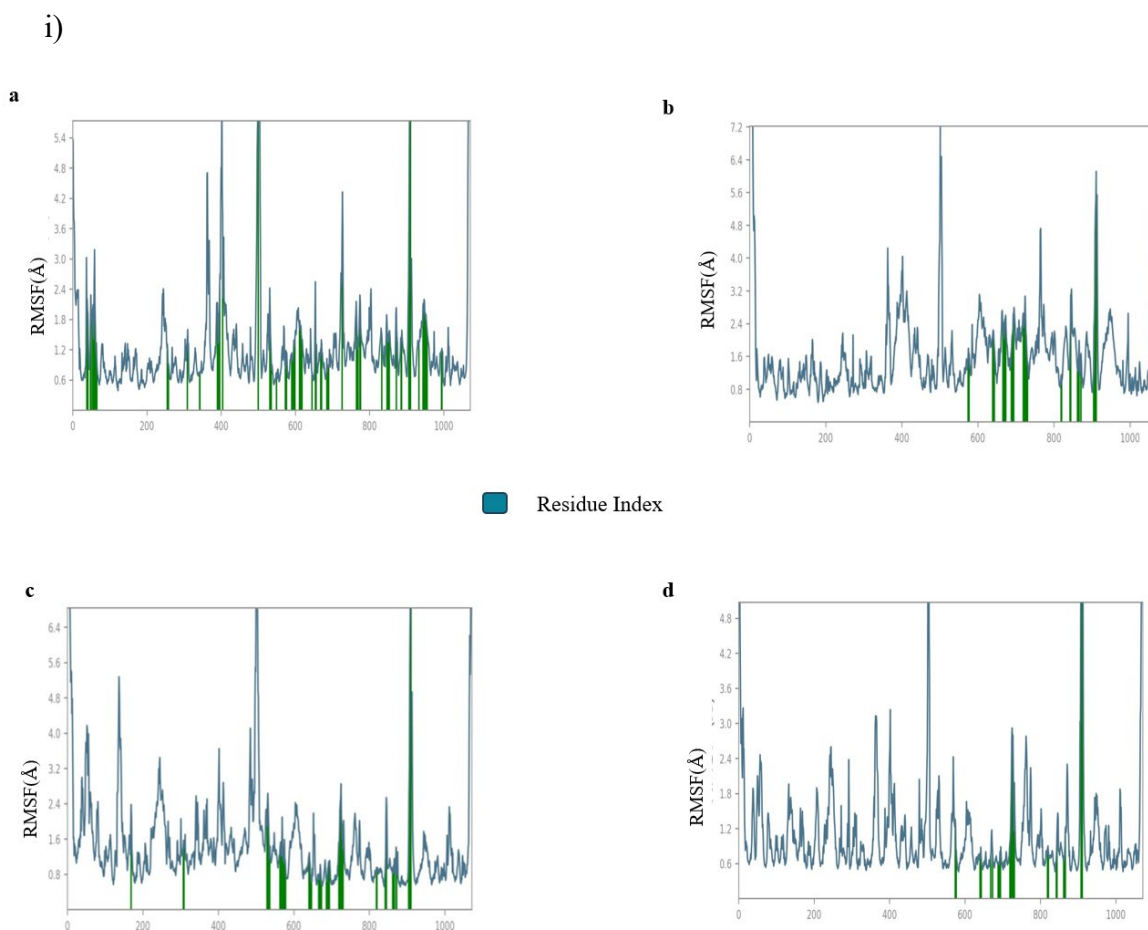
ii)
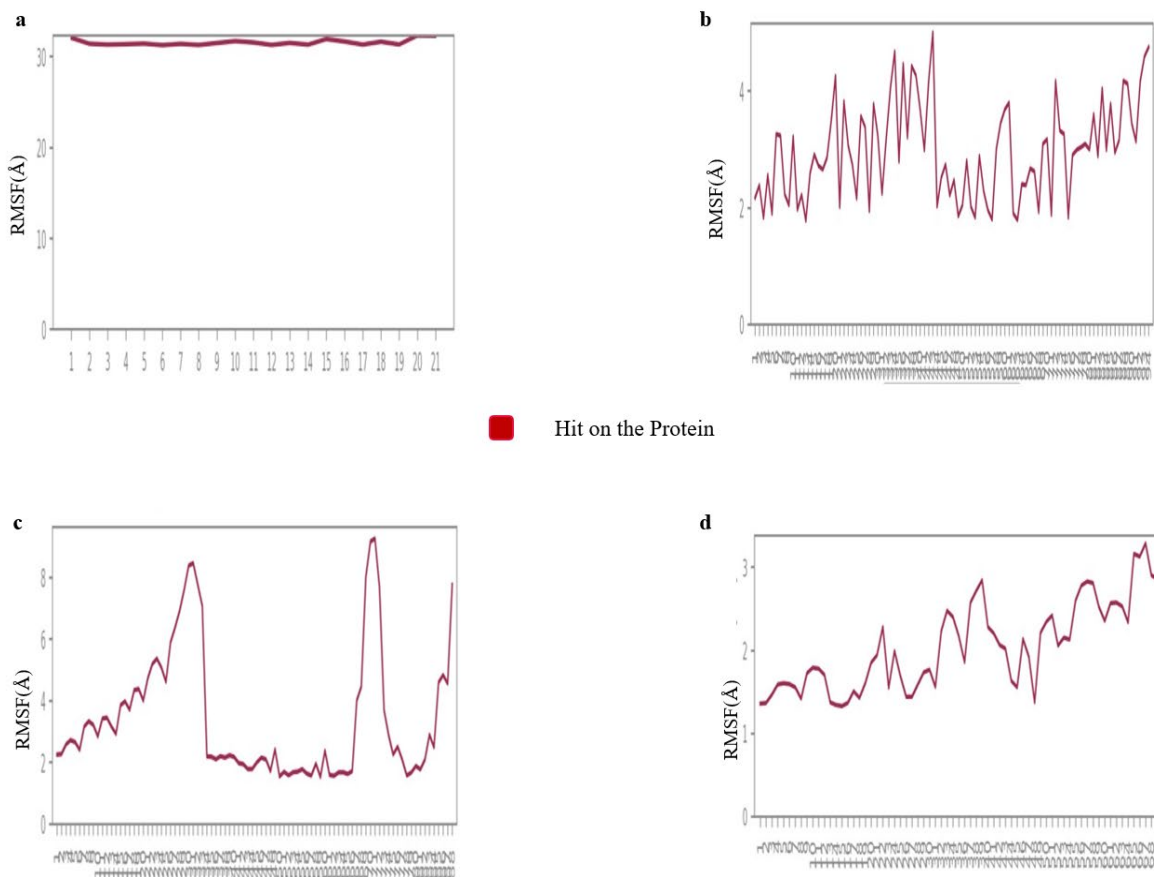
Figure 52(i): Protein RMSF graph of the protein-ligand complex viz control Amitriptyline, a: Hit1 b: Hit2 c: Hit3 (ii) Ligand RMSF of a: Hit1 b: Hit2 c: Hit3 and controls

3.3.9. Comparative Analysis of a) radius of gyration, b) hydrogen bonding, and c) SASA of CP protein and control and selected drugs:

The three selected ligands were compared with the control. The RMSD analysis showed good stability of all hits throughout the 200 ns simulation. Similarly, the hydrogen bonds remained stable throughout the simulation, with Hit 2 and Hit 1 exhibiting higher stability. Hit 1 also showed the highest Solvent Accessible Surface Area (SASA) (Figure 53).
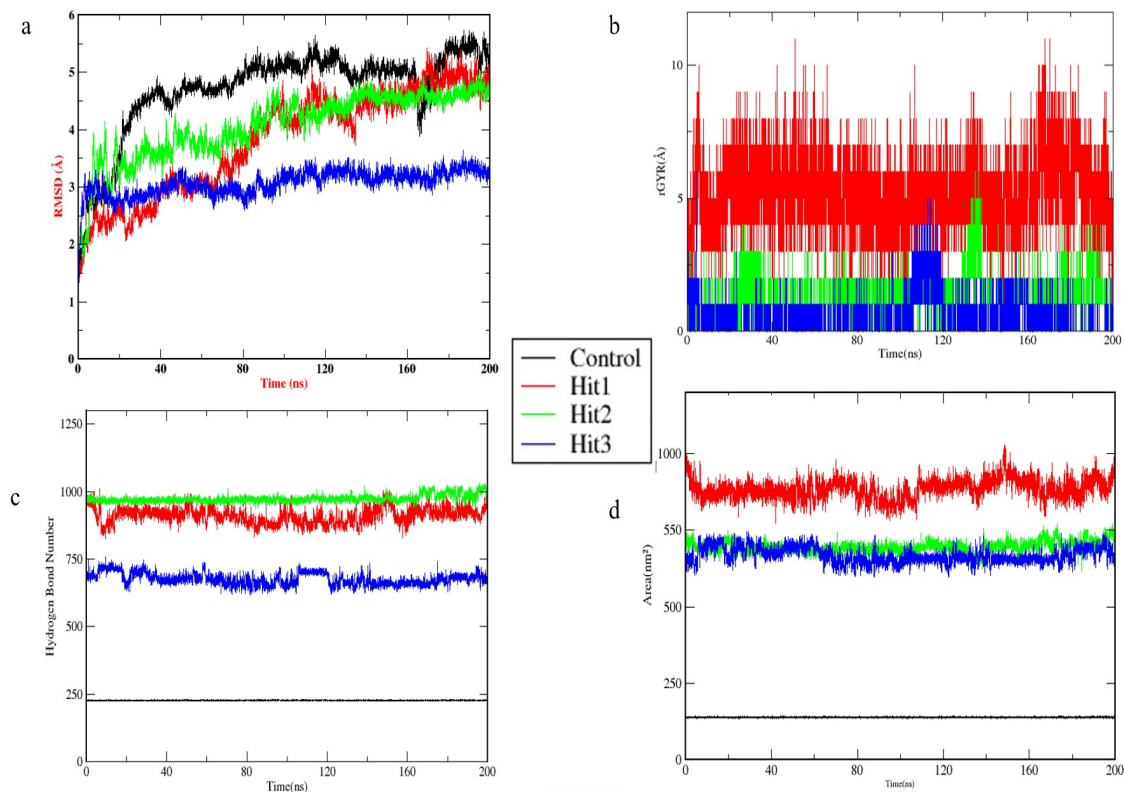
Figure 53. a) RMSD over the entire simulation of the Control and Hit 1, 2and 3, b) Radius of gyration (Rg) over the entire simulation, using time (ns) as the abscissa and Rg as the ordinate. c) Total H-bond count during the course of the simulation d) Solvent accessible surface area (SASA), with time (ns) as the abscissa and SASA as the ordinate.

Evaluation of Stable Protein-Ligand Interactions during MD:

Further analysis was conducted to evaluate the stable protein-ligand interactions during the MD simulation. The interactions were examined for subtypes of hydrogen bonds, such as backbone acceptor, backbone donor, side-chain acceptor, and side-chain donor. Protein-ligand hydrogen bonds were considered strong when the distance between the donor and acceptor atoms was 2.5 Å (D—H•••A), and the donor-hydrogen-acceptor atoms formed an angle of ≥120° (D—H•••A). The hydrogen-acceptor-bonded atom should have an acceptor angle of ≥90° (H•••A—X). Additionally, π-Cation, π-π, and other non-specific interactions were divided under the category of hydrophobic interactions (Varma et al., 2010)

133

For Hit 1, we observed 96% and 92% hydrogen bond interactions within the ligand (Fig. 11a).

Hit 2 displayed 10 hydrogen bonds along with three water bonds (>30%). It showed an 83% hydrogen donor bond interaction with SER703 (Fig. 11b).

Hit 3 exhibited 4 hydrogen bonds and one pi–pi stacking interaction. Considering hydrogen bonds are the strongest, we conclude that hit 2 i.e., Lycopersicon esculentum (TIP011972) is the best ligand to use for docking studies against CP.
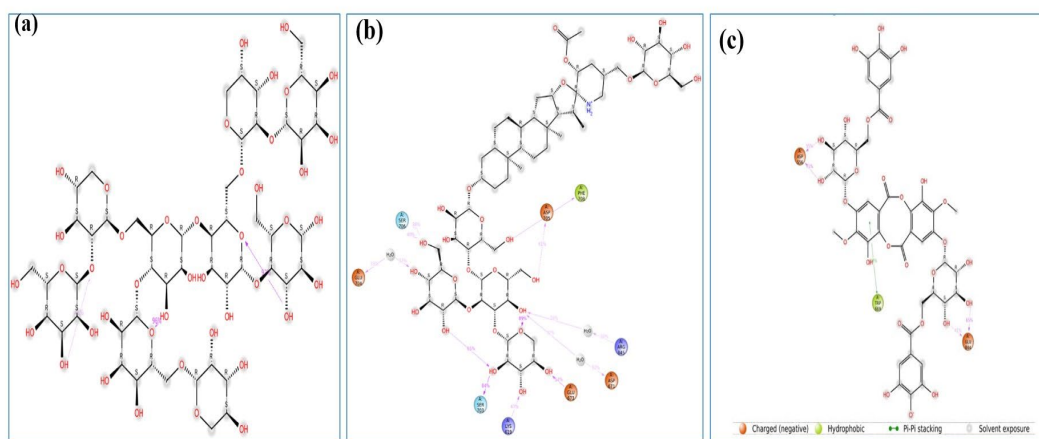
Figure 54. Desmond MD calculated protein−ligand contacts at CP binding site with Hit 1(a), 2(b), 3(b)

Discussion of part 3.3:

Following molecular docking studies, MD was used to rank the three compounds according to their binding energies and ADME characteristics as follows: Hit 2: Lycoperoside F> Hit1: XLLG xyloglucan oligosaccharide> Hit3: Ardimerin digallate

The above data shows all three drugs can be further explored and validated through further experimentation.

Hit 1: XLLG xyloglucan oligosaccharide:

PubChem CID: 52940189

A backbone of glucosyl residues that are β-(1→4)-linked glucosyl residues and α-(1→6)-substituted with xylosyl residues makes up xyloglucan. The majority of xyloglucan structures allow for the extension of the xylosyl substituents with galactosyl and fucosyl residues. The cotyledons of tamarind seeds can be used to obtain xyloglucans, which are mostly present in the main cell walls of higher plants and are commercially accessible as a thickening, stabilizer, gelling agent, ice-crystal stabilizer, and starch modifier. Clinical trials are being conducted with xyloglucan oligosaccharide on individuals with diarrhea and irritable bowel syndrome. In order to protect and strengthen the intestinal barrier, they created Gelsectan, a medical device combining xyloglucan (XG), pea protein and tannins (PPT) from grape seed extract, and xylo-oligosaccharides (XOS).In order to create drug-functionalized cellulosic biomaterials, efforts are being made to employ doxorubicin and xyloglucan glycoconjugates due to the severe side effects of anthracycline anticancer agents(Bliman et al., 2018).

XLLG showed a docking score of -18.93 in our docking studies with CP.
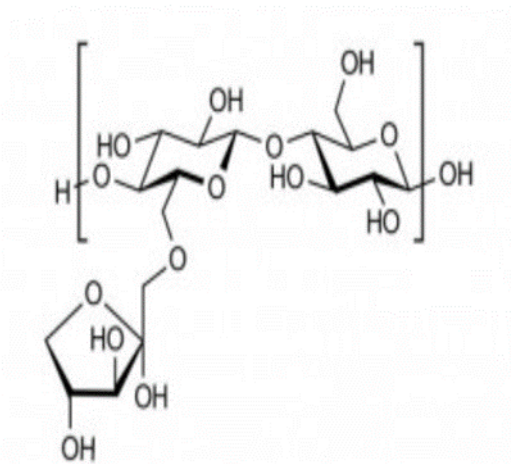
Xyloglucan oligosaccharide

Hit 2: Lycoperoside F:

Lycoperoside f is a steroidal alkaloid glycoside from tomato (Lycopersicon esculentum) with Pubchem ID 21577181(Yoshizaki et al., 2005).

Lycoperoside f obtained from Lycopersicon esculentum (TIP011972.sdf) that docked at our site of interest with a binding score of -15.553 with significant number of hydrogen bonds as well

as hydrophobic interactions. It showed good results of ADMET and drug likeness. Hence Lycoperoside f can be a suitable drug that can be further validated through *invitro* studies for binding at the MPO-CP interaction site.
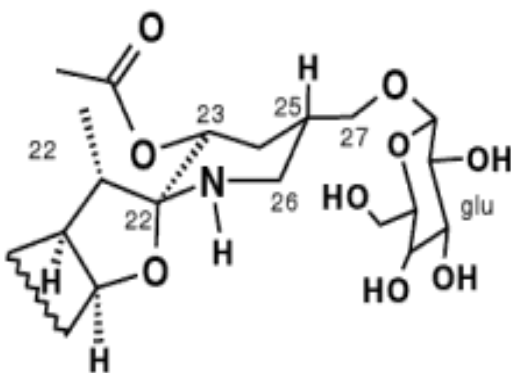
Lycoperoside F

Hit3: Ardimerin digallate

PubChem CID: 16681402

A C-glycosyl molecule called ardimerin digallate was discovered in the entire plants of Ardisia japonica. It is a dimeric lactone that has inhibitory effects on the enzymes Ribonuclease H226 and HIV-1. It functions as a metabolite and an inhibitor of the enzyme retroviral ribonuclease H. It is a C-glycosyl compound, a lactone, an aromatic ether and a gallate (C. F. Liu, 2022).
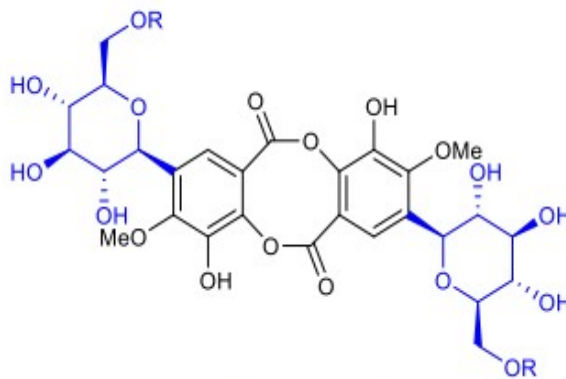
Ardemerin digallate

CHAPTER 4

CONCLUSION AND SUGGESTIONS FOR FUTURE WORK

CP, an abundant copper-binding protein, has been implicated in various aspects of tumor biology. In tumors, CP expression and activity has been seen to exhibit significant alterations, leading to potential implications for tumor progression and therapeutic outcomes.

One aspect of CP's involvement in tumors is its role in regulating oxidative stress. CP has antioxidant properties and can scavenge reactive oxygen species (ROS), thereby counteracting oxidative damage in tumor cells. Its ability to bind copper allows for efficient oxidation of substrates, including ferrous iron, which is important for tumor cell proliferation and survival. Moreover, CP has been associated with angiogenesis, the process of new blood vessel formation that is crucial for tumor growth and metastasis. CP can modulate angiogenesis by influencing the activity of pro-angiogenic factors, such as vascular endothelial growth factor (VEGF), and facilitating the remodeling of the extracellular matrix(Figure 55).
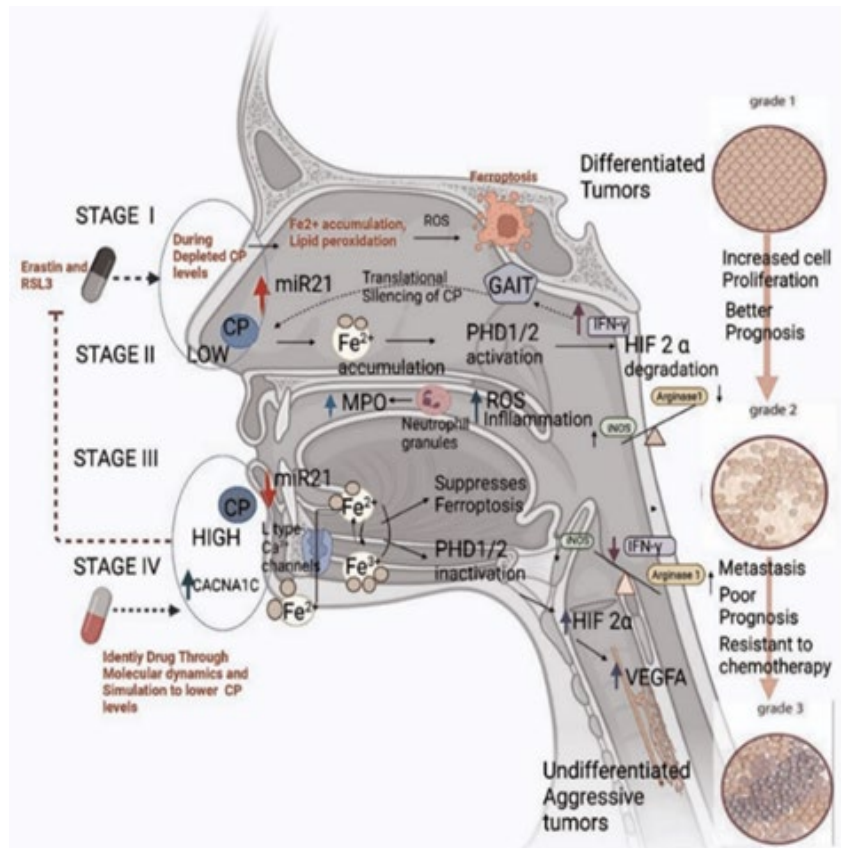
Figure 55: Proposed mechanism of ceruloplasmin action in oral cancer pathways

In addition to its roles in oxidative stress management and angiogenesis, the upregulation of CP in tumors may impact immune responses. It has been shown to regulate immune responses and modulate the function of immune cells within the tumor microenvironment. CP can influence the polarization of immune cells, such as macrophages, towards tumor-promoting phenotypes, thereby facilitating tumor immune evasion and immunosuppression. Furthermore, our network analysis results suggests a potential association between CP and cancer metastasis. CP may affect the epithelial-mesenchymal transition (EMT), a process involved in tumor cell invasion and metastasis. It can influence EMT-related signaling pathways, such as the transforming growth factor-beta (TGF-β) pathway, thereby promoting tumor cell migration and invasion.

Our study reports associations between CP expression levels and clinicopathological features, including tumor stage, grade, and patient survival rates, in HNC patients. The upregulation of CP in tumors has clinical implications as well. Elevated levels of CP have been associated with poor prognosis, advanced tumor stage, and reduced survival rates in certain cancer types. Therefore, CP upregulation may serve as a potential prognostic biomarker for assessing tumor aggressiveness and predicting patient outcomes.

The interaction between CP and MPO can suppress the peroxidase activity of MPO under normal physiological conditions. This inhibition prevents the production of HOCl (Hypochlorous acid) by MPO in Tumor-Associated Neutrophils within the tumor microenvironment. As a result, HOCl-mediated caspase activity, which typically leads to apoptosis, is suppressed. This mechanism may contribute to tumor survival in later stages. Our Tumor Immune Infiltration analysis revealed that high CP expression is correlated with the expression of PDL1 and TIM3, both of which activate NETosis (Neutrophil Extracellular Traps formation). These NETs have previously been linked to promoting tumor metastasis. Therefore by targeting CP-MPO interaction we are targeting CP's role in immune regulation in patients with head and neck cancer(Figure 56).
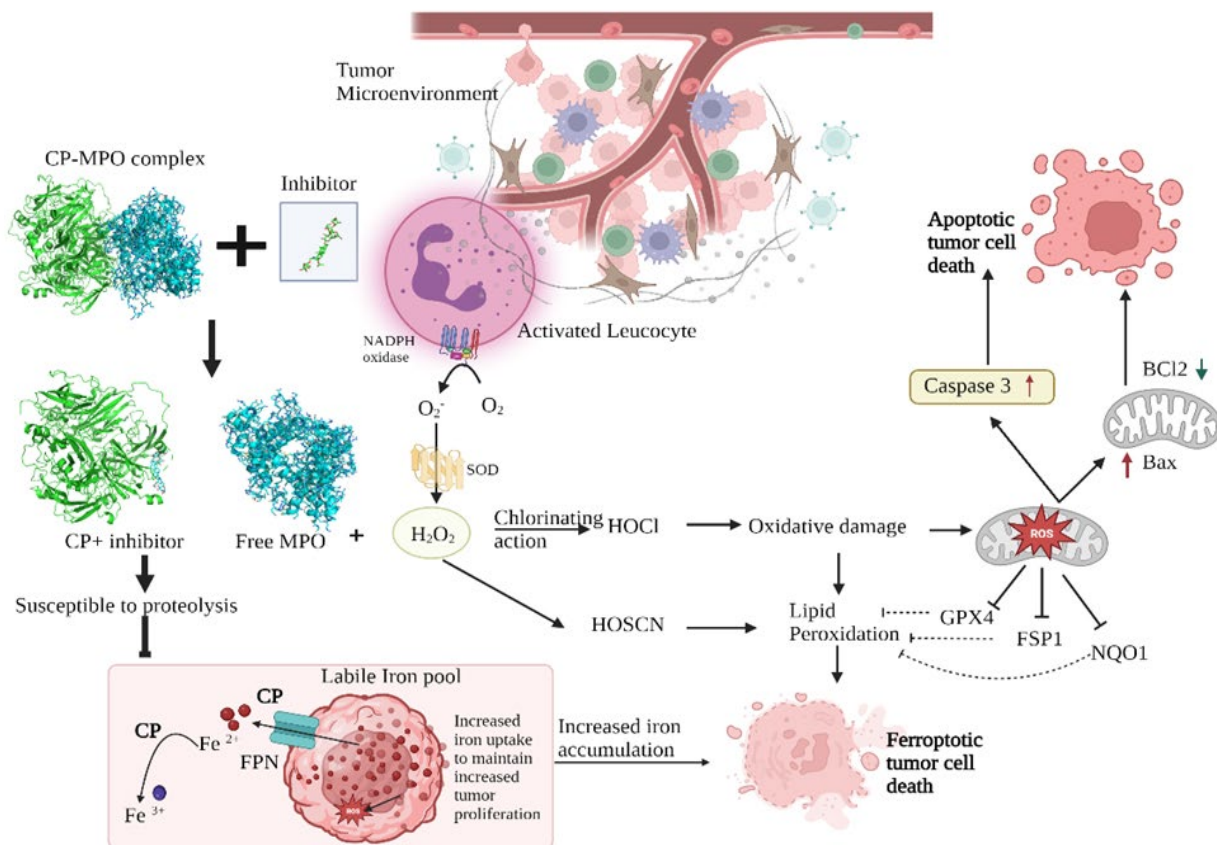
Figure 56: Proposed Role of MPO-CP interaction in the Tumor micro environment

Xyloglucan oligosaccharide and Ardimerin digallate metabolites showed good docking scores at the CP- MPO interaction site. We also identified the phytochemical lycoperoside f obtained from Lycopersicon esculentum (TIP011972.sdf) that docked at our site of interest with good binding score along with significant number of hydrogen bonds as well as hydrophobic interactions. They all showed good results of ADMET and drug likeness. This inhibition enables myeloperoxidase to carry out its chlorinating function, producing HOCl that triggers the caspase enzyme to kill tumor cells. Additionally, MPO and CP interaction shield CP from proteolysis. In order to achieve greater proliferation rates, tumor cells up-regulate CP to combat the elevated ROS caused by increased iron absorption. Therefore, CP is destroyed in the absence of MPO, which causes iron to build up inside of the tumor cells and eventually cause ferroptotic tumor cell death. We suggest further research into these compounds through additional *in vitro* and *in vivo* validation studies since they may be potential leads in the drug development for cancer therapy.

In summary, the upregulation of CP in tumors is associated with multiple aspects of tumor biology, including oxidative stress management, angiogenesis, immune modulation, and metastatic potential. Understanding the mechanisms underlying CP upregulation and its functional consequences in tumors has provided valuable insights for the development of novel therapeutic strategies targeting this protein in cancer treatment. Examining whether modulating CP expression or activity could have therapeutic benefits, either alone or in combination with existing therapies, could be an important area of future research.

The protein CP previously illustrated as a biomarker of cancer progression. Further,in this study, we revealed structure-based site specific docking investigations of a variety of active phytochemical compounds and marine chemicals against CP protein. Lycoperoside F, XLLG xyloglucan oligosaccharide, and Ardimerin digallate, which have the highest binding affinities to ceruloplamsin and exhibit strong interactions with the amino acids involved in CP-MPO interaction, raise the possibility of using these substances to inhibit CP-MPO. Invitro research could be used to learn more about these substances. With these advancements we hope drug repurposing could significantly contribute to the development of therapeutic medications and the efficient management of cancer.

REFERENCES

Abdelaal, G., & Veuger, S. (2021). Reversing oncogenic transformation with iron chelation. *Oncotarget*, *12*(2), 106. https://doi.org/10.18632/ONCOTARGET.27866

Aguilar-Cazares, D., Chavez-Dominguez, R., Carlos-Reyes, A., Lopez-Camarillo, C., Hernadez de la Cruz, O. N., & Lopez-Gonzalez, J. S. (2019). Contribution of Angiogenesis to Inflammation and Cancer. In *Frontiers in Oncology* (Vol. 9). https://doi.org/10.3389/fonc.2019.01399

Alhabbab, R., & Johar, R. (2022). Lip cancer prevalence, epidemiology, diagnosis, and management: A review of the literature. *Advances in Oral and Maxillofacial Surgery*, *6*, 100276. https://doi.org/10.1016/J.ADOMS.2022.100276

Aman, L. O., Kartasasmita, R. E., & Tjahjono, D. H. (2021). Virtual screening of curcumin analogues as DYRK2 inhibitor: Pharmacophore analysis, molecular docking and dynamics, and ADME prediction. *F1000Research*, *10*. https://doi.org/10.12688/f1000research.28040.1

Anastasiou, D., Poulogiannis, G., Asara, J. M., Boxer, M. B., Jiang, J. K., Shen, M., Bellinger, G., Sasaki, A. T., Locasale, J. W., Auld, D. S., Thomas, C. J., Vander Heiden, M. G., & Cantley, L. C. (2011). Inhibition of pyruvate kinase M2 by reactive oxygen species contributes to cellular antioxidant responses. *Science*, *334*(6060), 1278–1283. https://doi.org/10.1126/science.1211485

Andrews, L. P., Marciscano, A. E., Drake, C. G., & Vignali, D. A. A. (2017). LAG3 (CD223) as a cancer immunotherapy target. In *Immunological Reviews* (Vol. 276, Issue 1). https://doi.org/10.1111/imr.12519

Arner, E., Forrest, A. R. R., Ehrlund, A., Mejhert, N., Itoh, M., Kawaji, H., Lassmann, T., Laurencikiene, J., Rydén, M., & Arner, P. (2014). Ceruloplasmin is a novel adipokine which is overexpressed in adipose tissue of obese subjects and in obesity-associated cancer cells. *PLoS ONE*, *9*(3). https://doi.org/10.1371/journal.pone.0080274

Arnould, C., Lelièvre-Pégorier, M., Ronco, P., & Lelongt, B. (2009). MMP9 limits apoptosis and stimulates branching morphogenesis during kidney development. *Journal of*

the American Society of Nephrology, *20*(10). https://doi.org/10.1681/ASN.2009030312

AV, S., ET, Z., VA, K., VR, S., & VB, V. (2014). Lactoferrin, myeloperoxidase, and ceruloplasmin: complementary gearwheels cranking physiological and pathological processes. *Biometals : An International Journal on the Role of Metal Ions in Biology, Biochemistry, and Medicine*, *27*(5), 815–828. https://doi.org/10.1007/S10534-014-9755-2

B. Fernandes, T., C. F. Segretti, M., C. Polli, M., & Parise-Filho, R. (2016). Analysis of the Applicability and Use of Lipinski`s Rule for Central Nervous System Drugs. *Letters in Drug Design & Discovery*, *13*(10). https://doi.org/10.2174/1570180813666160622092839

Backes, C., Khaleeq, Q. T., Meese, E., & Keller, A. (2016). miEAA: microRNA enrichment analysis and annotation. *Nucleic Acids Research*, *44*(W1), W110–W116. https://doi.org/10.1093/NAR/GKW345

Bakhautdin, B., Goksoy Bakhautdin, E., & Fox, P. L. (2014). Ceruloplasmin has two nearly identical sites that bind myeloperoxidase. *Biochemical and Biophysical Research Communications*, *453*(4), 722–727. https://doi.org/10.1016/J.BBRC.2014.09.134

Bedford, M. R., Ford, S. J., Horniblow, R. D., Iqbal, T. H., & Tselepis, C. (2013). Iron chelation in the treatment of cancer: a new role for deferasirox? *Journal of Clinical Pharmacology*, *53*(9), 885–891. https://doi.org/10.1002/JCPH.113

Beeram, M., Patnaik, A., & Rowinsky, E. K. (2005). Raf: A strategic target for therapeutic development against cancer. *Journal of Clinical Oncology*, *23*(27), 6771–6790. https://doi.org/10.1200/JCO.2005.08.036

Bertucci, F., Finetti, P., Perrot, D., Leroux, A., Collin, F., Cesne, A. Le, Coindre, J.-M., Blay, J.-Y., Birnbaum, D., & Mamessier, E. (2017). PDL1 expression is a poor-prognosis factor in soft-tissue sarcomas. *Oncoimmunology*, *6*(3). https://doi.org/10.1080/2162402X.2016.1278100

BIOLOGICAL INORGANIC CHEMISTRY : structure and reactivity. (2018).

Blandino, G., & Di Agostino, S. (2018). New therapeutic strategies to treat human cancers expressing mutant p53 proteins. *Journal of Experimental & Clinical Cancer Research 2018 37:1*, *37*(1), 1–13. https://doi.org/10.1186/S13046-018-0705-7

Bliman, D., Demeunynck, M., Leblond, P., Meignan, S., Baussane, I., & Fort, S. (2018). Enzymatically Activated Glyco-Prodrugs of Doxorubicin Synthesized by a Catalysis-Free Diels-Alder Reaction. *Bioconjugate Chemistry*, *29*(7), 2370–2381. https://doi.org/10.1021/ACS.BIOCONJCHEM.8B00314

Bonaccorsi di Patti, M. C., Cutone, A., Polticelli, F., Rosa, L., Lepanto, M. S., Valenti, P., & Musci, G. (2018). The ferroportin-ceruloplasmin system and the mammalian iron homeostasis machine: regulatory pathways and the role of lactoferrin. *BioMetals*, *31*(3), 399–414. https://doi.org/10.1007/S10534-018-0087-5

Borse, V., Konwar, A. N., & Buragohain, P. (2020). Oral cancer diagnosis and perspectives in India. *Sensors International*, *1*, 100046. https://doi.org/10.1016/J.SINTL.2020.100046

Braicu, C., Buse, M., Busuioc, C., Drula, R., Gulei, D., Raduly, L., Rusu, A., Irimie, A., Atanasov, A. G., Slaby, O., Ionescu, C., & Berindan-Neagoe, I. (2019). A Comprehensive Review on MAPK: A Promising Therapeutic Target in Cancer. *Cancers*, *11*(10). https://doi.org/10.3390/CANCERS11101618

Brentnall, M., Rodriguez-Menocal, L., De Guevara, R. L., Cepero, E., & Boise, L. H. (2013). Caspase-9, caspase-3 and caspase-7 have distinct roles during intrinsic apoptosis. *BMC Cell Biology*, *14*(1). https://doi.org/10.1186/1471-2121-14-32

Brlek, P., Kafka, A., Bukovac, A., & Pećina-šlaus, N. (2021). Integrative cBioPortal Analysis Revealed Molecular Mechanisms That Regulate EGFR-PI3K-AKT-mTOR Pathway in Diffuse Gliomas of the Brain. *Cancers*, *13*(13). https://doi.org/10.3390/CANCERS13133247

Brown, R. A. M., Richardson, K. L., Kabir, T. D., Trinder, D., Ganss, R., & Leedman, P. J. (2020). Altered Iron Metabolism and Impact in Cancer Biology, Metastasis, and Immunology. In *Frontiers in Oncology* (Vol. 10). https://doi.org/10.3389/fonc.2020.00476

Brugere, J., Guenel, P., Leclerc, A., & Rodriguez, J. (1986). Differential effects of tobacco and alcohol in cancer of the larynx, pharynx, and mouth. *Cancer*, *57*(2). https://doi.org/10.1002/1097-0142(19860115)57:2<391::AID-

CNCR2820570235>3.0.CO;2-Q

Budanov, A. V. (2014). The role of tumor suppressor p53 in the antioxidant defense and metabolism. *Sub-Cellular Biochemistry*, *85*, 337. https://doi.org/10.1007/978-94-017-9211-0_18

Cabantchik, Z. I., Cabantchik, Z. I., Kakhlon, O., Epsztejn, S., Zanninelli, G., & Breuer, W. (2002). Intracellular and extracellular labile iron pools. *Springer*, *509*, 55–75. https://doi.org/10.1007/978-1-4615-0593-8_4

Cardama, G. A., Gonzalez, N., Maggio, J., Lorenzano Menna, P., & Gomez, D. E. (2017). Rho GTPases as therapeutic targets in cancer (Review). *International Journal of Oncology*, *51*(4), 1025–1034. https://doi.org/10.3892/IJO.2017.4093/HTML

Casas, B. S., Adolphe, C., Lois, P., Navarrete, N., Solís, N., Bustamante, E., Gac, P., Cabané, P., Gallegos, I., Wainwright, B. J., Palma, V., Casas, B. S., Adolphe, C., Lois, P., Navarrete, N., Solís, N., Bustamante, E., Gac, P., Cabané, P., … Palma, V. (2017). Downregulation of the Sonic Hedgehog/Gli pathway transcriptional target Neogenin-1 is associated with basal cell carcinoma aggressiveness. *Oncotarget*, *8*(48), 84006–84018. https://doi.org/10.18632/ONCOTARGET.21061

Castro, F., Cardoso, A. P., Gonçalves, R. M., Serre, K., & Oliveira, M. J. (2018a). Interferon-Gamma at the Crossroads of Tumor Immune Surveillance or Evasion. *Frontiers in Immunology*, *9*(MAY). https://doi.org/10.3389/FIMMU.2018.00847

Castro, F., Cardoso, A. P., Gonçalves, R. M., Serre, K., & Oliveira, M. J. (2018b). Interferon-Gamma at the Crossroads of Tumor Immune Surveillance or Evasion. *Frontiers in Immunology*, *0*(MAY), 847. https://doi.org/10.3389/FIMMU.2018.00847

Cerami, E., Gao, J., Dogrusoz, U., Gross, B. E., Sumer, S. O., Aksoy, B. A., Jacobsen, A., Byrne, C. J., Heuer, M. L., Larsson, E., Antipin, Y., Reva, B., Goldberg, A. P., Sander, C., & Schultz, N. (2012). The cBio Cancer Genomics Portal: An Open Platform for Exploring Multidimensional Cancer Genomics Data. *Cancer Discovery*, *2*(5), 401. https://doi.org/10.1158/2159-8290.CD-12-0095

Ceruloplasmin and acute phase protein levels are associated with cardiovascular disease in chronic dialysis patients - PubMed. (n.d.). Retrieved May 22, 2023, from

https://pubmed.ncbi.nlm.nih.gov/15593040/

Chandrashekar, D. S., Karthikeyan, S. K., Korla, P. K., Patel, H., Shovon, A. R., Athar, M., Netto, G. J., Qin, Z. S., Kumar, S., Manne, U., Crieghton, C. J., & Varambally, S. (2022). UALCAN: An update to the integrated cancer data analysis platform. *Neoplasia*, *25*, 18–27. https://doi.org/10.1016/J.NEO.2022.01.001

Chapman, A. L. P., Mocatta, T. J., Shiva, S., Seidel, A., Chen, B., Khalilova, I., Paumann-Page, M. E., Jameson, G. N. L., Winterbourn, C. C., & Kettle, A. J. (2013). Ceruloplasmin is an endogenous inhibitor of myeloperoxidase. *Journal of Biological Chemistry*, *288*(9). https://doi.org/10.1074/jbc.M112.418970

Checa, J., & Aran, J. M. (2020). <p>Reactive Oxygen Species: Drivers of Physiological and Pathological Processes</p>. *Journal of Inflammation Research*, *Volume 13*, 1057–1073. https://doi.org/10.2147/jir.s275595

Chen, C. Y., Chen, J., He, L., & Stiles, B. L. (2018). PTEN: Tumor suppressor and metabolic regulator. In *Frontiers in Endocrinology* (Vol. 9, Issue JUL). https://doi.org/10.3389/fendo.2018.00338

Chen, F., Han, B., Meng, Y., Han, Y., Liu, B., Zhang, B., Chang, Y., Cao, P., Fan, Y., & Tan, K. (2021). Ceruloplasmin correlates with immune infiltration and serves as a prognostic biomarker in breast cancer. *Aging*, *13*(16), 20438–20467. https://doi.org/10.18632/AGING.203427

Chen, I. J., & Foloppe, N. (2010). Drug-like bioactive structures and conformational coverage with the ligprep/confgen suite: Comparison to programs MOE and catalyst. *Journal of Chemical Information and Modeling*, *50*(5). https://doi.org/10.1021/ci100026x

Chen, M. T., Sun, H. F., Li, L. D., Zhao, Y., Yang, L. P., Gao, S. P., & Jin, W. (2018). Downregulation of FOXP2 promotes breast cancer migration and invasion through TGFβ/SMAD signaling pathway. *Oncology Letters*, *15*(6). https://doi.org/10.3892/ol.2018.8402

Chen, X., Yu, C., Kang, R., & Tang, D. (2020a). Iron Metabolism in Ferroptosis. *Frontiers in Cell and Developmental Biology*, *8*, 590226. https://doi.org/10.3389/FCELL.2020.590226

Chen, X., Yu, C., Kang, R., & Tang, D. (2020b). Iron Metabolism in Ferroptosis. *Frontiers in Cell and Developmental Biology*, *8*, 1089. https://doi.org/10.3389/FCELL.2020.590226/BIBTEX

Chuckran, C. A., Liu, C., Bruno, T. C., Workman, C. J., & Vignali, D. A. A. (2020). Neuropilin-1: a checkpoint target with unique implications for cancer immunology and immunotherapy. *Journal for ImmunoTherapy of Cancer*, *8*(2), e000967. https://doi.org/10.1136/JITC-2020-000967

Crabtree, H. G. (1929). Observations on the carbohydrate metabolism of tumours. *The Biochemical Journal*, *23*(3), 536–545. https://doi.org/10.1042/BJ0230536

Dai, L., Cui, X., Zhang, X., Cheng, L., Liu, Y., Yang, Y., Fan, P., Wang, Q., Lin, Y., Zhang, J., Li, C., Mao, Y., Wang, Q., Su, X., Zhang, S., Peng, Y., Yang, H., Hu, X., Yang, J., … Deng, H. (2016). SARI inhibits angiogenesis and tumour growth of human colon cancer through directly targeting ceruloplasmin. *Nature Communications*, *7*. https://doi.org/10.1038/NCOMMS11996

Das, M., Zhu, C., & Kuchroo, V. K. (2017). Tim-3 and its role in regulating anti-tumor immunity. In *Immunological Reviews* (Vol. 276, Issue 1). https://doi.org/10.1111/imr.12520

De Domenico, I., Ward, D. M. V., Di Patti, M. C. B., Jeong, S. Y., David, S., Musci, G., & Kaplan, J. (2007). Ferroxidase activity is required for the stability of cell surface ferroportin in cells expressing GPI-ceruloplasmin. *The EMBO Journal*, *26*(12), 2823–2831. https://doi.org/10.1038/SJ.EMBOJ.7601735

De Stefani, E., Boffetta, P., Ronco, A. L., Deneo-Pellegrini, H., Correa, P., Acosta, G., Mendilaharsu, M., Luaces, M. E., & Silva, C. (2012). Processed meat consumption and risk of cancer: A multisite casecontrol study in Uruguay. *British Journal of Cancer*, *107*(9). https://doi.org/10.1038/bjc.2012.433

Delierneux, C., Kouba, S., Shanmughapriya, S., Potier-Cartereau, M., Trebak, M., & Hempel, N. (2020). Mitochondrial Calcium Regulation of Redox Signaling in Cancer. *Cells*, *9*(2). https://doi.org/10.3390/CELLS9020432

Deng, M., Brägelmann, J., Kryukov, I., Saraiva-Agostinho, N., & Perner, S. (2017).

FirebrowseR: an R client to the Broad Institute's Firehose Pipeline. *Database*, *2017*(1). https://doi.org/10.1093/DATABASE/BAW160

Deryugina, E. I., & Quigley, J. P. (2006). Matrix metalloproteinases and tumor metastasis. In *Cancer and Metastasis Reviews* (Vol. 25, Issue 1). https://doi.org/10.1007/s10555-006-7886-9

Dongiovanni, P., Fracanzani, A., … G. C.-T. A. journal of, & 2010, undefined. (n.d.). Iron-dependent regulation of MDM2 influences p53 activity and hepatic carcinogenesis. *Elsevier*. Retrieved May 22, 2023, from https://www.sciencedirect.com/science/article/pii/S0002944010604105

Doustjalali, S. R., Yusof, R., Govindasamy, G. K., Bustam, A. Z., Pillay, B., & Hashim, O. H. (2006). Patients with nasopharyngeal carcinoma demonstrate enhanced serum and tissue ceruloplasmin expression. *Journal of Medical Investigation*, *53*(1–2). https://doi.org/10.2152/jmi.53.20

Drury, J., Rychahou, P. G., Kelson, C. O., Geisen, M. E., Wu, Y., He, D., Wang, C., Lee, E. Y., Evers, B. M., & Zaytseva, Y. Y. (2022). Upregulation of CD36, a Fatty Acid Translocase, Promotes Colorectal Cancer Metastasis by Increasing MMP28 and Decreasing E-Cadherin Expression. *Cancers*, *14*(1). https://doi.org/10.3390/CANCERS14010252/S1

Du, B., Liu, M., Li, C., Geng, X., Zhang, X., Ning, D., & Liu, M. (2019). The potential role of TNFAIP3 in malignant transformation of gastric carcinoma. *Pathology, Research and Practice*, *215*(8). https://doi.org/10.1016/J.PRP.2019.152471

Dubey, K., Tiwari, R., & Ojha, R. (2014). Recent Advances in Protein−Ligand Interactions: Molecular Dynamics Simulations and Binding Free Energy. *Current Computer Aided-Drug Design*, *9*(4). https://doi.org/10.2174/15734099113096660036

Eberhardt, J., Santos-Martins, D., Tillack, A. F., & Forli, S. (2021). AutoDock Vina 1.2.0: New Docking Methods, Expanded Force Field, and Python Bindings. *Journal of Chemical Information and Modeling*, *61*(8), 3891–3898. https://doi.org/10.1021/ACS.JCIM.1C00203/SUPPL_FILE/CI1C00203_SI_002.ZIP

Elekofehinti, O. O., Iwaloye, O., Josiah, S. S., Lawal, A. O., Akinjiyan, M. O., & Ariyo, E. O. (2021). Molecular docking studies, molecular dynamics and ADME/tox reveal

therapeutic potentials of STOCK1N-69160 against papain-like protease of SARS-CoV-2. *Molecular Diversity*, *25*(3). https://doi.org/10.1007/s11030-020-10151-w

Elmore, S. (2007). Apoptosis: A Review of Programmed Cell Death. *Toxicologic Pathology*, *35*(4), 495. https://doi.org/10.1080/01926230701320337

F, C., B, H., Y, M., Y, H., B, L., B, Z., Y, C., P, C., Y, F., & K, T. (2021). Ceruloplasmin correlates with immune infiltration and serves as a prognostic biomarker in breast cancer. *Aging*, *13*(undefined). https://doi.org/10.18632/AGING.203427

F, M., T, L., DM, K., F, O., I, F., CK, M., K, E., J, T., S, B., G, C., & RH, W. (2005). Copper-dependent activation of hypoxia-inducible factor (HIF)-1: implications for ceruloplasmin regulation. *Blood*, *105*(12), 4613–4619. https://doi.org/10.1182/BLOOD-2004-10-3980

Ficarra, G., & Eversole, L. E. (1994). HIV-related tumors of the oral cavity. In *Critical Reviews in Oral Biology and Medicine* (Vol. 5, Issue 2). https://doi.org/10.1177/10454411940050020201

Foyer, C. H., & Noctor, G. (2005). Redox Homeostasis and Antioxidant Signaling: A Metabolic Interface between Stress Perception and Physiological Responses. *The Plant Cell*, *17*(7), 1866. https://doi.org/10.1105/TPC.105.033589

Friesner, R. A., Banks, J. L., Murphy, R. B., Halgren, T. A., Klicic, J. J., Mainz, D. T., Repasky, M. P., Knoll, E. H., Shelley, M., Perry, J. K., Shaw, D. E., Francis, P., & Shenkin, P. S. (2004a). Glide: A New Approach for Rapid, Accurate Docking and Scoring. 1. Method and Assessment of Docking Accuracy. *Journal of Medicinal Chemistry*, *47*(7), 1739–1749. https://doi.org/10.1021/JM0306430/SUPPL_FILE/JM0306430_S.PDF

Friesner, R. A., Banks, J. L., Murphy, R. B., Halgren, T. A., Klicic, J. J., Mainz, D. T., Repasky, M. P., Knoll, E. H., Shelley, M., Perry, J. K., Shaw, D. E., Francis, P., & Shenkin, P. S. (2004b). Glide: A New Approach for Rapid, Accurate Docking and Scoring. 1. Method and Assessment of Docking Accuracy. *Journal of Medicinal Chemistry*, *47*(7), 1739–1749. https://doi.org/10.1021/JM0306430/SUPPL_FILE/JM0306430_S.PDF

Fu, Y., Zou, T., Shen, X., Nelson, P. J., Li, J., Wu, C., Yang, J., Zheng, Y., Bruns, C., Zhao, Y., Qin, L., & Dong, Q. (2021). Lipid metabolism in cancer progression and

therapeutic strategies. *MedComm*, *2*(1), 27. https://doi.org/10.1002/MCO2.27

Fulda, S., & Debatin, K. M. (2006). Extrinsic versus intrinsic apoptosis pathways in anticancer chemotherapy. In *Oncogene* (Vol. 25, Issue 34, pp. 4798–4811). Nature Publishing Group. https://doi.org/10.1038/sj.onc.1209608

Gagliardi, P. A., Puliafito, A., & Primo, L. (2018). PDK1: At the crossroad of cancer signaling pathways. *Seminars in Cancer Biology*, *48*, 27–35. https://doi.org/10.1016/J.SEMCANCER.2017.04.014

Garrido, C., Galluzzi, L., Brunet, M., Puig, P. E., Didelot, C., & Kroemer, G. (2006). Mechanisms of cytochrome c release from mitochondria. In *Cell Death and Differentiation* (Vol. 13, Issue 9). https://doi.org/10.1038/sj.cdd.4401950

Gherardi, E., Birchmeier, W., Birchmeier, C., & Woude, G. Vande. (2012). Targeting MET in cancer: rationale and progress. *Nature Reviews Cancer 2012 12:2*, *12*(2), 89–103. https://doi.org/10.1038/nrc3205

Giménez, B. G., Santos, M. S., Ferrarini, M., & Dos Santos Fernandes, J. P. (2010). Evaluation of blockbuster drugs under the rule-of-five. *Pharmazie*, *65*(2). https://doi.org/10.1691/ph.2010.9733

Golusiński, P., Pazdrowski, J., Szewczyk, M., Misiołek, M., Pietruszewska, W., Klatka, J., Okła, S., Kaźmierczak, H., Marszałek, A., Filas, V., Schneider, A., Masternak, M. M., Stęplewska, K., Miśkiewicz-Orczyk, K., & Golusiński, W. (2017). Is immunohistochemical evaluation of p16 in oropharyngeal cancer enough to predict the HPV positivity? *Reports of Practical Oncology and Radiotherapy*, *22*(3), 237. https://doi.org/10.1016/J.RPOR.2017.01.003

Gormley, M., Creaney, G., Schache, A., Ingarfield, K., & Conway, D. I. (2022). *Reviewing the epidemiology of head and neck cancer: definitions, trends and risk factors*. https://doi.org/10.1038/s41415-022-5166-x

Gostner, J. M., Becker, K., Fuchs, D., & Sucher, R. (2013). Redox regulation of the immune response. In *Redox Report* (Vol. 18, Issue 3). https://doi.org/10.1179/1351000213Y.0000000044

Guo, Q., Li, L., Hou, S., Yuan, Z., Li, C., Zhang, W., Zheng, L., & Li, X. (2021).

The Role of Iron in Cancer Progression. *Frontiers in Oncology*, *11*, 4571.
https://doi.org/10.3389/FONC.2021.778492/BIBTEX

Gupta, B., Bray, F., Kumar, N., epidemiology, N. J.-C., & 2017, undefined. (2017).
Associations between oral hygiene habits, diet, tobacco and alcohol and risk of oral cancer:
A case–control study from India. *Elsevier*, *51*, 7–14.
https://doi.org/10.1016/j.canep.2017.09.003

Gupta, N., Badeaux, M., Liu, Y., Naxerova, K., Sgroi, D., Munn, L. L., Jain, R. K.,
& Garkavtsev, I. (2017). Stress granule-associated protein G3BP2 regulates breast tumor
initiation. *Proceedings of the National Academy of Sciences of the United States of
America*, *114*(5), 1033–1038.
https://doi.org/10.1073/PNAS.1525387114/SUPPL_FILE/PNAS.201525387SI.PDF

Gwangwa, M. V., Joubert, A. M., & Visagie, M. H. (n.d.). *Crosstalk between the
Warburg effect, redox regulation and autophagy induction in tumourigenesis*.
https://doi.org/10.1186/s11658-018-0088-y

Haas, M. S., Kagey, M. H., Heath, H., Schuerpf, F., Rottman, J. B., & Newman, W.
(2021). mDKN-01, a novel anti-DKK1 mAb, enhances innate immune responses in the
tumor microenvironment A C. *Molecular Cancer Research*, *19*(4), 717–725.
https://doi.org/10.1158/1541-7786.MCR-20-0799/81376/AM/MDKN-01-A-NOVEL-
ANTI-DKK1-MONOCLONAL-ANTIBODY

Hammouda, Y., Halily, S., Oukessou, Y., Rouadi, S., Abada, R., Roubal, M., &
Mahtar, M. (2021). Malignant tumors of the hard palate: Report of 4 cases and review of the
literature. *International Journal of Surgery Case Reports*, *78*, 228.
https://doi.org/10.1016/J.IJSCR.2020.12.024

Han, Y., Liu, D., & Li, L. (2020). PD-1/PD-L1 pathway: current researches in
cancer. *American Journal of Cancer Research*, *10*(3).

Han, Y., Zhang, J., Hu, C. Q., Zhang, X., Ma, B., & Zhang, P. (2019). In silico
ADME and toxicity prediction of ceftazidime and its impurities. *Frontiers in
Pharmacology*, *10*(APR). https://doi.org/10.3389/fphar.2019.00434

Hanwell, M. D., Curtis, D. E., Lonie, D. C., Vandermeerschd, T., Zurek, E., &

Hutchison, G. R. (2012). Avogadro: An advanced semantic chemical editor, visualization, and analysis platform. *Journal of Cheminformatics*, *4*(8), 1–17. https://doi.org/10.1186/1758-2946-4-17/FIGURES/14

Hawkins, C. L., & Davies, M. J. (2021). Role of myeloperoxidase and oxidant formation in the extracellular environment in inflammation-induced tissue damage. *Free Radical Biology and Medicine*, *172*, 633–651. https://doi.org/10.1016/J.FREERADBIOMED.2021.07.007

Hayes, J. D., Dinkova-Kostova, A. T., & Tew, K. D. (2020). Oxidative Stress in Cancer. *Cancer Cell*, *38*(2), 167. https://doi.org/10.1016/J.CCELL.2020.06.001

He, X., Arslan, A. D., Ho, T. T., Yuan, C., Stampfer, M. R., & Beck, W. T. (2014). Involvement of polypyrimidine tract-binding protein (PTBP1) in maintaining breast cancer cell growth and malignant properties. *Oncogenesis 2014 3:1*, *3*(1), e84–e84. https://doi.org/10.1038/oncsis.2013.47

Head and neck cancer - The Lancet. (n.d.). Retrieved April 11, 2023, from https://www.thelancet.com/article/S0140-6736(21)01550-6/fulltext

Heiden, M. G. V., Cantley, L. C., & Thompson, C. B. (2009). Understanding the Warburg Effect: The Metabolic Requirements of Cell Proliferation. *Science*, *324*(5930), 1029–1033. https://doi.org/10.1126/SCIENCE.1160809

Helleday, T. (2010). Homologous recombination in cancer development, treatment and development of drug resistance. *Carcinogenesis*, *31*(6), 955–960. https://doi.org/10.1093/CARCIN/BGQ064

Hoesel, B., & Schmid, J. A. (2013). The complexity of NF-κB signaling in inflammation and cancer. In *Molecular Cancer* (Vol. 12, Issue 1). https://doi.org/10.1186/1476-4598-12-86

Hollingsworth, S. A., & Karplus, P. A. (2010). A fresh look at the Ramachandran plot and the occurrence of standard structures in proteins. *Biomolecular Concepts*, *1*(3–4), 271. https://doi.org/10.1515/BMC.2010.022

Horton, J. D., Knochelmann, H. M., Day, T. A., Paulos, C. M., & Neskey, D. M. (2019). Immune Evasion by Head and Neck Cancer: Foundations for Combination Therapy.

Trends in Cancer, *5*(4), 208. https://doi.org/10.1016/J.TRECAN.2019.02.007

Huang, D. W., Sherman, B. T., Tan, Q., Collins, J. R., Alvord, W. G., Roayaei, J., Stephens, R., Baseler, M. W., Lane, H. C., & Lempicki, R. A. (2007). The DAVID Gene Functional Classification Tool: A novel biological module-centric algorithm to functionally analyze large gene lists. *Genome Biology*, *8*(9), 1–16. https://doi.org/10.1186/GB-2007-8-9-R183/TABLES/3

Huang, H. Y., Lin, Y. C. D., Cui, S., Huang, Y., Tang, Y., Xu, J., Bao, J., Li, Y., Wen, J., Zuo, H., Wang, W., Li, J., Ni, J., Ruan, Y., Li, L., Chen, Y., Xie, Y., Zhu, Z., Cai, X., … Huang, H. Da. (2022). miRTarBase update 2022: an informative resource for experimentally validated miRNA–target interactions. *Nucleic Acids Research*, *50*(D1), D222–D230. https://doi.org/10.1093/NAR/GKAB1079

Ivanova, L., Tammiku-Taul, J., García-Sosa, A. T., Sidorova, Y., Saarma, M., & Karelson, M. (2018). Molecular Dynamics Simulations of the Interactions between Glial Cell Line-Derived Neurotrophic Factor Family Receptor GFRα1 and Small-Molecule Ligands. *ACS Omega*, *3*(9), 11407–11414. https://doi.org/10.1021/ACSOMEGA.8B01524/ASSET/IMAGES/LARGE/AO-2018-01524B_0008.JPEG

Jamali, L., Sadeghi, H., Ghasemi, M. R., Mohseni, R., Nazemalhosseini-Mojarad, E., Yassaee, V. R., Larki, P., Zali, M. R., & Mirfakhraie, R. (2022). Autophagy ATG16L1 rs2241880 impacts the colorectal cancer risk: A case-control study. *Journal of Clinical Laboratory Analysis*, *36*(1). https://doi.org/10.1002/JCLA.24169

Jian, J., Yang, Q., Shao, Y., Axelrod, D., Smith, J., Singh, B., Krauter, S., Chiriboga, L., Yang, Z., Li, J., & Huang, X. (2013). A link between premenopausal iron deficiency and breast cancer malignancy. *BMC Cancer*, *13*. https://doi.org/10.1186/1471-2407-13-307

Jiang, B., Liu, G., Zheng, J., Chen, M., Maimaitiming, Z., Chen, M., Liu, S., Jiang, R., Fuqua, B. K., Dunaief, J. L., Vulpe, C. D., Anderson, G. J., Wang, H., & Chen, H. (2016). Hephaestin and ceruloplasmin facilitate iron metabolism in the mouse kidney. *Scientific Reports*, *6*. https://doi.org/10.1038/srep39470

Jiang, X., Wu, J., Wang, J., & Huang, R. (2019). Tobacco and oral squamous cell

carcinoma: A review ofcarcinogenic pathways. *Tobacco Induced Diseases*, *17*(April). https://doi.org/10.18332/TID/105844

Jögi, A., Vaapil, M., Johansson, M., & Påhlman, S. (2012). Cancer cell differentiation heterogeneity and aggressive behavior in solid tumors. *Upsala Journal of Medical Sciences*, *117*(2), 217. https://doi.org/10.3109/03009734.2012.659294

Johnson, D. E., Burtness, B., Leemans, C. R., Lui, V. W. Y., Bauman, J. E., & Grandis, J. R. (2020). Head and neck squamous cell carcinoma. *Nature Reviews Disease Primers 2020 6:1*, *6*(1), 1–22. https://doi.org/10.1038/s41572-020-00224-3

Jończy, A., Mazgaj, R., Smuda, E., Żelazowska, B., Kopeć, Z., Starzyński, R. R., & Lipiński, P. (2021). The role of copper in the regulation of ferroportin expression in macrophages. *Cells*, *10*(9). https://doi.org/10.3390/cells10092259

Jung, M., Mertens, C., Tomat, E., & Brüne, B. (2019). Iron as a Central Player and Promising Target in Cancer Progression. *International Journal of Molecular Sciences 2019, Vol. 20, Page 273*, *20*(2), 273. https://doi.org/10.3390/IJMS20020273

Kalinowski, F. C., Giles, K. M., Candy, P. A., Ali, A., Ganda, C., Epis, M. R., Webster, R. J., & Leedman, P. J. (2012). Regulation of Epidermal Growth Factor Receptor Signaling and Erlotinib Sensitivity in Head and Neck Cancer Cells by miR-7. *PLoS ONE*, *7*(10). https://doi.org/10.1371/journal.pone.0047067

Kaltenmeier, C., Simmons, R. L., Tohme, S., & Yazdani, H. O. (2021). Neutrophil extracellular traps (Nets) in cancer metastasis. In *Cancers* (Vol. 13, Issue 23). https://doi.org/10.3390/cancers13236131

Kang, R., Zhang, Q., Zeh, H. J., Lotze, M. T., & Tang, D. (2013). HMGB1 in Cancer: Good, Bad, or Both? *Clinical Cancer Research : An Official Journal of the American Association for Cancer Research*, *19*(15), 4046. https://doi.org/10.1158/1078-0432.CCR-13-0495

Karakas, B., Bachman, K. E., & Park, B. H. (2006). Mutation of the PIK3CA oncogene in human cancers. *British Journal of Cancer 2006 94:4*, *94*(4), 455–459. https://doi.org/10.1038/sj.bjc.6602970

Kase, S., Baburin, A., Kuddu, M., & Innos, K. (2021). Incidence and Survival for

Head and Neck Cancers in Estonia, 1996–2016: A Population-Based Study. *Clinical Epidemiology*, *13*, 149. https://doi.org/10.2147/CLEP.S293929

Katoh, M. (2011). Network of WNT and other regulatory signaling cascades in pluripotent stem cells and cancer stem cells. *Current Pharmaceutical Biotechnology*, *12*(2), 160–170. https://doi.org/10.2174/138920111794295710

Keith, B., Johnson, R. S., & Simon, M. C. (2012). HIF1α and HIF2α: sibling rivalry in hypoxic tumor growth and progression. *Nature Reviews. Cancer*, *12*(1), 9. https://doi.org/10.1038/NRC3183

Kennedy, T., Ghio, A. J., Reed, W., Samet, J., Zagorski, J., Quay, J., Carter, J., Dailey, L., Hoidal, J. R., Devlin, R. B., Ghio, A. J., Reed, W., Samet, J., Zagorski, J., Quay, J., Carter, J., Dailey, L., Hoidal, J. R., & Devlin, R. B. (2012). Copper-dependent Inflammation and Nuclear Factor- κ B Activation by Particulate Air Pollution. *Https://Doi.Org/10.1165/Ajrcmb.19.3.3042*, *19*(3), 366–378. https://doi.org/10.1165/AJRCMB.19.3.3042

Koen, K., Robin, D. P., & Eline, N. (2022). CHEK2 mutations and papillary thyroid cancer: correlation or coincidence? *Hereditary Cancer in Clinical Practice*, *20*(1). https://doi.org/10.1186/s13053-022-00211-7

Kono, S., Yoshida, K., Tomosugi, N., Terada, T., Hamaya, Y., Kanaoka, S., & Miyajima, H. (2010). Biological effects of mutant ceruloplasmin on hepcidin-mediated internalization of ferroportin. *Biochimica et Biophysica Acta - Molecular Basis of Disease*, *1802*(11). https://doi.org/10.1016/j.bbadis.2010.07.011

Kory, N., Farese, R. V., & Walther, T. C. (2016). Targeting Fat: Mechanisms of Protein Localization to Lipid Droplets. *Trends in Cell Biology*, *26*(7), 535–546. https://doi.org/10.1016/J.TCB.2016.02.007

Kotsafti, A., Scarpa, M., Castagliuolo, I., & Scarpa, M. (2020). Reactive oxygen species and antitumor immunity—from surveillance to evasion. In *Cancers* (Vol. 12, Issue 7). https://doi.org/10.3390/cancers12071748

Kou, L., Jiang, X., Huang, H., Lin, X., Zhang, Y., Yao, Q., & Chen, R. (2020). The role of transporters in cancer redox homeostasis and cross-talk with nanomedicines. *Asian*

Journal of Pharmaceutical Sciences, *15*(2), 145–157. https://doi.org/10.1016/J.AJPS.2020.02.001

Koundouros, N., & Poulogiannis, G. (2019). Reprogramming of fatty acid metabolism in cancer. *British Journal of Cancer 2019 122:1*, *122*(1), 4–22. https://doi.org/10.1038/s41416-019-0650-z

Kozomara, A., Birgaoanu, M., & Griffiths-Jones, S. (2019). miRBase: from microRNA sequences to function. *Nucleic Acids Research*, *47*(D1), D155–D162. https://doi.org/10.1093/NAR/GKY1141

Kufareva, I., & Abagyan, R. (2012). Methods of protein structure comparison. *Methods in Molecular Biology*, *857*. https://doi.org/10.1007/978-1-61779-588-6_10

Kulp, K., Green, S., research, P. V.-E. cell, & 1996, undefined. (n.d.). Iron deprivation inhibits cyclin-dependent kinase activity and decreases cyclin D/CDK4 protein levels in asynchronous MDA-MB-453 human breast cancer cells. *Elsevier*. Retrieved May 22, 2023, from https://www.sciencedirect.com/science/article/pii/S0014482796903432

Kutler, D. I., Auerbach, A. D., Satagopan, J., Giampietro, P. F., Batish, S. D., Huvos, A. G., Goberdhan, A., Shah, J. P., & Singh, B. (2003). High incidence of head and neck squamous cell carcinoma in patients with Fanconi anemia. *Archives of Otolaryngology - Head and Neck Surgery*, *129*(1). https://doi.org/10.1001/archotol.129.1.106

Larsson, P. -A, Edström, S., Westin, T., Nordkvist, A., Hirsch, J. M., & Vahlne, A. (1991). Reactivity against herpes simplex virus in patients with head and neck cancer. *International Journal of Cancer*, *49*(1). https://doi.org/10.1002/ijc.2910490104

Lechner, M., Liu, J., Masterson, L., & Fenton, T. R. (2022). HPV-associated oropharyngeal cancer: epidemiology, molecular biology and clinical management. *Nature Reviews Clinical Oncology 2022 19:5*, *19*(5), 306–327. https://doi.org/10.1038/s41571-022-00603-7

Lee, C. M., Lo, H. W., Shao, R. P., Wang, S. C., Xia, W., Gershenson, D. M., & Hung, M. C. (2004). Selective Activation of Ceruloplasmin Promoter in Ovarian Tumors: Potential Use for Gene Therapy. *Cancer Research*, *64*(5). https://doi.org/10.1158/0008-5472.CAN-03-2551

Lee, J. C., Chiang, K. C., Feng, T. H., Chen, Y. J., Chuang, S. T., Tsui, K. H., Chung, L. C., & Juang, H. H. (2016). The iron chelator, Dp44mT, effectively inhibits human oral squamous cell carcinoma cell growth in vitro and in vivo. *International Journal of Molecular Sciences*, *17*(9). https://doi.org/10.3390/ijms17091435

Li, H., Jing, X., Yu, J., Liu, J., Zhang, T., Chen, S., & Zhang, X. (2020). A combination of cytokeratin 5/6, p63, p40 and MUC5AC are useful for distinguishing squamous cell carcinoma from adenocarcinoma of the cervix. *Diagnostic Pathology*, *15*(1), 104. https://doi.org/10.1186/S13000-020-01018-7

Li, J., Cao, F., Yin, H. liang, Huang, Z. jian, Lin, Z. tao, Mao, N., Sun, B., & Wang, G. (2020). Ferroptosis: past, present and future. *Cell Death & Disease 2020 11:2*, *11*(2), 1–13. https://doi.org/10.1038/s41419-020-2298-2

Li, T., Fan, J., Wang, B., Traugh, N., Chen, Q., Liu, J. S., Li, B., & Liu, X. S. (2017). TIMER: A web server for comprehensive analysis of tumor-infiltrating immune cells. *Cancer Research*, *77*(21), e108–e110. https://doi.org/10.1158/0008-5472.CAN-17-0307/SUPPLEMENTARY-VIDEO-S1

Li, Z., Liu, H., & Luo, X. (2020). Lipid droplet and its implication in cancer progression. *American Journal of Cancer Research*, *10*(12), 4112. /pmc/articles/PMC7783747/

Liberti, M. V., & Locasale, J. W. (2016). The Warburg Effect: How Does it Benefit Cancer Cells? *Trends in Biochemical Sciences*, *41*(3), 211. https://doi.org/10.1016/J.TIBS.2015.12.001

Lin, Y. C., Wang, C. C., Chen, I. S., Jheng, J. L., Li, J. H., & Tung, C. W. (2013). TIPdb: a database of anticancer, antiplatelet, and antituberculosis phytochemicals from indigenous plants in Taiwan. *TheScientificWorldJournal*, *2013*. https://doi.org/10.1155/2013/736386

Liu, C. F. (2022). Recent Advances on Natural Aryl- C-glycoside Scaffolds: Structure, Bioactivities, and Synthesis-A Comprehensive Review. *Molecules (Basel, Switzerland)*, *27*(21). https://doi.org/10.3390/MOLECULES27217439

Liu, P., Cheng, H., Roberts, T. M., & Zhao, J. J. (2009). Targeting the

phosphoinositide 3-kinase (PI3K) pathway in cancer. *Nature Reviews. Drug Discovery*, *8*(8), 627. https://doi.org/10.1038/NRD2926

Łuczak, M. W., & Jagodziński, P. P. (2006). The role of DNA methylation in cancer development. In *Folia Histochemica et Cytobiologica* (Vol. 44, Issue 3).

Luo, Y., Ma, J., & Lu, W. (2020). The Significance of Mitochondrial Dysfunction in Cancer. *International Journal of Molecular Sciences*, *21*(16), 1–24. https://doi.org/10.3390/IJMS21165598

Lyu, C., Chen, T., Qiang, B., Liu, N., Wang, H., Zhang, L., & Liu, Z. (2021). CMNPD: A comprehensive marine natural products database towards facilitating drug discovery from the ocean. *Nucleic Acids Research*, *49*(D1). https://doi.org/10.1093/nar/gkaa763

Ma, D., Qiao, L., & Guo, B. (2021). Smad7 suppresses melanoma lung metastasis by impairing Tregs migration to the tumor microenvironment. *American Journal of Translational Research*, *13*(2).

Ma, J., Zheng, B., Goswami, S., Meng, L., Zhang, D., Cao, C., Li, T., Zhu, F., Ma, L., Zhang, Z., Zhang, S., Duan, M., Chen, Q., Gao, Q., & Zhang, X. (2019). PD1Hi CD8+ T cells correlate with exhausted signature and poor clinical outcome in hepatocellular carcinoma. *Journal for ImmunoTherapy of Cancer*, *7*(1). https://doi.org/10.1186/s40425-019-0814-7

Macfarlane, G. J., Zheng, T., Marshall, J. R., Boffetta, P., Niu, S., Brasure, J., Merletti, F., & Boyle, P. (1995). Alcohol, tobacco, diet and the risk of oral cancer: a pooled analysis of three case-control studies. *European Journal of Cancer. Part B: Oral Oncology*, *31*(3). https://doi.org/10.1016/0964-1955(95)00005-3

Mao, H., Zhao, Y., Li, H., & Lei, L. (2020). Ferroptosis as an emerging target in inflammatory diseases. *Progress in Biophysics and Molecular Biology*, *155*, 20–28. https://doi.org/10.1016/J.PBIOMOLBIO.2020.04.001

Marbaniang, C., & Kma, L. (2018). Dysregulation of Glucose Metabolism by Oncogenes and Tumor Suppressors in Cancer Cells. *Asian Pacific Journal of Cancer Prevention : APJCP*, *19*(9), 2377. https://doi.org/10.22034/APJCP.2018.19.9.2377

Marrocco, I., Altieri, F., & Peluso, I. (2017). Measurement and Clinical Significance of Biomarkers of Oxidative Stress in Humans. *Oxidative Medicine and Cellular Longevity*, *2017*. https://doi.org/10.1155/2017/6501046

Masucci, M. T., Minopoli, M., & Carriero, M. V. (2019). Tumor Associated Neutrophils. Their Role in Tumorigenesis, Metastasis, Prognosis and Therapy. In *Frontiers in Oncology* (Vol. 9). https://doi.org/10.3389/fonc.2019.01146

Matsuhashi, S., Manirujjaman, M., Hamajima, H., & Ozaki, I. (2019). Control Mechanisms of the Tumor Suppressor PDCD4: Expression and Functions. *International Journal of Molecular Sciences*, *20*(9). https://doi.org/10.3390/IJMS20092304

Matsuoka, R., Shiba, A., Sakashita, S., Minami, Y., & Noguchi, M. (2018). P1.09-30 Heterotopic Expression of Ceruloplasmin in Lung Adenocarcinoma and its Possible Clinical Use as a Tumor Biomarker. *Journal of Thoracic Oncology*, *13*(10). https://doi.org/10.1016/j.jtho.2018.08.806

McIlwain, D. R., Berger, T., & Mak, T. W. (2013). Caspase Functions in Cell Death and Disease. *Cold Spring Harbor Perspectives in Biology*, *5*(4), 1–28. https://doi.org/10.1101/CSHPERSPECT.A008656

Merugu, R., & Singh, K. V. (2018). Molecular docking of amitriptyline to ceruloplasmin, retinol-binding protein, and serum albumin. *Asian Journal of Pharmaceutical and Clinical Research*, *11*(2). https://doi.org/10.22159/ajpcr.2018.v11i2.22721

Modi, A., Purohit, P., Gadwal, A., Ukey, S., Roy, D., Fernandes, S., & Banerjee, M. (2022). In-Silico Analysis of Differentially Expressed Genes and Their Regulating microRNA Involved in Lymph Node Metastasis in Invasive Breast Carcinoma. *Cancer Investigation*, *40*(1), 55–72. https://doi.org/10.1080/07357907.2021.1969574

Mohanraj, K., Karthikeyan, B. S., Vivek-Ananth, R. P., Chand, R. P. B., Aparna, S. R., Mangalapandi, P., & Samal, A. (2018). IMPPAT: A curated database of Indian Medicinal Plants, Phytochemistry And Therapeutics. *Scientific Reports*, *8*(1), 4329. https://doi.org/10.1038/S41598-018-22631-Z

Morales, M., & Xue, X. (2021). Targeting iron metabolism in cancer therapy.

Theranostics, *11*(17), 8412. https://doi.org/10.7150/THNO.59092

Moratin, J., Mrosek, J., Horn, D., Metzger, K., Ristow, O., Zittel, S., Engel, M., Freier, K., Hoffmann, J., & Freudlsperger, C. (2021). Full-Thickness Tumor Resection of Oral Cancer Involving the Facial Skin—Microsurgical Reconstruction of Extensive Defects after Radical Treatment of Advanced Squamous Cell Carcinoma. *Cancers*, *13*(9). https://doi.org/10.3390/CANCERS13092122

Mukherjee, A., Kenny, H. A., & Lengyel, E. (2017). Unsaturated fatty acids maintain cancer cell stemness. *Cell Stem Cell*, *20*(3), 291. https://doi.org/10.1016/J.STEM.2017.02.008

Mukhopadhyay, B. P. (2019). Insights from molecular dynamics simulation of human ceruloplasmin (ferroxidase enzyme) binding with biogenic monoamines. *Bioinformation*, *15*(10), 750. https://doi.org/10.6026/97320630015750

Mukhopadhyay, R., Jia, J., Arif, A., Ray, P. S., & Fox, P. L. (2009). The GAIT system: a gatekeeper of inflammatory gene expression. *Trends in Biochemical Sciences*, *34*(7), 324. https://doi.org/10.1016/J.TIBS.2009.03.004

Musci, M. C. (2014). Ceruloplasmin-ferroportin system of iron traffic in vertebrates. *World Journal of Biological Chemistry*, *5*(2). https://doi.org/10.4331/wjbc.v5.i2.204

Mütze, S., Hebling, U., Stremmel, W., Wang, J., Arnhold, J., Pantopoulos, K., & Mueller, S. (2003). Myeloperoxidase-derived Hypochlorous Acid Antagonizes the Oxidative Stress-mediated Activation of Iron Regulatory Protein 1. *Journal of Biological Chemistry*, *278*(42). https://doi.org/10.1074/jbc.M307159200

Nemeth, E., & Ganz, T. (2009). The role of hepcidin in iron metabolism. In *Acta Haematologica* (Vol. 122, Issues 2–3). https://doi.org/10.1159/000243791

Nogueira, V., & Hay, N. (2013). Molecular Pathways: Reactive Oxygen Species Homeostasis in Cancer Cells and Implications for Cancer Therapy. *Clinical Cancer Research : An Official Journal of the American Association for Cancer Research*, *19*(16), 4309. https://doi.org/10.1158/1078-0432.CCR-12-1424

O'Boyle, N. M., Banck, M., James, C. A., Morley, C., Vandermeersch, T., & Hutchison, G. R. (2011). Open Babel: An Open chemical toolbox. *Journal of*

Cheminformatics, *3*(10), 1–14. https://doi.org/10.1186/1758-2946-3-33/TABLES/2

O'Brien, P. J., & Bruce, W. R. (William R. (2010). *Endogenous toxins : diet, genetics, disease and treatment*. https://www.wiley.com/en-ie/Endogenous+Toxins%3A+Targets+for+Disease+Treatment+and+Prevention-p-9783527628100

Oral Cancer - India Against Cancer. (n.d.). Retrieved April 12, 2023, from http://cancerindia.org.in/oral-cancer/

Oudit, G. Y., Trivieri, M. G., Khaper, N., Liu, P. P., & Backx, P. H. (2006). Role of L-type Ca2+ channels in iron transport and iron-overload cardiomyopathy. *Journal of Molecular Medicine (Berlin, Germany)*, *84*(5), 349. https://doi.org/10.1007/S00109-005-0029-X

Pai, S. I., & Westra, W. H. (2009). Molecular Pathology of Head and Neck Cancer: Implications for Diagnosis, Prognosis, and Treatment. *Annual Review of Pathology*, *4*, 49. https://doi.org/10.1146/ANNUREV.PATHOL.4.110807.092158

Pan, C., Jin, L., Wang, X., Li, Y., Chun, J., Boese, A. C., Li, D., Kang, H. B., Zhang, G., Zhou, L., Chen, G. Z., Saba, N. F., Shin, D. M., Magliocca, K. R., Owonikoko, T. K., Mao, H., Lonial, S., & Kang, S. (2019). Inositol-triphosphate 3-kinase B confers cisplatin resistance by regulating NOX4-dependent redox balance. *The Journal of Clinical Investigation*, *129*(6), 2431. https://doi.org/10.1172/JCI124550

Pani, G., Galeotti, T., & Chiarugi, P. (2010). Metastasis: Cancer cell's escape from oxidative stress. In *Cancer and Metastasis Reviews* (Vol. 29, Issue 2, pp. 351–378). Cancer Metastasis Rev. https://doi.org/10.1007/s10555-010-9225-4

Park, H. A., Brown, S. R., & Kim, Y. (2020). Cellular Mechanisms of Circulating Tumor Cells During Breast Cancer Metastasis. *International Journal of Molecular Sciences*, *21*(14), 1–19. https://doi.org/10.3390/IJMS21145040

Parrish, A. B., Freel, C. D., & Kornbluth, S. (2013). Cellular mechanisms controlling caspase activation and function. *Cold Spring Harbor Perspectives in Biology*, *5*(6). https://doi.org/10.1101/cshperspect.a008672

Patil, M. B., Lavanya, T., Meena Kumari, C., Shetty, S. R., Gufran, K., Viswanath,

V., Swarnalatha, C., Suresh Babu, J., & Nayyar, A. S. (2021). Serum ceruloplasmin as cancer marker in oral pre-cancers and cancers. *Journal of Carcinogenesis*, *20*(1), 15. https://doi.org/10.4103/JCAR.JCAR_10_21

Pawar, S. S., & Rohane, S. H. (2021). Review on Discovery Studio: An important Tool for Molecular Docking. *Asian Journal Of Research in Chemistry*, *14*(1). https://doi.org/10.5958/0974-4150.2021.00014.6

Paz, N., Levanon, E. Y., Amariglio, N., Heimberger, A. B., Ram, Z., Constantini, S., Barbash, Z. S., Adamsky, K., Safran, M., Hirschberg, A., Krupsky, M., Ben-Dov, I., Cazacu, S., Mikkelsen, T., Brodie, C., Eisenberg, E., & Rechavi, G. (2007). Altered adenosine-to-inosine RNA editing in human cancer. *Genome Research*, *17*(11). https://doi.org/10.1101/gr.6493107

Peluso, M., Russo, V., Mello, T., & Galli, A. (2020). Oxidative Stress and DNA Damage in Chronic Disease and Environmental Studies. *International Journal of Molecular Sciences*, *21*(18), 1–4. https://doi.org/10.3390/IJMS21186936

Prajapat, R., Marwal, A., & Gaur, R. K. (2014). Recognition of Errors in the Refinement and Validation of Three-Dimensional Structures of AC1 Proteins of Begomovirus Strains by Using ProSA-Web. *Journal of Viruses*, *2014*. https://doi.org/10.1155/2014/752656

Pu, F., Chen, F., Zhang, Z., Shi, D., Zhong, B., Lv, X., Tucker, A. B., Fan, J., Li, A. J., Qin, K., Hu, D., Chen, C., Wang, H., He, F., Ni, N., Huang, L., Liu, Q., Wagstaff, W., Luu, H. H., … Shao, Z. (2022). Ferroptosis as a novel form of regulated cell death: Implications in the pathogenesis, oncometabolism and treatment of human cancer. *Genes & Diseases*, *9*(2), 347. https://doi.org/10.1016/J.GENDIS.2020.11.019

Purohit, V., Simeone, D. M., & Lyssiotis, C. A. (2019). Metabolic Regulation of Redox Balance in Cancer. *Cancers*, *11*(7). https://doi.org/10.3390/CANCERS11070955

Rainey, N. E., Moustapha, A., Saric, A., Nicolas, G., Sureau, F., & Petit, P. X. (2019). Iron chelation by curcumin suppresses both curcumin-induced autophagy and cell death together with iron overload neoplastic transformation. *Cell Death Discovery 2019 5:1*, *5*(1), 1–15. https://doi.org/10.1038/s41420-019-0234-y

Rajan, C., Roshan, V. G. D., Khan, I., Manasa, V. G., Himal, I., Kattoor, J., Thomas, S., Kondaiah, P., & Kannan, S. (2021). MiRNA expression profiling and emergence of new prognostic signature for oral squamous cell carcinoma. *Scientific Reports*, *11*(1), 7298. https://doi.org/10.1038/S41598-021-86316-W

Raldine Gentric, G., Mieulet, V., & Mechta-Grigoriou, F. (n.d.). *Heterogeneity in Cancer Metabolism: New Concepts in an Old Field*. https://doi.org/10.1089/ars.2016.6750

Reczek, C. R., Birsoy, K., Kong, H., Martínez-Reyes, I., Wang, T., Gao, P., Sabatini, D. M., & Chandel, N. S. (2017). A CRISPR screen identifies a pathway required for paraquat-induced cell death. *Nature Chemical Biology*, *13*(12), 1274–1279. https://doi.org/10.1038/NCHEMBIO.2499

Rhodes, D. R., Yu, J., Shanker, K., Deshpande, N., Varambally, R., Ghosh, D., Barrette, T., Pandey, A., & Chinnaiyan, A. M. (2004). ONCOMINE: A Cancer Microarray Database and Integrated Data-Mining Platform. *Neoplasia (New York, N.Y.)*, *6*(1), 1. https://doi.org/10.1016/S1476-5586(04)80047-2

Rivera, C. (2015). Essentials of oral cancer. *International Journal of Clinical and Experimental Pathology*, *8*(9), 11884. /pmc/articles/PMC4637760/

Rivera, C., & Venegas, B. (2014). Histological and molecular aspects of oral squamous cell carcinoma (Review). *Oncology Letters*, *8*(1), 7. https://doi.org/10.3892/OL.2014.2103

Rizo-Téllez, S. A., Sekheri, M., & Filep, J. G. (2022). Myeloperoxidase: Regulation of Neutrophil Function and Target for Therapy. In *Antioxidants* (Vol. 11, Issue 11). https://doi.org/10.3390/antiox11112302

Robinson, N. J., & Schiemann, W. P. (2022). Telomerase in Cancer: Function, Regulation, and Clinical Translation. In *Cancers* (Vol. 14, Issue 3). https://doi.org/10.3390/cancers14030808

Roeser, H. P., Lee, G. R., Nacht, S., & Cartwright, G. E. (1970). The role of ceruloplasmin in iron metabolism. *The Journal of Clinical Investigation*, *49*(12), 2408–2417. https://doi.org/10.1172/JCI106460

Roig, E. M., Yaromina, A., Houben, R., Groot, A. J., Dubois, L., & Vooijs, M.

(2018). Prognostic Role of Hypoxia-Inducible Factor-2α Tumor Cell Expression in Cancer Patients: A Meta-Analysis. *Frontiers in Oncology*, *8*(JUN), 224. https://doi.org/10.3389/FONC.2018.00224

Rupaimoole, R., Lee, J., Haemmerle, M., Ling, H., Previs, R. A., Pradeep, S., Wu, S. Y., Ivan, C., Ferracin, M., Dennison, J. B., Millward, N. M. Z., Nagaraja, A. S., Gharpure, K. M., McGuire, M., Sam, N., Armaiz-Pena, G. N., Sadaoui, N. C., Rodriguez-Aguayo, C., Calin, G. A., … Sood, A. K. (2015). Long Noncoding RNA Ceruloplasmin Promotes Cancer Growth by Altering Glycolysis. *Cell Reports*, *13*(11). https://doi.org/10.1016/j.celrep.2015.11.047

Sallmyr, A., Fan, J., & Rassool, F. V. (2008). Genomic instability in myeloid malignancies: Increased reactive oxygen species (ROS), DNA double strand breaks (DSBs) and error-prone repair. In *Cancer Letters* (Vol. 270, Issue 1). https://doi.org/10.1016/j.canlet.2008.03.036

Samet, J. M. (1992). The health benefits of smoking cessation. In *Medical Clinics of North America* (Vol. 76, Issue 2). https://doi.org/10.1016/S0025-7125(16)30359-5

Samygina, V. R., Sokolov, A. V., Bourenkov, G., Petoukhov, M. V., Pulina, M. O., Zakharova, E. T., Vasilyev, V. B., Bartunik, H., & Svergun, D. I. (2013a). Ceruloplasmin: Macromolecular Assemblies with Iron-Containing Acute Phase Proteins. *PLoS ONE*, *8*(7), 67145. https://doi.org/10.1371/JOURNAL.PONE.0067145

Samygina, V. R., Sokolov, A. V., Bourenkov, G., Petoukhov, M. V., Pulina, M. O., Zakharova, E. T., Vasilyev, V. B., Bartunik, H., & Svergun, D. I. (2013b). Ceruloplasmin: Macromolecular Assemblies with Iron-Containing Acute Phase Proteins. *PLoS ONE*, *8*(7), 67145. https://doi.org/10.1371/JOURNAL.PONE.0067145

Samygina, V. R., Sokolov, A. V., Bourenkov, G., Petoukhov, M. V., Pulina, M. O., Zakharova, E. T., Vasilyev, V. B., Bartunik, H., & Svergun, D. I. (2013c). Ceruloplasmin: Macromolecular Assemblies with Iron-Containing Acute Phase Proteins. *PLoS ONE*, *8*(7), 67145. https://doi.org/10.1371/JOURNAL.PONE.0067145

Sathishkumar, K., Chaturvedi, M., Das, P., Stephen, S., & Mathur, P. (2023). Cancer incidence estimates for 2022 & projection for 2025: Result from National Cancer Registry

Programme, India. *Indian Journal of Medical Research*, *0*(0), 0. https://doi.org/10.4103/IJMR.IJMR_1821_22

Scully, C., & Porter, S. (2001). Oral cancer. *Western Journal of Medicine*, *174*(5), 348. https://doi.org/10.1136/EWJM.174.5.348

Shah, A. T., Wu, E., & Wein, R. O. (2013). Oral squamous cell carcinoma in post-transplant patients. *American Journal of Otolaryngology - Head and Neck Medicine and Surgery*, *34*(2). https://doi.org/10.1016/j.amjoto.2012.11.004

Shah, J. P., & Gil, Z. (2009). CURRENT CONCEPTS IN MANAGEMENT OF ORAL CANCER – SURGERY. *Oral Oncology*, *45*(0), 394. https://doi.org/10.1016/J.ORALONCOLOGY.2008.05.017

Shang, Y., Luo, M., Yao, F., Wang, S., Yuan, Z., & Yang, Y. (2020a). Ceruloplasmin suppresses ferroptosis by regulating iron homeostasis in hepatocellular carcinoma cells. *Cellular Signalling*, *72*. https://doi.org/10.1016/J.CELLSIG.2020.109633

Shang, Y., Luo, M., Yao, F., Wang, S., Yuan, Z., & Yang, Y. (2020b). Ceruloplasmin suppresses ferroptosis by regulating iron homeostasis in hepatocellular carcinoma cells. *Cellular Signalling*, *72*. https://doi.org/10.1016/J.CELLSIG.2020.109633

Shannon, P., Markiel, A., Ozier, O., Baliga, N. S., Wang, J. T., Ramage, D., Amin, N., Schwikowski, B., & Ideker, T. (2003). Cytoscape: A Software Environment for Integrated Models of Biomolecular Interaction Networks. *Genome Research*, *13*(11), 2498. https://doi.org/10.1101/GR.1239303

Shin, Y. J., Vu, H., Lee, J. H., & Kim, H. D. (2021). Diagnostic and prognostic ability of salivary MMP-9 for oral squamous cell carcinoma: A pre-/post-surgery case and matched control study. *PLoS ONE*, *16*(3 March). https://doi.org/10.1371/journal.pone.0248167

Singel, K. L., & Segal, B. H. (2016). Neutrophils in the tumor microenvironment: trying to heal the wound that cannot heal. *Immunological Reviews*, *273*(1), 329. https://doi.org/10.1111/IMR.12459

Singh, S., Sharma, B., Kanwar, S. S., & Kumar, A. (2016). Lead Phytochemicals for Anticancer Drug Development. *Frontiers in Plant Science*, *7*(November 2016), 1667.

https://doi.org/10.3389/FPLS.2016.01667

Spitz, M. R., Fueger, J. J., Newell, G. R., Goepfert, H., & Hong, W. K. (1988). Squamous cell carcinoma of the upper aerodigestive tract. A case comparison analysis. *Cancer*, *61*(1). https://doi.org/10.1002/1097-0142(19880101)61:1<203::AID-CNCR2820610134>3.0.CO;2-6

Sticht, C., De La Torre, C., Parveen, A., & Gretz, N. (2018). miRWalk: An online resource for prediction of microRNA binding sites. *PLOS ONE*, *13*(10), e0206239. https://doi.org/10.1371/JOURNAL.PONE.0206239

Sukiennicki, G. M., Marciniak, W., Muszyńska, M., Baszuk, P., Gupta, S., Białkowska, K., Jaworska-Bieniek, K., Durda, K., Lener, M., Pietrzak, S., Gromowski, T., Prajzendanc, K., Łukomska, A., Waloszczyk, P., Wójcik, J. Z., Scott, R., Lubiński, J., & Jakubowska, A. (2019). Iron levels, genes involved in iron metabolism and antioxidative processes and lung cancer incidence. *PLoS ONE*, *14*(1). https://doi.org/10.1371/journal.pone.0208610

Szklarczyk, D., Gable, A. L., Lyon, D., Junge, A., Wyder, S., Huerta-Cepas, J., Simonovic, M., Doncheva, N. T., Morris, J. H., Bork, P., Jensen, L. J., & Von Mering, C. (2019). STRING v11: protein–protein association networks with increased coverage, supporting functional discovery in genome-wide experimental datasets. *Nucleic Acids Research*, *47*(Database issue), D607. https://doi.org/10.1093/NAR/GKY1131

Tan, M., & Yu, D. (2013). *Molecular Mechanisms of ErbB2-Mediated Breast Cancer Chemoresistance*. https://www.ncbi.nlm.nih.gov/books/NBK6194/

Tang, Z., Li, C., Kang, B., Gao, G., Li, C., & Zhang, Z. (2017). GEPIA: a web server for cancer and normal gene expression profiling and interactive analyses. *Nucleic Acids Research*, *45*(W1), W98–W102. https://doi.org/10.1093/NAR/GKX247

Tomczak, K., Czerwińska, P., & Wiznerowicz, M. (2015). The Cancer Genome Atlas (TCGA): an immeasurable source of knowledge. *Contemporary Oncology*, *19*(1A), A68. https://doi.org/10.5114/WO.2014.47136

Tongue Cancer — Cancer Stat Facts. (n.d.). Retrieved April 12, 2023, from https://seer.cancer.gov/statfacts/html/tongue.html

Torti, S. V., & Torti, F. M. (2020). Iron: The cancer connection. In *Molecular Aspects of Medicine* (Vol. 75). Elsevier Ltd. https://doi.org/10.1016/j.mam.2020.100860

Tsai, Y.-M., Wu, K.-L., Chang, Y.-Y., Chang, W.-A., Huang, Y.-C., Jian, S.-F., Tsai, P.-H., Lin, Y.-S., Chong, I.-W., Hung, J.-Y., & Hsu, Y.-L. (2020). Loss of miR-145-5p Causes Ceruloplasmin Interference with PHD-Iron Axis and HIF-2α Stabilization in Lung Adenocarcinoma-Mediated Angiogenesis. *International Journal of Molecular Sciences 2020, Vol. 21, Page 5081*, *21*(14), 5081. https://doi.org/10.3390/IJMS21145081

Ushio-Fukai, M., & Nakamura, Y. (2008). Reactive oxygen species and angiogenesis: NADPH oxidase as target for cancer therapy. In *Cancer Letters* (Vol. 266, Issue 1, pp. 37–52). Elsevier Ireland Ltd. https://doi.org/10.1016/j.canlet.2008.02.044

Vahabi, M., Blandino, G., & Di Agostino, S. (2021). MicroRNAs in head and neck squamous cell carcinoma: a possible challenge as biomarkers, determinants for the choice of therapy and targets for personalized molecular therapies. *Translational Cancer Research*, *10*(6), 3090. https://doi.org/10.21037/TCR-20-2530

Vahabi, M., Pulito, C., Sacconi, A., Donzelli, S., D'Andrea, M., Manciocco, V., Pellini, R., Paci, P., Sanguineti, G., Strigari, L., Spriano, G., Muti, P., Pandolfi, P. P., Strano, S., Safarian, S., Ganci, F., & Blandino, G. (2019). miR-96-5p targets PTEN expression affecting radio-chemosensitivity of HNSCC cells. *Journal of Experimental & Clinical Cancer Research : CR*, *38*(1). https://doi.org/10.1186/S13046-019-1119-X

Varela-Centelles, P. (2022). Early Diagnosis and Diagnostic Delay in Oral Cancer. *Cancers*, *14*(7). https://doi.org/10.3390/CANCERS14071758

Vasaikar, S. V., Straub, P., Wang, J., & Zhang, B. (2018). LinkedOmics: analyzing multi-omics data within and across 32 cancer types. *Nucleic Acids Research*, *46*(D1), D956–D963. https://doi.org/10.1093/NAR/GKX1090

Vashchenko, G., Bleackley, M. R., Griffiths, T. A. M., & MacGillivray, R. T. A. (2011). Oxidation of organic and biogenic amines by recombinant human hephaestin expressed in Pichia pastoris. *Archives of Biochemistry and Biophysics*, *514*(1–2), 50–56. https://doi.org/10.1016/J.ABB.2011.07.010

Vashchenko, G., & MacGillivray, R. T. A. (2013). Multi-copper oxidases and

human iron metabolism. In *Nutrients* (Vol. 5, Issue 7). https://doi.org/10.3390/nu5072289

Veluthattil, A., Sudha, S., Kandasamy, S., & Chakkalakkoombil, S. (2019). Effect of Hypofractionated, Palliative Radiotherapy on Quality of Life in Late-Stage Oral Cavity Cancer: A Prospective Clinical Trial. *Indian Journal of Palliative Care*, *25*(3), 383–390. https://doi.org/10.4103/IJPC.IJPC_115_18

Vermorken, J. B., Mesia, R., Rivera, F., Remenar, E., Kawecki, A., Rottey, S., Erfan, J., Zabolotnyy, D., Kienzer, H.-R., Cupissol, D., Peyrade, F., Benasso, M., Vynnychenko, I., De Raucourt, D., Bokemeyer, C., Schueler, A., Amellal, N., & Hitt, R. (2008). Platinum-based chemotherapy plus cetuximab in head and neck cancer. *The New England Journal of Medicine*, *359*(11), 1116–1127. https://doi.org/10.1056/NEJMOA0802656

Vogel, D. W. T., Vogel, T., Zbaeren, P., & Thoeny, H. C. (2010). Cancer of the oral cavity and oropharynx. *Cancer Imaging*, *10*(1), 62. https://doi.org/10.1102/1470-7330.2010.0008

Wade, R. C., & Goodford, P. J. (1989). The role of hydrogen-bonds in drug binding. *Progress in Clinical and Biological Research*, *289*.

Walker-Samuel, S., Ramasawmy, R., Torrealdea, F., Rega, M., Rajkumar, V., Johnson, S. P., Richardson, S., Gonçalves, M., Parkes, H. G., Årstad, E., Thomas, D. L., Pedley, R. B., Lythgoe, M. F., & Golay, X. (2013). In vivo imaging of glucose uptake and metabolism in tumors. *Nature Medicine*, *19*(8), 1067. https://doi.org/10.1038/NM.3252

Wang, H., Guo, M., Wei, H., & Chen, Y. (2021). Targeting MCL-1 in cancer: current status and perspectives. *Journal of Hematology & Oncology 2021 14:1*, *14*(1), 1–18. https://doi.org/10.1186/S13045-021-01079-1

Wang, M., Zhang, G., Zhang, Y., Cui, X., Wang, S., Gao, S., Wang, Y., Liu, Y., Bae, J. H., Yang, W. H., Qi, L. S., Wang, L., & Liu, R. (2020). Fibrinogen alpha chain knockout promotes tumor growth and metastasis through integrin-akt signaling pathway in lung cancer. *Molecular Cancer Research*, *18*(7), 943–954. https://doi.org/10.1158/1541-7786.MCR-19-1033/82219/AM/FIBRINOGEN-ALPHA-CHAIN-KNOCKOUT-PROMOTES-TUMOR

Wang, W., Li, D., Xiang, L., Lv, M., Tao, L., Ni, T., Deng, J., Gu, X., Masatara, S., Liu, Y., & Zhou, Y. (2019). TIMP-2 inhibits metastasis and predicts prognosis of colorectal cancer via regulating MMP-9. *Cell Adhesion & Migration*, *13*(1), 273. https://doi.org/10.1080/19336918.2019.1639303

Ward, D. M., & Kaplan, J. (2012). Ferroportin-mediated iron transport: expression and regulation. *Biochimica et Biophysica Acta*, *1823*(9), 1426. https://doi.org/10.1016/J.BBAMCR.2012.03.004

Warde-Farley, D., Donaldson, S. L., Comes, O., Zuberi, K., Badrawi, R., Chao, P., Franz, M., Grouios, C., Kazi, F., Lopes, C. T., Maitland, A., Mostafavi, S., Montojo, J., Shao, Q., Wright, G., Bader, G. D., & Morris, Q. (2010). The GeneMANIA prediction server: biological network integration for gene prioritization and predicting gene function. *Nucleic Acids Research*, *38*(Web Server issue), W214. https://doi.org/10.1093/NAR/GKQ537

Warnakulasuriya, S. (2009). Global epidemiology of oral and oropharyngeal cancer. *Oral Oncology*, *45*(4–5), 309–316. https://doi.org/10.1016/J.ORALONCOLOGY.2008.06.002

Wei, C. Y., Wang, L., Zhu, M. X., Deng, X. Y., Wang, D. H., Zhang, S. M., Ying, J. H., Yuan, X., Wang, Q., Xuan, T. F., He, A. Q., Qi, F. Z., & Gu, J. Y. (2019). TRIM44 activates the AKT/mTOR signal pathway to induce melanoma progression by stabilizing TLR4. *Journal of Experimental and Clinical Cancer Research*, *38*(1), 1–13. https://doi.org/10.1186/S13046-019-1138-7/FIGURES/7

Woodman, S. E., & Mills, G. B. (2010). Are oncogenes sufficient to cause human cancer? *Proceedings of the National Academy of Sciences of the United States of America*, *107*(48), 20599. https://doi.org/10.1073/PNAS.1015563107

Wu, G., Peng, H., Tang, M., Yang, M., Wang, J., Hu, Y., Li, Z., Li, J., Li, Z., & Song, L. (2021). ZNF711 down-regulation promotes CISPLATIN resistance in epithelial ovarian cancer via interacting with JHDM2A and suppressing SLC31A1 expression. *EBioMedicine*, *71*. https://doi.org/10.1016/J.EBIOM.2021.103558

Wu, J., Liu, G., An, K., & Shi, L. (2022). NPTX1 inhibits pancreatic cancer cell

proliferation and migration and enhances chemotherapy sensitivity by targeting RBM10. *Oncology Letters*, *23*(5), 1–9. https://doi.org/10.3892/OL.2022.13275/HTML

Wu, Y., & Zhou, B. P. (2010). TNF-α/NFκ-B/Snail pathway in cancer cell migration and invasion. In *British Journal of Cancer* (Vol. 102, Issue 4). https://doi.org/10.1038/sj.bjc.6605530

Xing, F., Hu, Q., Qin, Y., Xu, J., Zhang, B., Yu, X., & Wang, W. (2022a). The Relationship of Redox With Hallmarks of Cancer: The Importance of Homeostasis and Context. In *Frontiers in Oncology* (Vol. 12). https://doi.org/10.3389/fonc.2022.862743

Xing, F., Hu, Q., Qin, Y., Xu, J., Zhang, B., Yu, X., & Wang, W. (2022b). The Relationship of Redox With Hallmarks of Cancer: The Importance of Homeostasis and Context. *Frontiers in Oncology*, *12*, 1437. https://doi.org/10.3389/FONC.2022.862743/BIBTEX

Xue, X., Ramakrishnan, S. K., Weisz, K., Triner, D., Xie, L., Attili, D., Pant, A., Győrffy, B., Zhan, M., Carter-Su, C., Hardiman, K. M., Wang, T. D., Dame, M. K., Varani, J., Brenner, D., Fearon, E. R., & Shah, Y. M. (2016). Iron Uptake via DMT1 Integrates Cell Cycle with JAK-STAT3 Signaling to Promote Colorectal Tumorigenesis. *Cell Metabolism*, *24*(3), 447–461. https://doi.org/10.1016/J.CMET.2016.07.015

Y, M., H, I., Y, M., K, A., T, M., N, A., Y, N., T, M., H, S., & K, O. (2021). Ceruloplasmin Levels in Cancer Tissues and Urine Are Significant Biomarkers of Pathological Features and Outcome in Bladder Cancer. *Anticancer Research*, *41*(8), 3815–3823. https://doi.org/10.21873/ANTICANRES.15174

Y, Z., & Z, Z. (2020). The history and advances in cancer immunotherapy: understanding the characteristics of tumor-infiltrating immune cells and their therapeutic implications. *Cellular & Molecular Immunology*, *17*(8), 807–821. https://doi.org/10.1038/S41423-020-0488-6

Yang, H. L., Chang, H. C., Lin, S. W., Senthil Kumar, K. J., Liao, C. H., Wang, H. M., Lin, K. Y., & Hseu, Y. C. (2014). Antrodia salmonea inhibits TNF-α-induced angiogenesis and atherogenesis in human endothelial cells through the down-regulation of NF-κB and up-regulation of Nrf2 signaling pathways. *Journal of Ethnopharmacology*,

151(1), 394–406. https://doi.org/10.1016/J.JEP.2013.10.052

Yang, J., Qi, M., Fei, X., Wang, X., & Wang, K. (2021). Long non-coding RNA XIST: a novel oncogene in multiple cancers. *Molecular Medicine*, *27*(1), 1–19. https://doi.org/10.1186/S10020-021-00421-0/FIGURES/4

Yang, R., Yi, M., & Xiang, B. (2022). Novel Insights on Lipid Metabolism Alterations in Drug Resistance in Cancer. *Frontiers in Cell and Developmental Biology*, *10*. https://doi.org/10.3389/FCELL.2022.875318/FULL

Yang, X. H., Jing, Y., Wang, S., Ding, F., Zhang, X. X., Chen, S., Zhang, L., Hu, Q. G., & Ni, Y. H. (2020). Integrated Non-targeted and Targeted Metabolomics Uncovers Amino Acid Markers of Oral Squamous Cell Carcinoma. *Frontiers in Oncology*, *10*, 426. https://doi.org/10.3389/FONC.2020.00426

Yang, Y., Li, C., Liu, T., Dai, X., & Bazhin, A. V. (2020). Myeloid-Derived Suppressor Cells in Tumors: From Mechanisms to Antigen Specificity and Microenvironmental Regulation. *Frontiers in Immunology*, *11*, 1371. https://doi.org/10.3389/FIMMU.2020.01371/BIBTEX

Ying, J.-F., Lu, Z.-B., Fu, L.-Q., Tong, Y., Wang, Z., Li, W.-F., & Mou, X.-Z. (2021). The role of iron homeostasis and iron-mediated ROS in cancer. *American Journal of Cancer Research*, *11*(5).

YM, T., KL, W., YY, C., WA, C., YC, H., SF, J., PH, T., YS, L., IW, C., JY, H., & YL, H. (2020). Loss of miR-145-5p Causes Ceruloplasmin Interference with PHD-Iron Axis and HIF-2α Stabilization in Lung Adenocarcinoma-Mediated Angiogenesis. *International Journal of Molecular Sciences*, *21*(14), 1–19. https://doi.org/10.3390/IJMS21145081

Yoshizaki, M., Matsushita, S., Fujiwara, Y., Ikeda, T., Ono, M., & Nohara, T. (2005). Tomato new sapogenols, isoesculeogenin A and esculeogenin B. *Chemical and Pharmaceutical Bulletin*, *53*(7). https://doi.org/10.1248/cpb.53.839

You, J., Chen, W., Chen, J., Zheng, Q., Dong, J., & Zhu, Y. (2018). The oncogenic role of ARG1 in progression and metastasis of hepatocellular carcinoma. *BioMed Research International*, *2018*. https://doi.org/10.1155/2018/2109865

Young, L. S., & Dawson, C. W. (2014). Epstein-Barr virus and nasopharyngeal carcinoma. *Chinese Journal of Cancer*, *33*(12), 581. https://doi.org/10.5732/CJC.014.10197

Yuan, S., Chan, H. C. S., & Hu, Z. (2017). Using PyMOL as a platform for computational drug design. In *Wiley Interdisciplinary Reviews: Computational Molecular Science* (Vol. 7, Issue 2). https://doi.org/10.1002/wcms.1298

Yun, C. W., & Lee, S. H. (2018). The roles of autophagy in cancer. In *International Journal of Molecular Sciences* (Vol. 19, Issue 11). https://doi.org/10.3390/ijms19113466

Zambrano, A., Molt, M., Uribe, E., & Salas, M. (2019). Glut 1 in Cancer Cells and the Inhibitory Action of Resveratrol as A Potential Therapeutic Strategy. *International Journal of Molecular Sciences*, *20*(13). https://doi.org/10.3390/IJMS20133374

Zhan, T., Rindtorff, N., & Boutros, M. (2016). Wnt signaling in cancer. *Oncogene 2017 36:11*, *36*(11), 1461–1473. https://doi.org/10.1038/onc.2016.304

Zhang, B. D., Li, Y. R., Ding, L. D., Wang, Y. Y., Liu, H. Y., & Jia, B. Q. (2019). Loss of PTPN4 activates STAT3 to promote the tumor growth in rectal cancer. *Cancer Science*, *110*(7), 2258. https://doi.org/10.1111/CAS.14031

Zhang, X., Wang, Y., Cao, Y., Zhang, X., & Zhao, H. (2017). Increased CCL19 expression is associated with progression in cervical cancer. *Oncotarget*, *8*(43), 73817. https://doi.org/10.18632/ONCOTARGET.17982

Zhang, Y., Chen, Z., Chen, J. G., Chen, X. F., Gu, D. H., Liu, Z. M., Gao, Y. D., & Zheng, B. (2021a). Ceruloplasmin overexpression is associated with oncogenic pathways and poorer survival rates in clear-cell renal cell carcinoma. *FEBS Open Bio*, *11*(11), 2988–3004. https://doi.org/10.1002/2211-5463.13283

Zhang, Y., Chen, Z., Chen, J. G., Chen, X. F., Gu, D. H., Liu, Z. M., Gao, Y. D., & Zheng, B. (2021b). Ceruloplasmin overexpression is associated with oncogenic pathways and poorer survival rates in clear-cell renal cell carcinoma. *FEBS Open Bio*, *11*(11), 2988–3004. https://doi.org/10.1002/2211-5463.13283

Zhang, Y., Chen, Z., Chen, J. G., Chen, X. F., Gu, D. H., Liu, Z. M., Gao, Y. D., & Zheng, B. (2021c). Ceruloplasmin overexpression is associated with oncogenic pathways and poorer survival rates in clear-cell renal cell carcinoma. *FEBS Open Bio*, *11*(11), 2988.

https://doi.org/10.1002/2211-5463.13283

Zhang, Y., & Wang, X. (2020). Targeting the Wnt/β-catenin signaling pathway in cancer. *Journal of Hematology & Oncology 2020 13:1*, *13*(1), 1–16. https://doi.org/10.1186/S13045-020-00990-3

Zhang, Y., & Zhang, Z. (2020). The history and advances in cancer immunotherapy: understanding the characteristics of tumor-infiltrating immune cells and their therapeutic implications. *Cellular & Molecular Immunology*, *17*(8), 807–821. https://doi.org/10.1038/S41423-020-0488-6

Zhou, L., Zhao, B., Zhang, L., Wang, S., Dong, D., Lv, H., & Shang, P. (2018). Alterations in cellular iron metabolism provide more therapeutic opportunities for cancer. In *International Journal of Molecular Sciences* (Vol. 19, Issue 5). https://doi.org/10.3390/ijms19051545

Zhou, W. J., Geng, Z. H., Chi, S., Zhang, W., Niu, X. F., Lan, S. J., Ma, L., Yang, X., Wang, L. J., Ding, Y. Q., & Geng, J. G. (2011). Slit-Robo signaling induces malignant transformation through Hakai-mediated E-cadherin degradation during colorectal epithelial cell carcinogenesis. *Cell Research 2011 21:4*, *21*(4), 609–626. https://doi.org/10.1038/cr.2011.17

Ziello, J. E., Jovin, I. S., & Huang, Y. (2007). Hypoxia-Inducible Factor (HIF)-1 regulatory pathway and its potential for therapeutic intervention in malignancy and ischemia. In *Yale Journal of Biology and Medicine* (Vol. 80, Issue 2).

Zimpfer, A., Glass, Ä., Bastian, M., Schuff-Werner, P., Hakenberg, O. W., & Maruschke, M. (2021). Ceruloplasmin expression in renal cell carcinoma correlates with higher-grade and shortened survival. *Biomarkers in Medicine*, *15*(11). https://doi.org/10.2217/bmm-2020-0514

Zolkind, P., & Uppaluri, R. (2017). Checkpoint immunotherapy in head and neck cancers. *Cancer and Metastasis Reviews*, *36*(3). https://doi.org/10.1007/s10555-017-9694-9

ZQ, W., XL, S., YL, W., & YL, M. (2021). Agrin promotes the proliferation, invasion and migration of rectal cancer cells via the WNT signaling pathway to contribute to rectal cancer progression. *Journal of Receptor and Signal Transduction Research*, *41*(4),

363–370. https://doi.org/10.1080/10799893.2020.1811325

LIST OF PUBLICATIONS

Arfin, S., Kumar, D., Lomagno, A., Mauri, P. L., & Di Silvestre, D. (2023). Differentially Expressed Genes, miRNAs and Network Models: A Strategy to Shed Light on Molecular Interactions Driving HNSCC Tumorigenesis. Cancers, 15(17), 4420. https://doi.org/10.3390/cancers15174420

Arfin, S., Agrawal, K., Kumar, A., Kumar, A., Rathi, B., & Kumar, D. (2022). Metabolic dysregulation in cancer progression. In Autophagy and Metabolism: Potential Target for Cancer Therapy. https://doi.org/10.1016/B978-0-323-99879-6.00008-0

Arfin, S., Chauhan, S., Mani, N., Rathi, B., & Kumar, D. (2022). In Silico analysis of Ceruloplasmin alteration in Oral Squamous Cell Carcinoma. Chemical Biology Letters, 9(3), 342–342. https://pubs.thesciencein.org/journal/index.php/cbl/article/view/342

Arfin, S., Jha, N. K., Jha, S. K., Kesari, K. K., Ruokolainen, J., Roychoudhury, S., Rathi, B., & Kumar, D. (2021). Oxidative Stress in Cancer Cell Metabolism. Antioxidants (Basel, Switzerland), 10(5). https://doi.org/10.3390/ANTIOX10050642

Agrawal, K., **Arfin, S**., Mishra, M. K., Harihar, S., Kesari, K. K., Roychoudhury, S., & Kumar, D. (2022). Signaling pathways in metabolic dysregulation in solid tumors. In Autophagy and Metabolism: Potential Target for Cancer Therapy. https://doi.org/10.1016/B978-0-323-99879-6.00013-4

Agrawal, K., Chakraborty, P., Dewanjee, S., **Arfin, S**., Das, S. S., Dey, A., Moustafa, M., Mishra, P. C., Jafari, S. M., Jha, N. K., Jha, S. K., & Kumar, D. (2023). Neuropharmacological interventions of quercetin and its derivatives in neurological and psychological disorders. In

Neuroscience and Biobehavioral Reviews (Vol. 144).
https://doi.org/10.1016/j.neubiorev.2022.104955

James, S., **Arfin, S**., Mishra, M. K., Kumar, A., Jha, N. K., Jha, S. K., Kesari, K. K., Kumar, P., Srivastava, A., & Kumar, D. (2021). Role of Arsenic in Carcinogenesis. Molecular and Integrative Toxicology, 149–169. https://doi.org/10.1007/978-3-030-83446-3_7

Jha, N. K**., Arfin, S**., Jha, S. K., Kar, R., Dey, A., Gundamaraju, R., Ashraf, G. M., Gupta, P. K., Dhanasekaran, S., Abomughaid, M. M., Das, S. S., Singh, S. K., Dua, K., Roychoudhury, S., Kumar, D., Ruokolainen, J., Ojha, S., & Kesari, K. K. (2022). Re-establishing the comprehension of phytomedicine and nanomedicine in inflammation-mediated cancer signaling. Seminars in Cancer Biology. https://doi.org/10.1016/J.SEMCANCER.2022.02.022

Maurya, S., Srivastava, R., **Arfin, S.,** Hawthorne, S., Jha, N. K., Agrawal, K., Raj, S., Rathi, B., Kumar, A., Raj, R., Agrawal, S., Paiva-Santos, A. C., Malik, A. A., Dua, K., Rana, R., Ojha, S., Jha, S. K., Sharma, A., Kumar, D., El-Zahaby, S. A., … Nagar, A. (2022). Exploring state-of-the-art advances in targeted nanomedicines for managing acute and chronic inflammatory lung diseases. *Nanomedicine (London, England)*, *17*(30), 2245–2264. https://doi.org/10.2217/nnm-2021-0437

Arfin S, Kumar.D. (2023).Use of vitamins and minerals as dietary supplements for better health and cancer prevention. Nutraceuticals Academic Press, (3), 53-97. https://doi.org/10.1016/B978-0-443-19193-0.00003-4. https://www.sciencedirect.com/science/article/pii/B9780443191930000034

thesis

8%	**4**%	**6**%	**1**%
SIMILARITY INDEX	INTERNET SOURCES	PUBLICATIONS	STUDENT PAPERS

PRIMARY SOURCES

1	"Encyclopedia of Cancer", Springer Science and Business Media LLC, 2017 Publication	**2**%
2	pubs.thesciencein.org Internet Source	**2**%
3	dokumen.pub Internet Source	**1**%
4	storage.googleapis.com Internet Source	<**1**%
5	"2015 ACR/ARHP Annual Meeting Abstract Supplement", Arthritis & Rheumatology, 2015. Publication	<**1**%
6	Submitted to Universitaet Hamburg Student Paper	<**1**%
7	ia801702.us.archive.org Internet Source	<**1**%
8	Submitted to University of Birmingham Student Paper	<**1**%